

UNDERGROUND SUN.STORAGE



Final Report

31. October 2017

Projectnumber: **840705**

Programmsteuerung



Programmabwicklung



Projektkonsortium



Verbund



Ausschreibung	e!MISSION.at – 1. Ausschreibung
Projektstart	01.Juli 2013
Projektende	30.Juni 2017
Gesamtprojektdauer (in Monaten)	42 Monate
ProjektnehmerIn (Institution)	RAG
AnsprechpartnerIn	Hr. DI Stephan Bauer
Postadresse	1010 Wien, Schwarzenbergplatz 16
Telefon	0043(0)50724-5377
Fax	0043(0)50724-5383
E-Mail	stephan.bauer@rag-austria.at
Website	www.rag-austria.at ; www.underground-sun-storage.at

UNDERGROUND SUN STORAGE

Chemical storage of renewable energy in porous subsurface reservoirs with exemplary testbed

Authors:

RAG Austria AG

AXIOM angewandte Prozesstechnik GesmbH

VERBUND AG

MONTANUNIVERSITÄT LEOBEN

UNIVERSITÄT für Bodenkultur Wien

ENERGIEINSTITUT an der Johannes Kepler Universität Linz

1 Table of Contents

1	Table of Contents	4
2	Abridgment	7
3	Introduction	14
4	Geological, geochemical and geophysical processes in hydrogen bearing porous gas reservoirs	17
4.1	Introduction	17
4.2	Integrity of the Cap Rock	18
4.2.1	Task Definition	18
4.2.2	Content Presentation	19
4.2.3	Results and Conclusions	20
4.3	Changes in the behavior of the storage gas due to hydrogen admixture	20
4.3.1	Introduction	20
4.3.2	Task description DBI	21
4.3.3	DBI content presentation	21
4.3.4	Results and Conclusions DBI	22
4.3.5	Task definition MUL	24
4.3.6	Content presentation MUL	25
4.3.7	Results and conclusions MUL	28
4.4	Transport and diffusion modelling at the University of Leoben	42
4.4.1	Task	42
4.4.2	Content presentation	42
4.4.3	Results an conclusions	44
4.5	Artificial reservoir water	46
4.5.1	Task definition	46
4.5.2	Content presentation	46
4.5.3	Results and Conclusions	46
4.6	Alteration of the reservoir rock (reservoir alteration)	49
4.6.1	Task definition	49
4.6.2	Presentation of content	49
4.6.3	Results and conclusions	50
4.7	Geochemical Simulation	55
4.7.1	Task definition	55
4.7.2	Content representation of the static simulation RAG	56
4.7.3	Results and conclusions of the static simulation RAG	56
4.7.4	Dynamic Simulation RAG	60
4.7.5	Content of the MUL simulations	61
4.7.6	Results and conclusions MUL	64
4.8	Reference to publications and other documents	65
4.9	List of references	65
4.10	Contact details	67
5	Microbiological processes in hydrogen-loaded reservoirs	68
5.1	Task	68

5.2	Content presentation	68
5.2.1	Experimental setup.....	68
5.2.2	Test materials.....	69
5.2.3	Investigation methods	70
5.2.4	Test procedure	71
5.2.5	Possible microbiological conversions at hydrogen exposure.....	74
5.3	Results and conclusions.....	77
5.3.1	Hydrochemical analyses	77
5.3.2	Gas analyses.....	79
5.3.3	Characterization of the microbial consortium	84
5.3.4	Conclusions.....	85
5.4	Reference to publications and other documents	86
5.5	List of references	86
5.6	Contact details.....	87
6	Material integrity in hydrogen-loaded gas storage facilities.....	88
6.1	Tasks of metallic materials	88
6.2	Content presentation of metallic materials	88
6.3	Results and Conclusions of Metallic Materials	92
6.3.1	STTs.....	92
6.3.2	CLTs.....	95
6.3.3	Paging tests.....	95
6.4	Conclusions on metallic materials	96
6.5	Task Cement	96
6.6	Cement content presentation	96
6.7	Results and conclusions cement.....	97
6.8	Reference to publications and other documents	100
6.9	Contact details.....	100
7	Membrane technology in connection with hydrogen admixtures.....	101
7.1	Task definition	101
7.2	Content presentation	102
7.3	Results and conclusions.....	103
7.4	Reference to publications and other documents	106
7.5	Contact details.....	106
8	In-situ field trials	107
8.1	Task definition	107
8.2	Preparation, Planning and Building of the Test Facility	107
8.3	Experiment execution	109
8.4	Hydrogen balancing.....	109
8.4.1	Initial situation.....	109
8.4.2	Hydrogen produced.....	109
8.4.3	Hydrogen diffused	110
8.4.4	Conversion	111
8.4.5	Hydrogen Dissolved	112
8.5	Microbiology	113

8.5.1	Sampling formation water from the test field	113
8.5.2	Modification of the microbial consortium in the test field	115
8.5.3	Hydrochemical results of the formation water	117
8.5.4	Modification of reservoir parameters	118
8.6	Material tests	119
8.6.1	Cement.....	119
8.6.2	Steels	119
8.6.3	Elastomers	119
8.6.4	Well Integrity.....	119
8.7	Modeling	119
8.8	Summary of the results.....	121
8.9	Reference to publications and other documents	123
8.10	List of references	123
8.11	Contact details.....	124
9	Risk analysis and life cycle assessment	125
9.1	Task definition	125
9.2	Content presentation	125
9.2.1	Risk analysis	125
9.2.2	Life cycle assessment	127
9.3	Results and conclusions.....	128
9.3.1	Risk Analysis	128
	Life cycle assessment	134
9.4	Reference to publications and other documents	137
9.5	List of references	138
9.6	Contact details.....	140
10	Economic and legal analyses.....	141
10.1	Tasks	141
10.2	Content presentation	141
10.2.1	Legal analyses	142
10.2.2	Potential of hydrogen injection into the Austrian natural gas grid	142
10.2.3	Economic valuation	143
10.2.4	Social Acceptance of Power-to-Gas.....	144
10.3	Results and conclusions.....	144
10.3.1	Legal analyses	144
10.3.2	Potential of hydrogen injection into the Austrian natural gas grid	147
10.3.3	Economic valuation	152
10.3.4	Social acceptance of power-to-gas	156
10.3.5	Summary of the report.....	159
10.4	Reference to publications and other documents	162
10.5	List of references	163
10.6	Contact details.....	165
11	Outlook and recommendations	166
12	Appendix	168

2 Abridgment

The „Publizierbare Endbericht“ for the project Underground Sun Storage sums up the essential findings of this research project. Where it is necessary additional publications will be mentioned. For further details, researcher institutions from the different disciplines will be mentioned with their contact data.

The project was started in 2013 and lasted until 2017. The aim was to find out whether it is possible to store huge amounts of renewable energy in existing subsurface gas storages by using hydrogen generated from renewable electricity. This is shown in the long title of the project which reads: ” Chemical storage of renewable Energy in porous subsurface Reservoirs with exemplary Testbed”. The issue of storage of renewable energie is a key focus of the Austrian climate and energy fund.

The project was split into two phases one being the basic research with lab tests, literature review and simulation and the second was the planning, building, approval and execution of a field-test facility. In the first phase it was especially important to prove that the overall integrity of the subsurface reservoir is not compromised by the blending of 10% of hydrogen to the natural gas. The laboratory experiments were conducted based on the geological situation in the Austrian molass basin and took into account the technical conditions of RAG's (RAG Austria AG) commercial gas storage facilities. With this project it was possible for the first time to gain actual interdisciplinary insight into the storage of hydrogen in a subsurface gas storage with the inclusion of an actual field test.

The project was initiated by RAG and was executed together with high quality partners from universities and the industry. The consortium was made up of RAG, Montanuniversität Leoben, Universität für Bodenkultur – Department IFA Tulln, Axiom Angewandte Prozesstechnik GmbH, Energieinstitut an der JKU Linz und Verbund AG and was publically funded by the Austrian climate and energy fund.

Overall, ten work-packages have been defined. However, for better readability the summary is arranged into connected topics. Of special interest were the topics of geochemistry, geophysics and microbiology as well as material science to get a baseline understanding about possible issues in the subsurface concerning hydrogen. For the field test, it was also important to legally couple the project into the existing law. Additionally several reservoir engineering and process engineering issues needed to be addressed. The overall aim was to show a full storage cycle of a gas mixture with 10% of hydrogen blend. Finally, a Risk Assessment and a Life-Cycle Assessment were carried out and also social, legal and economic aspects of such a technology were analyzed.

Geological, geochemical and geophysical processes in hydrogen bearing porous subsurface gas reservoirs

Hydrogen is a highly reactive element, which made it a key necessity to investigate geochemical and geophysical aspects for this project. Therefore several laboratory experiments where conducted to determine the influence of hydrogen on the integrity of the reservoir and the surrounding seal rocks. Additionally it was investigated whether hydrogen-bearing gases have a different physical behavior in a subsurface reservoir than common natural gas. With this knowledge established, it was tried to develop geological and

geochemical dynamic simulation models, to rebuild and verify the results from the lab. Once this was done, the models were used to make predictions on long-term influences of hydrogen in the subsurface. The rocks used for the laboratory experiments were all taken from representative cores of the molass basin as this basin contains all of RAG's storage formations.

The movement of hydrogen-bearing gases in the reservoir was determined in the laboratory with the help of flow through experiments on wet reservoir rocks. To see these effects not only on small scale (a typical rock plug is only 3 inches long), but on reservoir scale, additional flow through experiments were done in huge high-pressure reactors at MUL. This 7m long reactors were filled with sand to resemble the pore space of a reservoir. It was then filled with a CH₄/H₂ mixture, (92 Vol.-% CH₄, 8 Vol.-% H₂) to conduct static and dynamic experiments. The static experiments were done in order to prove that there is no de-mixing of the gases during the duration of one 6 month and one 12 months storage cycle. (Isotherm conditions with 40°C mean temperature and three different pressures of 10, 25 and 40 bar(g)) It could be shown, that inside the measurement precision of the gas phase chromatograph (ABB Modell PGC 1000) no de-mixing is happening. The dynamic experiments should prove that there is also no de-mixing when gas is flowing through the reservoir due to different viscosities. The results of these experiments are hard to interpret, but generally, it can be seen that there are no differences in the travel speed of hydrogen and methane within a porous media. As the measurement, precision made it difficult to find the exact break through points of both gases these results should be used with care. It should be mentioned that the DBI Leipzig did similar experiments on reservoir plugs. Their interpretation of the experimental results was also that there is no difference in the travel speed of hydrogen and methane in the reservoir.

Using the sandstones and the reservoir water from the molass basin geochemical flow through experiments were also conducted at DBI Leipzig. Here wet reservoir rocks were kept under reservoir conditions and CH₄/H₂ atmosphere for several months. Afterwards the permeability was measured and thin-sections were made and compared to measurements and thin-section of the original rocks. It could be seen, that gases bearing a hydrogen share of 25 Vol.-% and 75 Vol.-% of hydrogen do not cause measurable changes under the physical conditions of the molass basin. This also proved the assumptions of a literature study, which also came to the result that the relative low temperatures of the molass basin would hamper geochemical reactions.

The data generated in the laboratory experiments was used as input for the dynamic geochemical reaction models, which were developed at MUL. To determine the movement of hydrogen in the reservoir a geological transport model of the test-reservoir was developed via simulation software. This model was then further used to appraise the losses of hydrogen due to diffusion into the cushion gas and the cap rock under different reservoir conditions. Another part of the simulation was related to geochemical reactions in the gas, water, solid system. For this a workflow was developed, which in several steps tried to predict the long-term as well as the time related effect of kinetics on geochemical reactions. The results showed that for the duration of the storage no significant reactions happen. The transport model on the other hand showed that for some scenarios losses of hydrogen due to diffusion and dissolution seem possible. This is why future work should focus on these aspects.

Microbiological Experiments

In the flagship project Underground Sun Storage the University of Natural Resources and Life Sciences, Vienna was responsible for the characterisation of microbiological transformation processes in hydrogen exposed natural gas reservoirs. Accordingly, the physio-chemical conditions of the test field were simulated in high-pressure bioreactors (see chapter 6). Drilling cores with mineralogical and petrological properties similar to the test field were placed in bioreactors, inoculated with formation water from the test field, and then incubated at 47 bar and 45°C. After the inoculation phase, gas mixtures of hydrogen (4-10 Vol.-%), carbon dioxide (0.3-2.5 Vol.-%) and methane (87.5-95.7 Vol.-%) were introduced into the high pressure bioreactors. For the assessment of a potential abiotic hydrogen depletion, two of ten reactors were sterilized using gamma radiation. The analysis of hydrochemical properties of the reactor fluids as well as the characterization of the microbiological consortia based on DNA sequencing was accomplished before the introduction of gas components (H₂, CO₂, CH₄) and upon opening of the reactors after approx. 180 days. During the lab-scale experiment, concentrations of gas components were monitored (H₂, CO₂, CH₄) together with pressure and temperature. Upon total consumption of hydrogen, selected reactors were refilled with a hydrogen containing gas mixture. Knowledge on microbiological transformation processes as gained from the lab scale study was applied to set up the hydrogen storage experiment in the field test. Several samplings of formation water were accomplished in the course of the field test experiment (see chapter 9) to monitor possible changes of hydrochemical properties and to detect shifts in the structure of the microbiological consortium.

Integrity of steels, cements and elastomers in hydrogen-bearing subsurface gas storages

The chemo-mechanical resistance of the steel grades L80, P110, 42CrMo4, L360, P235, J55 and K55, which are used in an Underground Gas Storage (UGS), against the degradation due to gaseous hydrogen up to a hydrogen partial pressure of 10 bar, has been investigated by means of slow strain rate and constant load tests. An experimental plan has been established, which enables a differentiation between the effects of hydrogen and other chemical species in the media, whose existence is theoretically possible during the operation of an UGS, on the mechanical properties of the materials. Pre-strained steel samples have been exposed in the UGS for a duration of one year. No rupture has been observed after field exposure. All investigations have shown that no additional embrittlement of the investigated steel grades is caused by the presence of hydrogen gas under the tested conditions. The elastomers NBR 80, HNBR 80, Viton 90, Packer Sealing 90, Packer Sealing 70, Fluorcarbon, HNBR und FPM 90 and O-Ring pieces also have been exposed to the UGS for one year. Optical conditions, masses and volumina of the elastomers have been investigated before and after the exposure test. Except HNBR, which has shown very slight mass and volume gain, no significant optical, gravimetric or volumetric differences have been observed.

Membrane-Technology in relation to hydrogen inclusion into the natural gas stream

Within the research project Underground Sun Storage the company Axiom angewandte Prozeßtechnik developed a membrane permeation system for the separation of hydrogen and for the adjustment of the hydrogen content in natural gas / hydrogen mixtures.

An experimental pilot plant with the nominal feed gas volume flow of 400 Nm³/h has been constructed and operated at field conditions at a gas storage facility of RAG Austria AG in Upper Austria.

The experimental plant proved its functionality and ability to adjust the hydrogen content with the assigned limits of 2-9 % (v/v) in the withdrawn gas from the storage. Furthermore, the field experiment confirmed the advantages of the membrane process: its high reliability, high energy efficiency, high process safety and low footprint.

Insitu test-bed facility

An essential part of the project was the execution of a field-test in one of RAG's small gas reservoirs. The reservoir was chosen after a thorough screening process which did not only take reservoir, but also logistic parameters (accessibility) into account. It has similar geological and dynamical parameters as RAG's major gas storage facilities. The test bed facility was planned, approved, built and executed at this location which is near Vöcklabruck in upper Austria.

It has to be noted that this field-test is unique, as it is the first project of it's kind where a hydrogen natural gas mixture is actually injected into a porous gas reservoir. Adding to the lab experiments, several baseline measurements in the reservoir and on the completion of the storage well have been done in order to make sure that any possible changes happening do to the field test could be accounted for. After this preliminary work was done, the approval and the construction of the facility was done and in April 2016 the injection of the hydrogen, natural gas mixture finally started. The injection of 1,22 Mio. Nm³ took about three months until the beginning of July. Afterwards a three months shut in phase was used to monitor the pressure and temperature behaviour as well as the changes in the gas composition. The gas was then reproduced until mid-January 2017. During all this stages pressure and temperature measurements were done on a continuous basis. Additionally several well tests were executed in order to see any possible changes in the reservoir behaviour. However, during the lifetime of the facility no hydrogen induced issues could be monitored. A final volume balance showed, that 82% of the injected hydrogen could be recovered. The other 18% are accounted for by, diffusion, solubility and conversion. None of this processes is harmful to the reservoir and apart from conversion these effects will only happen until a saturation equilibrium with hydrogen is reached in the reservoir. It is however emphasised to do additional research on this aspects in future research projects. It should be mentioned, that no damage was detected on materials or installations of the facility either. Therefore the field test showed, that the storage of 10 vol. % of hydrogen in a gas mixture is possible for RAG's storage facilities.

Risk and Life-Cycle Assessment

To determine the risks of subsurface hydrogen storage a risk assessment was done within the official international guidelines. Additionally a life cycle assessment was carried out to determine the effects on the environment as well as to generate business cases for future applications of this technology.

Risk Assessment

The risk assessment was carried out to identify all possible and probable risks and safety aspects for the storage of hydrogen in an underground pore storage facility, considering future activities of similar nature. The risk assessment led to display and to list all identified risks and safety aspects of all applied technologies in this project, and further, resulted in an improved model for risk evaluation for the underground storage of hydrogen. This model consists of a quantitative and qualitative risk assessment, and is supplemented by a Monte Carlo simulation, which enables a better understanding of possible repercussions of critical risks. The developed methodology encompasses all available test bed data and thus contributes to the development of a generic evaluation methodology for similar projects.

The, on the provided data based, result of the risk assessment for the assessed use case clearly lines out that the regarded storage of renewable energy as hydrogen admixture to Underground Gas Storage reservoirs will not exceed regulatory limits and thus will not display any significant risks or increased risks for man or environment.

Life-Cycle Assessment

The ecological assessment of selected Power-to-Gas applications, which were identified in WP 10, was conducted based on the standards of ISO 14040:2006f „Environmental Management – Life-Cycle Assessment“. Therefore the LCA was implemented in assistance of specific LCA software for two economic feasible scenarios, and its results were included in the Risk Assessment. The Impact Assessment to identify potential environmental impacts includes nine categories (a.o. climate change, ozone depletion, human toxicity, etc.) whereby sensitivity analyses for relevant parameters allow comparisons between fossil and renewable energy sources. The Impact Assessment showed clearly that the energy sources are relevant for the environmental impacts of PtG applications. With the fields of application the electrolysis unit was identified as the most relevant energy consumer, and its specific efficiency as the critical parameter. To sum up, no significant potential environmental impacts could be identified for the analysed applications. For a clear statement regarding the benefits and the environmental improvement potential of PtG for subsurface storage of renewables, further analyses including longer time frames and large scale applications are needed.

Economic and legal analyses

Economic and legal analyses deals with different fields of application and possible uses of the storage technology were analysed in the context of the whole power-to-gas system. Compared with relevant benchmarks of individual fields of application in the energy system, especially the production of a renewable product (green hydrogen or methane) and the provision of negative control energy are interesting from an economic point of view. Other individual fields of

application, when considered individually, are associated with high production costs and therefore are far away from competitiveness. On basis of the performed analyses an intelligent combination of individual fields of application in terms of an intelligent business model is recommended. The economic effects of the different fields of application have in common, that they lead to an increase in the gross domestic product in Austria.

Further the feed-in potential of hydrogen into the Austrian natural gas grid was determined. Latter is influenced by different factors such as prevailing standards and guidelines, H₂ compatibility of the components, gas grid structure and natural gas flow.

In addition to the technological and economic aspects, also the social acceptance of power-to-gas in public is an important factor. In order to achieve a positive impact on social acceptance for hydrogen applications, the respective target groups must be identified and the relevant influencing factors addressed.

The legal analysis in the project Underground Sun Storage mainly focusses on the possibility of (intermediate) storage of hydrogen and synthetic natural gas in the natural gas network. In the process, a classification of the power-to-gas plant into the electricity- and gas-market model is carried out. Then, questions concerning authorization regarding erection and operation, as well as general requirements concerning rules of professional conduct and plant permits are dealt with. Furthermore, it was important to describe the costs arising from the purchase of electricity and, if necessary, the natural gas and the (re-)feeding in of the power-to-gas products. Even if the GWG 2011 applies exclusively to natural and biogenic gases, it can be argued that it is compulsory to include grid-compatible natural gas-hydrogen mixtures as well as synthetic natural gas within the scope of the GWG 2011. The Natural Gas Directive 2009 supports this assumption.

Additionally, the analysis of the legal situation deals with aspects regarding possible reconversion in an external power plant as well as the participation of a power-to-gas installation in the balancing energy market, contributing to the (negative) secondary control. A further legal question is the underground storage of the power-to-gas products in accordance with the MinroG. In this context, the pure as well as the synthetic natural gas are subject to the term “hydrocarbons”, pure hydrogen on the other hand is classified as “material”. Finally, the topic of whether the power-to-gas system may be accessed in the event of a crisis accordance with the EnLG 2012 is touched on.

Based on the legal and economic analyses in the Underground Sun Storage project it can be stated, that the technology Power-to-Gas has to be further developed on a technological and regulatory point of view and as well as from the perspective of intelligent business models in order to make economically and systemically positive contributions.

Outlook

To answer the question whether hydrogen-storage in a real subsurface sandstone reservoir is possible the Underground Sun Storage project was initiated as the first project to address these questions with an interdisciplinary approach and a real world field test.

For the examined geochemical, geophysical and material science test no negative influence on the overall storage integrity, when blending 10% of hydrogen to the natural gas could be

found. It was found that during the first hydrogen exposure chemical and physical effects are happening in the reservoir. Especially the hydrogen solubility in reservoir water and the follow up reactions should be part of further investigations. Additionally it was found that there is the potential of using a subsurface reservoir as a bioreactor for methane generation. This happens because of microbes in the subsurface which can convert hydrogen and carbon dioxide to methane.

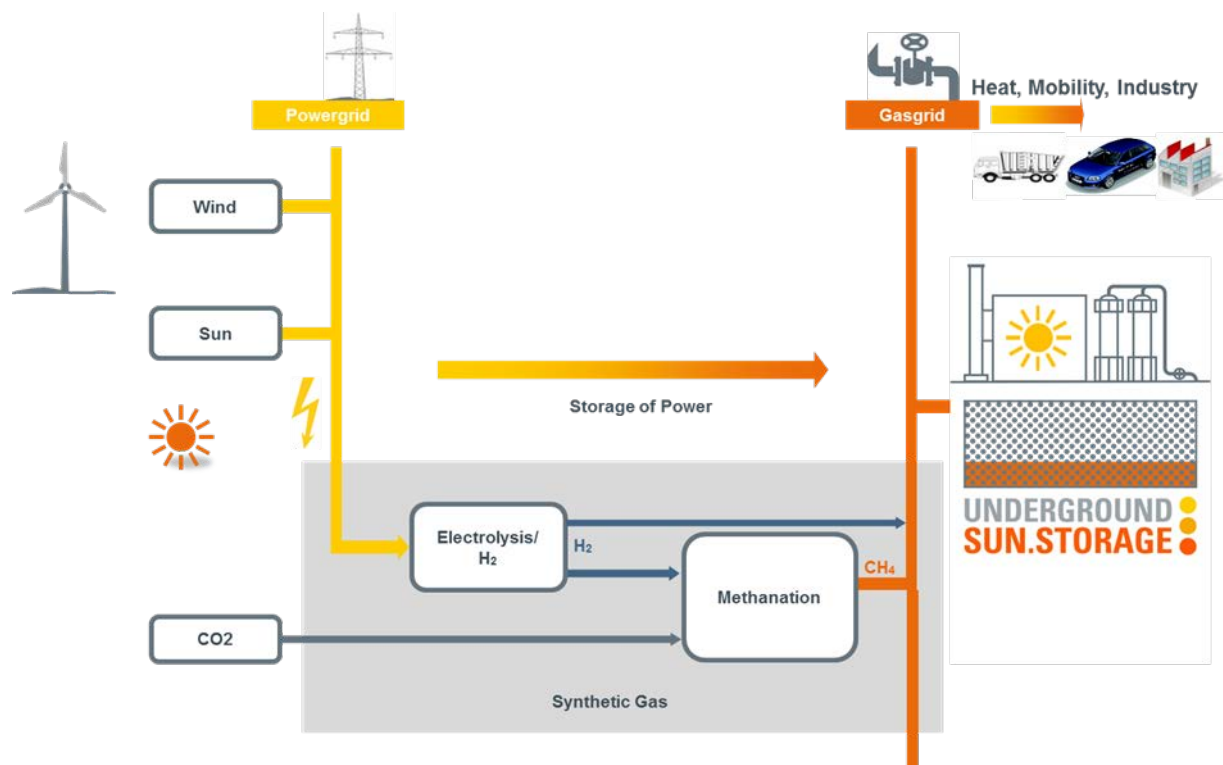
Due to the knowledge gained by different experimental approaches and an interdisciplinary working group, it is now possible to transfer this knowledge to other subsurface storages. Certain parameters which have to be looked at have been defined during the project.

There are also still open questions concerning operational issues when upgrading this to a commercial facility. This also concerns using different gas blends which would mean different caloric values instead of a homogenous gas quality.

During four years of research, the storage integrity could be sufficiently proven, and the storage facility was successfully planed and operated. Therefore, it was possible to add an essential scientific insight into the capability of a subsurface gas storage in a renewable energy system. The before mentioned conversion of hydrogen and carbon dioxide to methane will now be even further developed into a follow up project called „Underground Sun Conversion“. Apart from the option of seasonal storage of renewable energy, it should then also be possible to generate renewable methane in the same bio facility. Which makes this even more interesting is the fact that the vast European gas infrastructure could be set to a further sustainable use. Furthermore, a self-sustaining carbon cycle could be installed. For further information, please refer to: www.underground-sun-conversion.at

3 Introduction

In order to achieve the global climate targets, but also the national climate targets, there is no way around the expansion of energy generation from renewable sources. Energy generation from solar and wind power is volatile and does not meet the demand. In addition to short-term storages, which are already used today for day/night balancing and to guarantee grid stability, large-volume storage facilities are also required as electricity generation from renewable energy sources expands. These storage facilities must be able to provide a seasonal balance between fluctuations in energy supply and demand, as well as the usual security of supply. The only possibility to realize these storages according to today's criteria are chemical storages. For this purpose, the "Power to Gas" technology has been developed and propagated in recent years. Electricity is converted into gas, which is a chemical energy carrier.

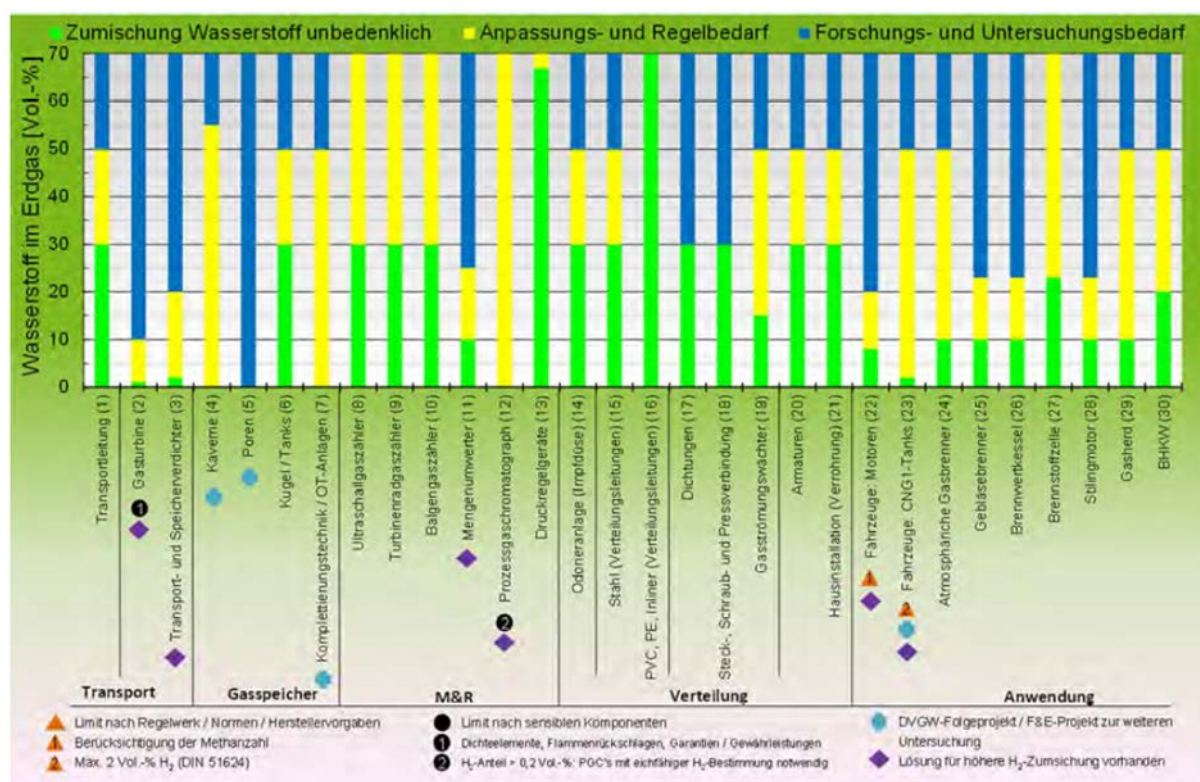


Source: RAG; modified after STERNER

Figure 1: System Image of energy storage via power to gas

Electrolyzers are used in which electricity from renewable energy sources is used to split water into its components hydrogen and oxygen. Hydrogen is thus the first and obvious chemical storable energy carrier for renewable electricity. In order to avoid further process steps, it has been examined for several years whether and to what extent hydrogen can be added to natural gas in the existing infrastructure. To name just a few the NaturalHy project, the DVGW studies "Development of modular concepts for the production, storage and feeding of hydrogen and methane into the natural gas grid" (G1-07-10), "Hydrogen tolerance of the natural gas infrastructure including all associated facilities" (G1-02-12) and the GERG project "Admissible Hydrogen Concentrations in Natural Gas Systems" can be mentioned here..

The result of all these studies is that hydrogen can be added in most of the parts of the natural gas infrastructure and that customers and end users can also deal with hydrogen admixture as long as it stays in the single digit region. However there are still some minor details which need further clarification. Figure 2 provides a good graphical overview on the efforts already taken.



Source: DVGW

Figure 2: Overview matrix H2 tolerance of selected elements in the natural gas network

From the figure above, however, it can also be seen that the underground porous storage facilities in particular are still largely unexplored with regard to hydrogen compatibility.

On the initiative of the WEG and some natural gas storage operators, the DGMK commissioned literature studies on the hydrogen compatibility of natural gas storage facilities. The results are available in the DGMK research reports 752 "Einfluss von Wasserstoff auf Untertagegasspeicher" and 756 "Einfluss von Biogas und Wasserstoff auf die Mikrobiologie in Untertagegasspeichern". In these papers, all conceivable influences and processes that can be caused by hydrogen were presented and described.

At the same time, RAG developed the Underground Sun Storage research project and, together with its partners the University of Leoben, the University of Natural Resources and Applied Life Sciences - Department IFA Tulln, Energieinstitut at the JKU Linz, Verbund AG, Axiom- Angewandte Prozesstechnik GesmbH, applied for national research funding in Austria. The Austrian Climate and Energy Fund has supported this project as a lead project within the framework of the energy research program. In the course of the project, cooperation agreements were concluded with international companies such as Nafta, Hychico and DVGW.

The Underground Sun Storage project was launched in mid-2013 and completed in mid-2017. The aim of the project was to investigate large-volume and seasonal storage possibilities for renewable energy in former natural gas reservoirs in the form of hydrogen admixtures. This is also expressed by the long title of the project "Chemical Storage of renewable Energy in porous subsurface Reservoirs with exemplary Testbed". The storage of renewable energy is one of the main topics of the Austrian Climate and Energy Fund.

The project was divided into two phases. Phase I comprised basic investigations with the aim of clarifying the feasibility of a field test. In particular, it had to be proven that the integrity of a storage facility is not impaired by hydrogen admixtures of 10 percent. Within the scope of targeted laboratory tests and simulations, the influence of hydrogen on the specific situation of the RAG natural gas storage facilities was tested.

Phase II included the planning, approval, construction and operation of a field test facility at a small isolated natural gas reservoir in the Vöcklabruck/Austrian area. The work was carried out on the basis of the geological situation in the foothills of the Alps (Molassezone) and took into account the technical conditions in commercial underground gas storage facilities (UGS) of RAG Austria AG (RAG). It was important to gain practical and interdisciplinary knowledge on the subject of hydrogen in porous reservoirs for the first time and to support it with a field test.

A total of 10 work packages were defined. For better readability, however, a thematic structure is given here. In particular, the topics geochemistry, geophysics, microbiology and materials science were addressed. During the execution of the field test itself, it was necessary to anchor it in the existing legal framework and to solve the reservoir and process engineering problems. The aim was to monitor and balance an approximately 10 percent hydrogen admixture over a full storage cycle.

The research was accompanied by a risk assessment, a life cycle assessment and an examination of economic and legal framework conditions.

Within a timeframe of four years, the integrity could be sufficiently confirmed and the field test with the associated plants, was planned, built and operated. This has made it possible not only to achieve valuable scientific results, but also to demonstrate the performance of gas storage facilities in a renewable energy scenario.

The project was initiated by RAG and implemented together with the partners Montanuniversität Leoben, Universität für Bodenkultur - Department IFA Tulln, Axiom Angewandte Prozesstechnik GmbH, Energieinstitut an der JKU Linz und Verbund AG and with support from the Austrian Climate and Energy Fund.

4 Geological, geochemical and geophysical processes in hydrogen bearing porous gas reservoirs

4.1 Introduction

RAG Austria AG has been working since the 1950s in the Molasse basin of Upper Austria and Salzburg, the area between the foothills of the Alps in the south and the Bohemian Massif in the north, in the exploration of hydrocarbons (crude oil, natural gas) and has also been active as a natural gas storage operator since 1980. All of RAG's underground natural gas storage facilities are located in formerly producing natural gas reservoirs. Crude oil and natural gas are produced here from porous sandstone deposits, with oil mainly occurring in the stratigraphy of the Eocene and Cenoman periods and natural gas reservoirs occurring in the lower Miocene strata (Burdigal, Haller series).

In the porous gas reservoirs of the molasse zone, the trap structures are covered with a thick gas-tight clay layer. The sandstone formations themselves are now sufficiently well-known thanks to a large number of rock cores and can be well described petrographically. The sandstones of the Haller and Puchkirchner series, which are located in the molasse basin, contain a large part of RAG's gas deposits and thus also all of RAG's gas storage facilities.

Depending on the depth, the temperatures vary between 30°C and 80°C with a low salinity of 14-18,000 ppm and a pH value between 6 and 8. Values from the Haller series (shallower and thus cooler and less saline) were used for the laboratory tests, as it was already clear that the test field would be in this region. The admixture of hydrogen in this system represents a change that has both physical and chemical relevance. On the one hand, it was proven that the clays responsible for the tightness of the reservoir are also impermeable to hydrogen. On the other hand, it was tested in flow experiments whether there are possible chemical changes in the minerals in the reservoir and in the overlying cap rock.

The diffusivity of hydrogen in the gas present in the reservoir is particularly interesting for depleted natural gas reservoirs. The literature assumes only a small mixing of the cushion gas (gas present in the reservoir) with the working gas containing hydrogen (gas volume effectively available for storage) [1] [2].

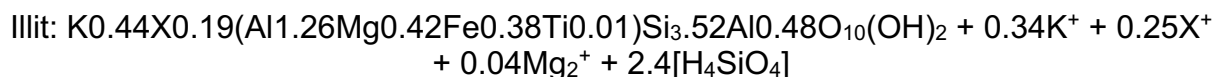
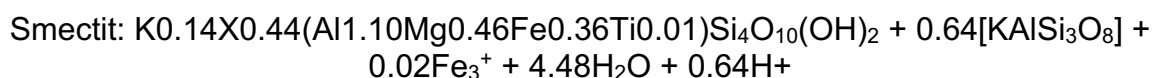
Nevertheless, this process is not yet fully understood and requires closer examination. Conversely, the same applies to the separation of hydrogen from the stored gas. If gas mixtures with a certain hydrogen content are stored, one would expect the gas mixture to remain largely stable. If, however, a gravimetric segregation of the gases takes place in the reservoir, higher hydrogen concentrations could occur at the top of the reservoir, which would then no longer comply with the specification and integrity considerations. In particular, the higher partial pressure of the hydrogen that would then be present could subsequently lead to stronger reactions with the reservoir rock. The integrity of the materials used would also have to be reassessed. Furthermore, it is possible that the different viscosities of hydrogen and natural gas could cause a mobility-dependent segregation [3]. This could then also lead to the problems already mentioned.

In order to answer these complex questions, laboratory tests and geochemical simulation were used to create a knowledge base on which the field test could be based.

4.2 Integrity of the Cap Rock

4.2.1 Task Definition

There are several scientific papers on the clays of the molasse zone, the work of Gier being one of the most comprehensive [4]. Here the pelitic sediments (clay fraction) of the cap rock above the gas deposits are discussed. The mineralogy of the younger sediments (Miocene to Middle Oligocene) is very monotonous: they consist of quartz, plagioclase, alkali feldspar, calcite, dolomite, gypsum, pyrite and the clay minerals smectite, kaolinite, mica and chlorite, whereby the clay minerals with 70-85 weight percent of the examined samples occupy the main component of the total rock. For the Haller series, one of the formations in which natural gas reservoirs are typically found, the cap rock consists mainly of mixed layer sediments (Illite/Smectite) and Illite in pure form. Chlorite is also found in a subordinate form. The gas permeability of the overlapping clays was determined on a fresh core and amounts to $0.2\text{--}1.64 \cdot 10^{-(20)} \text{ m}^2$. As can be seen from the subsequent investigations carried out by DBI Gas-Umwelttechnik GmbH Leipzig (DBI Leipzig), this permeability is also valid for hydrogen. Clay minerals are a mixture of many different elements, some of which can also react with hydrogen as electron acceptors. Here Gier developed a general structural formula which describes the statistical composition of the clays of the molasse zone.



It can be seen that the iron which can possibly react with hydrogen is only a small part of the clay fraction, so that it can be assumed that the clays of the molasse zone are resistant to a reaction with hydrogen.

Finally, at the University of Leoben, the movement of the hydrogen in the reservoir was also shown using a geologically dynamic transport model. The transport model focused on hydrogen migration in the reservoir and through the surrounding clay layers. Based on the resulting spatial distribution, it estimates the kinetic equilibrium of hydrogen at the boundaries of the reservoir. Due to the lack of data and uncertainties of different nature, scenarios and sensitivities were investigated that resulted in a risk assessment rather than in absolute numbers. However, it must be noted that transport processes can lead to potential losses due to gas diffusion into the surrounding layers. Even at low penetration depths, losses could be in the range of a few percent. However, it can be assumed that diffusion losses are only significant in the first storage cycles.

4.2.2 Content Presentation

The gas permeability of the overburden was determined at 40°C with methane and hydrogen as measuring gas. It was carried out on representative clay cores from the molasse zone. The permeability is determined according to the following equation:

$$k = \frac{\eta \cdot l \cdot Q}{A \cdot \Delta p \cdot (1 + \Delta p / 2)} \quad \text{Gl. (1)}$$

k	- Permeability Coefficient	[m ²]
Q	- Flow Rates	[m ³ /s]
A	- Cross-sectional area of the core	[m ²]
Δp	- Pressure Difference	[Pa]
l	- core length	[m]
η	- dynamic viscosity of the sample gas ¹	[Pa s]

The measurements were carried out under specified inlet pressure (0.5-0.6 bar) up to the constancy of the measured flow rate. The temperature- and pressure-dependent viscosity required for the permeability calculation was taken from the data provided by the National Institute of Standards and Technology (NIST).

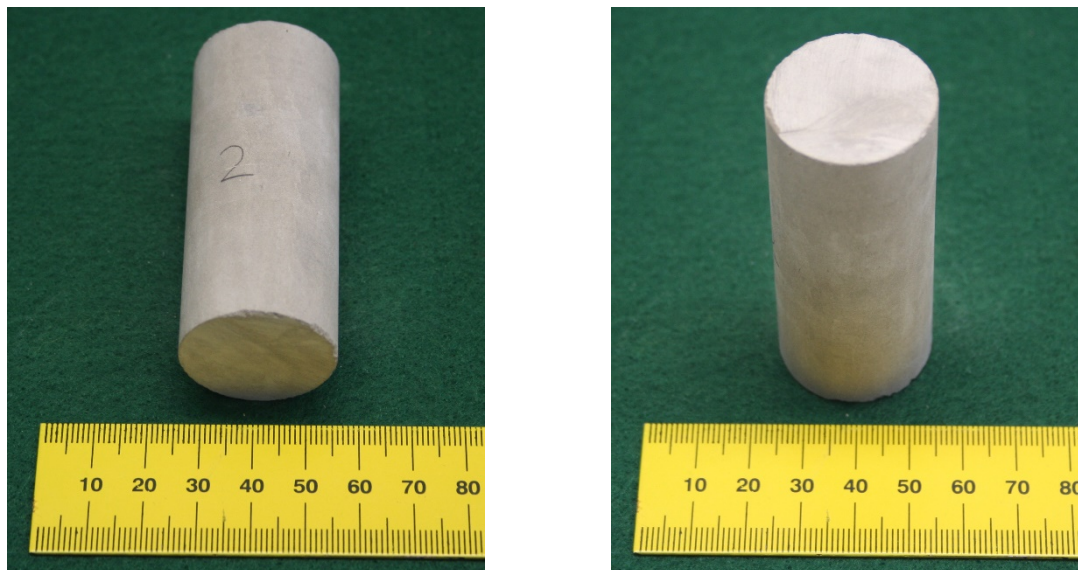


Figure 3: Core of the cap rock from the well NU C2

Since the rock samples are not "fresh" material, they were stored in the desiccator in a saturated steam atmosphere for preparation in order to achieve remoistening and thus a re-swell of the clays. However, it cannot be assumed that this remoistening is sufficient to restore the clay to its original state. Figure 3 shows an example of two of the dry cores used.

¹ Viscosity at measurement conditions (Pressure, Temperature)

4.2.3 Results and Conclusions

The influence of water saturation was demonstrated by again storing the cores in the desiccator for two weeks. Afterwards, a further reduction in permeability was observed. Table 1 summarizes the results of the two measurements.

Table 1: Measurement of Core 2 NU C2

	Permeability [m ²]	
	Methane	Hydrogen
1. Measurement	7,2 10 ⁻¹⁸	8,3 10 ⁻¹⁸
2. Measurement	2,5 10 ⁻¹⁸	2,7 10 ⁻¹⁸

The comparison of hydrogen and methane permeability does not show a clear trend and is approximately the same taking the measurement tolerance into account (Table 2). However, it can be seen that the hydrogen permeability is even lower than that of methane if the clay content of the sample is increased. It can therefore be assumed that the resistance of the cap rock to gas migration is not affected by hydrogen.

Table 2: Permeability of methane and hydrogen for the investigated cores

		Permeability [m ²]	
Formation	Core-Nr.	Methane	Hydrogen
NU C2	2	2,1 10 ⁻¹⁸	2,3 10 ⁻¹⁸
	3	2,5 10 ⁻¹⁸	2,7 10 ⁻¹⁸
WEG	1	8,5 10 ⁻¹⁹	8,2 10 ⁻¹⁹
	3	3,2 10 ⁻¹⁸	1,9 10 ⁻¹⁸

4.3 Changes in the behavior of the storage gas due to hydrogen admixture

4.3.1 Introduction

The flow of several components in a porous system is generally considered to be very complex. If a new component, in this case hydrogen, is introduced into such a system, additional influences have to be considered. Accordingly, several experiments were carried out at DBI Gas-Umwelttechnik GmbH Leipzig to determine the flow behavior of hydrogen in the reservoir. One could expect hydrogen to flow faster than natural gas due to its lower density and smaller molecule size. This effect is known from aquifer reservoirs and is described as "viscous finger ring" [5]. The less dense fluid penetrates the denser fluid on paths of high permeability and forms the so-called fingers. These can then only be partially or not at all produced back, since they either dissolve in the denser fluid or are enclosed by it [6]. In the case of the reservoir investigated in this project, both the possibility of mixing with the cushion gas and migration of the hydrogen into the aquifer were considered.

Another influencing factor is permeability. If several fluids move through one and the same pore space, then each fluid has a certain effective permeability depending on its saturation which assigns it a part of the total permeability. However, this seems to be more interesting for two phase systems (water/gas). Nevertheless, this aspect was also considered.

Since a new component is introduced into the storage system with hydrogen, the effects of solubility and adsorption must also be considered. Especially in the case of solubility, there are no robust models for saline fluids in the literature so far. A model developed by DeLucia in the course of the H2Store project [7] was used for forecasts.

For adsorption, methods are known from the literature in which the wettability of a rock is changed by means of small molecule CFCs [24]. A similar effect could be expected with H₂, whereby the adsorption forces of course also depend on the molecule size. Accordingly, the adsorption effect is considered negligible. Last but not least a gravimetric segregation and diffusion in porous media was considered.

4.3.2 Task description DBI

In order to evaluate the mobility of the gases, breakthrough experiments were carried out at the University of Leoben and at DBI Leipzig. The DBI Leipzig tests were carried out on actual reservoir rocks and aimed to demonstrate the breakthrough of hydrogen through a core saturated with methane in both a dry and moist state. The aim was to demonstrate whether flow velocity, water saturation and heterogeneity have an influence on the flow behavior of hydrogen in porous media. This was important to draw conclusions about viscous fingering as well as the dissolution behavior of hydrogen.

4.3.3 DBI content presentation

To determine the gas permeability, the applied pressure of the sample gas and the permeated gas volume were recorded. The volume flow was determined from the increase in permeated volume over time. Figure 4 shows the measuring station.

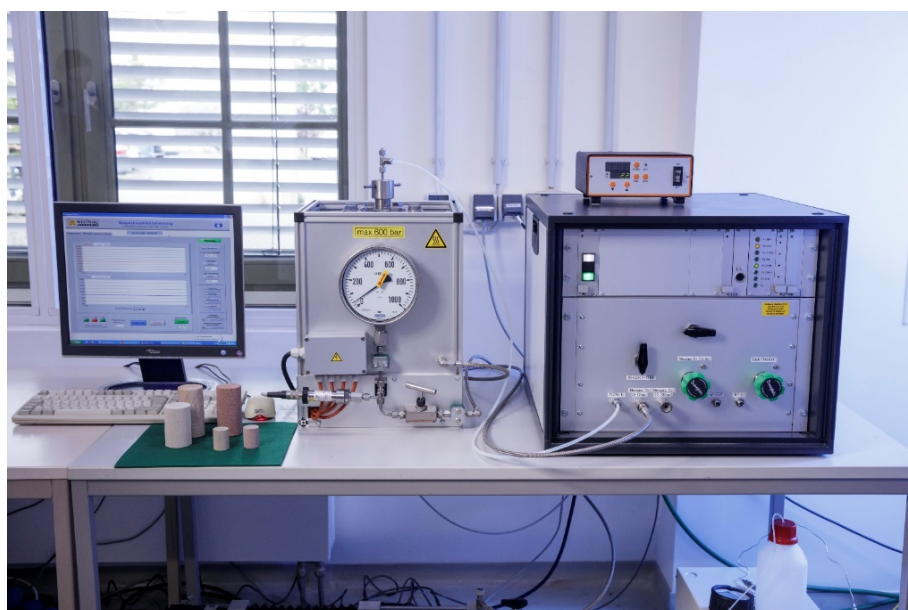


Figure 4: Measuring site for determining gas permeability

In order to assess the influence of gas permeability on the displacement functions, the gas permeability of the cores from the two different wellbores was determined before the displacement tests were carried out. Table 3 summarizes the determined gas permeability's.

Table 3: Gas permeability of the investigated rock cores

Formation	Core-Nr.	Permeability [m ²]
Haller Series	BA C1	3.6 E-13
Obere Puchkirchen Series	NU W8	2.3 E-14

To measure the displacement curves, methane flowed through the cores up to a constant flow velocity (Δp of ~ 0.5 bar) before the start of the test. The saturation was checked by gas chromatography using repeat measurements. Hydrogen was then injected into the core at a constant flow velocity.

4.3.4 Results and Conclusions DBI

In the cores tested at DBI Gas- und Umwelttechnik, there is no difference in the curve shape caused by the flow velocity. However, the breakthrough curve measured on the NU W8 core shows a more uniform increase or asymptotic curve of the H₂ content than in the BA C1 core. The breakthrough curve in the BA C1 core shows a renewed increase of the H₂ concentration in the later course of time. Figure 5 shows the measured breakthrough curves at the two core samples at constant flow velocity.

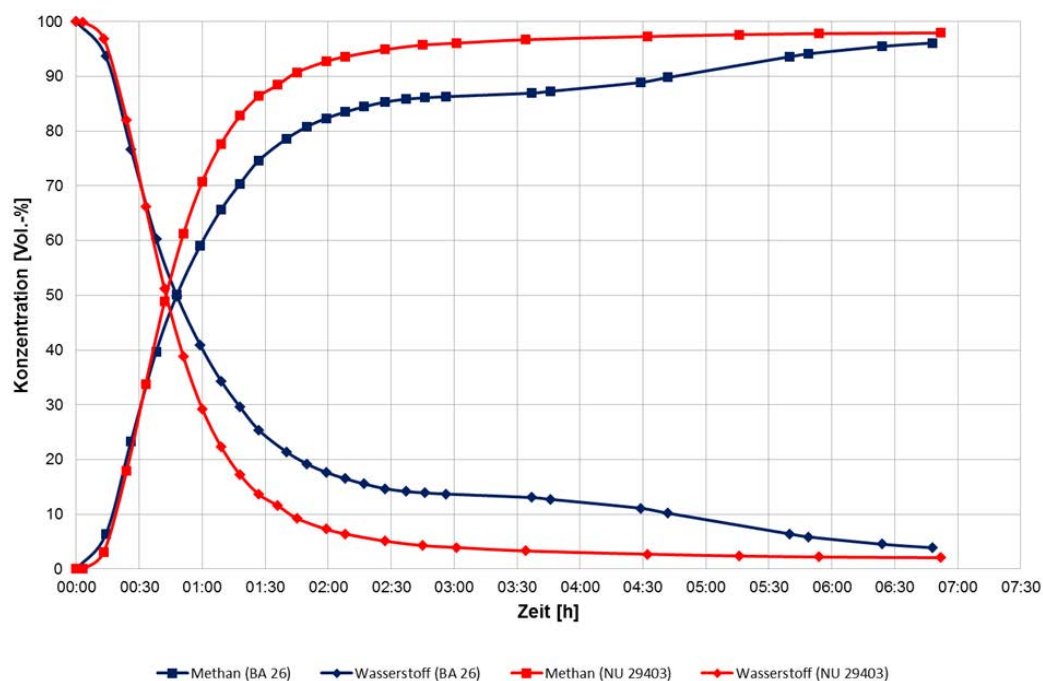


Figure 5: Determined breakthrough curves at dry cores BA C1 and NU W8 at flow velocities of 3.5 cm/min

One possible reason for the different curve shapes is the pore structure in the two cores. The NU W8 cores are significantly more heterogeneous than the BA C1 cores, which leads to a change in flow behavior.

The curve shape for flow-through tests in moist cores must be considered in a differentiated way. Thus, in both the NU W8 and the BA C1 core samples, the hydrogen first decreases again before it finally flows out into a plateau. In both cases the curve shape is similar but with NU W8 the hydrogen is slower at the breakthrough. Figure 6 shows the comparison of the displacement curves at the wet cores.

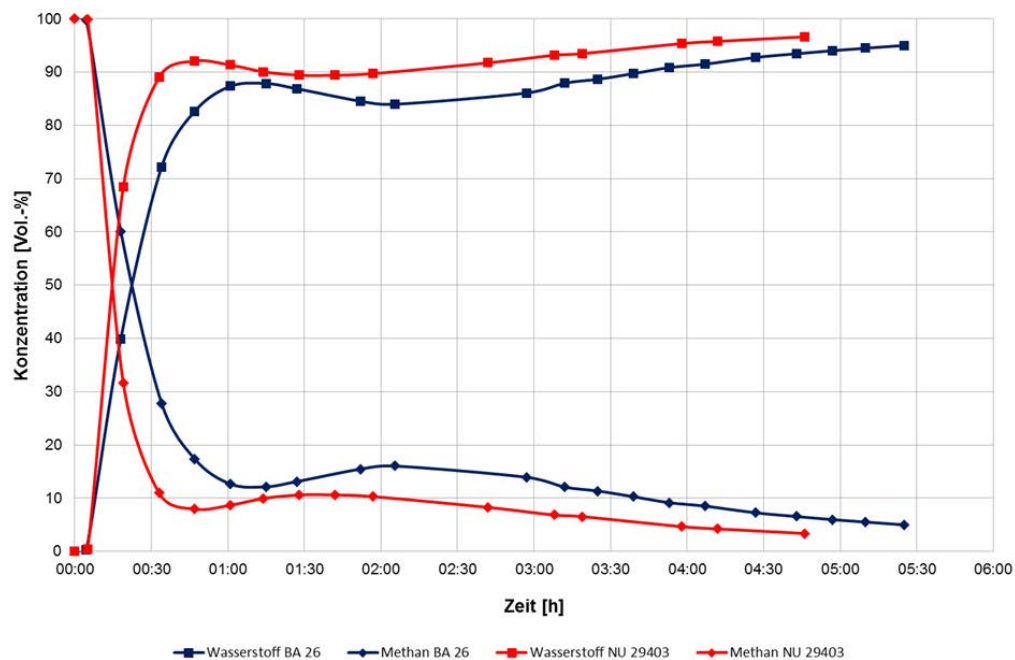


Figure 6: Comparison of the displacement function at the wet cores NU W8 (8.9 cm/min) and BA C1 (4.3 cm/min)

One possible explanation is the solubility of hydrogen and CH_4 in water. The solubility of hydrogen in salt water is different than in fresh water. Since this solubility also depends on the saturation of a substance in the gas phase, it can be assumed that an equilibrium occurs at a certain point at which a similar proportion of CH_4 is released from the water as H_2 is dissolved in the water. If more CH_4 is suddenly released than hydrogen is added due to the saturation of hydrogen in water, then an apparent decrease of hydrogen in the gas can occur for a short time.

Another possible explanation would be a reaction of the hydrogen in the aqueous phase with other components dissolved in the water. However, no evidence could be found for such a change. Figure 7 shows the displacement curves measured on the water-wetted core BA C1 at two different flow velocities of 4.3 and 6.5 cm/min.

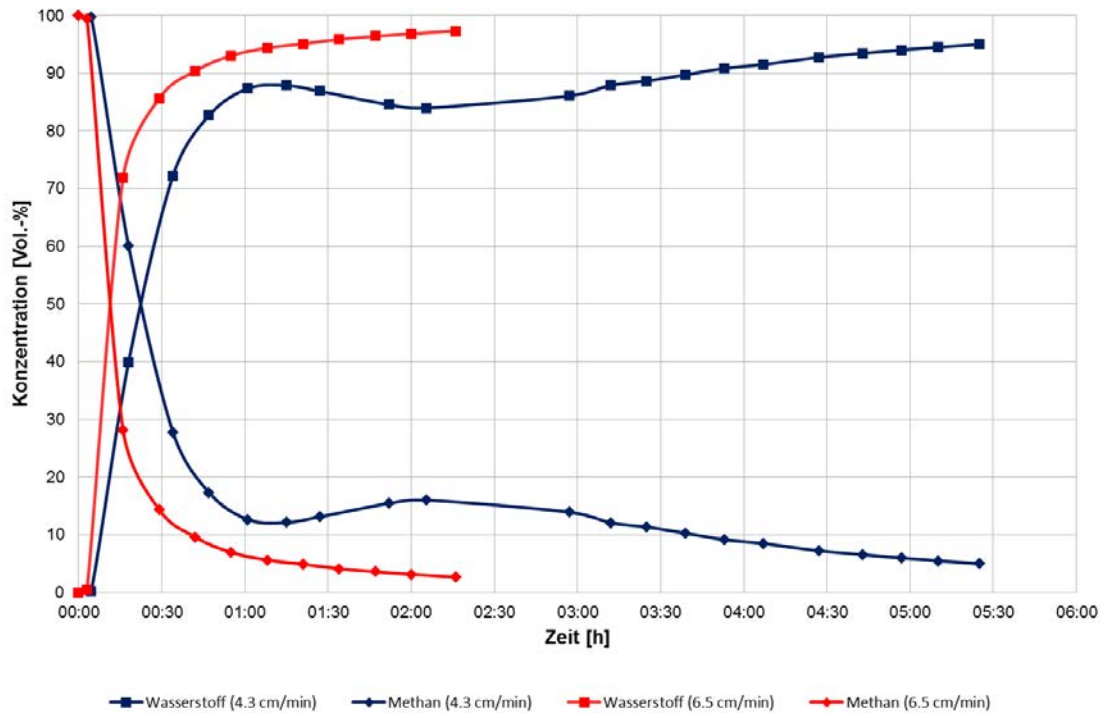


Figure 7: Comparison of the displacement curves measured on the water-saturated core BA C1 26 at flow velocities of 4.3 and 6.5 cm/min.

The comparison of the curves shows that at high flow velocities the course of the curve is aligned with the temporal course of the displacement function on the dry core. There is no maximum of the hydrogen concentration. This shows a clear influence of the flow velocity on the curve. At higher flow velocities, the mass transfer by adsorption, desorption and solution probably have a lesser impact.

4.3.5 Task definition MUL

The experiments of the Montanuniversität Leoben (MUL) were to investigate the theory of the gravimetric segregation on the one hand and on the other hand the flow experiments of the DBI Leipzig on a larger scale. Since the flow distance of the reactors at MUL was 7m, natural sand had to be used, as deposit cores of this length are rare and very difficult to extract. The comparison of the tests of the DBI Leipzig and the MUL, however, shows quite similar results, so that the chosen access is considered reasonable.

Finally, the laboratory experiments were also accompanied by a simulation model to transfer the findings to the size of the reservoir and to make a statement about the movement of the hydrogen in the subsurface.

Furthermore, the characterization of the behavior of mixtures of natural gas and hydrogen under static conditions was investigated by means of a test facility. This work was summarized in a separate work package under the title "De-Mixing of Natural Gas and Hydrogen".

In the static tests, a possible segregation of hydrogen and methane in closed reactors filled with sand was investigated in long-term tests at three different pressures. The dynamic tests

were intended to show insights into the segregation of both gases when flowing through a porous bed (porous rock).

4.3.6 Content presentation MUL

The pilot plant consists of three reactors. The pressure pipes are designed for pressures of 10 bar, 25 bar and 40 bar. The inner diameter is 150 mm and the length of each reactor is 7 m. This results in an internal volume of 123.7 liters per reactor (Figure 8).

The reactors were pressure tested and approved by TÜV.

The reactors are equipped with pressure sensors, temperature sensors, heating sleeves, a data acquisition system and connections for gas analysis.

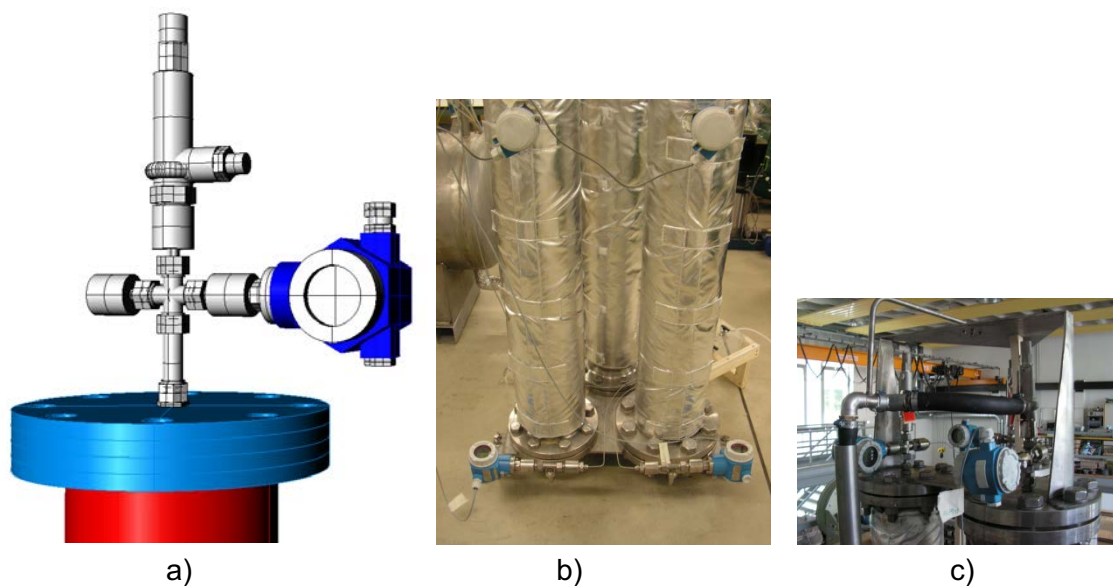


Figure 8: Pressure transmitter: a) Mounting position with safety valve; b) Lower reactor section; c) Upper reactor section

The reactors were heated to 40°C and the temperature was kept constant over the entire duration of the test. Heating was provided by heating sleeves.

The pressure and temperature values were recorded hourly over the entire duration of the test. The data acquisition system Field Point from National Instruments with the visualization software Lookout is used for data acquisition (Figure 9). The temperature control and data acquisition modules were installed in a control cabinet with power supply.

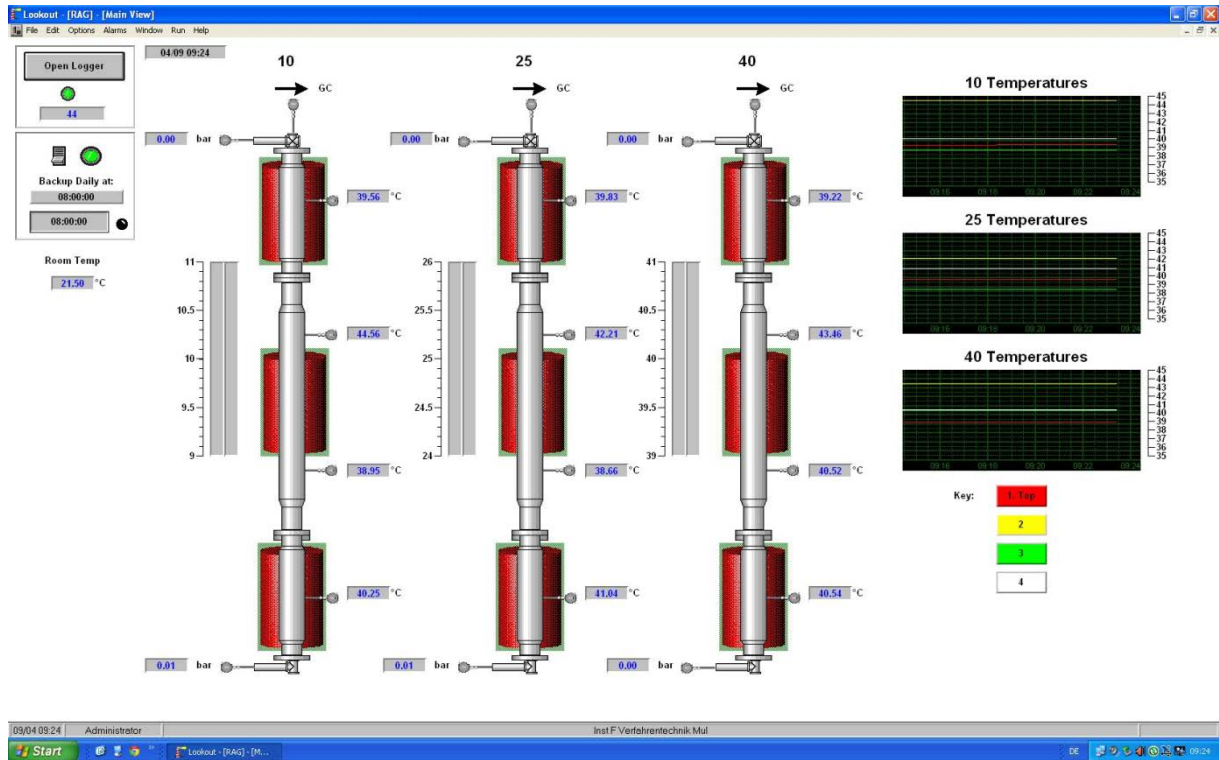


Figure 9: Data Acquisition Visualization

For the gas analysis a process gas chromatograph from ABB model PGC 1000 was used. The PGC was connected to the head and bottom of the reactors by capillary tubes (inner diameter 1 mm) for gas extraction (Figure 10).



Figure 10: Process - Gas - Chromatograph with display of capillary tubes

Test description: static tests

To reproduce the porous rock in the reservoir, the reactors were filled with sand (Figure 11). The sand was dried in a rotary kiln at over 100°C and filled into the reactors. Assuming a cubically dense ball packing (gap volume of 26%), the free gas volume in the reactors is 32 liters per reactor. For sand with the particle size distribution available, the gap volume of the

cubically densest spherical packing lies between the total porosity stated in the literature and the effective porosity. Thus, the gas volumes for the pressure reactors are given in Table 4.

Table 4: Gas volumes of the reactors as a function of the pressure stage

Reactor pressure [bar]	Gas volume [standard liter]
40	1286,5
25	801,1
10	321,3

Following installation, instrumentation, filling with sand and flushing with nitrogen, the reactors were pressurized with gas. The filling gas used was a test gas class 1 with 8% hydrogen and the remainder methane with a 12-month stability guarantee from Linde. For reactor 1 a pressure of 10 bar, for reactor 2 a pressure of 25 bar and for reactor 3 a pressure of 40 bar was set.

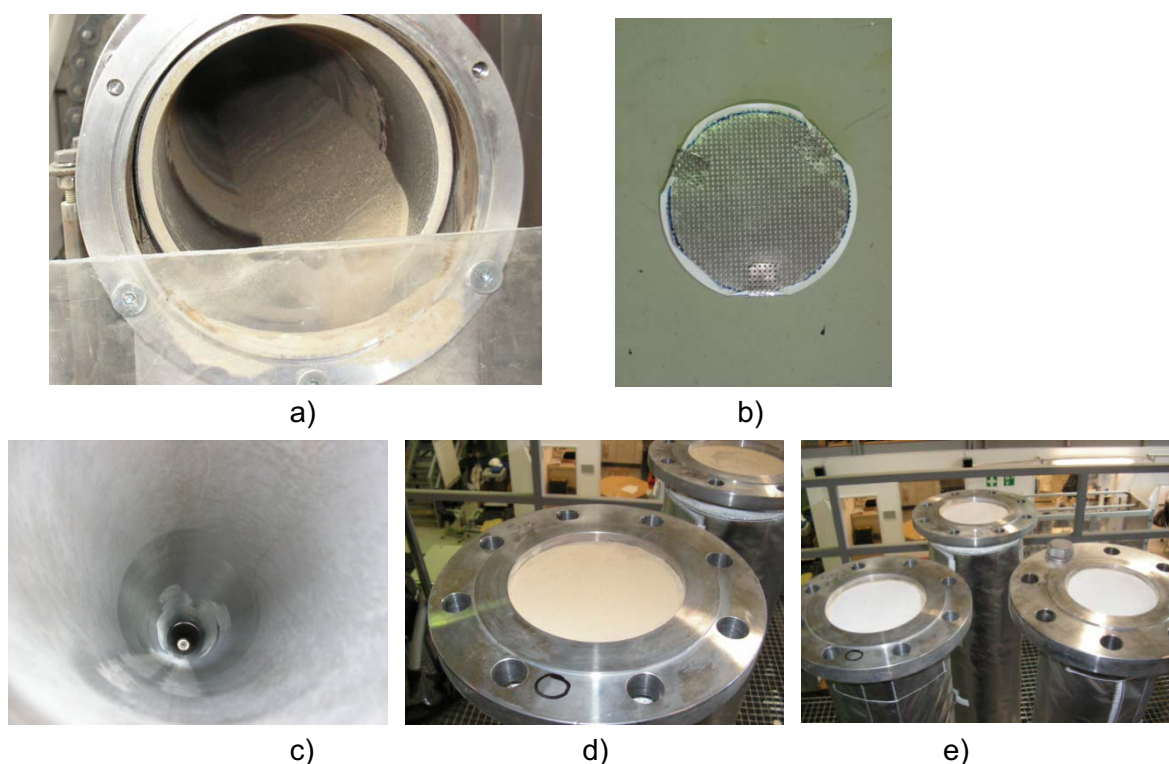


Figure 11: Drying of the sand in the rotating tube (a), perforated plate with filter paper (b), reactor empty (c), reactor filled (d-e)

Test description: dynamic tests

The dynamic tests were carried out dry and wet. During the wet tests, 5 liters of water were added to the lower part of the reactor. This corresponds to about 15 % of the free ideal gap volume. The dry tests were carried out with different gas concentrations, different pressures, different flow rates and different background gases.

In the dynamic tests, the reactor was first flushed with nitrogen and then a certain test pressure was set with nitrogen. Subsequently, the reactor was flushed with the test gas at test pressure.

4.3.7 Results and conclusions MUL

4.3.7.1 Results of the static tests

The test period of the reactor with 10 bar pressure was one year from 30.04.2014 to 27.04.2015. The course of the pressure and the temperature over the test period are exemplarily shown in Figure 12 and Figure 13. The pressure and temperature of the reactors with 25 and 40 bar respectively were also recorded and showed the same behavior.

The pressures P Top and P Bottom decrease over the test period due to sampling gas for analysis and smaller leakages. The variations in pressure are due to the influence of ambient temperature. Figure 14 shows examples of pressure and ambient temperature for the 10 bar reactor. This clearly shows the correlation between pressure and temperature.

The temperature sensors T1 and T4 are mounted in the middle of the upper and lower pipes, which are surrounded by heating sleeves. These sensors show very little variation. The temperature sensors T2 and T3 are mounted at the edge of the middle heating sleeve and show a dependence on the ambient temperature despite insulation of the adjacent pipe sections.

The average temperatures over the test period in the reactors are shown in Table 5. They correspond to the assumed reservoir conditions.

Table 5: Average temperatures of the reactors

	Average temperatures [°C]		
	Reactor 10 bar	Reactor 25 bar	Reactor 40 bar
T1	40.197	39.928	39.708
T2	40.093	40.923	41.734
T3	39.426	37.021	39.532
T4	40.28	40.283	40.406
Average value T1-T4	40.249	39.539	40.347

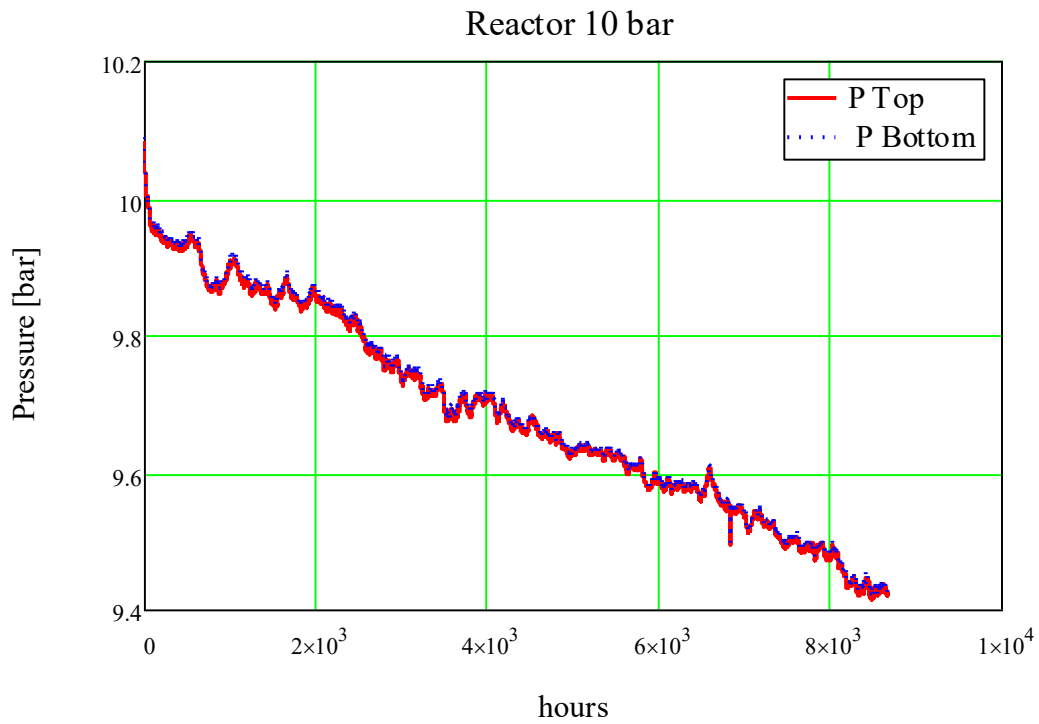


Figure 12: Pressure curve of reactor with 10 bar over the test period

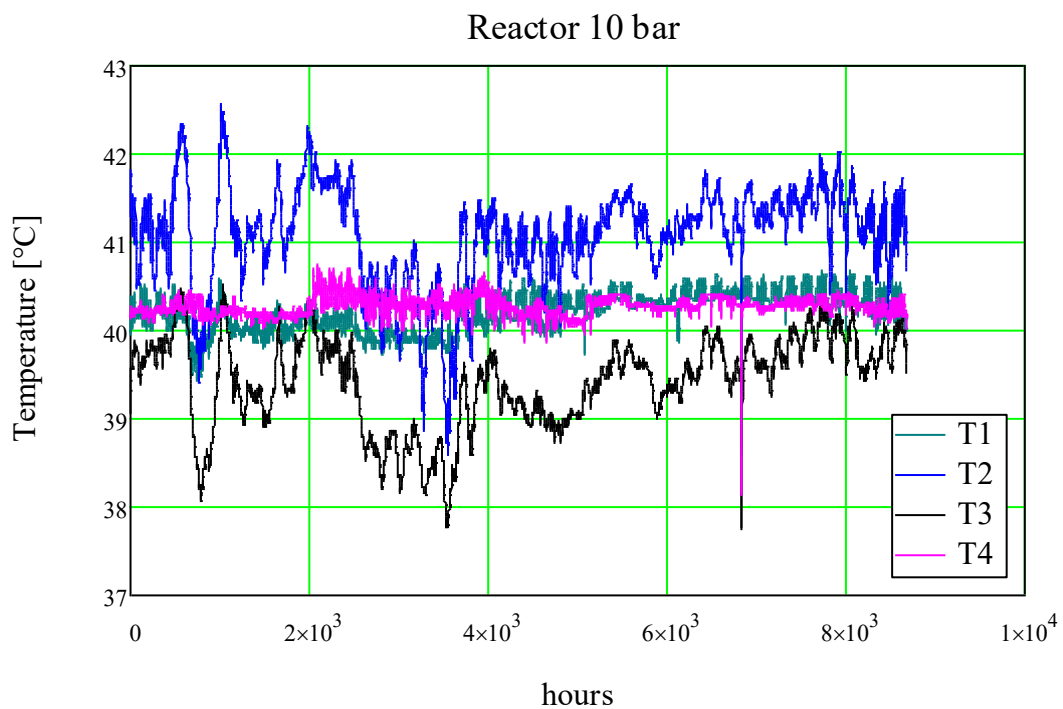


Figure 13: Temperature curves of reactor 10 bar over the test period

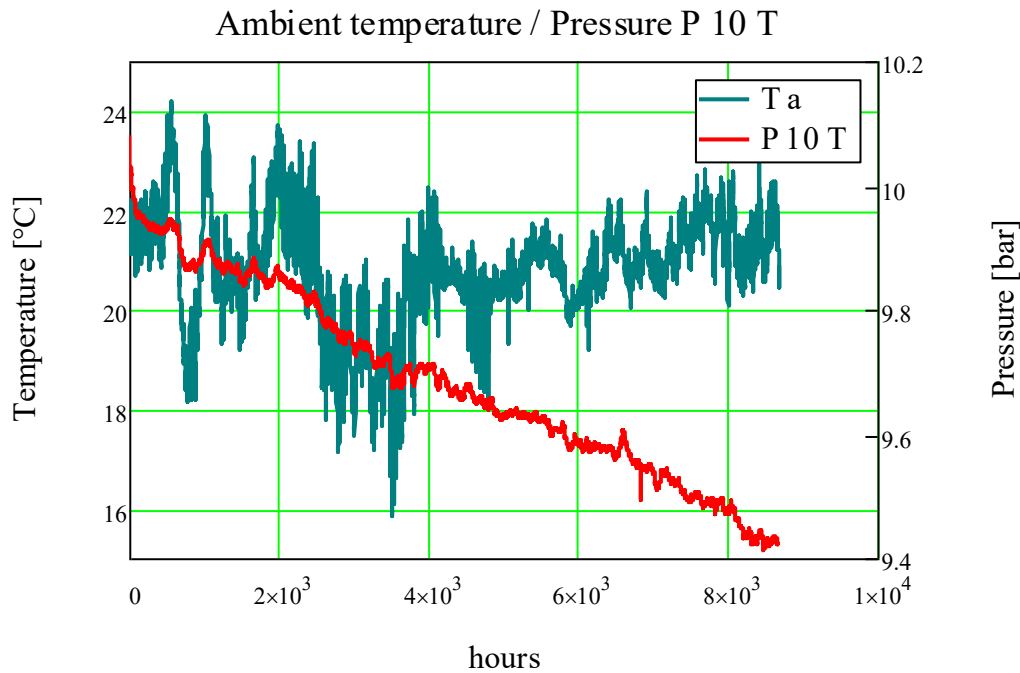


Figure 14: Pressure curve reactor 10 bar and ambient temperature.

During the duration of the test, a gas analysis was taken weekly from the head and bottom of the reactors using a process gas chromatograph. Before each sampling, the gas pipes to the PGC were purged with nitrogen, which is why it was also detected during the gas measurement. In order to eliminate the nitrogen content, the ratio of methane to hydrogen is used as the result. The measurement of the pure test gas from the bottle resulted in a ratio of methane to hydrogen of 12,227.

In the following figures (Figure 15; Figure 16; Figure 17) the ratio of methane to hydrogen at the top and bottom of the reactors is plotted over the weekly samples. The linear trends of the ratios does not show any drifting apart over the experimental time. A drifting apart of the measured values for ratio top and ratio bottom would indicate a segregation of the two components. In addition, the measured values are within the tolerance limits of the measuring instrument.

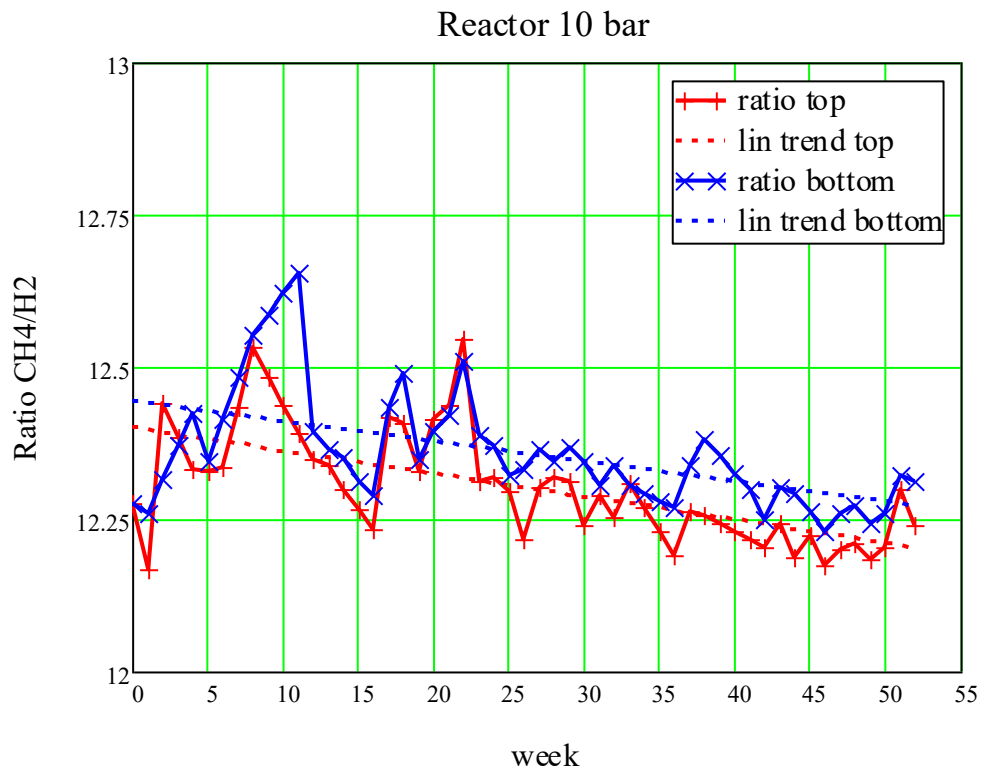


Figure 15: CH₄/H₂ ratio for reactor 10 bar

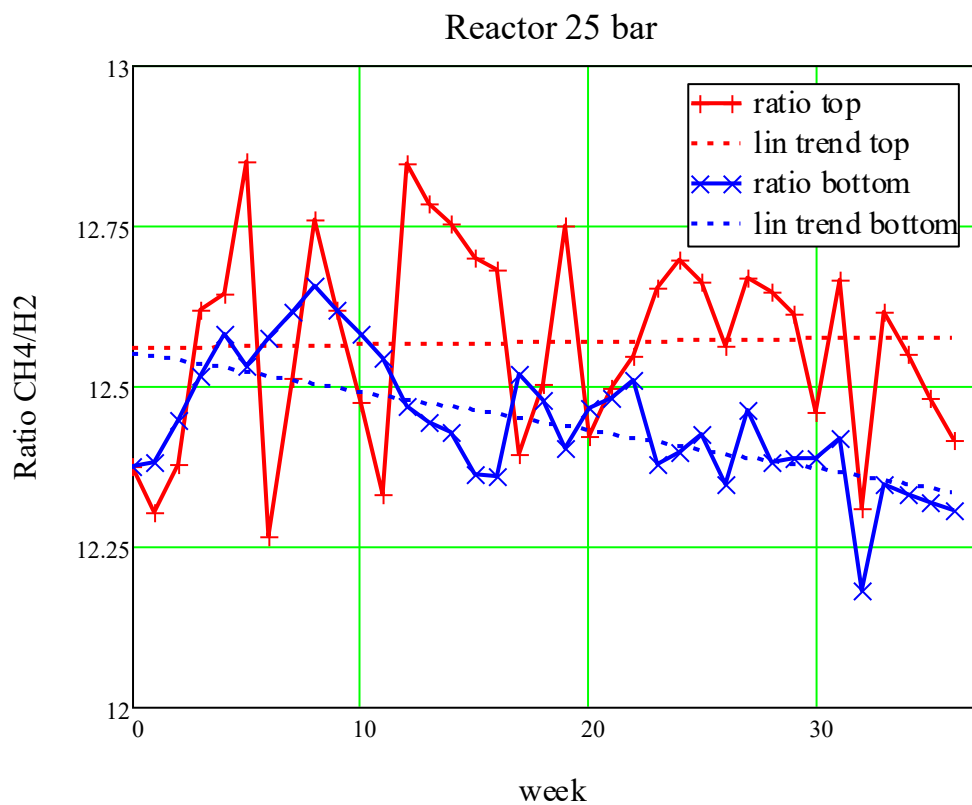


Figure 16: CH₄/H₂ ratio for reactor 25 bar

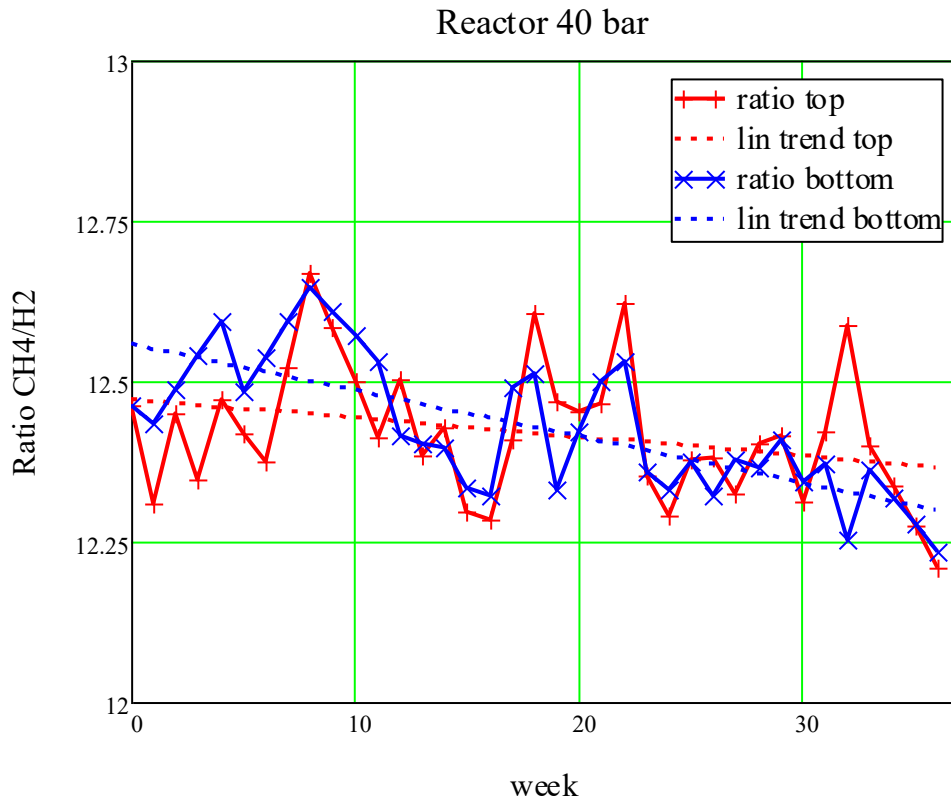


Figure 17: CH₄/H₂ ratio for reactor 40 bar

The statistical values of the gas measurements result in smaller deviations over the duration of the test than the deviations specified by the manufacturer of the analyzer. It can therefore be assumed that there is no segregation of the gases under static conditions.

4.3.7.2 Results of dynamic tests

The breakthrough curves with a reactor pressure of 10 bar are shown in Figure 18. The first derivative of the breakthrough curve is used in the following to better detect a delay or a leading of a gas component. The 1st derivative represents the change in concentration over time. It shows a maximum of the concentration change. The maxima of the individual gas components are shifted in time and show a delay of hydrogen when nitrogen is displaced.

When the test gas is displaced by nitrogen, methane is delayed. This effect is intensified at a reactor pressure of 20 bar. The delay times are given in Table 6.

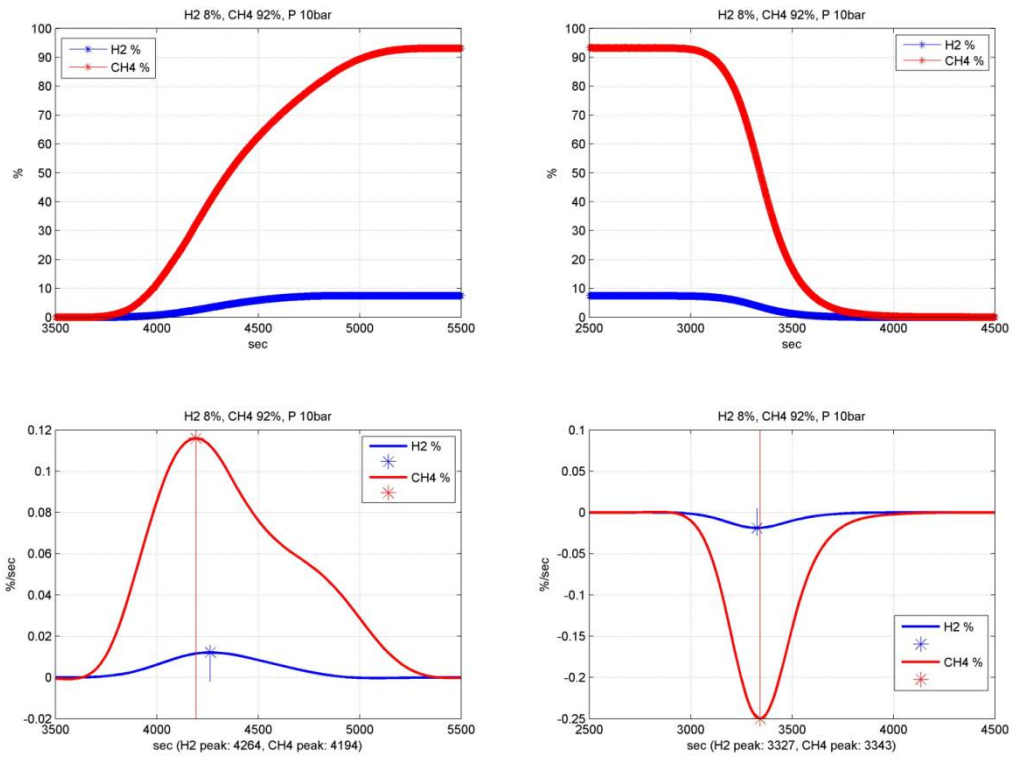


Figure 18: Breakthrough curves with 1st derivation at 10 bar reactor pressure

Table 6: Delay times at 10 and 20 bar reactor pressure with test gas 8% H₂ and 92% CH₄

	Displacement of N ₂ by test gas	Displacement of test gas by N ₂
	Delay from H ₂ in sec	Delay from CH ₄ in sec
10 bar	70	16
20 bar	493	28

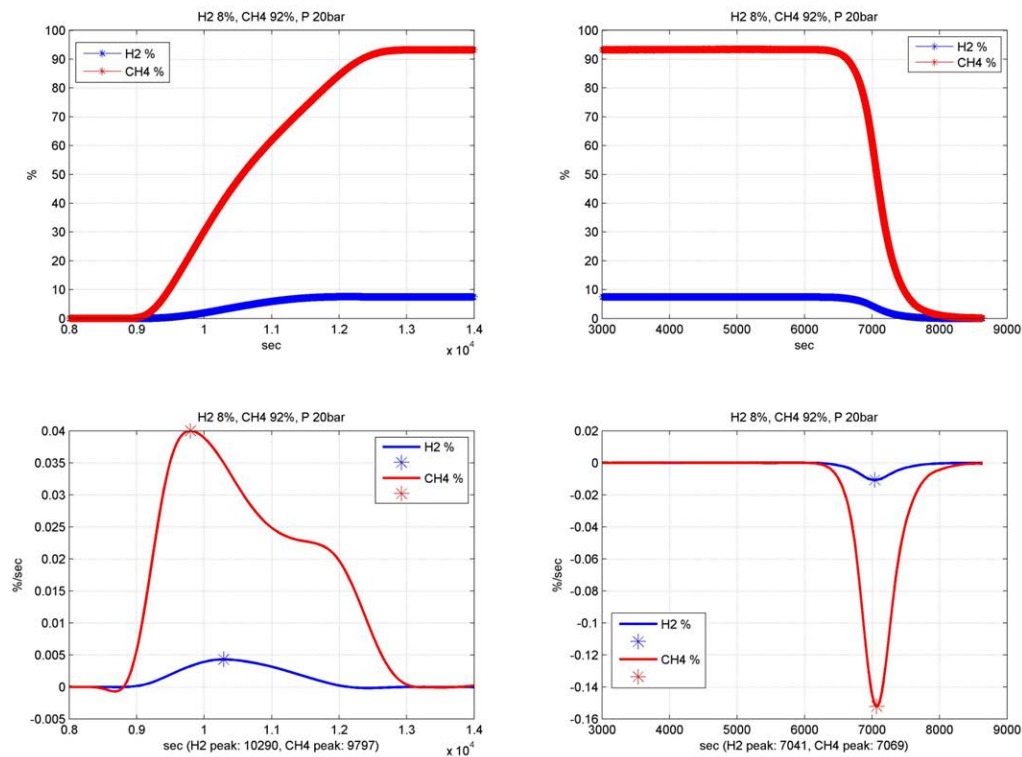


Figure 19: Breakthrough curves with 1st derivation at 20 bar reactor pressure

Tests with different gas concentrations were carried out with a test gas containing 20% hydrogen and 80% methane, each with 10 bar and 20 bar reactor pressure.

In these tests, too, there is a delay of H₂ during filling with test gas and vice versa a delay of CH₄ during displacement with N₂ (Figure 20; Figure 21). The resulting delay times are given in Table 7.

Table 7: Delay times at 10 and 20 bar reactor pressure with test gas 20%H₂ and 80% CH₄

	Displacement of N ₂ by test gas	Displacement of test gas by N ₂
	Delay from H ₂ in sec	Delay from CH ₄ in sec
10 bar	102	23
20 bar	420	44

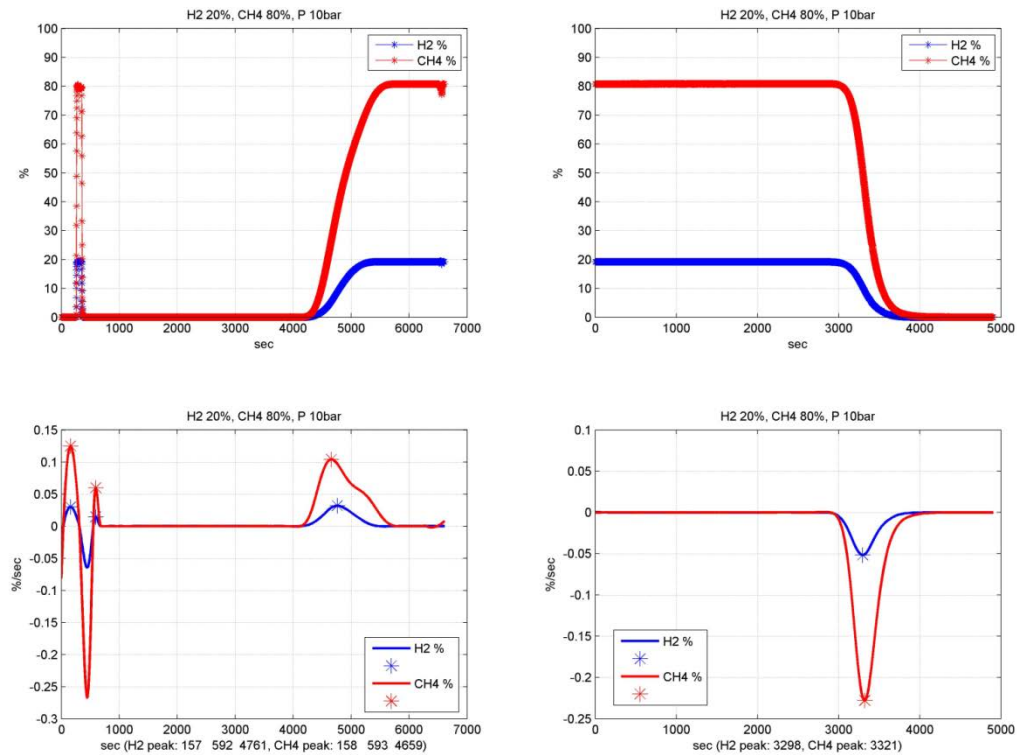


Figure 20: Breakthrough curves with 1st derivation at 10 bar reactor pressure

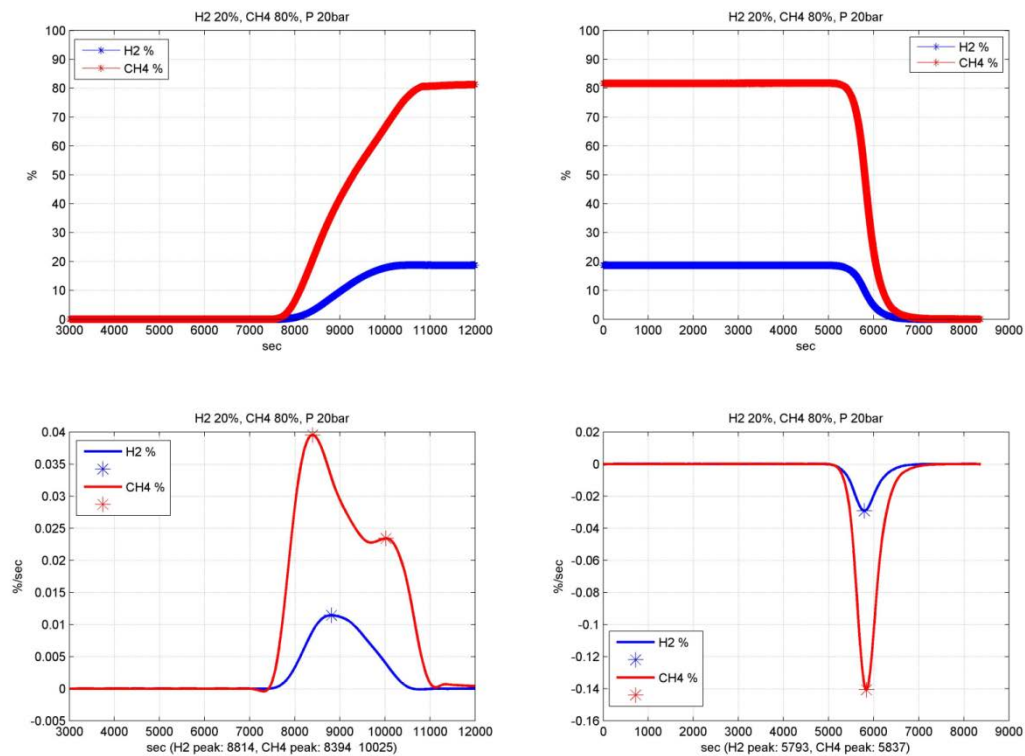


Figure 21: Breakthrough curves with 1st derivation at 20 bar reactor pressure

A test with increased flow (28 instead of 17 l/min) was carried out with test gas 8% H₂ and 92% CH₄ at a reactor pressure of 10 bar.

Table 8: Delay times at 10 bar and increased flow with test gas 20% H₂ and 80% CH₄

	Displacement of N ₂ by test gas	Displacement of test gas by N ₂
	Delay from H ₂ in sec	Delay from CH ₄ in sec
10 bar	58	13

The increased flow rate slightly reduces the delays (Table 8 and Figure 22), otherwise the results are the same as in the tests with a flow rate of 17 l/min.

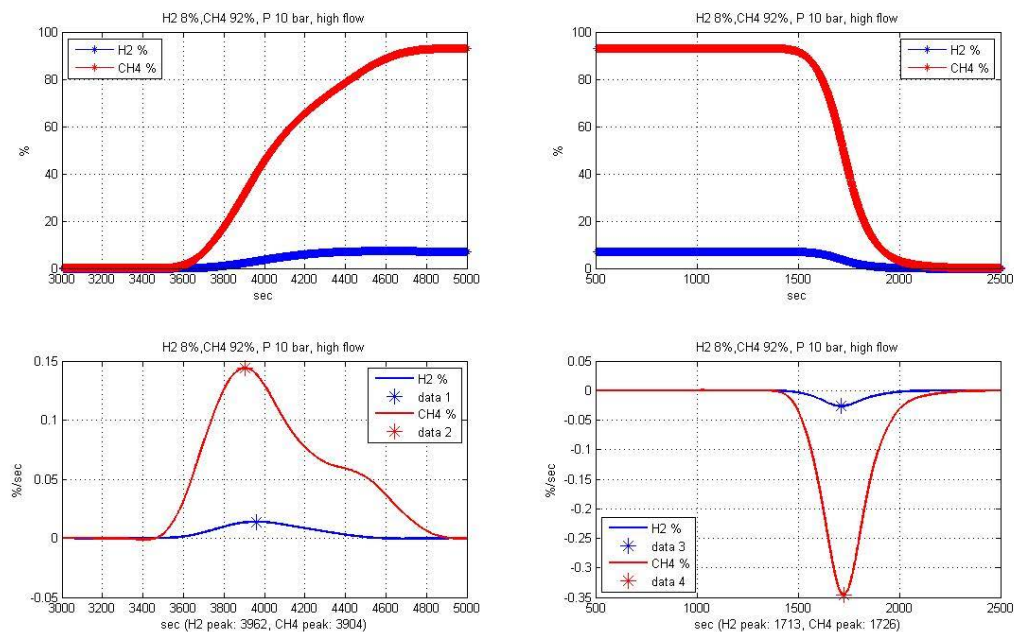


Figure 22: Breakthrough curves with 1st derivation at 10 bar reactor pressure and increased flow rate

Tests with methane instead of nitrogen as background gas were carried out with 2 test gases of different concentrations and a reactor pressure of 10 bar. The results are shown in Figure 23 and Figure 24. Here you can see the breakthrough curve of hydrogen with the resulting displacement of methane. The breakthrough curve does not differ from the other experiments.

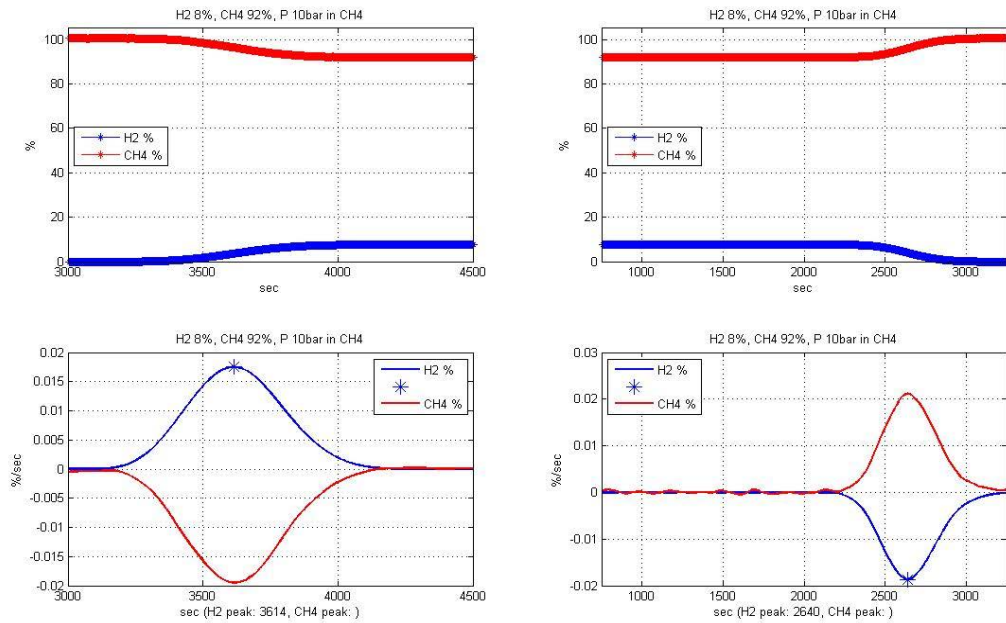


Figure 23: Breakthrough curves with 1st derivation with methane as background gas, pressure 10 bar and test gas 8% H₂ and 92% CH₄

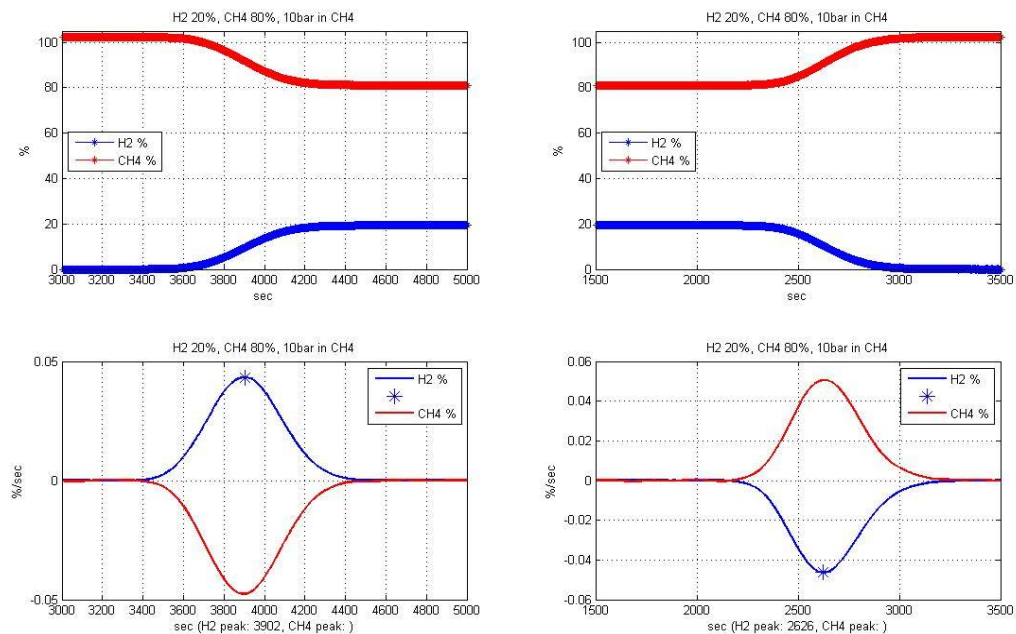


Figure 24: Breakthrough curves with 1st derivation with methane as background gas, pressure 10 bar and test gas 20% H₂ and 80% CH₄.

As an alternative to the results of the first derivation, an attempt was made in a second step to evaluate the overall test. Thus, the first derivative is an excellent example of which of the two gases shows a faster increase in concentration, but it is not yet possible to make a statement about the total flow. After the concentrations increased very abruptly, the second criterion used was a fraction filter, which measures the time up to which a certain proportion of the total concentration was reached. Here it can be seen that although methane sometimes rushes ahead in the beginning (faster increase in concentration), the hydrogen catches up very quickly and reaches a stable 100% flow faster. Accordingly, the dry through-flow tests showed that hydrogen rushes ahead regardless of the constellation. However, it should be noted that the difference is minimal (

Figure 25). This is attributed to latent adsorption forces that slightly slow down the hydrogen at the beginning. This is also supported by the fact that at the other end of the reactor there was always a reduced hydrogen content than was present in the original mixture. This did not change even with long flow times. It can therefore be assumed that CH_4 and H_2 move through the dry pore space at practically the same speed.

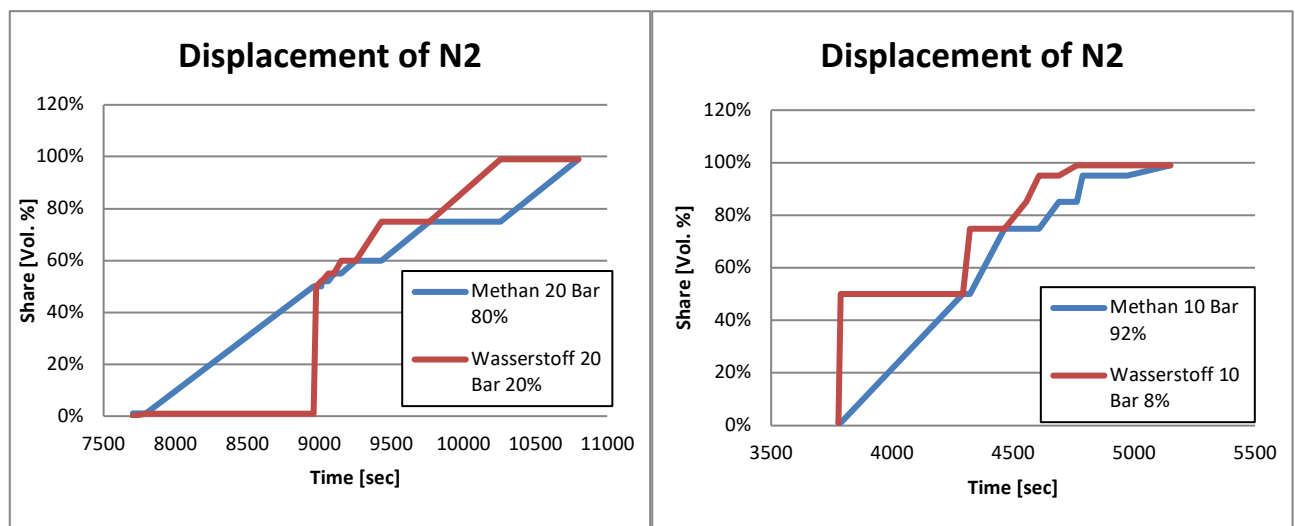


Figure 25: Displacement of nitrogen at 10 bar and 8% H_2 or at 20 bar and 20% H_2 .

When the reactors were rinsed again with nitrogen, the hydrogen was again somewhat faster, but the difference was so small that a uniform flow velocity can be assumed again Figure 26. Another series of experiments was started in which higher flow velocities were applied. Here, too, it was shown that practically both gases are equally fast.

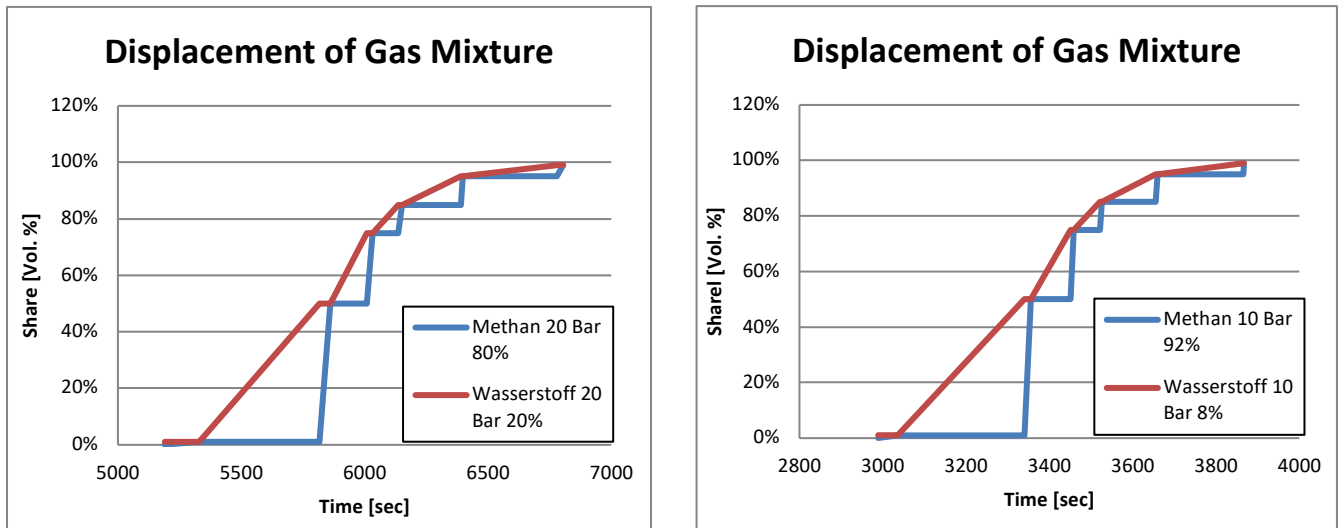


Figure 26: Displacement of the gas mixture at 10 bar and 8% or at 20 bar and 20% H₂.

In wet conditions, the delays are exactly the opposite of dry conditions. Methane is delayed when N₂ is displaced by the test gas and hydrogen is delayed when N₂ is displaced by the test gas. In addition to adsorption effects, absorption effects with different solubility of the gases in water also play a role. Methane is about 10 times more soluble in tap water than hydrogen ([9] [7]). The results are shown in Figure 28 and Figure 29 as well as the delay times in Table 9.

Table 9: Delay times at 10 and 20 bar under humid conditions with test gas 8% H₂ and 92% CH₄

Druck	Pressure Displacement of N ₂ by Test Gas	Displacement of Test Gas by N ₂
	Delay from CH ₄ in sec	Delay from H ₂ in sec
10 bar	121	23
20 bar	2	44

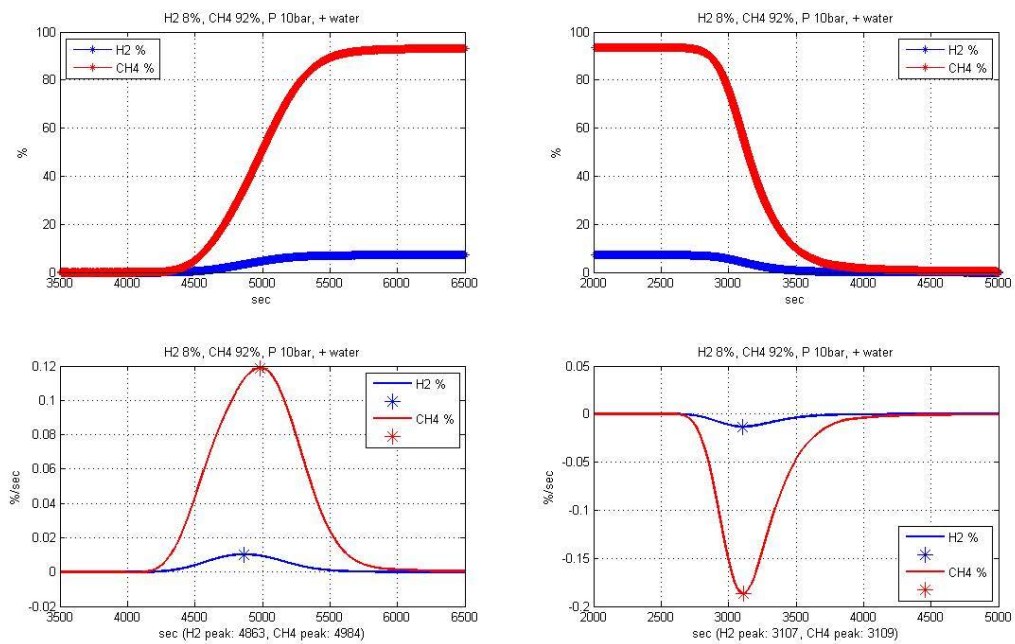


Figure 27: Breakthrough curves with 1st derivation in wet conditions, pressure 10 bar.

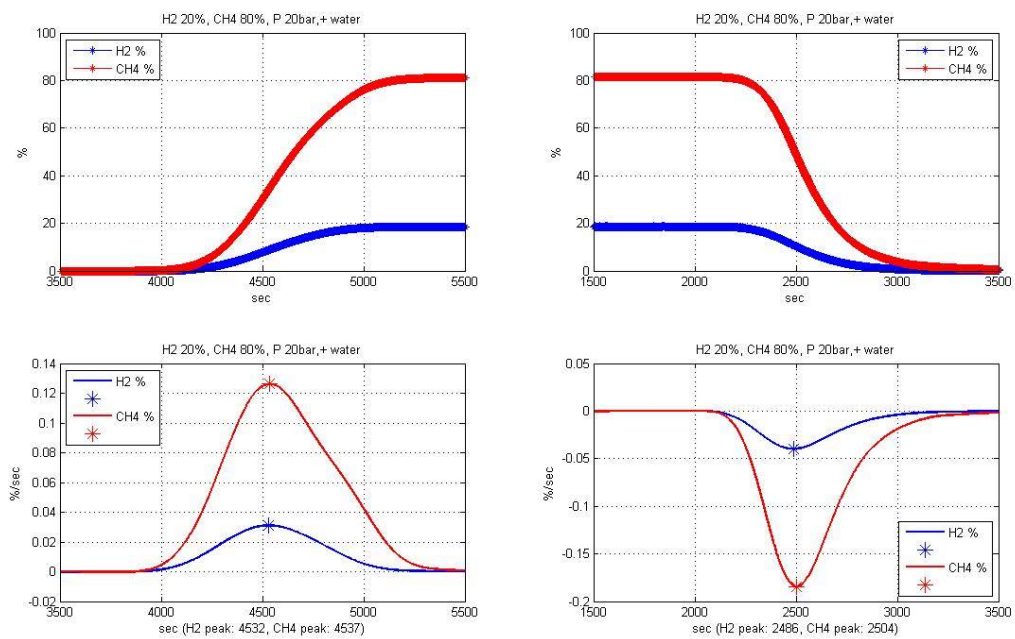


Figure 28: Breakthrough curves wet conditions, pressure 20 bar.

Here the results of the first derivation coincide with the results of the fractionation. In both cases the hydrogen breaks through somewhat faster. However, it should be noted that methane is slowed down even more by water because it dissolves more strongly in water than hydrogen.

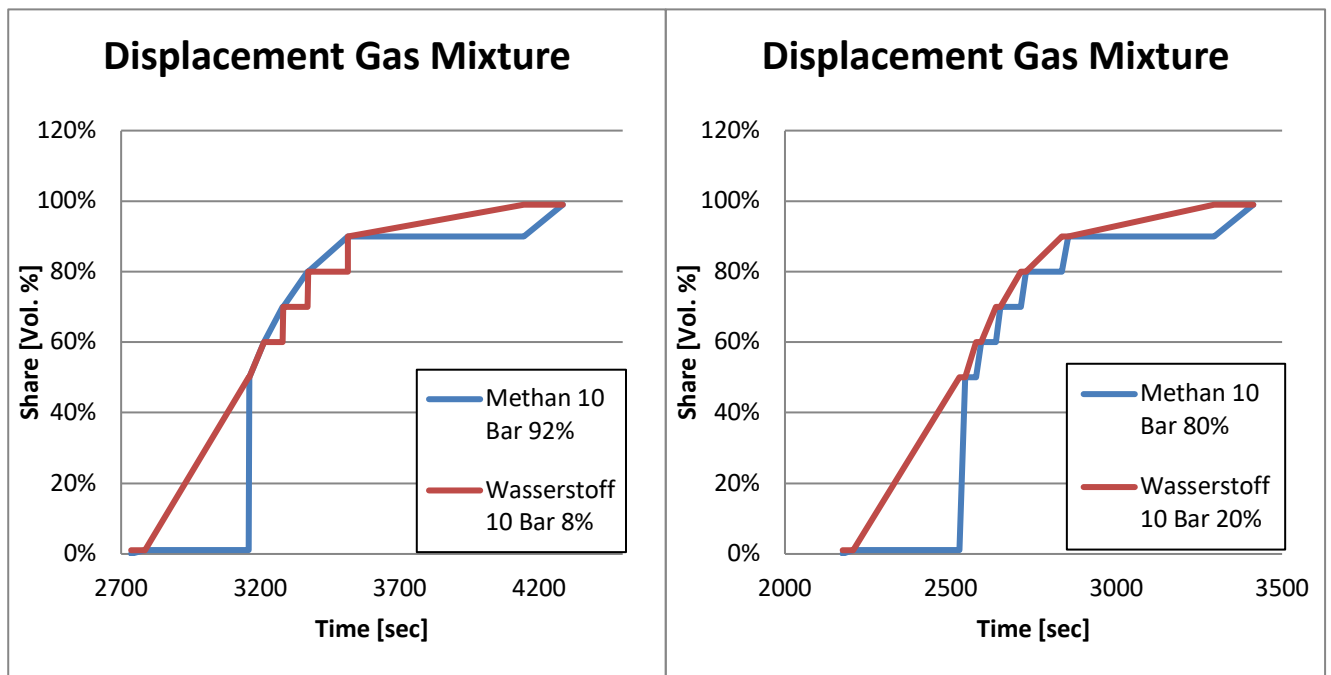


Figure 29: Displacement of the mixture at 10 bar and 8% H₂ at the wet core

Since the methane saturation is already given in a depleted natural gas reservoir, the unsaturated hydrogen will be slowed down somewhat by dissolution and adsorption. In general, however, it can be said that there is practically no speed difference between methane and hydrogen in the porous space. The differences measured in the experiments are within a few seconds and can therefore be attributed to measurement inaccuracies.

In general, however, the results of the dynamic experiments are very difficult to interpret. Thus it could be shown in a second approximation that the hydrogen is minimally ahead (as expected from the literature), but with regard to the measurement inaccuracy no definite answer is possible. For a possible further experiment it is considered to extend the flow distance again in order to be able to better represent the conditions in the reservoir. However, it should also be noted that even if the gases are separated by their different viscosities, mixing is to be expected again later, since diffusion in the porous space has proved to be strong. This might also be the explanation, why there was no segregation in the static experiments, because here the diffusion has a stronger influence and the system tries to get and maintain a saturation equilibrium.

4.4 Transport and diffusion modelling at the University of Leoben

4.4.1 Task

This part contains a summary of the steps taken to create transport and diffusion models and discusses the potential hydrogen movement in the porous geological layers.

A geological model of a specific reservoir was prepared as a basis for the transport modelling study, structural maps, drilling data, borehole markings, protocols and seismic data were evaluated and used to determine the geological model. The model steps are outlined in Figure 30.

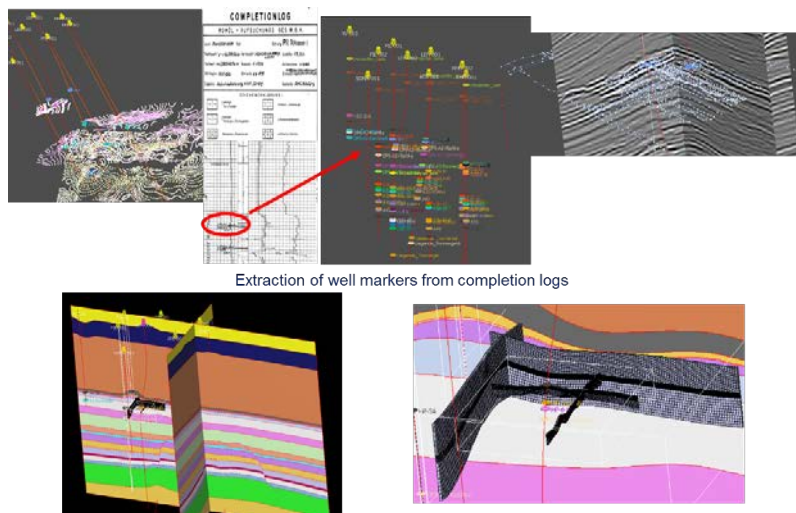


Figure 30: Sections of geological modelling: digitization of structural maps, extraction of drilling markers from drilling protocols, seismic cube interpretation and flow simulation grid construction.

4.4.2 Content presentation

After the static model was constructed, a reservoir model was created in CMG (Compositional Reservoir Simulator). Due to the small thickness of the reservoir and the lack of data, the distribution of porosity and permeability in the reservoir was assumed to be homogeneous. The Peng-Robinson (1978) equation of state was selected to describe the gas phase. A gas mixture (10% H_2 + 90% CH_4) was injected into the reservoir at an injection rate of 1000 Nm^3 (H_2)/h for three months. Advection and diffusion transport processes were used to describe the movement of the gas and the hydrogen concentrations in the reservoir. The expansion of the gas front was simulated and shown as spatial distribution of the hydrogen concentration as a function of time in Figure 31.

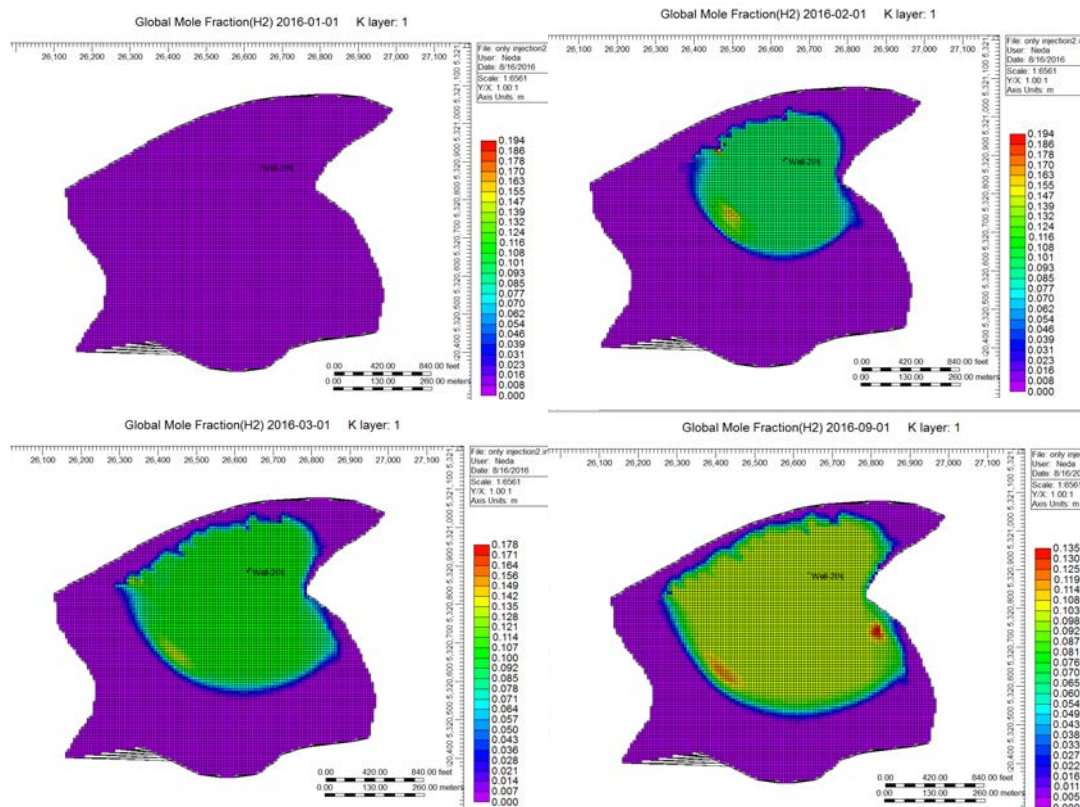


Figure 31: Distribution of hydrogen concentration in the deposit over time.

The model in Figure 32 shows a comparison of the hydrogen and methane distribution. The areas wetted by the hydrogen according to this model were entered into an analytical diffusion model to calculate the diffusion losses until the concentration balance of the hydrogen at the boundaries of the reservoir, as discussed below.

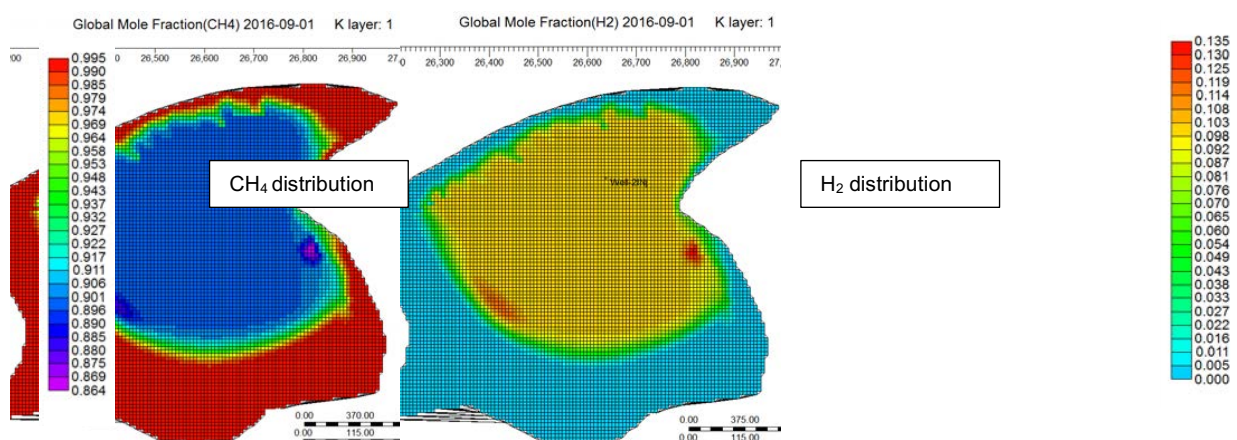


Figure 32: Comparison of the spatial distributions of CH4 and H2 in the reservoir.

4.4.3 Results and conclusions

While the reservoir provides storage capacity for a hydrogen-based energy supply, clay stones are sealing layers that are generally water-saturated as they have sufficient capillary displacement pressure to prevent the outflow of a light non-wetting fluid such as natural gas and hydrogen [10]. Nevertheless, a hydrogen loss by diffusion up to the concentration equilibrium could be possible. A concept model was developed to investigate the possibility of hydrogen losses due to diffusion into the sealing water-filled layers. The solubility of hydrogen and other gases in the formation water plays a decisive role. The injected mixture of hydrogen and methane touches the surrounding sealing layers. The hydrogen could dissolve in both interstitial clay and pore water and then be transported by diffusion. The amount of hydrogen that can be bound in the superimposed layers is one of the H₂ loss sources. It should be mentioned that the concentration gradient and thus the amount of gas loss is greatest in the first storage cycle and will decrease considerably in the following cycles [11]. Using the 1D diffusion equation, the diffusion loss of hydrogen was evaluated for a period of one year of storage, assuming three months of continuous hydrogen injection with the data from Table 10.

$$\text{Diffusion loss} = \frac{\text{amount of lost H}_2 \text{ during inclusion phase (e.g.: 1 year)}}{\text{amount of injected H}_2 \text{ in 3 months}}$$

Table 10: Injection and reservoir data for the calculation of the diffusion loss.

Hydrogen injection rate	1,000 Nm ³ /h
Gas FVF (at 75 bar)	0.0153 rm ³ /sm ³
Hydrogen deposits Injection rate	6,535 rm ³ /h
Injected hydrogen Volume	14,117,647rm ³
Deposit pressure after injection	75bar
Deposit temperature	40°C
Hydrogen Z-factor	1.05
Hydrogen concentration in the deposit	274 mol/m ³
Number of moles of injected hydrogen	3.88E+09 mole

Under the assumption that the diffusion coefficient of hydrogen is 4.5e-⁹[m²/s] [12], the concentration of H₂ in the covering layers and the respective penetration depth were calculated by means of an analytical solution. The result is summarized in Figure 33.

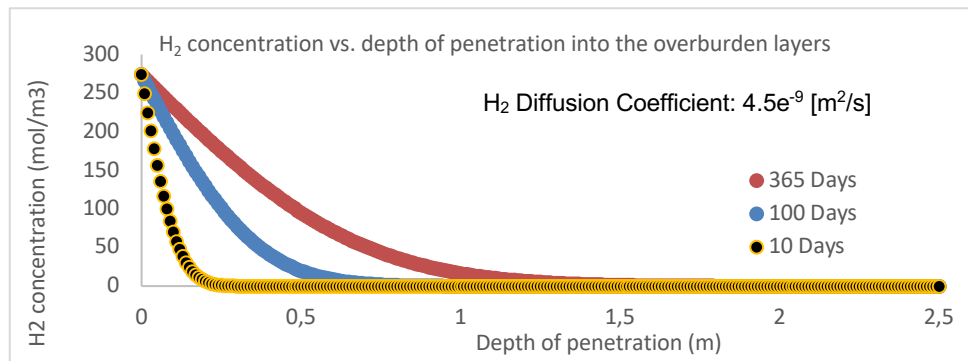


Figure 33: H₂ concentration vs. penetration depth of H₂ into the surface layers

Due to the small thickness of the reservoir, it can be assumed that the mixture of the injected gas is evenly distributed in the reservoir. Since diffusion takes place in 3D space, the hydrogen can diffuse into the entire mantle surface, which represents a maximum loss scenario. Table 11 summarizes different scenarios and the associated diffusion losses for different cases. Two diffusion coefficients for hydrogen in reservoir water (4.5e^{-9} and 4.5e^{-10} [m^2/s]) [11], the latter considering the heterogeneity of the reservoir. The diffusion loss of hydrogen was estimated for two cases. The first case considers only diffusion upwards through the surface layers and the second case also considers diffusion into the entire mantle surface. From the results we estimate the minimum diffusion loss at 0.16% and the maximum diffusion loss at 6.05%. As mentioned above, we expect a lower diffusion loss during subsequent storage cycles.

Table 11: Diffusion loss into the surface layers during 1 year hydrogen storage considering two diffusion coefficients.

Diffusion coefficient	Length (m)	Width (m)	Penetration Volume	diffusion losses Hydrogen	diffusion losses Cover Layer	diffusion losses mantle
4.5e^{-9} [m^2/s]	1000	1000	1.17E+08	3.02E-02	3.02%	6.05%
	800	600	5.62E+07	1.45E-02	1.45%	2.90%
	500	500	2.93E+07	7.56E-03	0.76%	1.51%
	400	400	1.87E+07	4.84E-03	0.48%	0.97%
4.5e^{-10} [m^2/s]	1000	1000	3.82E+07	9.87E-03	0.99%	1.97%
	800	600	1.83E+07	4.74E-03	0.47%	0.95%
	500	500	9.55E+06	2.47E-03	0.25%	0.49%
	400	400	6.11E+06	1.58E-03	0.16%	0.32%

4.5 Artificial reservoir water

4.5.1 Task definition

Artificial sterile reservoir water was used for the reservoir alteration experiments (see 4.9.6). The reason for this is that the results are made reproducible and there are no side effects due to microbiological metabolic processes. However, in order to exclude the possibility that this non-original reservoir water may have an influence on the cores used, a further series of tests was started. Rock material, which was also used in the alteration tests, was stored for 9 months in artificial reservoir water at reservoir temperature and pressure (40°C; 100 Bar).

4.5.2 Content presentation

In preparation for the experiments, a water sample was taken in a representative depleted gas reservoir. This was then used by DBI Gas-Umwelttechnik GmbH Leipzig as a reference to mix artificial water with the same number of dissolved ions and the same pH value.

Prior to storage, the water and gas permeability's of the cores used were determined. A homogeneous and a strongly heterogeneous reservoir were selected, whereby the heterogeneous one shows a higher diversity of minerals. The aim of this approach was to be able to make a general statement about the reactivity of different minerals and the influence of a larger proportion of clay (swelling).

At the end of the exposition process, the rock cores were removed from the reactors at slow pressure release (risk of fracture at fast pressure release) and investigated both optically (deposits) and physically (permeability).

4.5.3 Results and Conclusions

Figure 34 and Figure 35 show the cores after storage. Original samples were kept for comparison to determine changes.



Figure 34: Core of hole BA C1 original sample (left) and after storage (right)



Figure 35: Photos of the cores from the NU original sample (left) and after storage (right)

Apparently, the rock cores turned brownish. This can be explained by the precipitation of iron from the reservoir water and the clays. A similar discoloration could also be observed in the rock cores used in other experiments.

Table 12 summarizes the determined gas and water permeability's of the rock cores before and after nine months of storage.

Table 12: Comparison of water and gas permeability's before and after storage

		$k_{w,g} [m^2]$	$k_w [m^2]$
BA C1	before storage	$9.73 \cdot 10^{-14}$	$1.45 \cdot 10^{-14}$
	after storage	$7.00 \cdot 10^{-14}$	$2.73 \cdot 10^{-14}$
NU W8	before storage	$3.36 \cdot 10^{-15}$	$8.20 \cdot 10^{-16}$
	after storage	$3.14 \cdot 10^{-15}$	$9.68 \cdot 10^{-16}$

$k_{w,g}$ -gas permeability in case of saturation of the adhesive water

k_w -water permeability

Furthermore, an increase in water permeability and a decrease in gas permeability was observed. Both can be attributed to the age and long atmospheric storage of the rock cores. For example, the rock cores were not water-saturated before the start of the experiments, as they had dried out due to long storage in the RAG core house. After storage, the relative permeability's shifted due to the increased water saturation, which meant that the gas could now flow more slowly and the water faster. A swelling of the clays as well as possible dissolution phenomena at mineral grains could not be proven neither in the thin section nor in the permeability measurements.

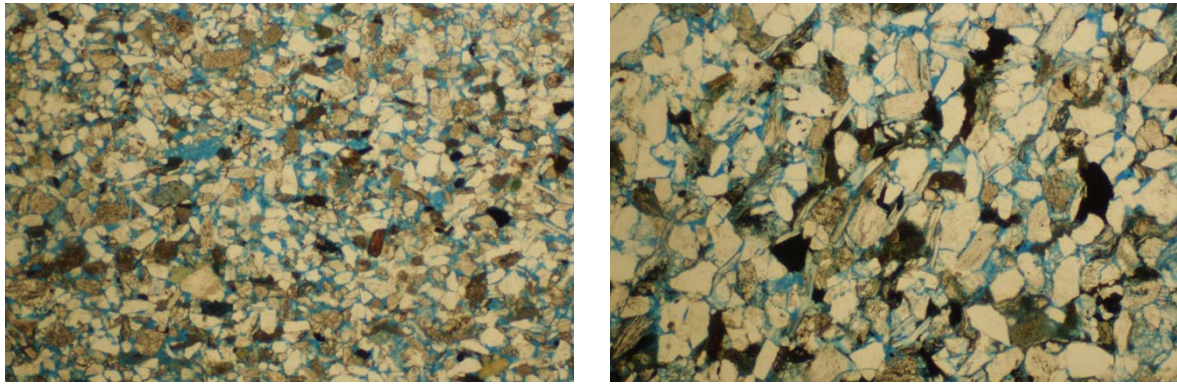


Figure 36: Core BA C1, (left) and core NU W8, (right); brightfield transmitted light, detail: 3.6 mm x 2.4 mm

Figure 37 and Figure 38 show thin section images of the cores BA C1 and NU W8 before and after storage.

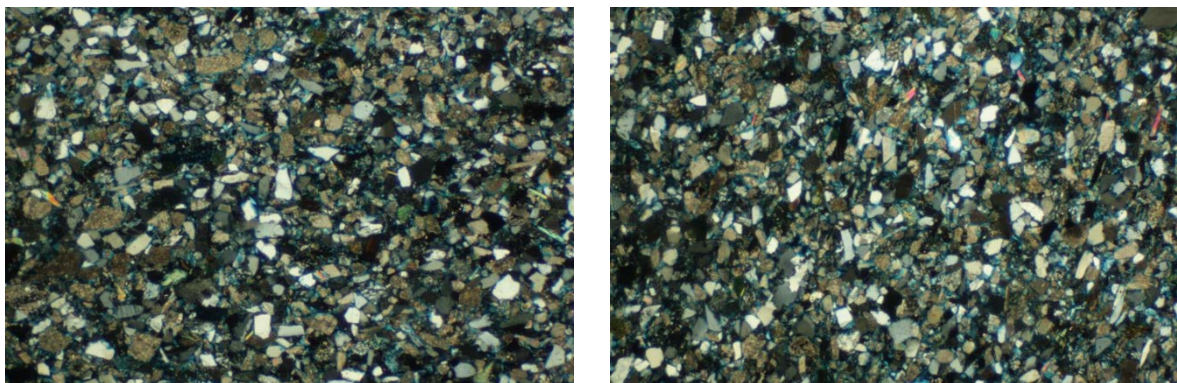


Figure 37: Core BA C1, depth: 1319.14 m, (left: before storage, right: after storage), crossed polarizers, image section: 3.6 mm x 2.4 mm

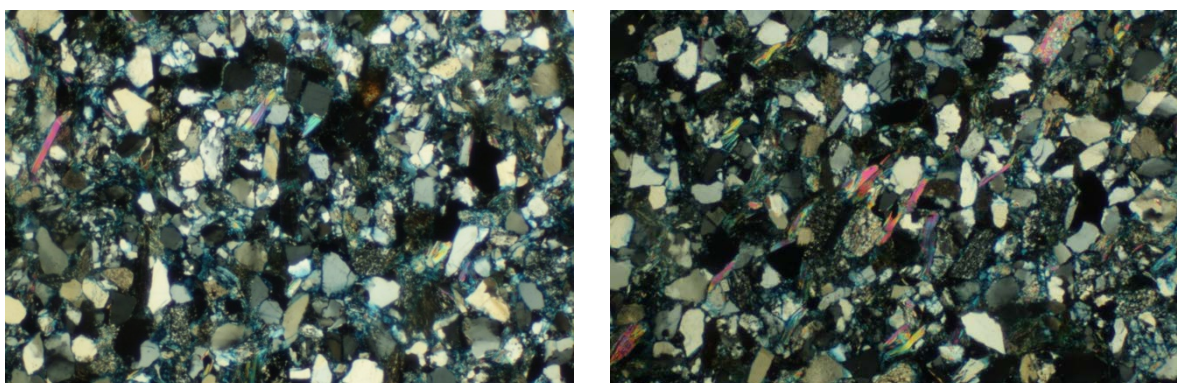


Figure 38: Core NU W8, (left: before storage, right: after storage), crossed polarizers, image section: 3.6 mm x 2.4 mm

However, since the swelling of the clays is time-dependent (kinetic effect), it can be assumed that further shifts may occur during longer storage. For the reservoir alteration experiments,

however, these results were classified as sufficiently accurate, since the storage times roughly coincide.

4.6 Alteration of the reservoir rock (reservoir alteration)

4.6.1 Task definition

Hydrogen is generally considered to be highly reactive. In the atmosphere in particular, it reacts quickly with oxygen or is quickly distributed due to its high diffusivity. In natural gas reservoirs, the oxygen component is completely absent as it cannot exist stably under the prevailing reducing conditions but reacts immediately with the reservoir fluids. However, the question remains whether hydrogen will react with other molecules in the reservoir. From the literature the reaction with sulfur to H_2S [13] and the reaction with iron to Götthit [14] are known. The possible transverse effects of the buffering of carbonates and the influence of the rich clay minerals on the geochemical system are also described in the literature [9]. The topic of hydrogen sulphide naturally received special attention in the project development, as this would have been a clear exclusion criterion for further experiments due to its properties and the fact that the plants were not designed for this case. Theoretically, Sulphur is available in the reservoir under consideration. It exists as the mineral pyrite as well as dissolved in the reservoir water as SO_4 . Accordingly, tests on this topic were carried out at DBI Leipzig.

4.6.2 Presentation of content

As in the other experiments, cores from representative reference reservoirs with a mineralogical composition similar to that of the RAG gas storage facilities were used.

In preparation, the cores were cut and measured and the gas and water permeability's were determined. In addition, thin sections were prepared as reference samples in order to be able to measure and evaluate possible dissolution phenomena or growth fringes. The cores intended for the experiment were soaked in artificial reservoir water in order to remoisten them.



Figure 39: Flow apparatus

After preparation, the cores were installed in the flow apparatus Figure 39, where the test was carried out at a temperature of 40°C (reservoir property). The prefabricated gas mixture of 25% H₂ and 75% CH₄ was passed over a water-saturated activated carbon in order to moisten the gas to prevent the cores from drying out. The cores were then flowed through for 3, 6, 10 and 12 months. The experiments were repeated under otherwise identical conditions with a gas mixture of 75% H₂ and 25% CH₄.

4.6.3 Results and conclusions

After the opening of the reactors, the first visual assessment of the cores showed a reddish discoloration of the cores, indicating an oxidation of iron. The iron probably reacted with the residual oxygen present in the artificial reservoir water. A connection with hydrogen could not be found, since the red coloration also occurred in the test reactors without hydrogen. A biofilm could not be found, which excludes microbiological reactions during storage.

Figure 40 and Figure 41 show a comparison of the cores stored for 12 months before and after storage.



Figure 40: Core BA C1, depth: 1312.97 m, (left: before storage, right: after storage for 12 months)



Figure 41: Core NU W8 (left: before storage, right: after storage for 12 months)

After removal of the cores, the gas and water permeability's were determined again.

Table 13: Comparison of water and gas permeability's before and after storage at the cores from borehole BA C1

Water permeability k_w [m ²]			Gas permeability k_{wg} [m ²]	
Months	before	after	before	after
2	$2.77 \cdot 10^{-14}$	$2.86 \cdot 10^{-14}$	$2.43 \cdot 10^{-13}$	$2.31 \cdot 10^{-13}$
3	$5.55 \cdot 10^{-14}$	$3.16 \cdot 10^{-14}$	$2.17 \cdot 10^{-13}$	$2.57 \cdot 10^{-13}$
6	$4.07 \cdot 10^{-14}$	$3.75 \cdot 10^{-14}$	$1.60 \cdot 10^{-13}$	$1.45 \cdot 10^{-13}$
9	$3.87 \cdot 10^{-14}$	$2.58 \cdot 10^{-14}$	$1.31 \cdot 10^{-13}$	$1.11 \cdot 10^{-13}$
12	$2.59 \cdot 10^{-14}$	$7.19 \cdot 10^{-14}$	$1.95 \cdot 10^{-13}$	$1.06 \cdot 10^{-13}$

k_w -water permeability

$k_{w,g}$ -gas permeability in case of saturation of the adhesive water

Table 14: Comparison of water and gas permeability's before and after storage at the cores from borehole NU W8

Water permeability k_w [m ²]			Gas permeability k_{wg} [m ²]	
Months	before	after	before	after
2	$5.95 \cdot 10^{-16}$	$2.77 \cdot 10^{-16}$	$4.10 \cdot 10^{-15}$	$11.0 \cdot 10^{-15}$
3	$6.27 \cdot 10^{-15}$	$0.25 \cdot 10^{-15}$	$4.65 \cdot 10^{-14}$	$3.80 \cdot 10^{-14}$
6	$3.90 \cdot 10^{-15}$	$1.07 \cdot 10^{-15}$	$1.94 \cdot 10^{-14}$	$0.76 \cdot 10^{-14}$
9	$4.48 \cdot 10^{-15}$	$1.13 \cdot 10^{-15}$	$2.95 \cdot 10^{-14}$	$2.15 \cdot 10^{-14}$
12	$1.34 \cdot 10^{-15}$	$2.8 \cdot 10^{-15}$	$7.68 \cdot 10^{-15}$	$9.51 \cdot 10^{-15}$

k_w -water permeability

$k_{w,g}$ - gas permeability in case of saturation of the adhesive water

Interestingly, the water permeability's of the short-stored cores decreased and those of the 12-monthly cores increased. The decrease can be explained by the properties of the clay minerals, which tend to swell at different water saturations. This is a kinetic effect, which of course is time-dependent. The initial slight increase in water permeability can be explained by the water saturation of the cores. The higher the initial saturation (due to re-moistening), resulted in an increased relative water permeability, since the water moves faster through saturated pores.

As explained below, the thin sections (Figure 42; Figure 43) give no indication that the increase in permeability is connected to the dissolution of minerals.



Figure 42: Moderately sorted, fine-grained, calcitically cemented litharenite



Figure 43: Overview of a porous, well sorted, fine-grained litharenite. The free pore space is blue.

The gas permeability decreased in all cores used due to the re-moistening of the rock cores. As the reservoir rock used for the experiments is very heterogeneous the permeability's and water saturations are also quite different. The reason is, that the water saturation does also depend on the rock type. The water saturation decreases the relative gas permeability in the cores. Gas permeability increased only in two rock cores from the well NU. No reasonable explanation could be found for the rock core which was tested for 2 months and increased its

permeability to $11 \cdot 10^{-15} \text{ m}^2$ and so it might be an anomaly caused by the rock properties. The other core that was stored for 12 months had an increase in permeability due to micro fractures that resulted from the depressurization of the reactor. Therefore, not only the gas, but also the water permeability increased. It should again be mentioned that there was no indication for dissolution phenomena in the thin section.

Since the results of the permeability measurement did not yield any clear results, thin sections were prepared to see possible changes at microscopic level. No growth seams by precipitation or smoothing by dissolution were observed on the carbonate grains of the sandstone.

Figure 44 and Figure 45 show exemplary thin section images of cores 8 and 10 before and after the storage of 2 and 12 months, respectively.

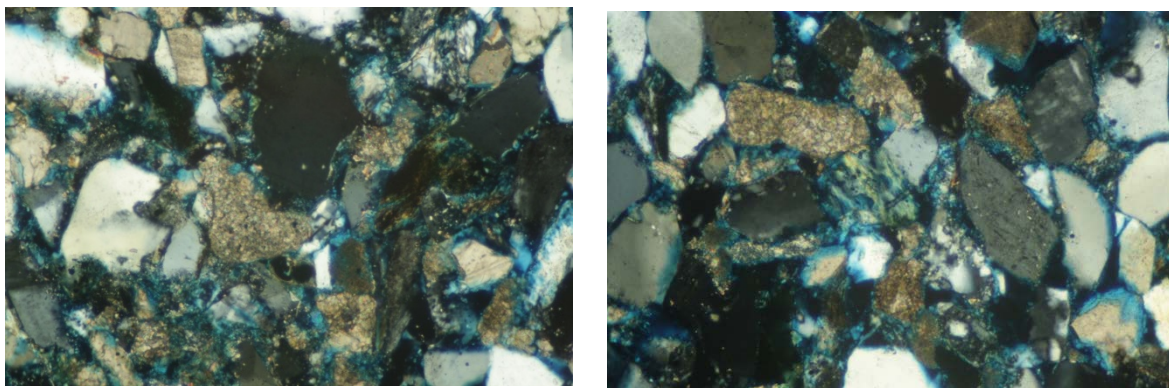


Figure 44: Core BA C1, depth: 1310.94 m, (left: before storage, right: after storage for 12 months), crossed polarizers; detail: 900 μm x 600 μm

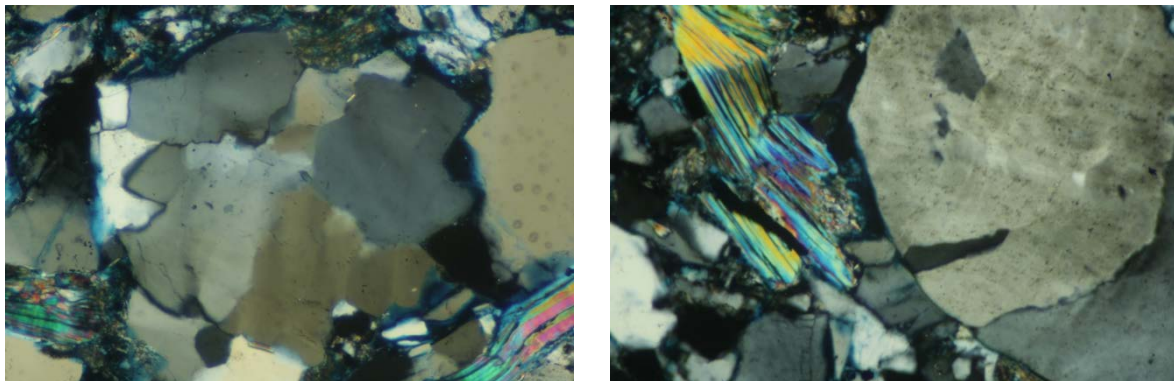


Figure 45: Core NU W8, (left: before storage, right: after storage for 12 months), crossed polarizers; image detail: 900 μm x 600 μm

As can be seen, the grains are still sharply separated from each other without showing the holes typical for dissolution phenomena.

RAG also interpreted these thin sections petrographically. On the basis of the thin sections provided by DBI Leipzig, no changes are discernible after the tests.

Furthermore, cores used in the microbiological experiments of the IFA Tulln were subjected to the same investigation. However, no changes in permeability, pore structure or mineralogical composition were found either.

In similar investigations (H₂Store), partly significant dissolution phenomena were measured in the carbonates of the sandstones. Apart from the fact, that the changes due to the re-moistening were not measured, the author assumes, however, that this is not an effect of the hydrogen, but rather has to do with the test conditions prevailing in this project (higher temperatures, lower pH values, significantly higher salinity). The high temperatures of course also imply a much higher energy in the system, which can lead to reactions without the influence of hydrogen.

For the Underground Sun Storage project, a separate series of experiments was carried out on the influence of artificial reservoir water on the rock cores (4.5). Unfortunately, similar experiments or at least their results are not available for the H₂Store project. Accordingly, it can only be assumed whether the changes measured in the H₂Store are due to hydrogen or to the artificial reservoir water or as has been mentioned due to the test conditions.

In conclusion, it can be said that no measurable geochemical changes could be observed for the reservoir conditions existing in RAG's storage reservoir. These very positive results from the operator's point of view were very important for the planning and execution of the field test.

4.7 Geochemical Simulation

4.7.1 Task definition

The topic of geochemistry was given high priority from the outset, as hydrogen is generally considered to be highly reactive and the literature also assumes that significant reactions will occur in the subsurface reservoir.

University of Leoben Department Reservoir Engineering

Within the framework of this work, possible reactions and integrity of the depleted gas deposits in the Upper Austrian molasse basin with regard to the injection of hydrogen were examined. Possible sources of hydrogen loss associated with geochemical equilibrium and transport processes are investigated. Since the time scales of chemical reactions and transport phenomena are well separated, separate geochemical and transport modelling studies were carried out to estimate hydrogen utilization paths. A geochemical workflow was developed to predict the fluid-fluid and rock-fluid interactions due to hydrogen injection within the period of a storage cycle and to investigate the final reactions of hydrogen.

Within the geochemical study a multi stage approach was developed and performed to study equilibrium and kinetic batch simulations. Appropriate assumptions were taken into account for each type of model. Equilibrium "batch models" estimate long-term consequences of hydrogen storage (what happens to hydrogen when the reaction potential of a system is zero). On the other hand, kinetic "batch models" estimate the temporal evolution and make a statement about the loss during a storage cycle possible. Two steps were considered in the kinetic "batch models". In the first kinetic models, mineral reactions are kinetically controlled while hydrogen reactions are assumed to be in equilibrium. In the second kinetic batch model,

hydrogen reactions in reservoir water are considered kinetically controlled. The results show that reactions between the injected hydrogen and the formation within a typical storage cycle are insignificant.

RAG

A geochemical simulation was also carried out by RAG, using existing and available software. Specifically, the open source software Phreeqc [T] was used to enable other storage operators to compare the results of Underground Sun Storage with their geological input. It should be made possible to make fast investigation by means of water, temperature and rock data, whether other formations are suitable for the storage of hydrogen. As a preliminary work, a master thesis was carried out in which static batch experiments were simulated with the simulator GEMS [T] in order to gain a rough understanding of the geochemical processes in the subsurface [15]. These simulations showed some possible reactions of the hydrogen with the carbonates of the reservoir as well as a possible increase of the pH-value due to the dissolution of hydrogen into the reservoir brine. A possible formation of H₂S was also discussed and some experiments known from literature (e.g. Truche's pyrite experiment [13]) were performed to verify the model. However, this static model could not give a statement on the duration of a reaction, since the code was not able to take reaction kinetics into account. With Phreeqc, the static experiments were first repeated in order to ensure that the results obtained in the master thesis could also be represented by Phreeqc.

4.7.2 Content representation of the static simulation RAG

A series of simulations were carried out to determine the equilibrium state of a system after (theoretically) infinitely long time (static simulation) and a statement about the effects occurring here to some. In addition, a sensitivity analysis was performed to determine the influence of various factors on the state of equilibrium.

4.7.3 Results and conclusions of the static simulation RAG

The results for the simulation of a varying H₂ content in the gas are shown in the next diagram Figure 46.

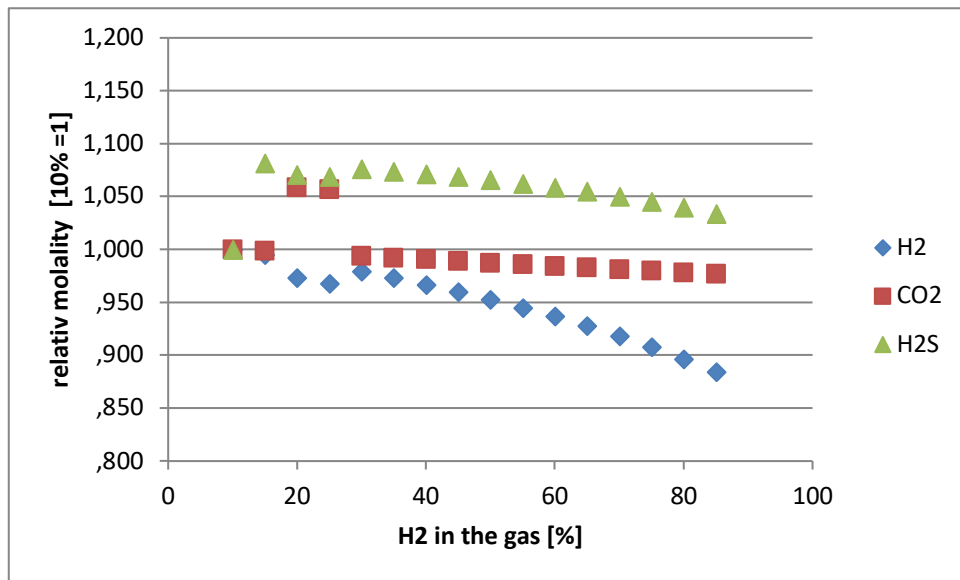


Figure 46: H₂ Sensitivity

One can observe clearly recognizable trends. Paradoxically, the molalities of H₂ and H₂S decrease with increased H₂ content, while the molality of CO₂ remains roughly the same. The outliers of 20% H₂ may be a limited phenomenon or numerical errors. A more detailed analysis of the affected area (10% to 34% H₂ in hydrogen) indicates numerical errors (Figure 47). While the trends are clear and approximately linear, there are some outliers.

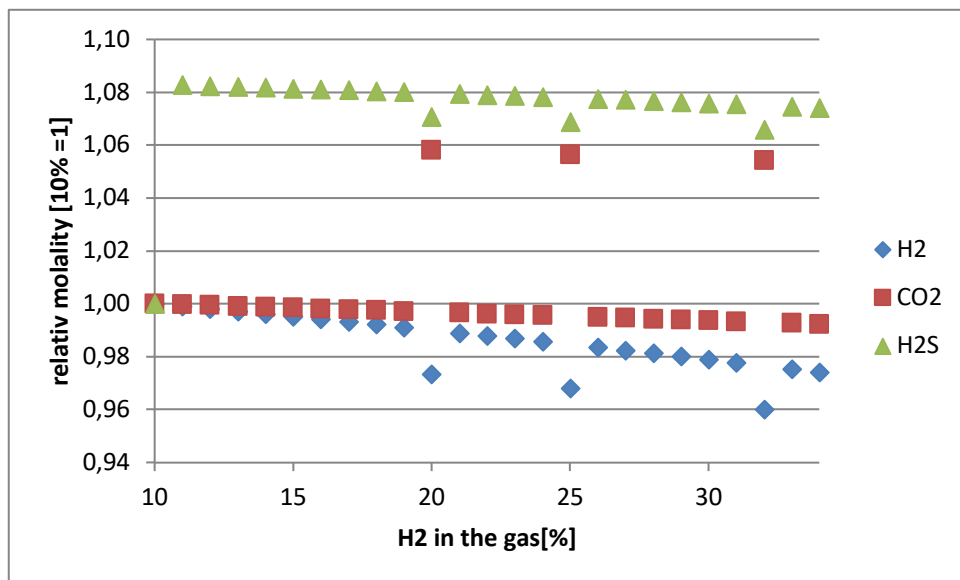


Figure 47: Numerical errors

The results of the simulation of a varying pyrite content in the rock are shown in the next diagram (Figure 48).

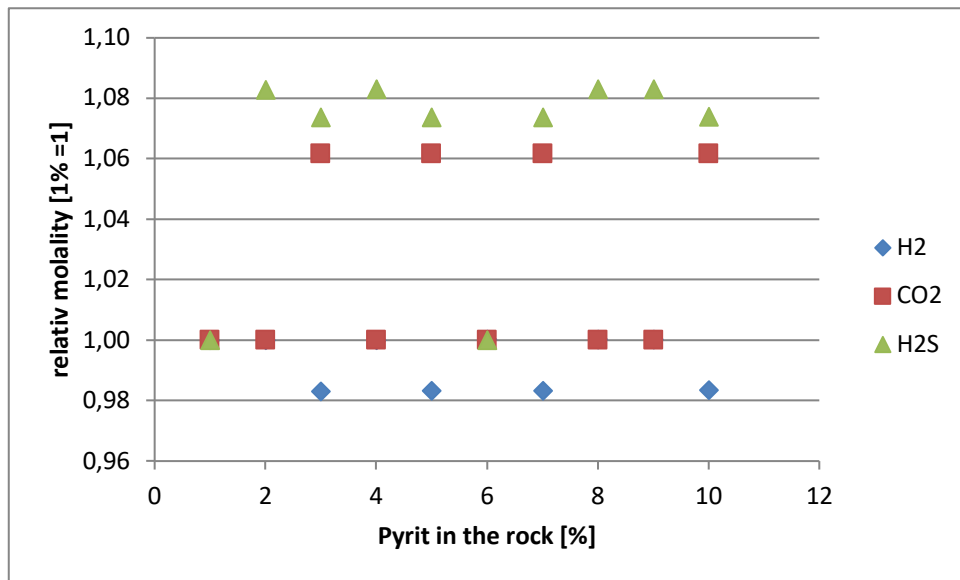


Figure 48: Pyrite Sensitivity

No clear trend is discernible in the molalities. An occurrence of numerical errors due to the oscillations of the values is conceivable. The next diagram shows a clearer reaction relationship (Figure 49).

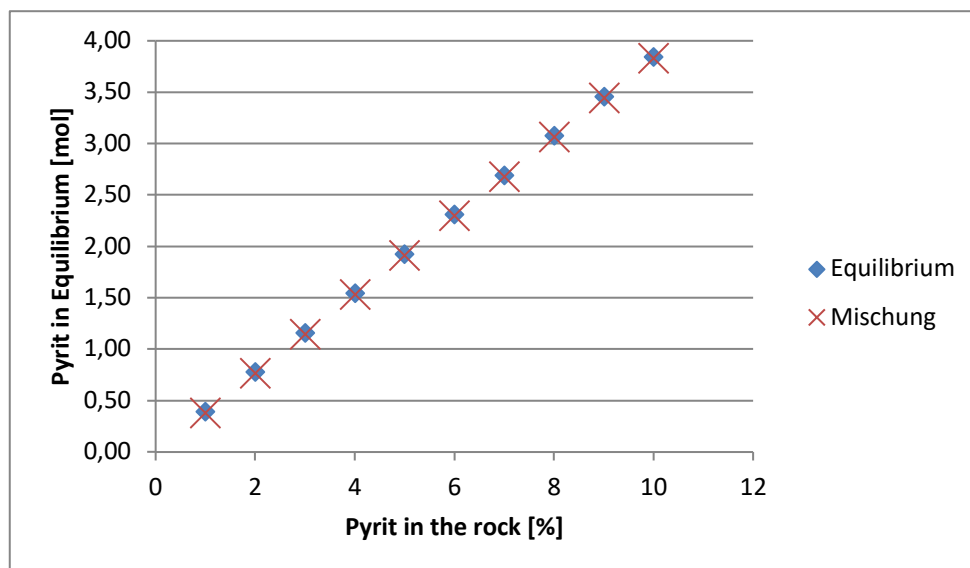


Figure 49: Pyrite sensitivity II

The moles of pyrite in equilibrium are practically identical to the amount of pyrite in the source rock for every percentage of pyrite in the rock. This means that regardless of the pyrite content, this rock remains inert.

Phreeqc makes it possible to identify substances (solid or gaseous) that are thought to be produced during the reaction. The software then trims the numeric in such a way that these substances are actually produced in the equilibrium. This process was performed for gaseous H_2 . It turned out that a large amount of hydrogen was necessary to end up with gaseous hydrogen in the system as the hydrogen does react with multiple substances in the reservoir.

The following diagram provides information about the limit value at which gaseous H_2 occurs in the equilibrium (Figure 50).

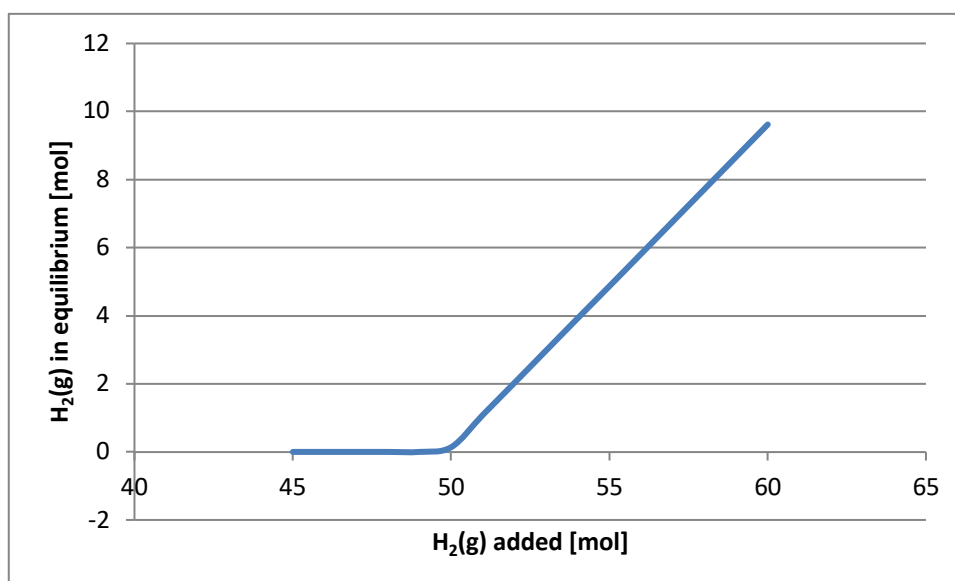


Figure 50: Limit value $H_2(g)$

The limit value necessary for the formation of gaseous H_2 is about 50 mol H_2 in the initial mixture. However, it should be borne in mind that these values refer to 1 litre of pore volume, which according to the ideal gas law can only absorb about one mole of gas (water saturation and other assumptions according to the standard case; temperature and pressure constant). In reality, the pressure and temperature in the system would change considerably (if at all possible). However, this simulation shows that under realistic conditions gaseous hydrogen can never be present in the equilibrium after infinite time.

The equilibrium changes considerably if one assumes that neither calcite nor dolomite are present in the rock (the amount of other minerals increases proportionally). The changes in the limit value for the formation of gaseous hydrogen in the equilibrium are most obvious (Figure 51).

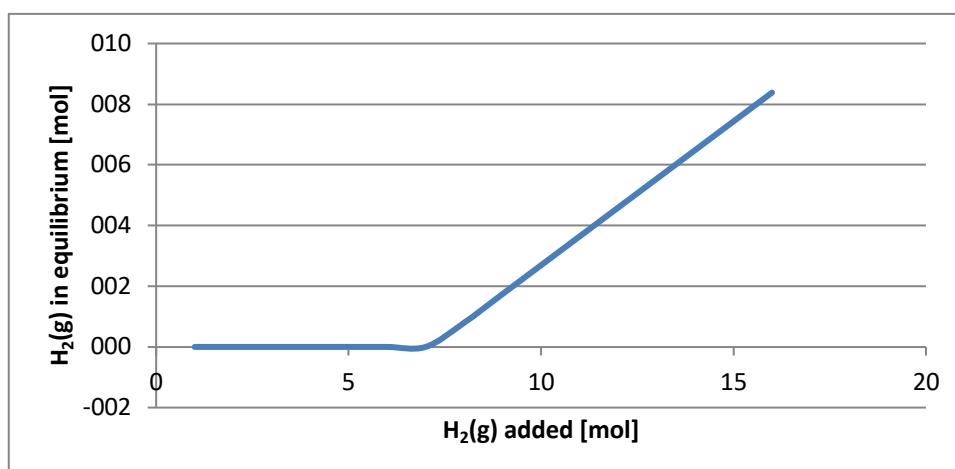


Figure 51: Limit value $H_2(g)$ without calcite and dolomite

This threshold value is also clearly reflected in the change in the pH value (Figure 52).

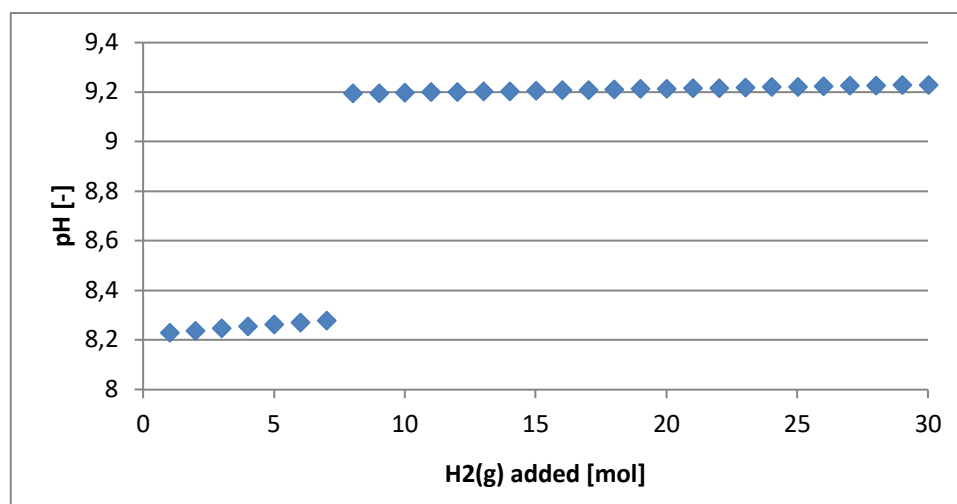


Figure 52: pH value as a function of the added amount of substance H₂(g), without calcite/dolomite in the rock

If the siderite is also removed from the original composition, this effect can be seen even more clearly. The limit value necessary for gaseous hydrogen shifts even further to the left (less than 1 mol). It is also possible to create material balances for individual atoms. For example, it can be determined that calcium atoms in equilibrium only occur in solution and in the minerals calcite and dolomite.

Under realistic conditions, no gaseous hydrogen is found in equilibrium in all simulations in the standard case. Since hydrogen is a highly reactive/highly diffuse substance, this result is realistic. The molality of gaseous hydrogen in the solution is comparatively low. Pyrite is never dissolved in the system, no matter in which concentration it was present in the source rock.

In practice, however, the effects described will hardly be measurable in the reservoir, as they simply run too slowly under reservoir conditions. Especially the low temperature of only 40°C is an obstacle, as the system contains far too little energy to start the only slightly exothermic reactions. This could also be verified with the laboratory tests of IFA Tulln and DBI Leipzig.

4.7.4 Dynamic Simulation RAG

In order to obtain more detailed and meaningful results, it is advisable to carry out dynamic simulations. These provide information about the timing of the chemical reactions and not only about the geochemical equilibrium. Since the equilibrium state is de facto never reached in nature, the first phase of the reactions is particularly relevant. In general, this is also where the reaction rates are highest. Due to the complexity of dynamic processes, such simulations require a series of laboratory experiments and a robust kinetic database. It was already known from [15] that kinetic models and values, especially for clay minerals, are not available. Unfortunately, these cannot be omitted so easily because they contain a significant amount of iron, which also tends to react with hydrogen to FeOOH (Göthite). In addition, the data situation for ferrocalcite was very poor, which obviously raises the same issue as the clays.

Since the geochemical system is also very complex, a great deal of programming would be necessary in order to visualize and evaluate all possible reactions in the system. So, at some

point it had to be admitted that the effort to generate a robust model would have gone far beyond the scope of the project.

Last but not least, it would not have been possible to verify the results of the simulation. Neither in the laboratory tests nor in the field tests could reactions be measured, except for the increase of the pH value. The missing basis made a geochemical simulation impossible, which is why it had to be abandoned.

4.7.5 Content of the MUL simulations

As part of the hydrogen storage feasibility study, a multi-stage workflow was proposed to characterize the behavior of the geochemical system in the presence of hydrogen. The workflow is shown in Figure 53. In this approach different modelling steps are proposed to investigate the short and long term effects of hydrogen on the reservoir. Appropriate assumptions were made for all sections of the modelling. The modelling steps are: (1) the equilibrium "batch model" assuming instantaneous reactions (equilibrium) for hydrogen and minerals; (2) the primary kinetic "batch model" assuming that mineral reactions are kinetically controlled while hydrogen reactions are assumed to occur at local thermodynamic equilibrium; this section consists of two modeling steps. In the first model, mineral reaction data from the literature were used. In the second step, it was assumed that reactions of pyrite and pyrrhotite take place in equilibrium. This is due to experimental findings [16] indicating that these reactions are relatively fast in the presence of hydrogen, whereas most literature data do not take this into account. Further discussions can be found in the results section. The final step (3) is the final batch model in which mineral and hydrogen reactions are considered kinetically controlled. A "sensitivity analysis" of the hydrogen reaction rate (low/medium/high) and the assumption of equilibrium/imbalance for redox pairs was made to investigate their influence on the results.

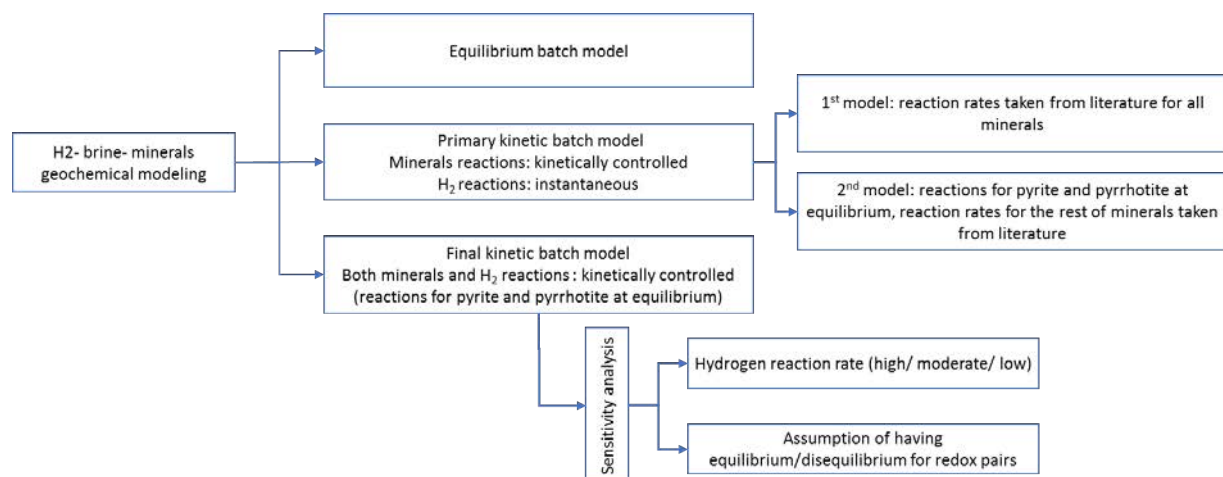


Figure 53: Proposed geochemical modelling workflow as described in the text.

The general findings of geochemical modelling show that hydrogen can react with reservoir water and formation rock under certain conditions and assumptions leading to a partial loss of hydrogen. There are some uncertainties due to the lack of experimental knowledge. This study could serve as a guideline for further experimental investigations (e.g.: experimental quantification of reactions with respect to the kinetic reaction rate in the presence of hydrogen, kinetic hydrogen reaction rates in reservoir water).

Static simulation MUL

As proposed above, in the first step, all possible reactions in the different physical phases under the equilibrium assumption for hydrogen reservoir water-mineral reactions are identified. The results of the model suggest that hydrogen can significantly affect the integrity of the reservoir. If there is enough time for all reactions to take place (e.g. carbonate dissolution/failure, redox reactions and aqueous speciation), this results in a substantial pH increase. The $\text{CH}_4\text{-HCO}_3^-$, $\text{HS}^- \text{-SO}_4^{2-}$, and $\text{CH}_4\text{-CH}_3\text{COO}^-$ redox pairs are the main sinks for hydrogen (consumption) in the system. Furthermore, the presence of H_2 in this system influences the thermodynamic stability of pyrite and the redox reaction in which pyrite is reduced to pyrrhotite.

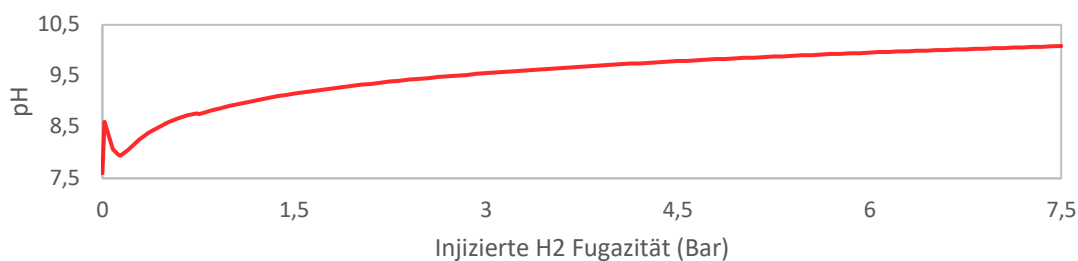


Figure 54: Development of the pH static equilibrium model as a function of injected hydrogen fugacity.

Dynamic simulation MUL

The next section includes kinetic response parameters for primary and secondary minerals in the basic kinetic model. The $\text{CH}_4\text{-HCO}_3^-$ and $\text{CH}_4\text{-CH}_3\text{COO}^-$ redox pairs are decoupled to achieve realistic conditions. The results suggest that geochemical reactions of H_2 with minerals generally have slow kinetic reaction rates, as confirmed by literature. Nevertheless, the kinetic parameters are mostly generated in the absence of hydrogen; therefore, an uncertainty must be considered in view of these rates, especially for the reduction of pyrite to pyrrhotite, which can be significant at low temperatures in the presence of hydrogen gas [16]. A case study in which pyrite-pyrrhotite reactions were considered equilibrium estimates which of the found hydrogen reactions with these minerals are fast enough to effectively increase the pH of the system. The last model is most relevant for application to underground hydrogen storage

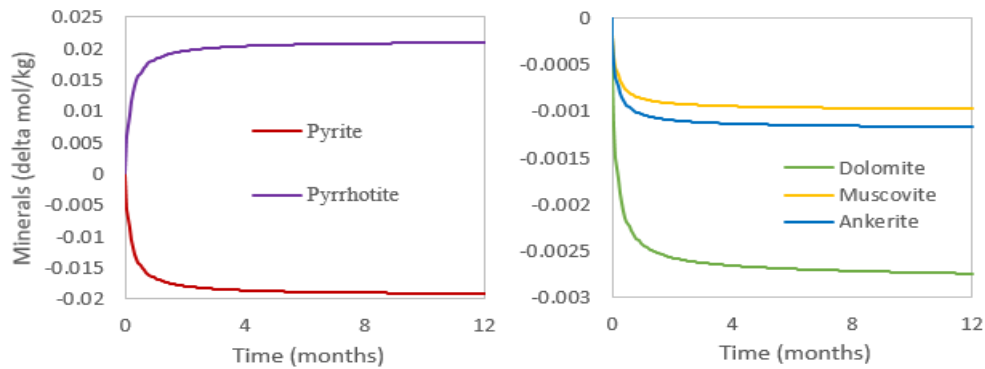


Figure 55: Change in mineral composition during an injection year with an H_2 partial pressure of 7.5 bar (Basic kinetic model based on the initial system of case study 3 and assuming the reactions of pyrite and pyrrhotite are in equilibrium).



Figure 56: pH change (Basic kinetic model based on the initial system of case study 3 and assuming the reactions of pyrite and pyrrhotite are in equilibrium).

Final kinetic „batch model“

In the last section of geochemical modelling, the kinetics of hydrogen solubility were added to the model. Due to the lack of data for hydrogen dissolution reactions, some scenarios were defined to understand under which conditions the probability of hydrogen loss is significant. Furthermore, we compared the same models with cases where the reactions of redox pairs remained in equilibrium. If assumptions are made of both kinetic and equilibrium reactions of redox pairs and the hydrogen reaction rate remains low, the pH increase is small and hydrogen behaves like an inert gas. In the case of moderate to high hydrogen reaction rates, a larger pH increase is observed; nevertheless, this amount remains insignificant if an imbalance is assumed for redox pair reactions and is considerable in the case of an equilibrium assumption for these reactions.

Table 15: Sensitivity analysis of kinetic reaction parameters for hydrogen reactions; three reaction rates (high, medium and slow) were tested by changing the specific reaction areas and the external hydrogen fugacity (after 12 months with a fugacity of 7.5 bar).

Case	Hydrogen Reaction Rate* Surface (mol/(kg water s))	pH Increase	
		Blocking of redox pairs and CH ₄ formation	Assumption of equilibrium of redox pairs
High H ₂ reaction rate	1E-07	0.1148	3.67
Average H ₂ reaction rate	1E-10	0.1148	2.88
Low H ₂ reaction rate	1E-13	0.0191	0.0039

4.7.6 Results and conclusions MUL

In summary, a geochemical workflow has been developed that investigates and quantifies potential geochemical processes that can lead to potential hydrogen loss in porous reservoirs. The geochemical processes were modelled both statically and dynamically at constant pressure and temperature. The modelling method considers both site-specific mineralogy and kinetic reaction rates taken from the literature. In addition, there is a coupling to fast equilibrium processes, such as aqueous speciation reactions. In order to test short- and long-term influences of hydrogen on the reservoir, different geochemical models with different compositions were simulated.

From the modelling results it can be concluded that the main reason for the pH value increase and thus a hydrogen loss is the equilibrium assumption among redox pairs and the pyrite reduction to pyrrhotite. The question of whether a local equilibrium for redox pairs is an appropriate assumption must be clarified by further experimental investigations of the corresponding reactions and data. The abiotic hydrogen redox reaction is kinetically limited and many of the hydrogen-induced redox reactions tend to be negligible at low temperatures. The exception for hydrogen-induced redox reactions is pyrite reduction to pyrrhotite, which already shows significant reduction rates at low temperatures. Alkaline pH conditions could further support pyrrhotite precipitation. However, the quantification of how much hydrogen is lost due to geochemical reactions was outside the scope of this paper. Additionally, the reservoir rock in the investigated are only contains minor fractions of pyrite which makes this sink further neglect able.

Given the full range of uncertainties mainly caused by the lack of reliable kinetic data, the loss of hydrogen and the influence of hydrogen on reservoir parameters cannot be completely excluded. The potential risk of hydrogen loss increases if it is assumed that the redox pair reactions are in equilibrium. The reaction rates used in this work, taken from literature data, are mainly derived from laboratory experiments. It is important to note that in real applications the reaction rates are usually several orders of magnitude smaller than the laboratory values. Consequently, for the field test only a moderate influence can be assumed compared to the laboratory values. In summary, this work package should not only serve as a simulation, but also as a contribution to risk assessment.

4.8 Reference to publications and other documents

No.	Study/Report/ Presentation	Year	Author
1	Power to Gas: Technology and Business Models. Springer Briefs in Energy, Cham, p. 16. 2014	2014	Lehner et al
2	Panel Discussion Economic Factor Natural Gas - Future of the Market, Vienna http://www.report.at/energie/aufmacher/item/88152-kurzbericht-podiumsgespraech-wirtschaftsfaktor-erdgas-zukunft-des-marktes	2015	Lehner
3	GeoTirol Presentation: Underground Sun Storage; A study on properties of hydrogen admixture in porous Underground Gas Storage facilities by means of an in-situ experiment	2016	Pichler
4	SPE Chapter Meeting Leoben and SPE Vienna: Presentation of the results of the geochemical experiments.	2016	Pichler
5	Hydrogen compatibility in pore storages; DVGW report in preparation	TBD	Bauer et al
6	Underground Sun Storage: Store renewable energy underground. DVGW energy water practice, 9:50-54	2014	Bauer et al
7	Underground Sun Storage: A Research Project the hydrogen compatibility of natural gas porous storage facilities. DVGW energy water practice, 8:64–69	2017	Bauer; Pichler
8	DBI final reports: overburden, cement, reservoir water	2016	Lubenau; Rockmann
9	DBI Final Report: Reservoir alteration at 25 and 75 vol.% H ₂ in natural	2017	Lubenau: Rockmann
10	DBI Report Change in the properties of gases through the addition of hydrogen	2014	Lubenau

4.9 List of references

- [1] Chen und e. al, Binary Gas Diffusion of Methane-Nitrogen Through Porous Solids, Michigan, US: AIChE Journal (Vol. 23, No. 3), 1977.
- [2] B. S. Srinivasan, „THE IMPACT OF RESERVOIR PROPERTIES ON MIXING OF INERT CUSHION AND NATURAL GAS IN STORAGE RESERVOIRS,“ Department of Petroleum & Natural Gas Engineering, College of Engineering and Mineral Resources, West Virginia University, Morgantown, West Virginia, US, 2006.
- [3] Paterson, „THE IMPLICATIONS OF FINGERING IN UNDERGROUND HYDROGEN STORAGE,“ Int. J. Hydrogen Energy, Vol. 8, No. 1, pp. 53-59, 1983/ International Association for Hydrogen Energy, Canberra, Australia, 1982.
- [4] S. Gier, „DIAGENESE PELITISCHER SEDIMENTE IN DER MOLASSEZONE OBER.STERREICHS,“ Österreichische Mineralogischen Gesellschaft, Wien, 1998.

- [5] G. Homsey, „Viscous Fingering in Porous Media,“ Department of Chemical Engineering, Stanford University, Stanford, 1987.
- [6] Paterson, „THE IMPLICATIONS OF FINGERING IN UNDERGROUND HYDROGEN STORAGE,“ Int. J. Hydrogen Energy, Vol. 8, No. 1, pp. 53-59, Great Britain, 1982.
- [7] Lucia, „Measurements of H₂ solubility in saline solutions under reservoir conditions: preliminary results from project H₂STORE,“ European Geosciences Union General Assembly, Potsdam, 2015.
- [8] Y.-L. Wang, „Wettability Alteration of Sandstone by Chemical Treatments,“ Hindawi Journal of Chemistry, China, 2013.
- [9] Lassin und e. al, Hydrogen solubility in pore water of partially saturated argillites: Application to Callovo-Oxfordian clayrock in the context of a nuclear waste geological disposal, Fontenay-aux-Roses, France: Physics and Chemistry of the Earth 36 (2011) 1721–1728, 2011.
- [10] K. Taeyoun, H. Seho und J. Seonghyung, „Petrophysical approach for estimating porosity, clay volume, and water saturation in gas bearing shale: A case study from the Horn River Basin, Canada,“ Austrian Journal of Earth Science, Vienna, 2016.
- [11] P. Carden und L. Paterson, Physical, Chemical and Energy Aspects of Underground Hydrogen Storage, Bd. Vol. 4, I. A. f. H. Energy, Hrsg., Canberra: International Journal Hydrogen Energy, 1979.
- [12] A. Hoch und M. James, „Gas Migration and Rock-matrix Diffusion in Higher Strength Rocks,“ AMEC/000450/001, Issue 4, Harwell Oxford, 2013.
- [13] Truche, „Experimental reduction of aqueous sulphate by hydrogen under hydrothermal conditions: Implication for the nuclear waste storage,“ Elsevier, Geochimica et Cosmochimica Acta 73 (2009) 4824–4835, 2009.
- [14] Garrels et al, Solutions Minerals and Equilibria, Freeman, Cooper & Co, 1995.
- [15] M. Pichler, Assessment of Hydrogen Rock Interaction During geological Storage of CH₄-H₂ Mixtures, Bd. Master Thesis, Leoben: Montanuniversität Leoben, 2013.
- [16] S. Betelu, C. Lerouge, G. Berger, E. Giffaut und I. Ignatiadis, „Mechanistic and kinetic study of pyrite (FeS₂)-hydrogen (H₂) interaction at 25°C using electrochemical techniques,“ BRGM, France, 2015.

4.10 Contact details

RAG Austria AG
Department UGS Entwicklung und Management
Schwarzenbergplatz 16
1015 Wien
+43(0)50724-0
www.rag-austria.at

MONTANUNIVERSITÄT LEOBEN
Univ.-Prof. Dr.-Ing. Markus Lehner
Lehrstuhl für Verfahrenstechnik des industriellen Umweltschutzes
Department Umwelt- und Energieverfahrenstechnik
Montanuniversität Leoben
Franz-Josef-Str. 18
A-8700 Leoben, Austria
<http://vtiu.unileoben.ac.at>
vtiu@unileoben.ac.at
Phone: +43 3842 402-5001
Fax: +43 3842 402-5002

MONTANUNIVERSITÄT LEOBEN
Univ.-Prof. Dipl.-Phys. Dr.rer.nat. Holger Ott
Lehrstuhl für Reservoir Engineering
Department Petroleum Engineering
Montanuniversität Leoben
Parkstraße 27
A-8700 Leoben, Austria
Mail: holger.ott@unileoben.ac.at
Phone: +43 43 3842 402 3000

Authors: Dipl.-Ing. Fritz Kittinger, Dipl.-Ing. Markus Pichler, Dipl.-Ing. Neda Hassannayebi

5 Microbiological processes in hydrogen-loaded reservoirs

This chapter summarizes the results of the laboratory tests carried out at the Institute for Environmental Biotechnology (IFA-Tulln). The results were used as an important basis for the performance of the field tests (see chapter 8).

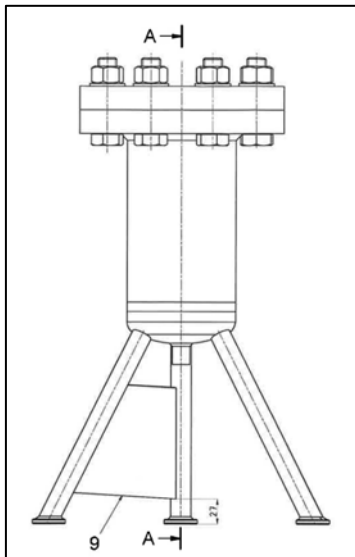
5.1 Task

In this work package, the microbiological consortium present in the test field was to be characterized and the hydrochemical properties of the formation water was determined. Subsequently, it should be investigated how the microbiological consortium reacts to hydrogen exposure, whether hydrogen-converting processes occur and if/how these can be prevented.

5.2 Content presentation

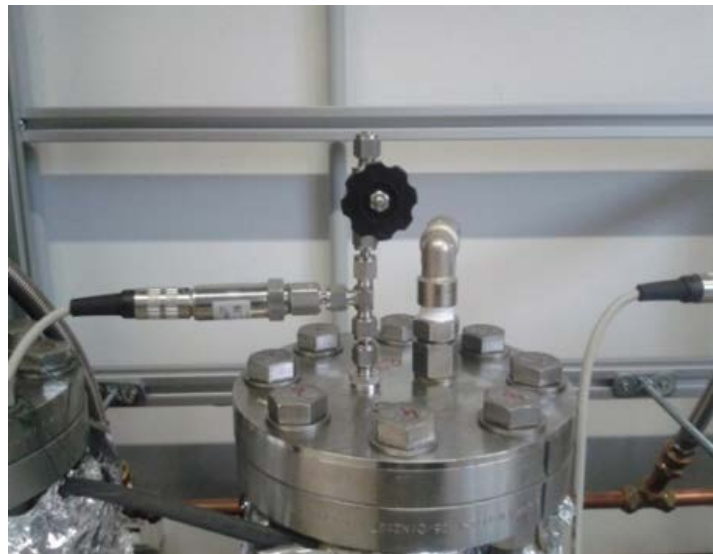
5.2.1 Experimental setup

A central point was to simulate the conditions in the natural gas storage facility (test field) in the laboratory. Ten high-pressure bioreactors were used for this purpose. These were made of a special steel quality suitable for hydrogen exposure and corrosion resistant to increased salinity (reservoir water) and hydrogen sulphide. The selection of suitable sealing materials also had to be taken into account in this context. In addition, all legal safety regulations for the handling of gaseous hydrogen had to be fulfilled. Before the start of the test, the reactors were inspected by the Technical Inspection Agency (TÜV) and, as a result, calculated in accordance with ATEX (explosive atmospheres) for the intended installation site. Based on these specifications, the high-pressure bioreactors could be operated at max. 55 bar and max. 45°C. Although the selected operating pressure of 45 bar is below the storage pressure for the test field (80 bar), microbiological processes caused by hydrogen exposure can also be expected under the selected test conditions. Figure 57 shows a schematic diagram of a reactor, Figure 58 shows a detailed view of a reactor with the attached fittings (needle valve, bursting disc, pressure sensor). Figure 59 shows all the reactors in operating condition with the insulation required due to the operating temperature of 45°C. The reactor is mounted with the valves (needle valve, bursting disc, pressure sensor).



Source: MAL

Figure 57: Diagram



Source: BOKU Wien

Figure 58: Reactor head with fittings

Figure 59: Isolated high-pressure bioreactors



Source: BOKU Wien

5.2.2 Test materials

For the successful simulation of the test field or natural gas storage facility in bioreactors, the following components were required in addition to the approximation of the pressure and the prevailing temperature: (i) fresh **reservoir water** (see Figure 60) extracted from the test field in autumn 2013, (ii) **drill cores** from a biogenic natural gas reservoir - drill cores from a natural gas reservoir were used which had a mineralogical distribution very similar to that of the test field and which originated from the same geological stratification (Haller series) (see Figure 61). (iii) In order to simulate hydrogen exposure in the presence of natural gas, appropriate

gas mixtures were required. Mixtures of hydrogen in methane with a hydrogen content of 4-10% (v/v) were used.



Source: BOKU Wien (RAG)

Figure 60: Reservoir water



Source: BOKU Wien (RAG)

Figure 61: Drill core

5.2.3 Investigation methods

5.2.3.1 Hydrochemical analyses

For determination of **pH** value, **redox potential** (mV) and **conductivity** (mS/cm) a measuring instrument from HACH (*HQ40d multi base unit*), equipped with the following sensors, was used: pH - *HACH IntelliCAL PHC101 Standard Gel Filled pH Electrode*, redox potential - *HACH IntelliCAL MTC301 Standard Refillable ORP Electrode*, conductivity - *HACH IntelliCAL CDC401 standard conductivity probe*.

Dissolved **chloride** (Cl^-), **nitrate** (NO_3^-), **sulfate** (SO_4^{2-}) and **phosphate** (PO_4^{3-}) were quantified by ion chromatography (THERMOFISHER Scientific *Dionex ICS 900*). Dr. LANGE cell tests were used to determine the dissolved contents of **iron** ($\text{Fe}^{2+}/\text{Fe}^{3+}$), **ammonium** (NH_4^+) and **carbon dioxide** (CO_2). **TOC** (total organic carbon), **TIC** (total inorganic carbon) and **TC** (total carbon) were determined with a TOC analyzer from SHIMADZU (*TOC-V CPH*). The elements **Al** - aluminum, **As** - arsenic, **Ba** - barium, **Ca** - calcium, **Cd** - cadmium, **Co** - cobalt, **Cr** - chromium, **Cu** - copper, **Fe** - iron, **K** - potassium, **Mg** - magnesium, **Mn** - manganese, **Mo** - molybdenum, **Na** - sodium, **Ni** - nickel, **P** - phosphorus, **Pb** - lead, **S** - sulfur, **Se** - selenium, **Zn** - zinc were determined with a *HORIBA Ultima Expert ICP-OES* spectrometer.

5.2.3.2 Gas analyses

Methane, **carbon dioxide**, **hydrogen**, **oxygen** and **nitrogen** were determined with a modified *AGILENT 7890a gas chromatography* equipped with a FID (flame ionization detector) and a

PDD (pulsed discharge ionization detector). For the separation of the gas mixture a combination of the following columns was used: *PlotQ15 Agilent 19095P-Q03*, *PlotMS Agilent 19095P-MS6*, *PlotQ30 Agilent 19095P-Q04*.

Gas components such as **hydrogen sulfide**, **acetic acid** and **carbon monoxide** were determined with *Dräger-Röhrchen®*.

5.2.3.3 Molecular biological analyses

DNA was extracted using phenol/chloroform (cf. [1]) to determine the microbiological consortium in the reservoir water of the test field and in the water of the high-pressure bioreactors. Subsequently, the 16S rDNA was amplified with PCR (polymerase chain reaction) using the primer pair for amplicon V4 (see Figure 62). The 16S rDNA was sequenced by *Microsynth AG*.

- **NGS_515f**
(5'-TCG TCG GCA GCG TCA GAT GTG TAT AAG AGA CAG GTG CCA GCM GCC GCG GTA A-3')
- **NGS_806r**
(5'-GTC TCG TGG GCT CGG AGA TGT GTA TAA GAG ACA GGG ACT ACH VGG GTW TCT AAT-3')

Figure 62: Primer pair V4

The extraction of DNA from drill cores was carried out with the FastDNA Spin Kit for Soil from *MP Biomedicals*. The further procedure is identical with the methods for reservoir water described above.

5.2.4 Test procedure

5.2.4.1 Preincubation phase of the drill cores

The drill cores originate from a strictly anaerobic environment (no oxygen in the deposit), but they were stored under aerobic conditions for several years, which significantly changed the original microbiological consortium. In order to create growth conditions similar to those in the test field, the cores were incubated under anaerobic conditions together with formation water in gas-tight aluminium-plastic bags at 35°C for several weeks.

5.2.4.2 Inoculation phase

The high-pressure bioreactors were filled under argon atmosphere with the preincubated drill cores and with fresh reservoir water from the test field (see Figure 63). This was to ensure microbial colonization of the cores comparable to that in the test field. Two of the ten high-pressure bioreactors served as abiotic controls (no living microorganisms present). They were sterilized with 35 kGy and, in order to exclude post-germination, mixed with a biocide. The reactors were insulated with mineral wool and aluminum foil, and tempered to 45°C. The

reactors were then sterilized with a biocide. The inoculation was carried out over a period of one month.



Figure 63: Filling of high-pressure bioreactors *Source: BOKU Wien*

5.2.4.3 Methane phase

To simulate a natural gas reservoir, the high pressure bioreactors were filled with methane (45 bar at 45°C). In the process, reactor water was extracted to a residual content of approx. 20 % (close to the water content of the test field which is 35%). The extracted water was hydrochemically examined and characterized by molecular biology. The microbial community found is subsequently referred to as the microbial start-up consortium prior to hydrogen exposure. The methane phase lasted 86 days.

5.2.4.4 Hydrogen phase

Methane was removed from the reactors to a residual pressure of 0.5 bar, followed by a further withdrawal of reactor water for hydrochemical investigations. The reactors were then filled with gas mixtures (4-10 % hydrogen and 0.3-2.5 % carbon dioxide in methane) (45 bar). Table 16 shows the allocation of the different gas mixtures to the ten high-pressure bioreactors at the start of the hydrogen phase. Directly after gas filling, the first gas sample was taken with a "gas mouse" (see Figure 64). Subsequently, a gas sample was taken weekly. The hydrogen phase took a total of 186 days. Selected reactors were refilled with a corresponding gas mixture after complete hydrogen consumption.

Table 16: Assignment of the individual gas mixtures at the start of the hydrogen phase

Reactor		H ₂	CO ₂	CH ₄	further components
Nr.		(Vol.-%)	(Vol.-%)	(Vol.-%)	(mg/m ³)
1	biotic	4	0,3	95,7	
2	biotic	10	0,3	89,7	
3	biotic	10	2,5	87,5	
4	biotic	4	0,3	95,7	
5	biotic	10	0,3	89,7	
6	biotic	10	2,5	87,5	
7	abiotic	10	2,5	87,5	
8	abiotic	10	2,5	87,5	
9	biotic	4	0,3	~95,7	6,2 Carbonyl sulfide;
10	biotic	4	0,3	~95,7	5,2 Hydrogen sulphide; 13,6 Propylmercaptan



Figure 64: Gas sampling Source: BOKU Wien

5.2.4.5 Opening of the reactors

After a maximum hydrogen exposure of 186 days, the reactors were opened (see Figure 65). The remaining reactor water was hydrochemically analyzed and subjected to a determination of the microbiological final consortium. DNA was also extracted from parts of the drill cores. The drill cores were mineralogically and petrographically examined (RAG, OMV Laboratory) in order to determine possible dissolution processes, especially with regard to calcite and dolomite.



Figure 65: Opening of a reactor *Source: BOKU Wien*

5.2.5 Possible microbiological conversions at hydrogen exposure

5.2.5.1 Background

Microbiological consortia in oil reservoirs, most of which are comparable to natural gas reservoirs, are usually divided into three metabolic groups: (i) methane-forming archaea (methanogens), (ii) sulfate-reducing bacteria and (iii) fermentative bacteria (cf. [2], p. 115 ff). It should also be borne in mind that the sampling of reservoir water and thus the evaluation of the microbiological consortium in the reservoir is only possible via wells (boreholes). Thus, besides autochthonous (originally present), allochthonous (externally introduced) microorganisms may also be present. The introduction can take place either by the drilling itself, the drilling mud or during technical overhauls. The presence of allochthonous microorganisms is all the more probable if the reservoir water has a low salt content and mesophilic (20-40°C) temperatures (see [2]). However, the microorganisms must be able to survive and multiply under oxygen-free conditions.

The storage of hydrogen in natural gas deposits can lead to increased microbiological activity (see [3]). This is especially true if suitable terminal electron acceptors (CO_2 , SO_4^{2-} , Fe^{3+} , Mn^{4+}) are present. In the following, hydrogenotrophic (hydrogen-consuming) microbiological processes are described which are important for natural gas reservoirs.

5.2.5.2 Sulphate-reducing bacteria (SRB)

Sulphate-reducing bacteria and Archaea (SRB) are among the first microorganisms to have developed on earth. They are believed to have been active before oxygen photosynthesis. SRB are anaerobic, heterotrophic microorganisms that can use oxygen-containing sulfur compounds (such as sulfate, sulfite, thiosulfate, trithionate, etc.) as well as elemental sulfur

(S°) as terminal electron acceptors (see [2]). The end product is hydrogen sulphide (H₂S), which is toxic, flammable and highly corrosive to metals and concrete. In the natural gas industry, natural gas containing hydrogen sulphide is also referred to as sour gas, the permitted proportion in natural gas in Austria is regulated in the ÖVGW Guideline G31 (H₂S 5 mg/m³). SRB's are therefore among the best-studied microorganisms in natural gas and oil deposits. They can be found indigenously in the reservoir, especially when kerogens with high sulphur contents are used as starting materials for crude oil and natural gas (cf. [4]). If sufficient sulphate is present, complete hydrogen spiking can occur in the natural gas storage facility (cf. equation 6-1), which in addition to the generation of undesirable H₂S also means a total energy loss of the stored hydrogen.

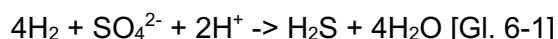


Table 1 gives an overview of SRBs found and isolated in oil fields. It also shows the wide range of salinity and temperature in which SRB can occur.

Table 17: Mesophilic and thermophilic SRB (adapted [5])

Species	Salinity (%)		Temperature (°C)		Complete Oxidizer
	Range	Optimum	Range	Optimum	
<i>Archaeoglobus fulgidus</i>	0.02–3	2	60-85	76	+
<i>Desulfacinum infernum</i>	0–5	1	40-65	60	+
<i>Desulfobacter vibrioformis</i>	1–5	ND	5-38	33	+
<i>Desulfobacterium cetonicum</i>	Up to 5	1	20-37	30-35	+
<i>Desulfomicrobium apsheronum</i>	0–8	ND	4-40	25-30	-
<i>Desulfotomaculum halophilum</i>	1–14	4-6	30-40	35	-
<i>Desulfotomaculum kuznetsovii</i>	0–3	0	50-85	60-65	+
<i>Desulfotomaculum nigrificans</i>	Up to 4	1	40-70	60	-
<i>Desulfotomaculum thermocisternum</i>	Up to 5	0.3-1.2	41-75	62	-
<i>Desulfovibrio gabonensis</i>	1-17	5-6	15-40	30	-
<i>Desulfovibrio longus</i>	0-8	2	10-40	35	-
<i>Desulfovibrio vietnamensis</i>	0-10	5	12-45	37	-
<i>Thermodesulfobacterium mobile</i>	ND	ND	45-85	65	-
<i>Thermodesulfurhabdus norvegicus</i>	0-5.6	1.6	44-74	60	+

5.2.5.3 Fermentative bacteria

Fermentative bacteria, which occur indigenously in oil fields, metabolize organic substrates such as alkanes and aromatic compounds. Among them is the chemoorganotrophic genus *Thermotoga*. End products of the metabolism here are acetate, CO₂ and H₂ (cf. [6]). Gases produced in a reservoir by fermentative processes can lead to an increase in reservoir pressure. Fermentative bacteria are also used for microbial enhanced oil recovery (MEOR) (see [2]). Table 18 shows fermentative bacteria isolated from oil fields. It is noteworthy that some fermentative bacteria can reduce elemental sulphur or sulphur oxides, which in turn can produce undesirable hydrogen sulphide.

Table 18: Fermentative bacteria isolated from oil fields (adapted [5])

Species	NaCl (%)		Temperature (°C)		Reduction of sulfur compound	
	Range	Optimum	Range	Optimum	S°	S ₂ O ₃ ²⁻
<i>Acetoanaerobium romashkovii</i>	ND	ND	30-60	37	ND	ND
<i>Anaerobaculum thermoterrenum</i>	0-2	1	28-60	55	+	+
<i>Dethiosulfovibrio peptidovorans</i>	1-10	3	20-45	42	+	+
<i>Geotoga petraea</i>	0.5-10	3	30-55	50	+	ND
<i>Geotoga subterranea</i>	0.5-10	4	30-60	45	+	ND
<i>Haloanaerobium acetoehtylicum</i>	6-20	10	15-45	34	ND	ND
<i>Haloanaerobium congolense</i>	4-24	10	20-45	42	+	+
<i>Haloanaerobium salsugo</i>	6-24	9	22-51	40	ND	ND
<i>Petrotoga miortherma</i>	0.5-10	3	35-65	55	+	ND
<i>Spirochaeta smaragdinae</i>	1-10	5	20-40	37	+	+
<i>Thermoanaerobacter brockii</i>	0-4.5	ND	37-75	55-60	+	+
<i>Thermotoga elfii</i>	0-2.4	1.2	50-72	66	-	+
<i>Thermotoga hypogea</i>	0-1.5	0-0.2	56-90	70-75	-	+
<i>Thermotoga subterranea</i>	0-2.4	1-2	50-75	70	-	+
*ND - not detected						

Homoacetogenesis is one of the most relevant processes in the group of fermentative bacteria for the storage of hydrogen (cf. equation 6-2). As with the reduction of sulfate (equation 6-1), this conversion results in a total loss of the energy of the stored hydrogen, unless Archaea is present in the reservoir. If these are active, they can form methane from the acetate.



Acetogens (acetate-forming microorganisms) are obligatory anaerobic bacteria, they form acetate by fermentation of organic substances. Homoacetogenic microorganisms, on the other hand, form acetate directly from carbon dioxide (electron acceptor) and hydrogen (electron donor). Prominent examples are the bacteria "*Clostridium aceticum*" and "*Acetobacterium woodii*" (see [7]).

5.2.5.4 Methanogenic microorganisms

Methanogenic microorganisms belong to the domain of the Archaea, just as bacteria do not possess any cell organelles. Some species of methanogens include the term "Bacteria" in their name, but they are currently classified as belonging to the Archaea domain. Methanogenic microorganisms form methane (CH₄) from alcohols, acetate and the gases H₂ and CO₂. Depending on the substrate used, they are divided into 3 main groups:

- Methylotrophic methanogens use methanol and methylamines to produce methane (cf. [5], [6]).
- Acetoclastic methanogens use acetate for methanogenesis, only the order of methanosarcinales (domain Archaea, Phylum Euryarchaeota, class Methanomicrobia) is capable of this metabolic process (see [7]).
- Hydrogenotrophic methanogens use CO₂ and H₂ to form methane (cf. [8] & cf. equation 6-3). This is the only microbial process in which methane is formed directly from gases.

$$\text{CO}_2 + 4\text{H}_2 \rightarrow \text{CH}_4 + 2\text{H}_2\text{O} \text{ [Gl. 6-3]}$$

Table 19 gives an overview of methanogens isolated from oil fields and shows their tolerance to temperature and salinity with common reference to possible substrate utilization.

Table 19: Mesophilic and thermophilic methanogens isolated from oil fields (adapted [5])

Species	Optimum	Temperature (°C)		Substrates used		
	NaCl (%)	Range	Optimum	Methyl- amines	Acetate	Hydrogen
<i>Methanobacterium bryantii</i>	0-2	25-40	37	-	-	+
<i>Methanobacterium ivanovii</i>	0.09	10-55	45	-	-	+
<i>Methanobacterium thermoaggregans</i>	2-4	40-70	60	-	-	+
<i>Methanobacterium thermoalcaliphilum</i>	0-2	30-80	65	-	-	+
<i>Methanobacterium thermoautrophicum</i>	0-30	40-70	60	-	-	+
<i>Methanocalculus halotolerans</i>	5	25-45	38	-	-	+
<i>Methanococcus thermolithotrophicus</i>	1.4-2.4	17-62	60	-	-	+
<i>Methanohalophilus euhalobius</i>	6	10-50	28-37	+	-	-
<i>Methanoplanus petrolearius</i>	1-3	28-43	37	-	-	+
<i>Methanosarcina mazei</i>	0.1-2	10-50	37	+	+	-
<i>Methanosarcina siciliae</i>	2.4-3.6	20-50	40	+	-	-

Finally, it can be stated that any excessive proliferation of microorganisms also carries the risk of blocking the pores of the natural gas reservoir, in addition to other undesirable processes such as in situ acidification, e.g. in the case of acetate formation, and corrosion of technical installations in the case of hydrogen sulphide formation.

5.3 Results and conclusions

Test data and results that are relevant for the storage of hydrogen in porous underground natural gas storage facilities served as a basis for the decision to carry out the field test (test field).

5.3.1 Hydrochemical analyses

In the following, the measured values of the hydrochemical analyses and the changes that occurred during the experiments are listed. Table 20 shows the pH value and sulphate content of the start methane phase, start hydrogen phase and end (reactor opening). In addition, the values of the formation water from the gas storage tank are given.

Table 20: pH value and sulphate contents of the reactors and the test field

Reaktor	Start Methan-phase	Reaktor-öffnung	Start Methan-phase	Start Wasserstoff-phase	Reaktor-öffnung
	pH	pH	SO ₄ ²⁻ (mg/L)	SO ₄ ²⁻ (mg/L)	SO ₄ ²⁻ (mg/L)
Testfeld	8,7	-	17	-	-
1	8,4	9,5	327	378	x
2	8,2	10,5	167	237	45
3	8,0	9,6	313	328	45
4	8,0	10,6	483	380	145
5	8,2	10,4	478	441	14
6	8,1	8,6	506	362	<2,4
7	9,0	x	450	548	253
8	9,0	x	411	449	54
9	7,5	x	1282	1163	306
10	7,5	9,7	1096	1455	17
(x nicht gemessen da Probenmenge unzureichend)					

The increase in the pH value in the course of gas exposure is clearly visible. Furthermore, a very strong increase of the sulphate contents in the reactor water compared to the formation water of the test field was recorded, although no sulphate-containing mineral was found in the cores (see Table 21). In-depth investigations with drill cores not installed in reactors showed that the increased sulphate contents were due to the drilling mud used during coring operation (cf. [9]).

Table 21: Distribution of the minerals of the drill core used at different depths (data in %)

Sample name	Depth (m)	Quartz	K-Feldspar	Plagioclase	Calcite	Dolomite	Ankerite	Siderite	Clay Tot + Mica
Sample 1	1158.32	21	2	6	17	11	5	3	35
Sample 2	1164.04	47	3	8	5	13	5	0	20
Sample 3	1165.80	48	3	7	4	12	6	0	17
Sample 4	1169.13	45	3	8	5	11	6	0	22

Source: RAG

The main source for the input of sulphate into the reactor water was therefore barite (barium sulphate) as a component of the drilling mud used. Sulfate penetrated the outer layer of the core during drilling and was washed out of the core during incubation in the reactor (cf. [10]). A further investigation of the drill core revealed a leaching potential of ~ 3 mg sulphate per g core. The individual cores in the reactors had a mass between 2.7 and 3 kg. Since sulfate, as already mentioned in chapter 5.2.5, can act as a terminal electron acceptor for SRB, this is also an explanation for the decrease of the sulfate content at the end of the test series. The mean decrease in sulfate concentration is lower in the abiotic controls. No hydrogen depletion was observed for these reactors either (see Figure 69).

5.3.2 Gas analyses

All reactors were sampled at regular intervals (see Figure 64 in Chapter 72). Figure 66 shows the concentration curve of hydrogen, carbon dioxide and methane (vol.%) for reactors 1 and 4 from day 0 to day 109. Both reactors were started with a gas mixture containing 4 % hydrogen and 0.3 % carbon dioxide in methane.

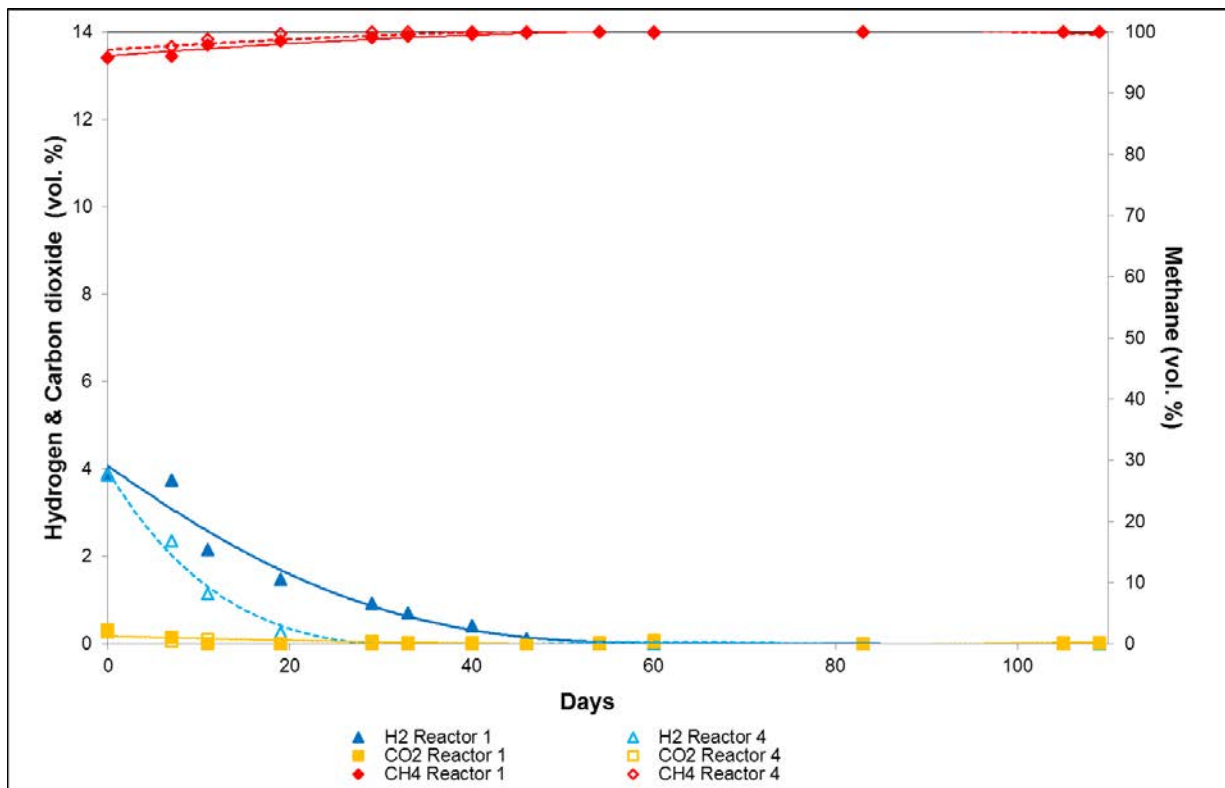


Figure 66: Concentration curve of the gas components in reactors 1 and 4: 4 % H₂, 0.3 % CO₂ in methane *Source: BOKU*

After 109 days, the reactors were refilled with a gas mixture with a higher hydrogen content (10 % hydrogen and 0.3 % carbon dioxide in methane - see Figure 67).

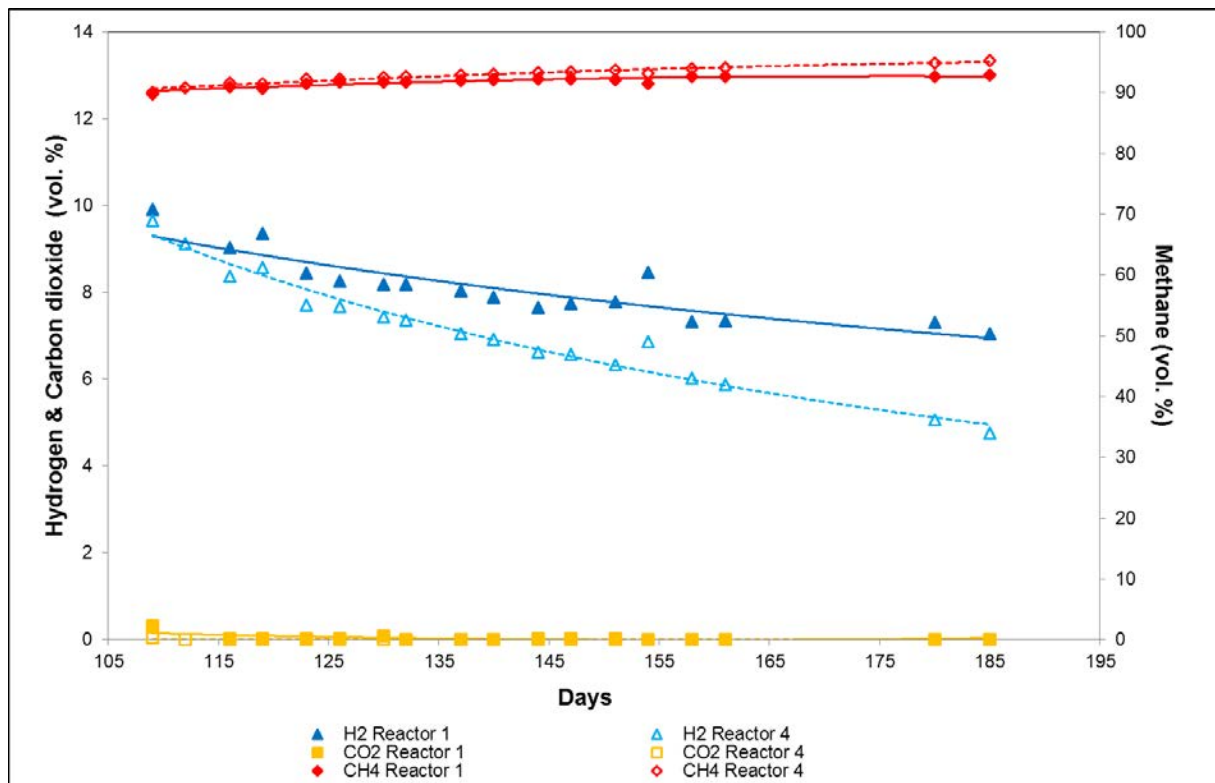


Figure 67: Concentration curve of the gas components in reactors 1 and 4: 10 % H₂, 0.3 % CO₂ in methane, refilling on day 109 Source: BOKU

Figure 66 clearly shows that the hydrogen content drops from 4 vol. % to 0 vol. % within 30-50 days. Carbon dioxide is also close to zero, but at 0.3 vol. % it is sub-stoichiometrically present for hydrogenotrophic methanogenesis and thus cannot explain the decrease in hydrogen; even after refilling, the decrease in hydrogen is disproportionate to the existing carbon dioxide content (see Figure 67). However, both reactors had a high sulphate content of 380 mg/L at the start of the hydrogen phase, which decreased sharply during the course of the experiment. It is assumed that sulphate, in addition to carbon dioxide, acted as an additional terminal electron acceptor for microorganisms (see equation 6-1). However, no increased hydrogen sulphide content could be measured in the gas phase. This can be explained by the fact that the high content of dissolved bivalent iron in the reactor water led to a precipitation of iron sulphide. This is confirmed by a black discoloration observed on the outer layer of the cores (penetration depth of the drilling mud) (see Figure 68 and [9]). Another component of the drilling fluid is potassium carbonate (K₂CO₃), which was also detected in the outer layer of a drill core. This can act as a CO₂ source and thus as an electron acceptor for hydrogenotrophic methanogenesis.



Figure 68: Discoloration of the outer edge of a drill core when the reactors are opened *Source: BOKU*

Figure 69 shows the concentration curve of the gas components over the entire test period for reactors 2 and 5. In this case, the initial hydrogen concentration was 10 vol. % and the reactors were not refilled with gas. Here, too, a complete or almost complete decrease in hydrogen can be observed, which in turn can be explained by sulphate and CO₂ from the drilling mud.

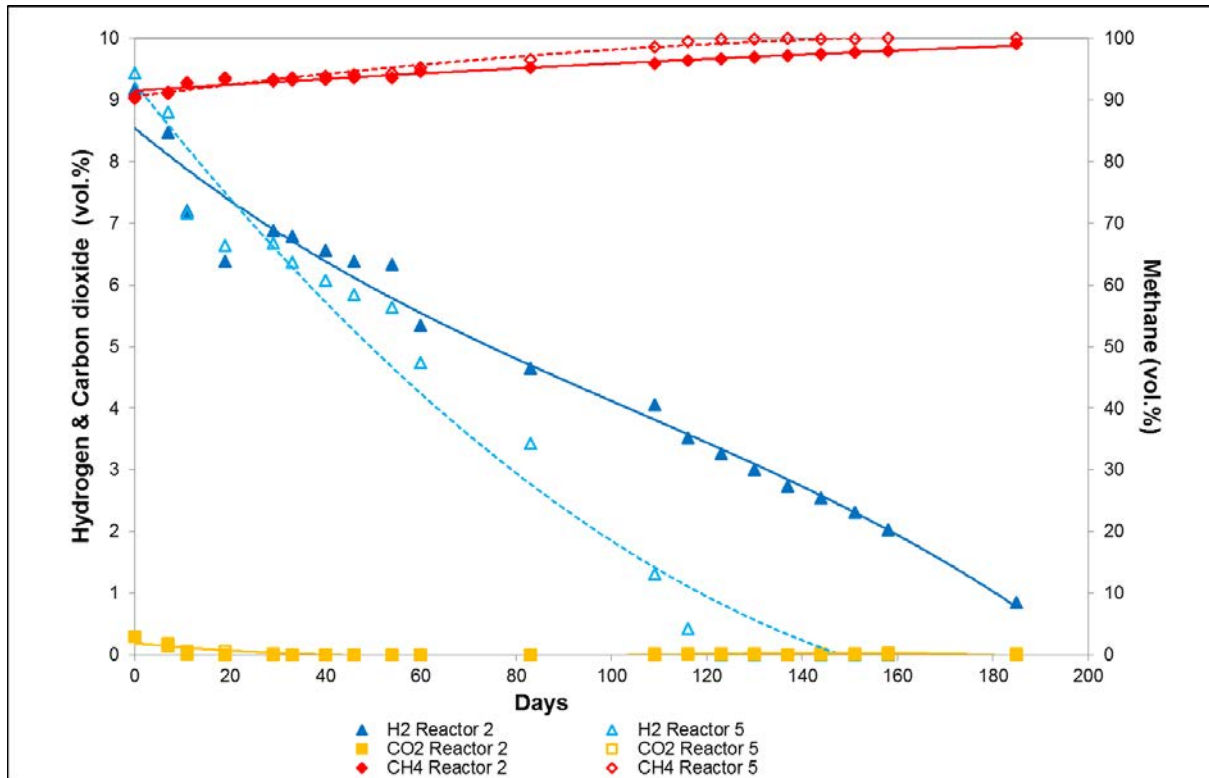


Figure 69: Concentration curve of the gas components in reactors 2 and 5: 10 % H₂, 0.3 % CO₂ in methane Source: BOKU

Figure 70 shows the concentration curve of the gas components for the abiotic controls (reactors 7 and 8). A significant decrease in the hydrogen concentration was not observed (≈ 0.05). This suggests that abiotic hydrogen consumption processes do not occur to any relevant extent under the selected experimental conditions.

The initial decrease of carbon dioxide in the abiotic control reactors confirms that the initial decrease of carbon dioxide concentration in the biotic reactors (Figure 66, Figure 67 and Figure 69) is due to dissolution of carbon dioxide in the reactor water.

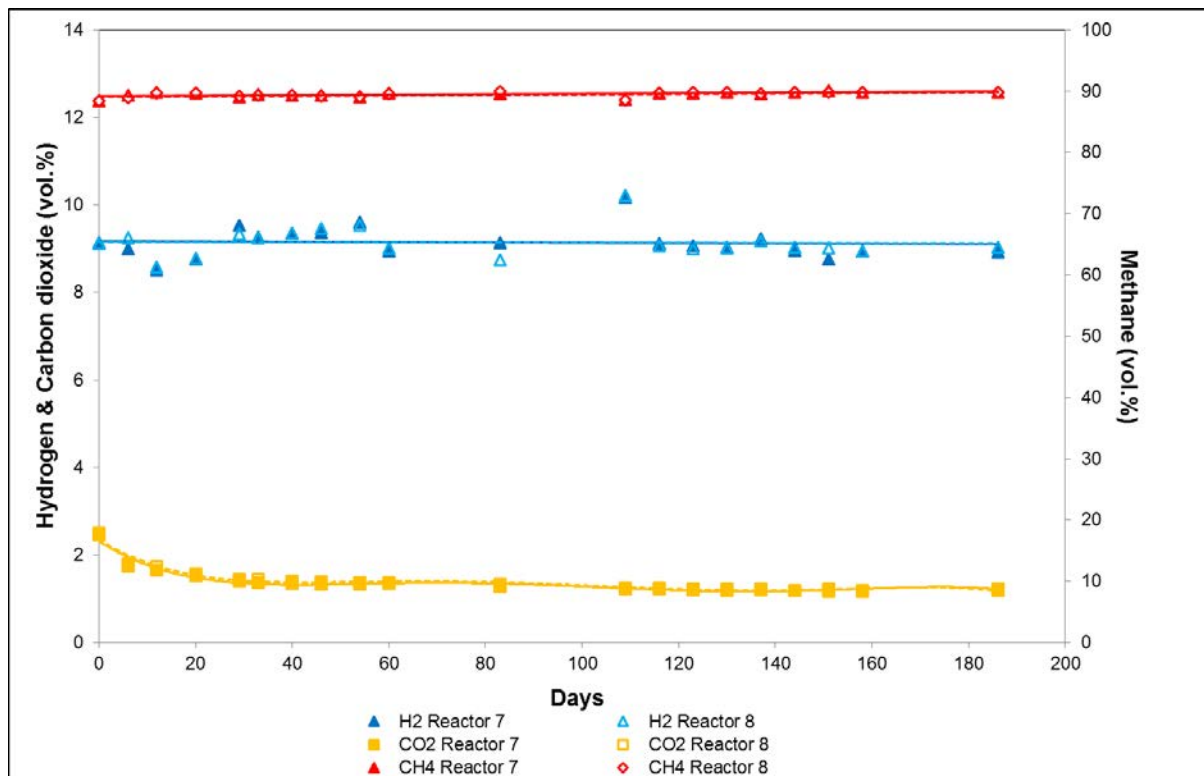


Figure 70: Concentration curve of gas components in abiotic reactors 7 and 8: 10 % H₂, 2.5 % CO₂ in methane Source: BOKU

5.3.3 Characterization of the microbial consortium

Figure 71 shows the shifts of the microbial consortium in the course of hydrogen exposure for four reactors (start consortium and end consortium). For comparison purposes the consortium of the formation water (sampling test field autumn 2013) was inserted.

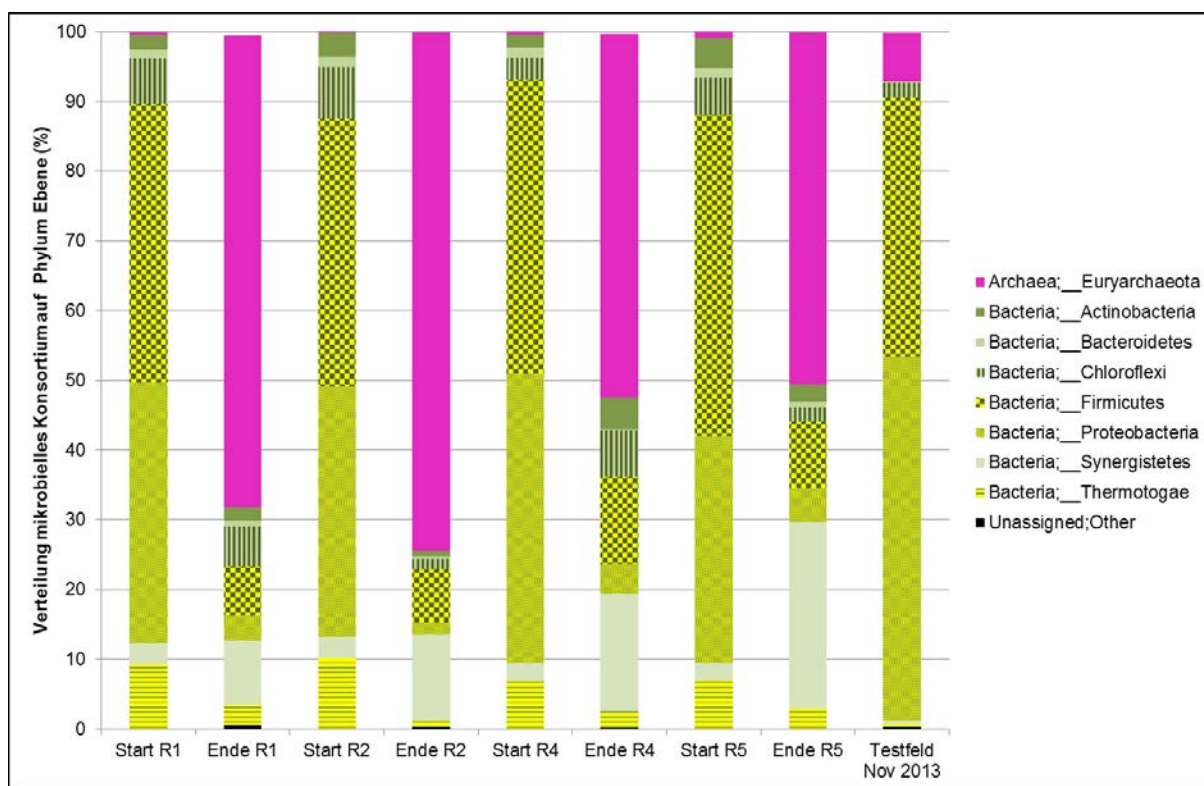


Figure 71: Microbial consortia in reactors (start vs. end of hydrogen exposure) and formation water (test field). Representation on phylum level. Source: BOKU

The green color comprises groups of bacteria that are capable of fermentative metabolic processes. This means that they are specialized in the degradation of organic compounds and use intermediate products of degradation as electron acceptors. The green-yellow bars also stand for fermentative bacteria, which can also use sulphate or elemental sulphur as terminal electron acceptors. The pink coloration encloses the group of methanogenic archaea. Figure 71 shows the shift of the microbial consortium depending on the nutrient supply and availability of terminal electron acceptors. If one compares the rightmost bar (test field November 2013) with the start consortia (R1, R2, R4, R5), it can be seen that methanogenic archaea were hardly present in the reactors any more while sulfate-reducing fermentative bacteria increased. The reason for this is, as already mentioned above, a sulphate entry due to drilling mud residues in the drill cores. Comparing the start and end consortia of the reactors R1, R2, R4 and R5, it is easy to see that the methanogenic archaea have a share of up to 75 % after hydrogen exposure and thus represent the dominant group of the entire consortium. This can be attributed to the conversion of carbon dioxide and hydrogen to methane, with a portion of the required carbon dioxide coming from the potassium carbonate of the drilling mud.

5.3.4 Conclusions

By simulating storage conditions of the test field in the laboratory, it has been shown that from a microbiological point of view, hydrogen can also be stored as a blend of 10 vol. % in natural gas as long as terminal electron acceptors are not present or available to a considerable extent. This statement can also be transferred to other porous natural gas fields, but each natural gas field should be tested in terms of its mineralogical-petrographic and hydrochemical composition. In addition, the existing microbiological consortium should be evaluated with regard to a possible hydrogen conversion. As can be seen in chapter 5.3.3, the microbiological consortium present in the storage adapts to changing conditions such as the availability of nutrients and terminal electron acceptors as well as changes in temperature, salinity and pH. Possible undesired processes can lead to pore blockages due to biomass growth or to a change of the chemical equilibrium in the natural gas storage due to the enrichment of microbial metabolites (e.g. acetate). Another hydrogen-consuming process is hydrogenotrophic methanogenesis, in which carbon dioxide and hydrogen are directly converted into methane. This reduces the total energy of the stored gas, but generates a chemical energy carrier with the biogenous methane. As can be seen in Chapters 5.3.2 and 5.3.3, hydrogenotrophic methanogenesis has taken place in individual reactors. To assess the technological potential of this conversion, the lead project Underground Sun Conversion (funded by the Climate and Energy Fund) was launched in March 2017. In the end, the results of the laboratory experiments formed the basis for the decision to carry out the field test in which natural gas with a hydrogen content of 10 % by volume was stored. Changes in the microbial consortium in the course of the field test are described in Chapter 8.

5.4 Reference to publications and other documents

The following table lists all publications and documents created in the course of the Underground Sun Storage project.

No.	Title	Year	Authores
1	Abstract: Geobatteries: is there a limitation to adding hydrogen to porous natural gas storages?	2015	Schritter Loibner
2	Geobatteries: is there a limitation to adding hydrogen to porous natural gas storages?	2015	Schritter Loibner
3	Abstract: Microbial processes in hydrogen exposed porous underground gas storages (UGS)	2015	Schritter Loibner
4	Microbial processes in hydrogen exposed porous underground gas storages (UGS)	2015	Schritter Loibner
5	Abstract: Microbial processes in hydrogen exposed porous underground gas storages (UGS)- results from lab scale simulation experiments - ABE Workshop	2016	Schritter Loibner
6	Microbial processes in hydrogen exposed porous underground gas storages (UGS) - results from lab scale simulation experiments - ABE Workshop	2016	Schritter Loibner
7	Master Thesis: Microbially induced changes upon the storage of a H ₂ / CH ₄ / CO ₂ Mixture in porous rock	2016	Komm
8	Constraints and potential of exploiting microbial capabilities for sub-surface applications	2016	Loibner

5.5 List of references

[1] SAMBROOK, J., & RUSSELL, D. W. (2006): *Purification of nucleic acids by extraction with phenol: chloroform*. Cold Spring Harbor Protocols, 2006(1), pdb-prot4455

[2] WOLICKA, D., BORKOWSKI, A., (2012), *Microorganisms and Crude Oil*, University of Warsaw Poland, (2012)

[3] PANFILOV, M., GRAVIER, G., & FILLACIER, S. (2006): *Underground storage of H₂ and H₂-CO₂-CH₄ mixtures*. In ECMOR X-10th European Conference on the Mathematics of Oil Recovery.

[4] DRIVER, L., & FREEDMAN, E. (1993): *Report to congress on hydrogen sulfide air emissions associated with the extraction of oil and natural gas. Final report (No. PB-94-131224/XAB; EPA--453/R-93/045)*. Environmental Protection Agency, Research Triangle Park, NC (United States). Office of Air Quality Planning and Standards

- [5] MAGOT, M., OLLIVIER, B., & PATEL, B. K. (2000): *Microbiology of petroleum reservoirs*. Antonie van Leeuwenhoek, 77(2), 103-116.
- [6] YOUSSEF N., ELSHAHED M.S., MCINERNEY M.J. (2009): *Microbial Processes in Oil Fields: Culprits, Problems, and Opportunities; Advances in Applied Microbiology*, Volume 66 © 2009 Elsevier Inc. ISSN 0065-2164, DOI: 10.1016/S0065- 2164(08)00806-X
- [7] DIEKERT G., WOHLFARTH G. (1994): *Metabolism of homoacetogens*, Anton Leeuw Int. J.Gen. Mol. Microbiol. 66, 209-221
- [8] JONES J.W., NAGLE D.P., WHITMAN W.B. (1987): Methanogens and the Diversity of Archaeobacteria, Microbiological Reviews Mar. 1987, p. 135-177.
- [9] BOTTIG M. (2008): *Diagenetische Umwandlungen in Sandsteinen der gasgesättigten, der sekundär verwässerten, der Wasser-, und der Übergangszone des Erdgas – Speichers Haidach in der Molasse Zone, Österreich*. Diploma thesis, University of Vienna
- [10] WANDREY M., MOROZOVA D., ZETTLITZER M., WÜRDEMANN H. (2010): *Assessing drilling mud and technical fluid contamination in rock core and brine samples intended for microbiological monitoring at the CO₂ storage site in Ketzin using fluorescent dye tracers*. International Journal of Greenhouse Gas Control 4 (2010) 972–980, doi:10.1016/j.ijggc.2010.05.012

5.6 Contact details

UNIVERSITÄT FÜR BODENKULTUR WIEN

Department IFA-Tulln

Institut für Umweltbiotechnologie

a.o.Prof.DI Dr. Andreas P. Loibner

Konrad Lorenz Str. 20, A-3430 Tulln

Tel.: +43-1-47654-97470

Fax: +43-1-47654-97409

E-Mail: andreas.loibner@boku.ac.at

www.boku.ac.at

Autoren: J. Schritter, A.P. Loibner

6 Material integrity in hydrogen-loaded gas storage facilities

6.1 Tasks of metallic materials

The aim of this work package was to investigate the chemical resistance of the steel grades L80, P110, 42CrMo4 QT, 42CrMo4 QTT, L360 and P235 used in the underground gas storage on degradation due to gaseous hydrogen up to a maximum hydrogen partial pressure of 10 bar at 25 °C.

6.2 Content presentation of metallic materials

The susceptibility of different steel grades to embrittlement by gaseous hydrogen was investigated using specific corrosion tests. For this purpose, a test plan was developed which enables a differentiation of the influences of H₂ and the theoretically possible components in the corrosive medium on the mechanical material properties during the operation of an underground gas storage facility (Table 22). In order to quantify the material Embrittlement supported by H₂, slow tensile tests (STTs) were carried out at a strain rate of 10⁻⁶ s⁻¹ and at a total pressure of 1 and 12 bar in specific corrosive media. On the basis of the measured elongations at break, the effects of the species present in the corrosive medium on the mechanical properties of the material could be evaluated. The test setup for the STTs is shown in Figure 72.

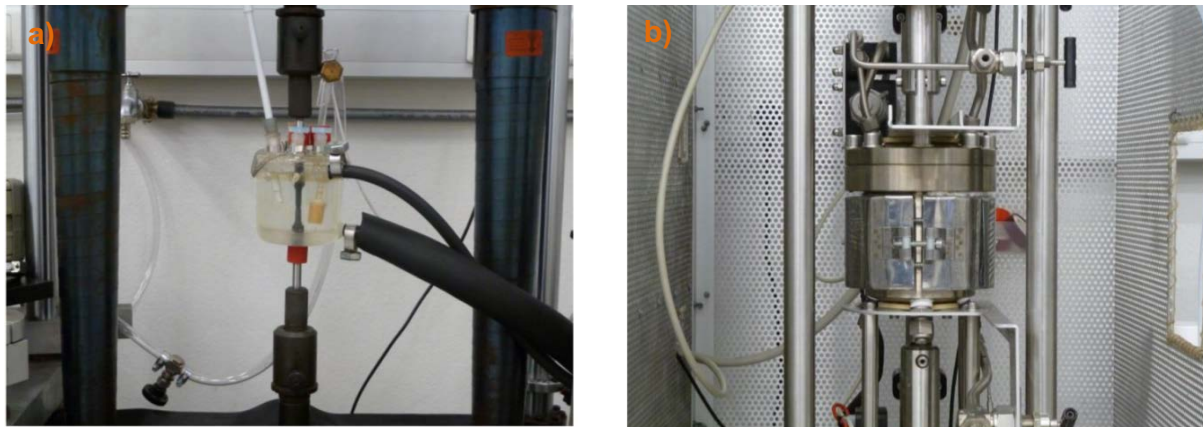


Figure 72: Test setup for SSRTs, a) Tensile testing device with glass cell for the SSRTs at 1 bar, b) Tensile testing device with autoclave for the SSRTs at 12 bar

In order to investigate premature material damage caused by molecular hydrogen, tests were carried out under constant load. The effect of H₂ in the presence of a defined mechanical stress was determined on the basis of the service life.

The CLTs were mounted on a mechanical lever apparatus with a constant load of 100 % $R_{P0.2}$, for a maximum test duration of 720 hours. At the beginning it was determined that a sample which does not break under the selected load in the respective medium during a maximum running time of 720 h is considered a run-through. The test setup of the CLTs is shown in Figure 73.



Figure 73: Test setup for CLTs at 1 bar

In order to investigate the influence of the different media on the hydrogen absorption and the hydrogen content of the materials L80 and P110, three cuboid samples of each steel grade and each ageing period were aged in selected corrosive media at a temperature of 25 °C and a pressure of 1 bar. The experimental set-up is illustrated in Figure 74: Experimental set-up for ageing tests at 1 bar.

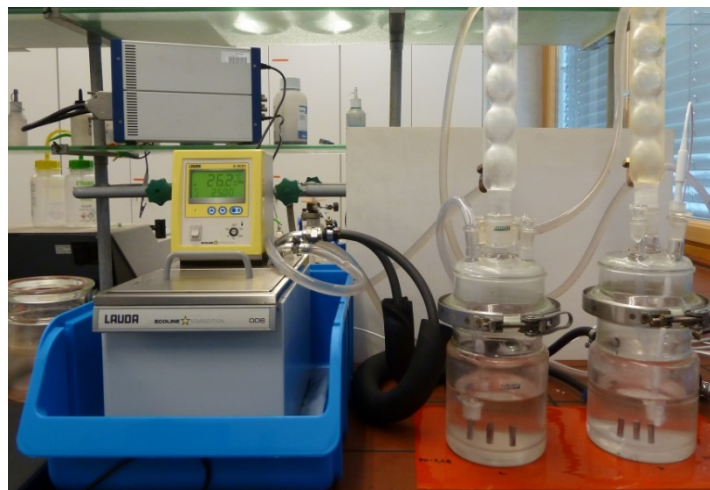



Figure 74: Test setup for ageing tests at 1 bar

The experimental design is shown in Table 22. The specified test conditions (Tcs) are arranged from 1 to 7 with increasing aggressiveness. With each Tc, the gaseous and liquid components in the aggressive medium change in such a way that a differentiation of the corrosion influences of the individual components of the test medium is possible.

Table 22: Test plan for the investigation of the materials L80, P110, 42CrMo4 QT, 42CrMo4 QTT, P235 and L360 for embrittlement by H₂

Vb [Nr.]	Medium	Druck p [bar]	Werkstoffe L80 P110	
1	Glycerin	1	2 x	2 x
	Glycerin 100 Vol.-% N ₂	12	2 x	2 x
2	5 Gew.-% NaCl 100 Vol.-% N ₂	1	2 x	2 x
		12	2 x	2 x
3	5 Gew.-% NaCl 100 Vol.-% CO ₂	1	2 x	2 x
		12	2 x	2 x
4	5 Gew.-% NaCl, 17 Vol.-% CO ₂ 83 Vol.-% H ₂	1	2 x	2 x
		12	2 x	2 x
5	5 Gew.-% NaCl 0,5 Vol.-% HAc 100 Vol.-% N ₂	1	2 x	2 x
6	5 Gew.-% NaCl 0,5 Vol.-% HAc 7 Vol.-% H ₂ S 93 Vol.-% N ₂	1	2 x	2 x
7	5 Gew.-% NaCl 0,5 Vol.-% HAc 7 Vol.-% H ₂ S 93 Vol.-% H ₂	1	2 x	2 x



Aggressivität der Versuchsbedingungen

The STTs in the inert medium (Tc 1) and in the chloride-containing test solutions, which were each rinsed with N₂, CO₂ and CO₂ + H₂ (Tc 2, 3 and 4), were carried out at a pressure of 1 and 12 bar. The tests in the test solutions containing chloride and acetic acid with the purge gases N₂, H₂S + N₂ and H₂S + H₂ (Tc 5, 6 and 7) were carried out at a pressure of 1 bar. Tcs 2, 3 and 4 were used to investigate the different influences of chloride, carbon dioxide and hydrogen. With a hydrogen content in the test gas of 83 vol. % and a pressure of 12 bar, the hydrogen

partial pressure corresponded to $p_{H_2} = 9.96$ bar (Tc 4). This allowed the materials to be tested under environmental conditions as close to operation as possible. Tc 5, 6 and 7 were used to investigate the different influences of acetic acid, hydrogen sulphide and hydrogen. Since hydrogen sulphide inhibits the recombination of adsorbed H atoms to molecular H_2 and supports the absorption of atomic H, Tc 6 and Tc 7 can be classified as very aggressive. The composition of the test gas at Tc 6 was determined according to NACE TM 0177 (mild conditions). Under Tc 7 the nitrogen in the test gas with 7 vol.% H_2S + 93 vol.% N_2 (Tc 6) was replaced by gaseous hydrogen. This ensured that the influence of molecular hydrogen can be represented in a differentiated way.

The materials L80 and P110 were tested using SSRTs in Tc 1 - 7 at 1 and 12 bar, CLTs in Tc 3 and 4 at 1 bar and outsourcing tests in Tc 3 - 7 at 1 bar. The remaining steel grades were tested with STTs in Tc 1 at 1 bar and in Tc 3 and 4 at 12 bar. The samples of the materials L80 and P110 tested with the SSRTs and CLTs were fractographically examined and their microstructure characterized by means of stereo and scanning electron microscopes. The materials L80 and P110 were investigated by ageing tests and subsequent hydrogen analysis. These were performed at Tc 3, 5, 6 and 7 for 72 h each. At Tc 4 the samples were stored for 48, 72 and 168 h respectively. Thus, the temporal influence of hydrogen absorption on exposure to gaseous hydrogen and carbon dioxide could be investigated more precisely. Hot gas extraction was used to analyse the hydrogen content of the two materials in the as-delivered state and after their removal from storage.

6.3 Results and Conclusions of Metallic Materials

6.3.1 STTs

The arithmetic mean values of the elongations at break of the material L80 are shown in Figure 75.

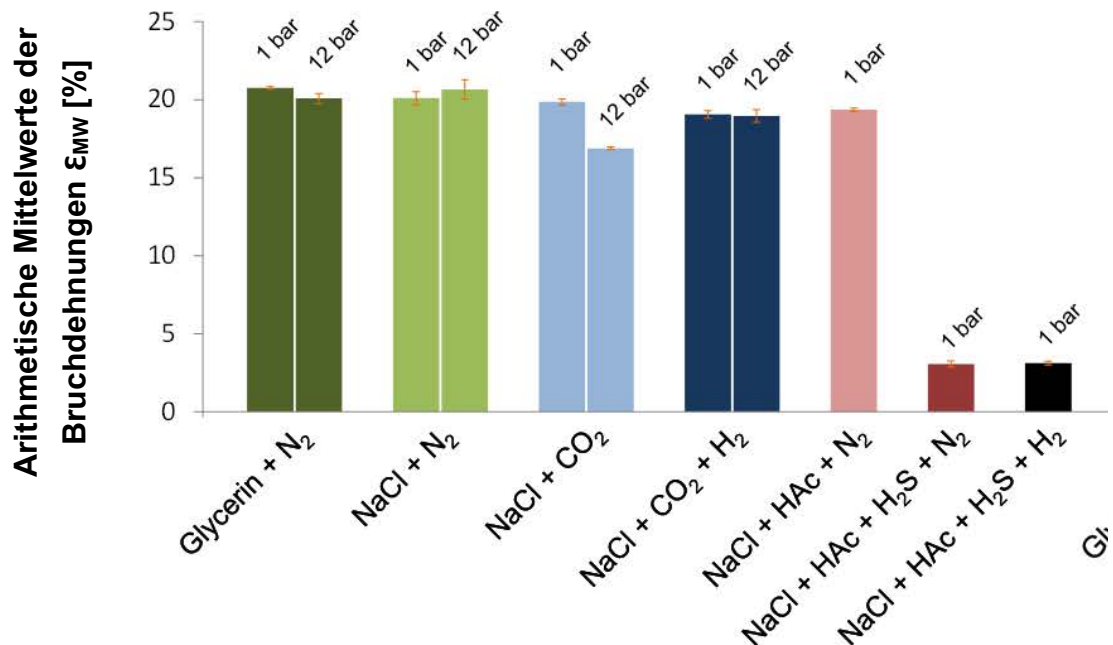


Figure 75: Arithmetic mean values of the elongations at fracture of the material L80

Compared to the tests in glycerin (Tc 1), the chloride-containing solution has no significant influence on the toughness of the material at a pressure of 1 bar and at 12 bar 100 vol.% N₂ (Tc 2).

The presence of 100 vol.% CO₂ (Tc 3) with $p_{\text{CO}_2} = 1$ bar does not lead to a significant reduction in elongation at break. The tests at 100 vol.% CO₂ (Tc 3) and $p_{\text{CO}_2} = 12$ bar show that, compared to the tests in glycerol (Tc 1) and those in 5 wt.% NaCl + 100 vol.% N₂ (Tc 2), a slight embrittlement occurs, which is due to the increased CO₂ concentration in the electrolyte. In Tc 4, molecular hydrogen and carbon dioxide are added to the electrolyte together for the first time. The comparison of the tests in the chloride-containing medium with 100 vol.% CO₂ (Tc 3) and 17 vol.% CO₂ + 83 vol.% H₂ (Tc 4), each at a pressure of 1 bar, shows that the elongation at break in the presence of H₂ is not significantly lower than in pure CO₂. The absorption of hydrogen from the gas phase must be excluded, as the thermodynamic and chemical conditions are too mild for this reaction path. At a total pressure of 12 bar, the partial pressure ratio is $p_{\text{H}_2} : p_{\text{CO}_2} = 10 : 2$. The aggressiveness of the medium is primarily increased by the increased CO₂ partial pressure, but the elongation at break difference to the tests at 1 bar is not significant. The observed decrease in elongation at break is uncritical as the value achieved is far ahead of the uniform elongation. The present degradation of toughness can be attributed to CO₂, which is readily soluble and dissociated in the electrolyte relative to H₂. Furthermore, the elongation at break in the presence of CO₂ + H₂ (Tc 4) is somewhat higher

than that under the influence of pure CO₂ (Tc 3). In this respect, the corrosive effect of pure carbon dioxide can be attributed to a dominant effect. The presence of CO₂ leads to a lowering of the pH value in the medium. The anodic dissolution of the iron as well as the occurrence of pitting corrosion can be promoted.

In the test solution 5 wt.% NaCl + 0,5 vol.% HAc + 100 vol.% N₂ (Tc 5) the content of acetic acid leads to a reduction of the pH-value and causes an increase of the general corrosion attack. However, no significant reduction in elongation at break was observed in this medium. The addition of 7 vol.% H₂S + 93 vol.% N₂ (Tc 6) leads to a dramatic reduction of elongation at break. The low pH-value of the medium and the H-absorption, increased by the catalytic effect of hydrogen sulphide, lead to a very rapid embrittlement of the L80. In Tc 7, the test solution containing chloride and acetic acid is rinsed with a mixture of 7 vol.% H₂S and 93 vol.% H₂. Analogous to the results under Tc 6, a very strong decrease in elongation at break can also be observed here, which is primarily due to the effect of the hydrogen promoter in the acid medium and not to the presence of the molecular hydrogen. The elongations at break of the tests in 7 vol.-% H₂S + 93 vol.-% N₂ (Tc 6), as well as those in 7 vol.-% H₂S and 93 vol.-% H₂ (Tc 7) do not differ significantly, from which it can be concluded that the presence of molecular H₂ has no effect. Figure 76 shows the arithmetic mean values of the elongations at break of the material P110.

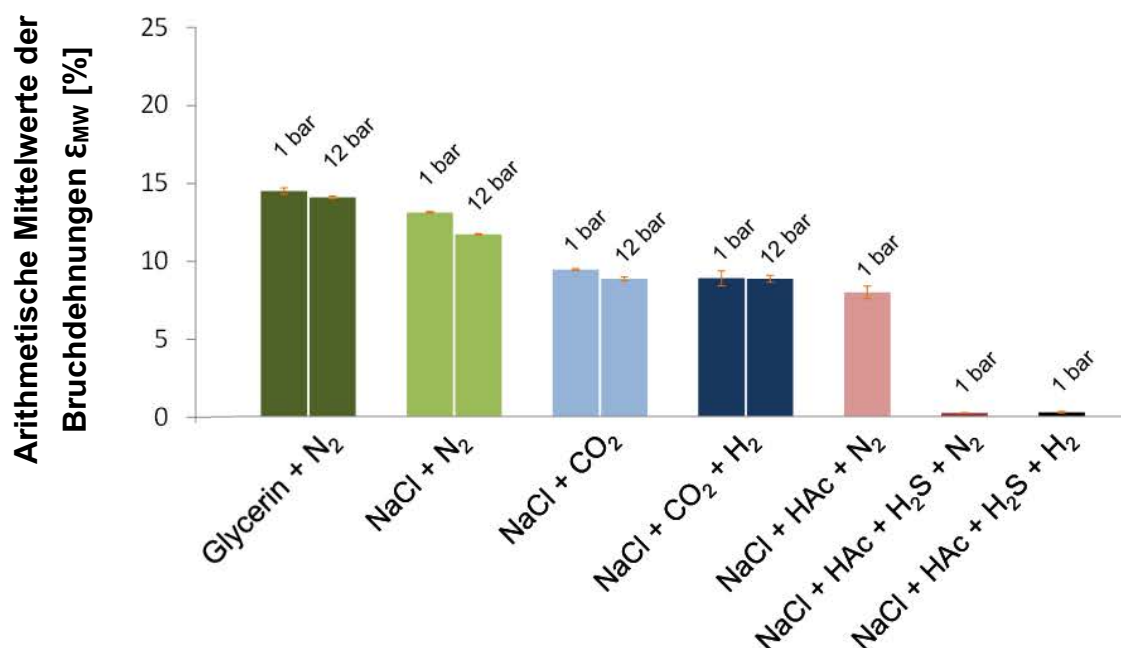


Figure 76: Arithmetic mean values of the elongations at break of the material P110

Compared to the measurements in glycerol with 100 vol.-% N₂ (Tc 1), the test in 5 wt.-% NaCl with 100 vol.-% N₂ (Tc 2) results in a slight reduction of ductility at both partial pressure levels. However, at 12 bar this effect is somewhat more pronounced.

If the test solution is rinsed with 100 % by volume CO₂ (Tc 3), an uncritical reduction in elongation at break is observed compared to the tests in glycerol. Here, too, embrittlement at 12 bar is slightly greater than at 1 bar. This fact is due to the increased CO₂ concentration in the test solution and the resulting lower pH value as well as the increased aggressiveness of the medium. The tests under Tc 4 were carried out with a test gas composition of 17 vol.-%

CO₂ and 83 vol.% H₂. In this medium, the material P110 behaves very similarly to Tc 3. There is a slight embrittlement, but this is to be classified as non-critical, since the elongation at break achieved is significantly greater than the uniform elongation. The comparison of the results in 5 wt.-% NaCl + 100 vol.-% CO₂ (Tc 3) with those in 5 wt.-% NaCl + 17 vol.-% CO₂ + 83 vol.-% H₂ (Tc 4) shows that gaseous hydrogen has no damaging effects on the mechanical properties of the material. The corrosive effect of the aggressive carbon dioxide has a dominant effect on the reduction of ductility.

The addition of acetic acid leads to an increased aggressiveness of the test solution containing chloride. As a result, the elongation at break of P110 in the medium 5 wt.-% NaCl + 0.5 vol.% HAc + 100 vol.% N₂ (Tc 5) is slightly lower than that in the HAc-free test media (Tc 1 to 4). When using the purge gas mixture 7 vol.% H₂S + 93 vol.% N₂ (Tc 6) in the same aqueous medium as Tc 5, it becomes clear what dramatic effects the mere presence of the hydrogen promoter H₂S has on the toughness of the steel. The material P110 reacts even more sensitively to the effect of hydrogen sulphide with its somewhat higher strength compared to L80 and embrittles rapidly. The low pH value and the increased hydrogen absorption cause the tensile specimens of the P110 to break at the beginning of the plastic range. Compared to these tests in the H₂S + N₂-containing medium (Vb 6), the test solution rinsed with H₂S + H₂ (Vb 7) does not show a significantly higher elongation at break. The presence of gaseous hydrogen in this medium therefore does not lead to any additional reduction in toughness.

Figure 77 shows the determined elongations at break of the materials 42CrMo4 QT, 42CrMo4 QTT, L360 and P235.

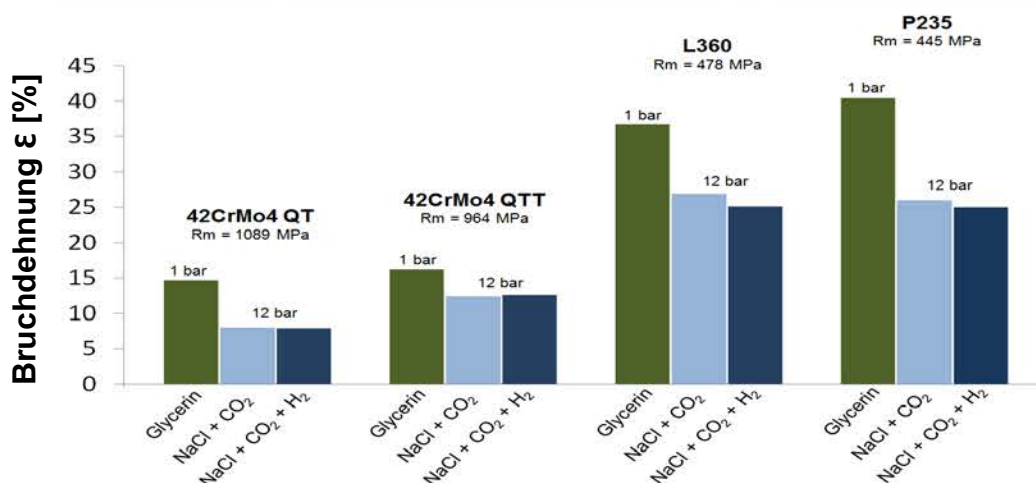


Figure 77: Elongations at break of materials 42CrMo4 QT, 42CrMo4 QTT, L360 and P235

Figure 77 shows that neither the 42CrMo4 QT nor the 42CrMo4 QTT, L360 or P235 suffer from significant embrittlement due to the action of H₂. The acidifying effect of the carbon dioxide has a dominant influence on the reduction of the ductility of the investigated materials, since the elongations at break achieved in the CO₂-purged medium do not differ significantly from those measured in the CO₂ + H₂-purged medium. As expected, the 42CrMo4 embrittles in both states

QT (quenched and tempered) and QDT (quenched and double tempered) slightly more than the relatively ductile materials L360 and P235 in the carbon dioxide-containing media.

6.3.2 CLTs

Under a constant tensile load of 100 % $R_{p0.2}$, the materials L80 and P110 in 5 w. % NaCl with 100 vol. % CO_2 (Tc 3) and in 5 w. % NaCl with 17 vol. % CO_2 + 83 vol. % H_2 (Tc 4) were each used to achieve 1 run at a maximum test duration of 720 hours. This shows that neither the aggressive carbon dioxide nor the gaseous hydrogen at the yield point leads to a time-delayed fracture. This test is an important criterion with regard to hydrogen-induced stress corrosion cracking, as the absorption and diffusion processes have sufficient time to accumulate atomic hydrogen at lattice imperfections and initiate a damage process. The load of 100 % $R_{p0.2}$ is a relatively harsh test, since there is a proportional dependence between the applied stress and the diffusive, damaging hydrogen content.

6.3.3 Paging tests

The analysis of the hydrogen content of the material L80 in the delivery condition resulted in 0.14 ppm. This value is compared with the measured contents of those specimens that were stored for a certain time in different test solutions at 1 bar and 25 °C respectively. The exposure in the chloride-containing solutions, which was rinsed with 100 vol. % CO_2 (Tc 3) or with 17 vol.% CO_2 + 83 vol.% H_2 (Tc 4), did not lead to a significant increase of the H content within 72 h. The H content of the samples was not significantly increased by the exposure. A relationship between the ageing time and the absorbed hydrogen content could not be established in the tests under Tc 4, since no significant hydrogen absorption occurred during the entire test period (168 h). The aging of L80 in the solution with 5 w. % NaCl + 0.5 vol.- HAc, which was rinsed with 100 vol.% N_2 (Vb 5) for 72 h, resulted in a slightly increased H concentration of 0.26 ppm. If this test solution was rinsed with 7 vol. % H_2S + 93 vol. % N_2 (Tc 6), the H concentration in the material increased to 3.49 ppm. The introduction of 7 vol. % H_2S + 93 vol. % H_2 (Tc 7) also led to a significant increase of the H content to 3.11 ppm. The increased contents are due to the catalytic effect of H_2S , as the effect of which reduces the recombination rate of the superficially adsorbed hydrogen and promotes H absorption. The comparison of Tc 6 and Tc 7 shows that the supply of gaseous hydrogen does not lead to any additional H-absorption.

A hydrogen analysis was also carried out on the material P110 in the as-delivered state, which resulted in an H content of 0.20 ppm. The results of the P110 samples stored in the different media at 1 bar and 25 °C were then compared with this initial value. The exposure of the samples in the solution with 5 w. % NaCl, which was rinsed with 100 vol. % CO_2 (Tc 3) or with 17 vol.% CO_2 + 83 vol.% H_2 (Tc 4), respectively, for 72 h, did not lead to any additional absorption of hydrogen. A correlation between exposure duration and absorbed hydrogen content could not be established under Tc 4, since there was no increase in the hydrogen concentration in the material even after a prolonged aging period of 168 hours. The ageing of P110 in 5 w. % NaCl + 0.5 vol.- HAc with 100 vol.% N_2 (Tc 5) resulted in an H-concentration of 0.16 ppm. The test in the same aqueous test solution, but with the much more aggressive purge gas of 7 vol. % H_2S + 93 vol.% N_2 (Tc 6), resulted in a significantly increased H content

of 3.41 ppm. Also in the purge gas mixture 7 vol. % H_2S + 93 vol.% H_2 (Tc 7) the H content increased to 3.97 ppm. The small difference in the hydrogen concentrations of the samples exposed to these two media suggests that the presence of molecular H_2 does not significantly influence H absorption. The increased H content in both cases is determined by the presence of H_2S , as this species reduces the recombination rate of superficially adsorbed hydrogen atoms and significantly facilitates H absorption.

6.4 Conclusions on metallic materials

The aim of this work package was to investigate the susceptibility of the materials L80 and P110, 42CrMo4 QT, 42CrMo4 QTT, P235 and L360 to embrittlement by gaseous hydrogen up to a maximum hydrogen partial pressure of 10 bar. The slow tensile tests showed that no additional degradation of the mechanical properties such as elongation at break, tensile strength or yield strength occurs due to the action of gaseous hydrogen on the materials tested under the selected test conditions. Only the pH-value-reducing effect of the carbon dioxide led in part to a slight reduction in elongation at break. The introduction of test gases containing H_2S into the respective test media, on the other hand, led to a massive reduction in elongation at break and to increased hydrogen absorption. The introduction of H_2 into the medium containing H_2S did not lead to an additional loss of ductility of the tested materials L80 and P110. The tests under constant load led to the result that there was no premature material failure of the materials L80 and P110 in 5 w.% NaCl with a purge gas composition of 100 vol.% CO_2 (Tc 3), nor with 17 vol.% CO_2 + 83 vol.% H_2 (Tc 4). Neither the presence of carbon dioxide nor the action of gaseous hydrogen could cause premature material failure under the selected test conditions. The results of fractography indicate that with increasing aggressiveness of the test conditions, but independent of the presence of molecular hydrogen, the materials L80 and P110 tend to become more brittle.

Overall, the results of all the tests carried out support the assumption that under the tested conditions no additional embrittlement occurs due to the action of gaseous hydrogen.

6.5 Task Cement

For the cements, it was important to determine whether they show a change in permeability, density or composition due to exposure to hydrogen in aqueous solution. To determine this, permeation experiments before and after exposure and X-ray diffraction measurements (XRD) were performed.

Since the permeation tests are similar to those of the rock cores from the breakthrough tests, no further description is given here.

6.6 Cement content presentation

The same methodology was used as for the overburden investigation. Description see 4.6.

6.7 Results and conclusions cement

Before assessing the results, it should be noted that it was not possible to produce cement samples with the same compaction as the cement actually used in the borehole. The density is lower and the permeability significantly higher than with curing under corresponding pressure conditions. However, this was accepted for the laboratory tests, since the air inclusions resulted in a higher permeability or porosity and thus a larger wetted area. In the case of a reaction with the hydrogen, this would then be stronger and more clearly distinguishable.

In preparation, the cement was poured into a PVC pipe and after curing, 1 inch plugs were cut from this "pseudo-core". Figure 78 shows an example of one of these cores.



Figure 78: Exemplary cement core

The cement plugs were then moistened with artificial reservoir water and confined in reactors under hydrogen atmosphere for several months. The reactors were heated to 40°C and pressurized to 70 Bar(a) which resembles the conditions in the reservoir. At regular intervals, some cement plugs were removed and analyzed in order to measure gradual changes. Table 23 summarizes the measured gas permeability's before and after the storage of all cores. Both measurements were carried out under analogous experimental conditions.

Table 23: Comparison of gas permeability's of the cement cores before and after the storage period

Storage period [Months]	Core No.	Pemeability [m ²]	
		before storage	after storage
2	6	1.04 10 ⁻¹⁷	1.73 10 ⁻¹⁷
	8	2.10 10 ⁻¹⁷	2.55 10 ⁻¹⁷
6	4	1.78 10 ⁻¹⁷	2.25 10 ⁻¹⁷
	3	3.97 10 ⁻¹⁷	4.88 10 ⁻¹⁷
12	9	2.21 10 ⁻¹⁷	1.97 10 ⁻¹⁷
14	2	2.26 10 ⁻¹⁷	9.21 10 ⁻¹⁷
	5	2.74 10 ⁻¹⁷	3.24 10 ⁻¹⁷

The XRD measurements showed that the portlandite in the cement was converted to vaterite during storage (XRD image) ($\text{Ca(OH)}_2 \rightleftharpoons \text{CaCO}_3$). This also happens naturally after cements are cured and is known under the term of carbonation. It further decreases the permeability of the cement as vaterite has a higher volume than portlandite. Figure 79 shows a comparison of the X-ray diffractograms of the cement sample before and after storage.

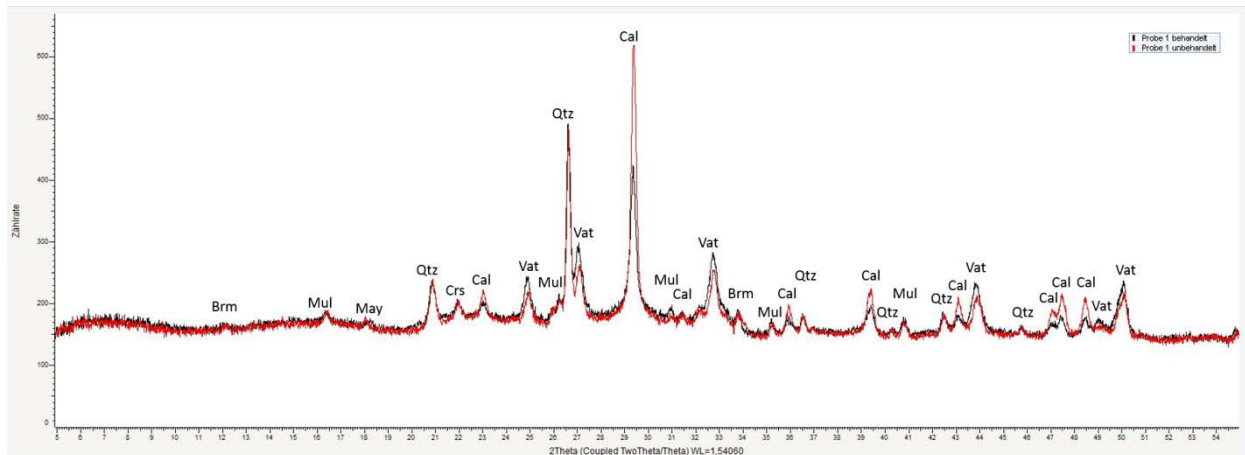


Figure 79: Comparison of X-ray diffractograms of the cement sample before and after storage.

Figure 80 and Figure 81 show the cement sample before and after storage.

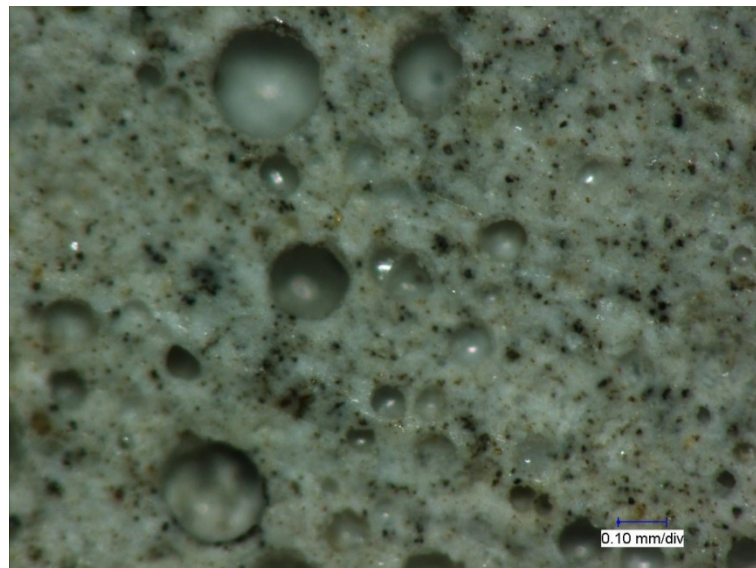


Figure 80: Cement stone before storage at 200x magnification.

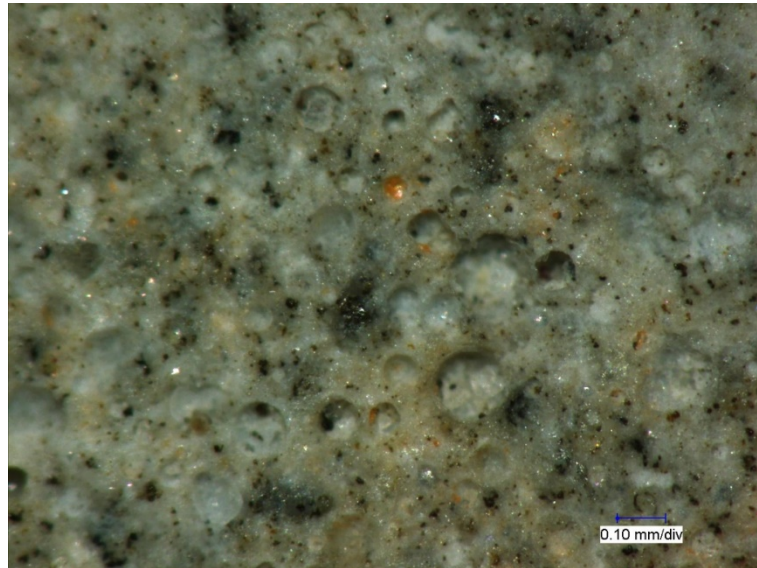


Figure 81: Cement paste after H₂ storage at 200-fold magnification

Subsequently, blank samples were stored to clarify the influence of nitrogen and methane on the cores. These experiments clearly showed that the change in composition is independent of hydrogen (Table 24). It is assumed that the change is due to the reaction with the CO₂ in the formation water or mixing water. However, since the change in permeability before and after storage is not significant, it was proven in the tests that the integrity of the cement, i.e. the tightness, against hydrogen is given.

The gas permeability's of hydrogen, nitrogen and natural gas in cement are, according to the measurement, approximately the same.

These results contradict assumptions from the literature and were therefore surprising for the project (DGMK, 2014). It could be proven that no new cementation of the well or special measures to protect it are necessary when hydrogen is added.

Table 24: Change of the cement permeability after storage in nitrogen and methane

Medium	Core No.	Permeability [m ³]	
		before storage	after storage
Methan	10	1.04E-17	3.44E-17
	11	8.53E-18	2.27E-17
Nitrogen	12.1	1.04E-17	n.b.*
	12.2	1.50E-17	1.32E-15*

*With nitrogen, unfortunately, the autoclave was relieved of pressure too quickly and the cores broke (Figure 82).



Figure 82: Fragmented core after autoclave opening

6.8 Reference to publications and other documents

In the course of this work package the diploma thesis was written by Dipl.-Ing. Karl Jojo Vidic at the Institute for General and Analytical Chemistry at the University of Leoben. The results of this work were presented at the following events:

- Congress and Trade Fair Gas - Water, 20.04.2016, Wels (A)
- Eurocorr, 13.09.2016, Montpellier (Fri)

6.9 Contact details

LEHRSTUHL FÜR ALLGEMEINE UND ANALYTISCHE CHEMIE

Montanuniversität Leoben

Dipl.-Ing. Karl Jojo Vidic

Franz-Josef-Straße 18

A-8700 Leoben

Tel.: +43 3842 - 402 1217

E-Mail: karl.vidic@gmx.at

RAG Austria AG

Department UGS Entwicklung und Management

Schwarzenbergplatz 16

1015 Wien

+43(0)50724-0

www.rag-austria.at

Autoren: K. J. Vidic, M. Pichler, S. Bauer

7 Membrane technology in connection with hydrogen admixtures

7.1 Task definition

The main task of this work package in the research project Underground Sun Storage was the development and experimental investigation of a process for the adjustment and separation of hydrogen into/from natural gas/hydrogen mixtures.

In the energy storage method investigated in the research project, the underground porous storage is adapted for storing higher quantities of hydrogen and thus for storing renewable energy. This energy, mainly obtained from wind and solar power, is generated at different times and at different intensities. Consequently, the stored hydrogen concentrations in the storage reservoir will vary in time and location. If the hydrogen/natural gas mixtures are withdrawn, there will also be variations in the hydrogen concentration.

From the point of view of a natural gas network operator, however, it is necessary to bring the hydrogen concentration in the stored gas to a constant level that is permissible for the network infrastructure. This makes it necessary to condition the gas at the interface between the bivalently operated storage facility (storage of natural gas and hydrogen) and the natural gas network. In general, such gas conditioning has two functions:

- 1) Compensation of the hydrogen fluctuations in the stored gas to achieve a targeted concentration in the natural gas network [1], whereby the separated hydrogen flow is returned to the gas storage.
- 2) Reduction of the hydrogen concentration to a value permissible for the natural gas network, in which case the separated hydrogen stream is fed into a hydrogen recovery process (typically for the production of electrical energy).

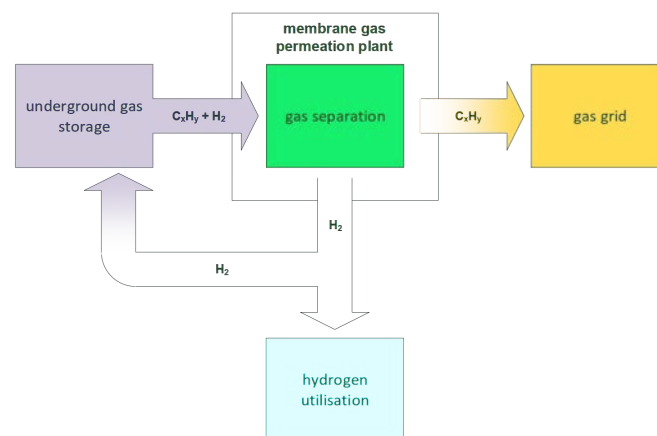


Figure 83: Integration and function of a hydrogen separation plant on a pore storage tank

Depending on the variation in hydrogen concentration in the gas storage, the permissible hydrogen concentration in the natural gas network and the target concentration in the natural gas network, the hydrogen separation plant may be designed for operation mode 1) or 2) or for a combination of both. The function and integration of the gas conditioning at a gas storage facility is shown schematically in Figure 83.

In the current research project, membrane gas permeation was selected for the hydrogen separation process. The selection is based on the following advantages of membrane technology for the separation process under consideration:

- 1) High selectivity between hydrogen and hydrocarbons.
- 2) Compactness, modularity and small footprint.
- 3) High process reliability, operation without chemicals.
- 4) Continuous separation process and easy integration with downstream processes.
- 5) Direct use of the pressure available in the storage tank for gas separation, thus high energy efficiency.

7.2 Content presentation

The activities in the work package are divided into two parts. In the first, theoretical and design fundamentals are laid for the field test. The second part deals with the construction of the hydrogen separation plant and with the field test itself. The workflow in the work package is described in the list below:

Part 1:

- Short study on the state of membrane technology in the separation of hydrogen/methane mixtures,
- Comparison of the separation parameters of the available membrane materials for the investigated gas separation task,
- Selection of a suitable membrane and assessment of its gas separation properties,
- Modelling of the separation process with the membrane parameters obtained in the laboratory under different operating conditions,
- Determination of the operating parameters for the design of the field experiment,

Part 2:

- Detail engineering of the experimental hydrogen separation plant for the field test,
- Risk analysis, selection and implementation of safety technology,
- Construction of the plant and delivery of the plant to the site of the field test,
- Commissioning of the plant together with connected gas storage components,
- Gas separation test with different feed gas parameters during a withdrawal cycle,
- Evaluation of the process performance and determination of the gas separation properties of the membrane used under field conditions.

7.3 Results and conclusions

The comparison of different membrane materials carried out in the first work package part pointed to the selection of anisotropic hollow polyimide fibers. Polyimides characterize very high hydrogen/hydrocarbon selectivity's (Figure 84). For the hydrogen-methane gas pair, the ideal selectivity is about 100. For longer aliphatic hydrocarbons, polyimides exhibit even higher selectivity values. This makes the realization of efficient gas separation processes possible. In addition, the hollow fibers mentioned above are mechanically robust and allow a pressure load of over 100 bar. They can therefore be operated directly with the pressure from the gas storage tank without pressure reduction.

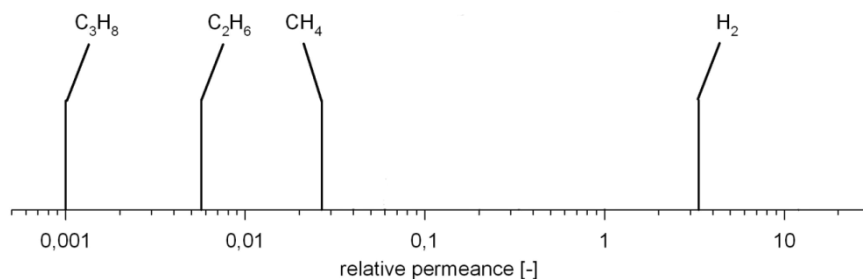


Figure 84: Relative permeances for hydrogen and hydrocarbons of a glassy polymer (polyimides)

In a subsequent step, a membrane cartridge with several thousand hollow polyimide fibers was installed in a high-pressure housing and subjected to a series of clean gas permeation tests for the gases H_2 , CH_4 , CO_2 and N_2 in the Axiom pilot plant. The ideal separation properties of the membrane were determined under laboratory conditions.

The experimental data obtained in the pilot plant test were then used to calibrate the membrane simulation tool. The simulation tool is based on a numerical finite volume method [2] and allows detailed modeling and optimization of membrane gas permeation systems. The tool was used to model several operating cases of the planned hydrogen separation plant. The plant behavior was numerically predicted and analyzed for different feed gas parameters. The results of the process simulation were the expected operating parameters of the plant in the field test. These data also served as a basis for the dimensioning of the secondary components of the hydrogen separation plant and for the correct integration of the plant with the upstream and downstream components of the gas storage system.

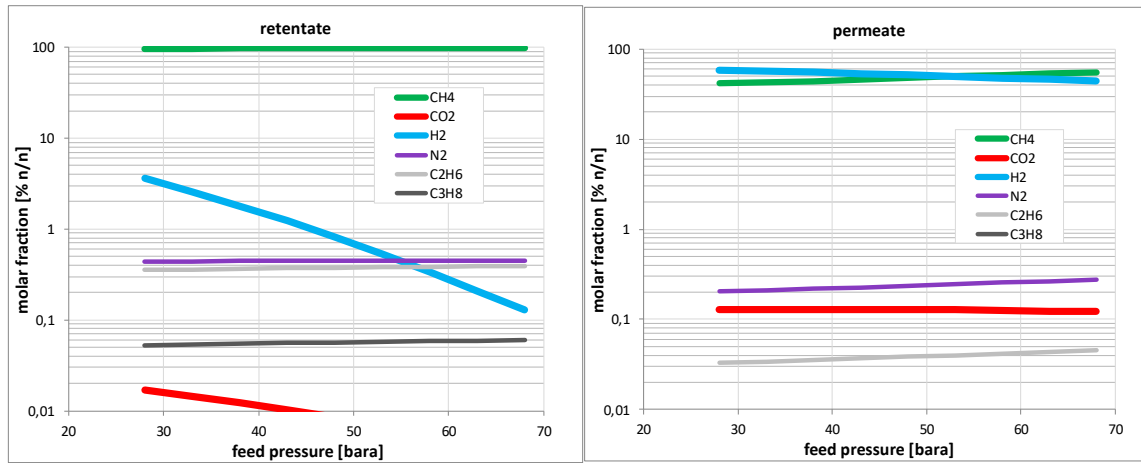


Figure 85: Concentration processes in the retentate-flow and in the permeate flow of the hydrogen separation plant during a storage-out process

A modelling result of a numerically simulated operating case is shown in the diagrams in Figure 85. The diagrams show the concentration curves for the permeate and the retentate flows during a withdrawal test. In the example presented, the system is operated directly with the storage pressure, resulting in a pressure ramp from 68 bar to 28 bar. The plant processes 400 Nm³/h natural gas with a constant hydrogen content of 10% (v/v). The aim is to reduce the hydrogen content to at least 4% (v/v) hydrogen (maximum value in ÖVGW G31) in the gas fed into the grid. In this case, no process control processes are simulated in the model to balance the gas concentrations in permeate and retentate. The resulting methane yield in the retentate stream is about 90%. The hydrogen yield in the permeate varies between 70% and 98% depending on the storage pressure.

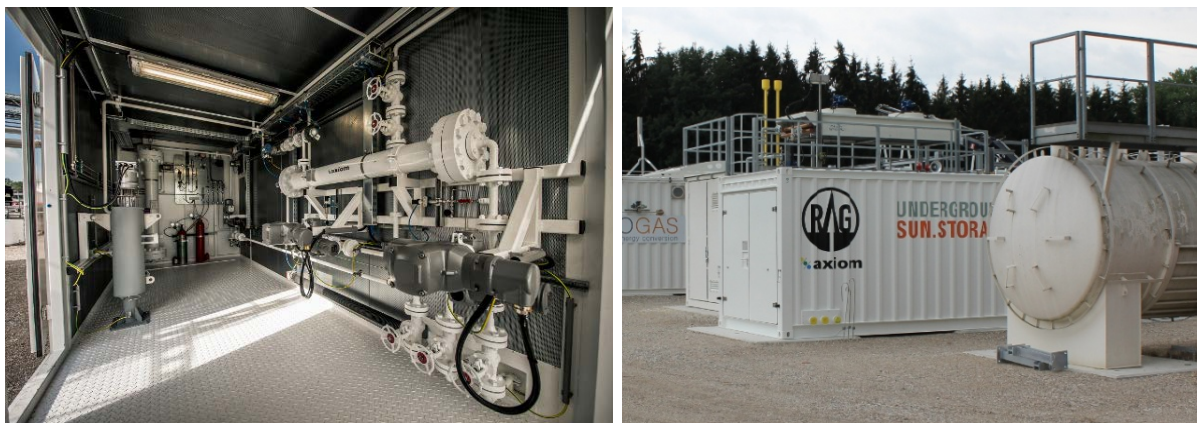


Figure 86: Experimental membrane plant for the separation of hydrogen/natural gas mixtures in the research project Underground Sun Storage

The hydrogen separation plant constructed for the research project was designed as a container unit. It is a standardized ISO container with a special length of 7 m. The hydrogen

separation plant is designed as a hydrogen separation unit. The container contains a polyimide hollow fiber module with all the ancillary components required for operation, such as an activated carbon bed, gas filter and a gas heater. The nominal throughput of the plant is 400 Nm³/h. The pressure stage is 100 bar. In terms of space requirements, the container enables the enclosure of 4-5 further modules and thus an expansion of the gas treatment capacity to approx. 2000 Nm³/h. The test plant was constructed in the assembly hall of Axiom and subsequently delivered to the field test plant of RAG in Upper Austria.

Flow measurements and gas analyzers were implemented for the complete balancing of the test. The gas analysis was carried out by means of a sound velocity measurement for the determination of the hydrogen content and infrared sensors for the determination of the methane and carbon dioxide content. The gas analyzers could be used alternately for retentate and permeate measurements thanks to a flow selector switch. The feed gas composition was determined by means of a gas chromatograph upstream of the hydrogen separation plant. The field test took place during the gas withdrawal phase between November 2016 and January 2017.

During this period several operating modes of the plant were experimentally investigated. The test results for an operating case in which a reduction of a 9% (v/v) hydrogen peak on the ÖVGW value was involved are shown in Figure 87. The plant achieves a methane yield of 93% in the retentate. The hydrogen content in the permeate is about 54% (v/v) with a hydrogen yield of about 60%.

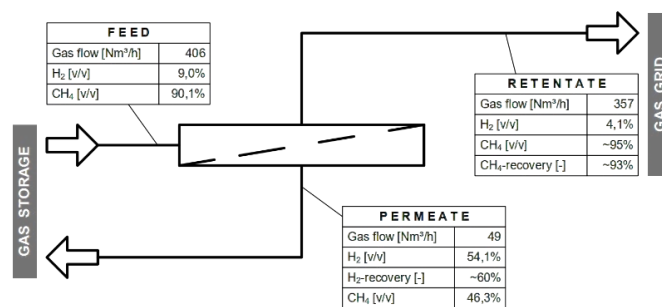


Figure 87: Separation parameters of the plant in a hydrogen balancing mode

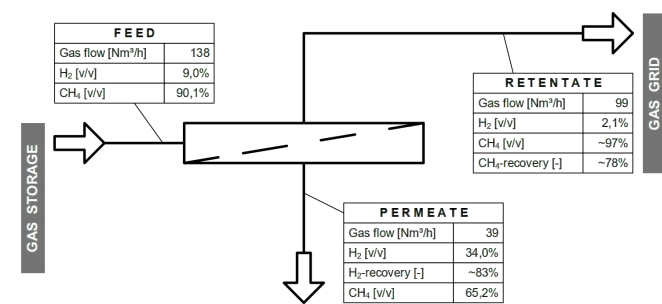


Figure 88: Separation parameters of the plant in a hydrogen separation plant

Figure 88 summarizes operating parameters for an operation case involving maximizing hydrogen yield. The hydrogen yield achieved in the permeate is 83%, the hydrogen content

34% (v/v). The hydrogen content in the retentate could be reduced to about 2% (v/v) for the grid feed-in.

In summary, the field tests carried out has proven the function of the hydrogen content setting for the energy storage system. The data obtained from the test serves as a sound basis for the engineering of the first pilot plants and for the development of optimized concepts for controlling the hydrogen concentration in natural gas networks.

7.4 Reference to publications and other documents

[1] S. Bauer, M. Prem, J. Szivacz, Device and method for storing and distributing renewable energy, EPO 2016.

[2] A. Makaruk, Numerical modeling, optimization and design of membrane gas permeation systems for the upgrading of renewable gaseous fuels, Dissertation, Vienna University of Technology 2011.

[3] A. Makaruk, J. Szivacz, S. Bauer and L. Schlegl, Key role of membrane gas separations in the utilisation of an underground natural gas reservoir for the renewable energy storage, Proceedings of GPA Spring Conference 2016, Making Natural Gas the Sustainable Fuel of the Future, 20-22 April 2016, Paris

7.5 Contact details

Axiom angewandte Prozeßtechnik GmbH

Dr. Aleksander Makaruk

Wiener Straße 114 Halle I-J

2483 Ebreichsdorf, Austria

Tel: 0043 2254 762 82

Fax: 0043 2254 746 75

E-Mail: a.makaruk@axiom.at

Website: www.axiom.at

Autor: A. Makaruk

8 In-situ field trials

8.1 Task definition

A crucial part of the Underground Sun Storage project was the demonstration of the storability of renewable energy in the form of hydrogen admixtures under real conditions of a scientific field test. This is of particular importance, as laboratory experiments and models can provide fundamental information, but due to simplified assumptions and boundary conditions they can never give a full picture, which makes verification in the field necessary. The decision to carry out this field test, which is unique in the world, was made on the basis of robust results from laboratory tests which confirmed the integrity of the storage tank under sharper conditions with regard to the hydrogen load (comparison: 25-100% hydrogen content in the laboratory to 10% hydrogen content in the field test). The hydrogen content of 10% was chosen due to various regulatory requirements in Europe.

A suitable small and isolated reservoir was selected in advance, which is geologically and geophysically well comparable with the commercial storage facilities of RAG, but on the other hand allows a test to be carried out with justifiable effort.

This is the Lehen-002 reservoir near the city of Vöcklabruck in the district of Upper Austria. The reservoir rock is a Litharenitic sandstone with a weakly carbonated non-cemented matrix. This sandstone body is enclosed by clay rock and lies isolated in the shallower layers of the molasse zone (Haller series) at a depth of around 1,022 meters. The initial pressure in the deposit was 107 bar. The permeability is 700 mD [mille Darcy]. For the test, the reservoir was operated in a pressure range of 30 to 78 bar(a). The temperature of the deposit is about 40 °C. It is a sweet gas deposit (pH value reservoir brine 8.1) with low salinity (14,000 mg/l NaCl). Communication with other layers or an active aquifer can be excluded due to the volumetric behavior of the reservoir. Furthermore, the reservoir is only accessed by a single existing well, which is very convenient for scientific consideration, as the inlet and outlet parameters can be clearly defined. With a gas volume of approx. 6 million Nm³, the deposit is extremely small and therefore made a test possible under real conditions and with justifiable effort.

8.2 Preparation, Planning and Building of the Test Facility

In preparation for the field test, a large number of measurements were made to confirm the suitability of the reservoir for this field test and to present the actual state of the reservoir as accurately as possible with basic measurements prior to the test. Thus already at the beginning of the project pressure and temperature measuring instruments were installed in the wellbore to observe the natural change of pressure and temperature in the reservoir. Water samples were used to determine the geochemical condition of the reservoir. This was supported by a short geological study which defined the expected mineralogical composition of the reservoir on the basis of analogous reservoirs in the vicinity. The water sample was also used to determine the existing microbiological consortium in the reservoir.

In addition, an injection test, a production test and analyses of the natural gas still present in the reservoir were carried out to determine the basic suitability of the reservoir as a gas storage

formation and to measure any damage or dilution caused by production. In addition, the expansion, volume and heterogeneity of the reservoir, which was assumed on the basis of the production history, was verified or, where necessary, modified by means of pressure build-up measurements.

A preservation of evidence at the wellbore casing was carried out by means of ultrasonic measurement, and at the cementation by means of log measurement. The original well completion which was installed for a production well, was adapted to the standard of a storage well.

In addition to the preparatory measures described, the planning, approval and construction of the surface facilities had to be completed. The surface installations essentially consist of a compressor that presses the gas mixture into the reservoir, an electrolysis plant for hydrogen production and various measuring systems and auxiliary systems. Figure 89 shows a systematic overview of the plant.

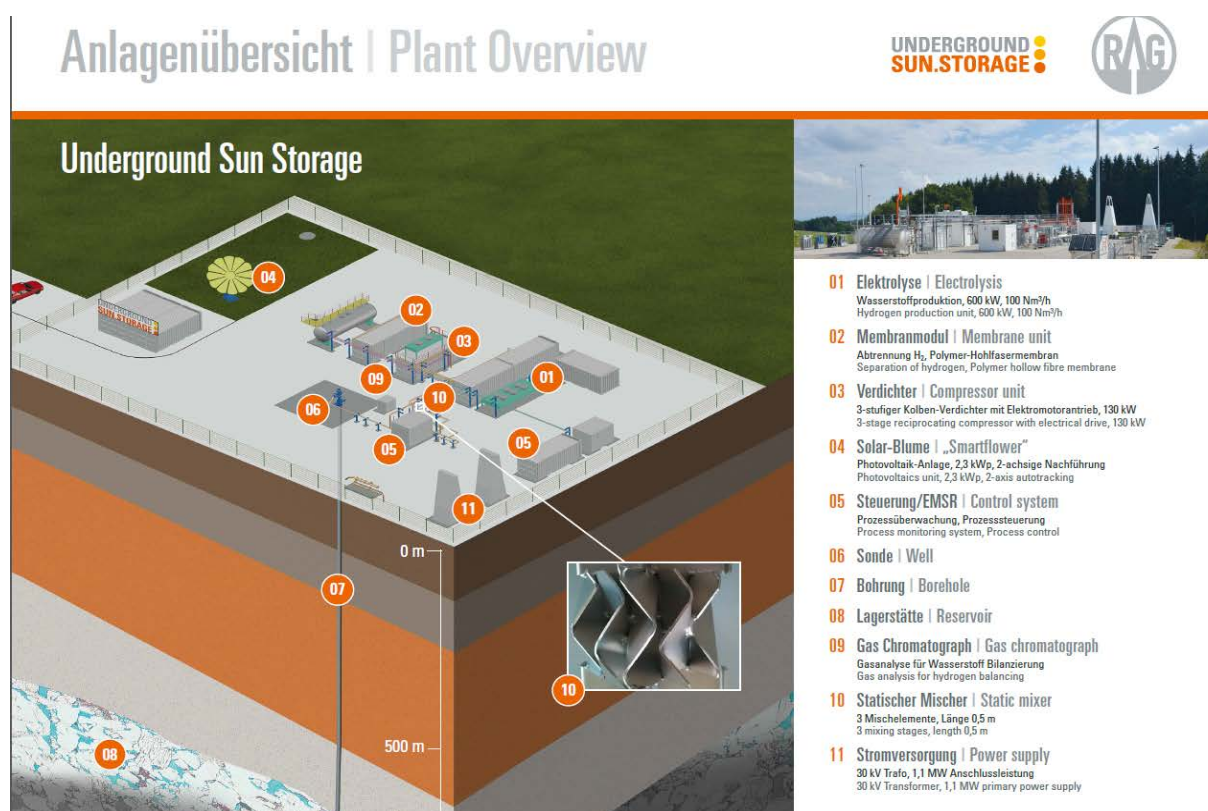


Figure 89: Schematic plant overview - main plants (Source: RAG)

All plants were approved in accordance with the applicable legal provisions, which affected a large number of legal matters. The plant was built in a construction period of approx. 5 months and subsequently put into operation.

8.3 Experiment execution

Within the framework of the Underground Sun Storage project, a complete storage cycle consisting of injection phase, shut in phase and withdrawal phase was implemented. Natural gas was mixed with approx. 10% hydrogen and injected into the experimental storage reservoir. This process of injection took about 3 months. During the shut in phase, which lasted about 4 months, gas samples were only taken selectively. Subsequently, the gas mixture was withdrawn over a period of approx. 3 months. During the test, the gas quantities were recorded by orifice measurements and the gas qualities by gas chromatography. A large number of other data points were recorded. In the test facility, different materials were additionally exposed to the gas flow and subsequently analyzed. During the entire field test, no unusual operating conditions, damage or unexpected test sequences were detected. The following sections deal with individual results and test evaluations.

8.4 Hydrogen balancing

8.4.1 Initial situation

Hydrogen balancing was one of the central tasks in the field test. The required data was collected by suitable quantity measurements and gas quality measurements.

A total of 1.22 million Nm³ of gas mixture was injected into the Lehen natural gas reservoir. Of these, 115,444 Nm³ were hydrogen. After the shut in phase, 1.24 million Nm³ were withdrawn. Of these, 94,549 Nm³ were hydrogen. This results in a shortfall of hydrogen of 20,895 Nm³. In addition to hydrogen and methane, the following components were recorded by gas chromatography:

Table 25: Detected gas components in the storage gas of the test storage Lehen (* this has a cross sensitivity with methanol which was added to the gas flow to avoid hydrate formation)

Component	Range of fluctuation Percentage [Vol.%]
Carbon dioxide [CO ₂]	0.22 – 0.01
Nitrogen [N ₂]	0.48 – 0.45
Ethane [C ₂ H ₆]	0.41 – 0.39
Propane [C ₃ H ₈]	0.3* - 0.13
C ₄ +	0.014-0.013
Total sulphur	0

In the following, the balance sheet change of the gas composition and its course over time is interpreted.

8.4.2 Hydrogen produced

In total, around 82% of the hydrogen volume injected could be withdrawn again. Since the extracted gas has too high a hydrogen content to be fed into the natural gas grid according to

the standard, it was mixed with gas from other RAG reservoirs so that the hydrogen content was less than one percent when it was fed into the natural gas grid.

8.4.3 Hydrogen diffused

At the end of the production phase, the hydrogen content in the gas was still ~3%. At this point, the total volume of gas, but not the volume of hydrogen, had already been removed. Thus it was clear that hydrogen had migrated into the cushion gas (original gas in the reservoir) already present in the reservoir. This can be explained by the fact that there is a saturation gradient between the gas introduced and the cushion gas (simplifies 10% H₂ on the one hand and 0% H₂ on the other). However, a closed system always tends towards equilibrium. This is why hydrogen diffused from the saturated gas into the unsaturated gas. If this process were to continue and the stored gas were no longer removed, the hydrogen would sooner or later be evenly distributed throughout the entire reservoir. In order to quantify the amount of hydrogen diffusing into the cushion gas, the drop in hydrogen concentration in the last third of the production was smoothed by various functions and then extrapolated (Figure 90). Depending on the smoothing function used, a share of 4-5 percent of the hydrogen volume introduced could be accounted to diffusion.

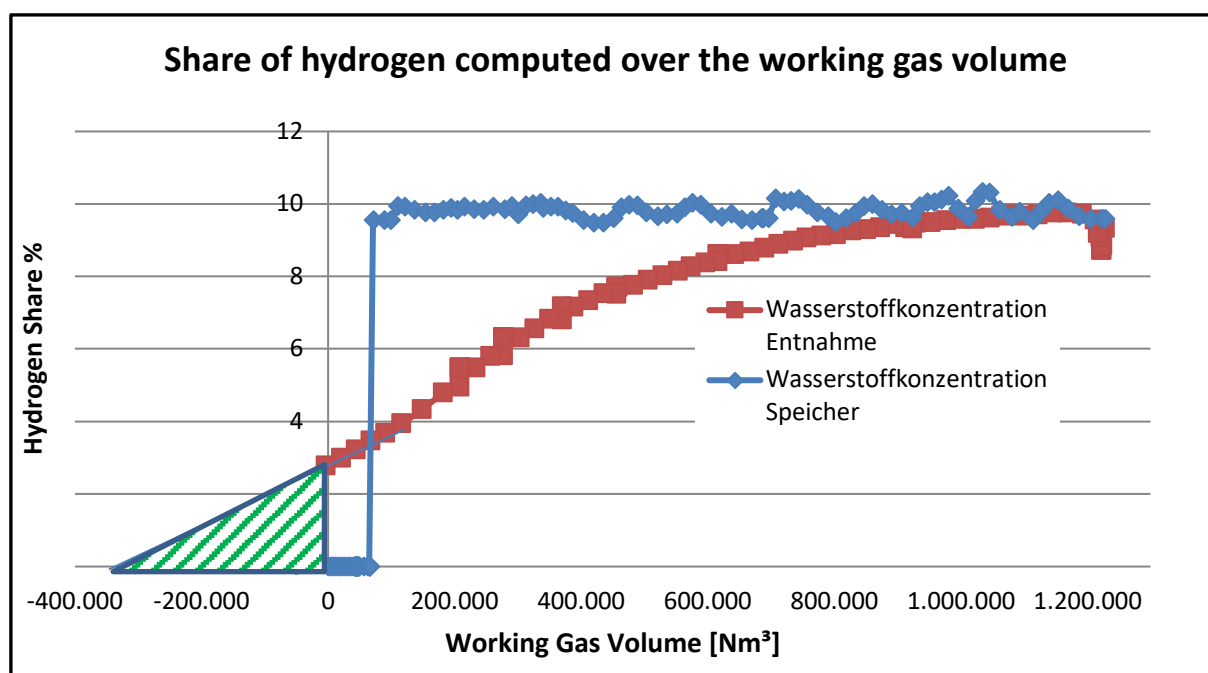


Figure 90: Course of the hydrogen concentration over the storage level

The diffusion of hydrogen into the surrounding rock layers was not considered. There is also a difference in concentration here. However, the pore space of these rock layers is 100% filled with water, which is why the decisive factor here is the water solubility of hydrogen. This is dealt with in paragraph 8.4.5.

8.4.4 Conversion

It was already known from literature and laboratory tests that reactions of hydrogen and elements present in the reservoir could occur. Among other things, the reaction of hydrogen and carbon dioxide to methane (methanogenesis) and the reaction of hydrogen and sulfur to hydrogen sulfide are known.

The carbon dioxide concentration in the stored gas gradually decreased, similar to the hydrogen concentration during the production phase (Figure 91).

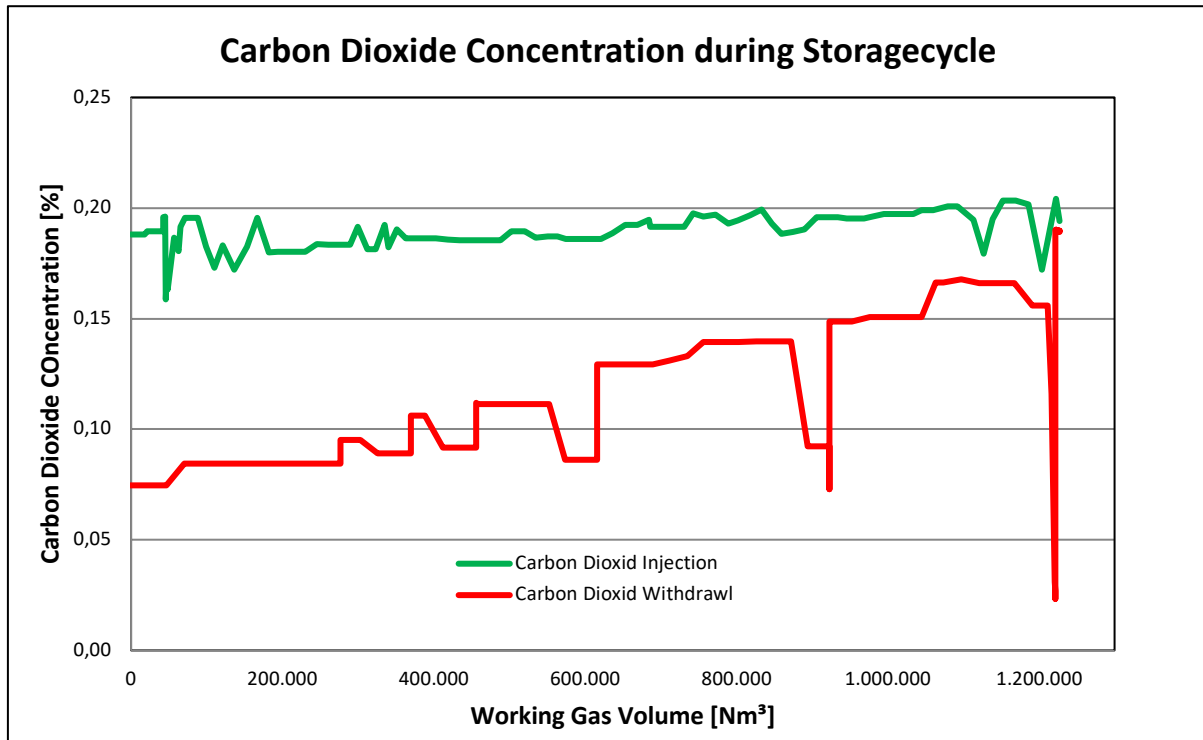


Figure 91: Course of the carbon dioxide concentration over the storage level

A carbon dioxide balance was drawn up to determine the amount of converted carbon dioxide. This resulted in a potential for the conversion of hydrogen, which mathematically explains the whereabouts of a further 3% of the hydrogen introduced. This is a microbiological process. Chemical methanogenesis cannot take place at such low temperatures (40°C) and pressures (~78 Bar(a)) as which are present in the reservoir. Microbes serve as catalysts and metabolize hydrogen via the hydrogenotrophic methanogenesis to methane. This process could also be proven by Isodetect's isotope measurements. In addition, however, it should be noted that the CO₂ balance only includes the gas injected into the reservoir. Natural gas with a CO₂ content of 0.2 vol. % was already present in the Lehen reservoir (cushion gas) before the start of the field test. In addition, CO₂ is also dissolved in the reservoir water. If these quantities are roughly calculated, there is a much higher potential for the conversion of hydrogen, which, however, cannot be precisely evaluated.

From the literature there are great concerns that the hydrogen introduced could react with the sulphur present in the reservoir due to microbiological processes. The test reservoir also contains sulphur dissolved in the reservoir water (SO₄) and as a solid in the form of the mineral pyrite. The IFA Tulln was able to detect sulphur-reducing bacteria (SRB) in the reservoir water.

For this reason, the hydrogen sulphide content in the production gas was measured continuously. However, no hydrogen sulphide was detected in the gas stream during the entire field test.

Apart from hydrogenotrophic methanogenesis, the reaction potential of hydrogen in the reservoir can be classified as low. This is also supported by the pressure and temperature records from the field test. If major reactions had taken place, these energies would have been released, leading to an increase in the reservoir temperature. However, as can be seen in Figure 92, the temperature in the deposit remains almost constant.

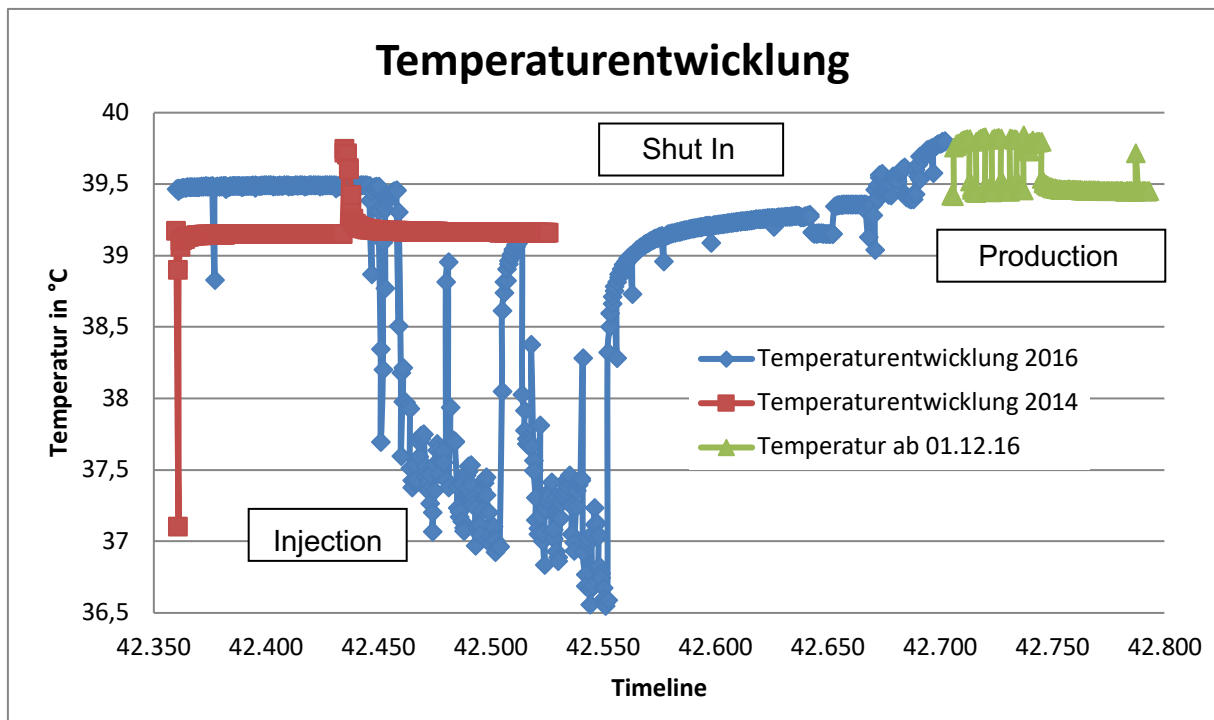


Figure 92: Comparative course of temperature development during the field test and the preparation phase

In addition, the Boyle-Mariotte law was used to calculate the pressure loss due to the change in volume associated with the conversion (see [6]). This could be calculated at 1.3 bar. If one compares this with the pressure before the start of the injection (32 bar(g)) and after the withdrawal (30 bar(g)), the assumption seems quite accurate. However, it should be noted that a natural gas reservoir is no tank and therefore influenced by various physical parameters (supercharging, aquifer expansion, etc.) that can change the reservoir pressure.

8.4.5 Hydrogen Dissolved

According to literature, the solubility of hydrogen in water is very low, at least less than methane. However, during the Underground Sun Storage project new findings were published in the H₂Store project, which indicated that this topic needs to be reassessed. Thus, it could be proven that the solubility of hydrogen strongly depends on the amount and type of ions dissolved in water. Accordingly, the solubility can vary within a relatively wide range. For the project Underground Sun Storage 2 solubility models were used to estimate the amount of

dissolved hydrogen (see [5]). The amount of water available for solution was calculated to be $\sim 9850\text{m}^3$ due to the water saturation in the pores of the hydrogen wetted space. If Lassin's model (cf. [5]) is used for solubility, a solution of up to 10% of the initially introduced hydrogen volume is conceivable. This model provides quite good results for low saline fluids, but is empirically determined and probably also influenced by the reaction of hydrogen with the ions dissolved in water. The model developed by De Lucia (see [4]) predicts a solubility of about 7.5% of the introduced volume. However, it should be noted that this model is particularly difficult to apply in the low-pressure range and also applies to systems with a significantly higher salinity than the water from the Lehen deposit (comparison 14,000 ppm NaCl to 200,000 ppm NaCl). Last but not least, the Henry constant should also be mentioned here, which gives a value for the solubility of pure substances in condensed water. If one calculates the dissolved H_2 volume with this, one arrives at a value that is lower by a factor of 10 than that of the other models used (0.88 % of the volume introduced). Here we see the need for further investigations.

8.5 Microbiology

8.5.1 Sampling formation water from the test field

In order to characterize the microbiological consortium in the natural gas storage facility and also to obtain an inoculum for the high-pressure bioreactors (see Chapter 6), several sampling campaigns were carried out over the entire project period. The sampling was carried out together with the RAG measurement team, which carried out technical measures such as water level measurement, bailer ride, etc. at the wellbore. A bailer was used for sampling (see Figure 94), which was cleaned beforehand. Oxygen was largely removed before the bailer was introduced into the pneumatic gas lock. The bailer's withdrawal volume was approx. 1.8 liters. The depth for sampling was around 1200 m TVD. After sampling, the reservoir water was transferred to sterile Pyrex bottles under continuous argon fumigation (see also Figure 93).



Figure 93: Filling of the reservoir water (Source: BOKU Vienna (RAG))



Figure 94: Sampler before entering the pneumatic gas lock (Source: BOKU Vienna (RAG))

The methods used for DNA extraction can be found in Chapter 71, for hydrochemical analyses in Chapter 70.

8.5.2 Modification of the microbial consortium in the test field

Figure 95 shows the change of the microbial consortium in the formation water of the test field. The assignment of the existing phyla was based on the DNA sequence, active microorganisms were detected by the detection of the corresponding RNA sequences. The coloring of the individual phyla is congruent as in Chapter 5.3.3 (Figure 71) - "Shifts in consortia due to hydrogen exposure in the reactors". The dominance of the fermentative bacteria (green bars) can be clearly seen; subgroups of the sulfur and sulfate reducers (yellow-green bars) can also be found here. The methanogenic Euryarchaeota are shown in pink, the fermentative Euryarchaeota in green. These include the class of thermoplasmata and belong to the extremophiles, since they have been isolated from hot springs, sulphatars and in the presence of mineral pyrite or arsenopyrite (ore deposits) (cf.[1]). If the individual **consortia (DNA)** are compared, for all five sampling campaigns (November 2013, April 2015, October 2015, November 2016 and March 2017) the proportion of fermentative bacteria (green) including sulphate-reducing bacteria (yellow-green) remains constant. The phylum of Thermotogae contained therein was originally isolated from oil fields (cf. [2]). With the sampling campaign in November 2016 the phylum of Atribacteria was added, which was isolated from anoxic sediments with methane production. It is assumed that these microorganisms can form a syntrophic connection with the methanogens (cf. [3]).

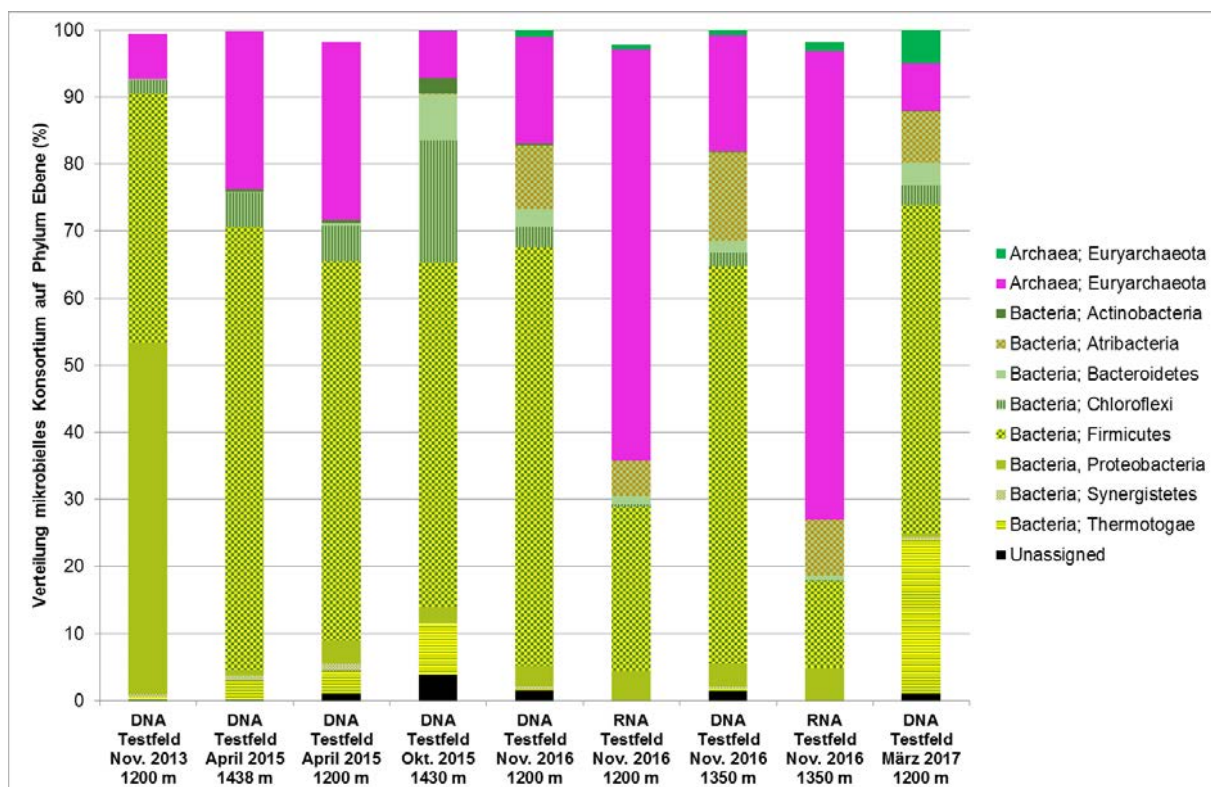


Figure 95: Shifts of the microbial consortium in the formation water of the test field.
Representation on phylum level (Source: BOKU)

Looking at the sampling of November 2016, the largest shifts in the microbial consortium can be found in a comparison of RNA and DNA. This sampling took place in the withdrawal cycle in order to extract the largest possible amount of original formation water from the probe. Although methanogens are not the main microorganisms present (see Figure 95), they account for up to 60% of the total **microorganisms active** in the natural gas storage facility. The **RNA-based consortia** of the two different depths (1200 m TVD and 1350 m TVD) show that the methanogens were the dominant group in this operating phase of the test field and therefore a formation of methane can be expected ($\text{CO}_2 + 4\text{H}_2 \rightarrow \text{CH}_4 + 2\text{H}_2\text{O}$). This is possible because a carrier gas (natural gas) with a carbon dioxide content of 0.2 % by volume was used for the storage of hydrogen (Figure 96).

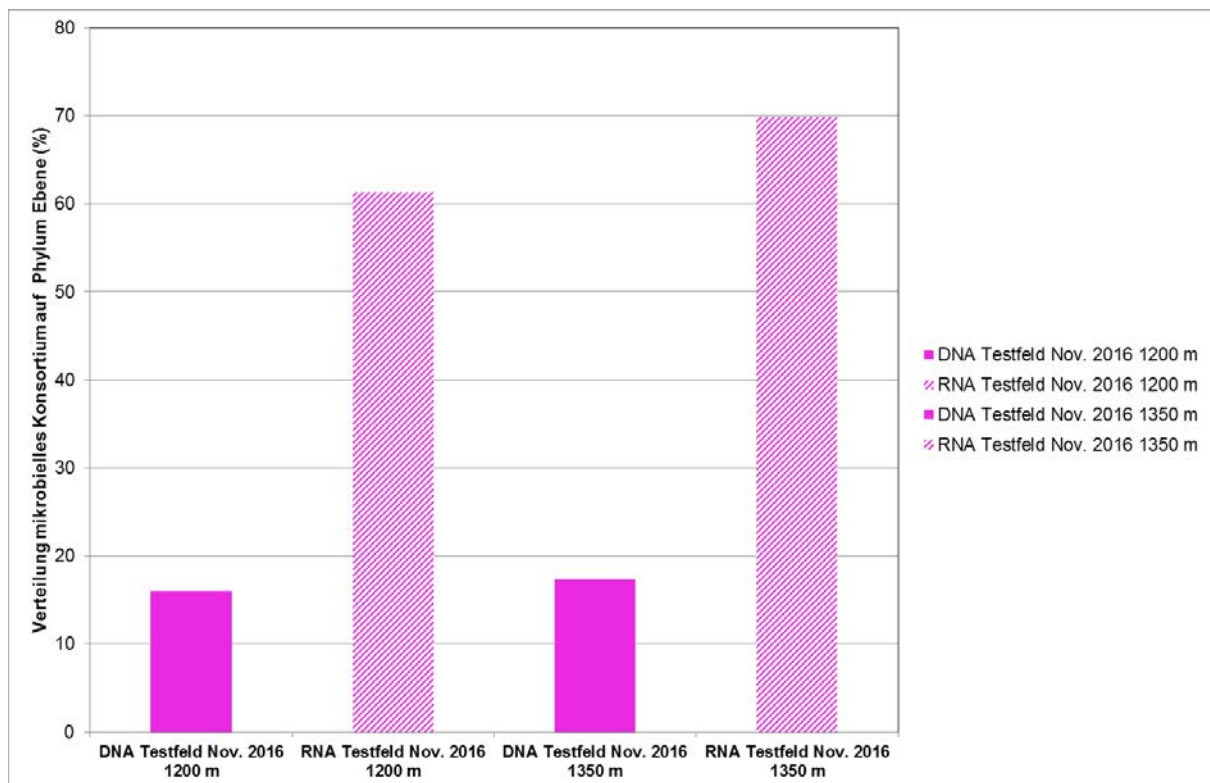


Figure 96: Comparison of the proportion of existing (DNA) and active (RNA) methanogens in the microbial consortium in the formation water of the test field (Source: BOKU)

Different potentials of hydrogen consumption can be derived from the microbial consortium in the formation water of the test field. When sulphur or sulphate is added, these electron acceptors can be reduced to undesired hydrogen sulphide by using hydrogen. At the same time, the proportion of sulfate-reducing bacteria would increase, with associated corrosive technical side effects. If carbon dioxide is present, it can be converted to methane by the microbes together with hydrogen (hydrogenotrophic methanogenesis), but acetate can also be generated (homoacetogenesis). Homoacetogenesis can cause a pH reduction and thus a shift in the chemical equilibrium, which can intensify various processes (dissolution processes of the mineral matrix, shifting of the microbial consortium). Whether hydrogen is used in the presence of carbon dioxide to form methane or acetate depends on various factors (pH, concentration of the gas components, microbiological consortium present, trace elements and

nutrients, etc.). Therefore, a careful preliminary investigation of the gas field selected for storage was needed (see Chapter 5).

8.5.3 Hydrochemical results of the formation water

Figure 97 shows the course of pH, chloride, sulphate and acetate in the formation water of the test field. The x-axis was scaled to "days" in order to display the sampling times correctly. In Table 26 the days of the corresponding sampling campaign are assigned to the dates, the orange background indicates the sampling at the time of withdrawal.

Table 26: Sampling times of the test field

Sampling Time Test field (depth m)	Days
Sept. 2013 (1200 m)	0
Nov. 2013 (1200 m)	57
April 2015 (1438 m)	565
Oct. 2015 (1430 m)	749
Nov. 2016 (1350 m)	1162
March 2017 (1194 m)	1260

The chloride content shows a slight slope due to wellbore overhauls of the test field with potassium chloride. The sulphate content of the first two sampling campaigns was 16 and 36 mg/L, the following decreasing trend shows possibly a microbial consumption of the dissolved sulphate, since the subsequent supply from the drilling mud is no longer given and no mineral containing sulphate occurs in the reservoir, also a possible dilution effect by probe overhauling or fresh formation water can be considered. The conductivity is increasing (probe overhaul with KCl) until the last sampling in March 2017, which could indicate original reservoir water. The pH value decreased from pH 8.7 (November 2013) to pH 8.65 (April 2015), to pH 8.4 (November 2016) and to pH 8 (March 2017) during storage. However, no microbiological pH-lowering processes due to hydrogen consumption were found, as the acetate content was ~100 mg/L one year before the storage experiment (April 2015) and ~100 mg/L in March 2017 (Figure 97). Thus, significant homoacetogenesis is unlikely.

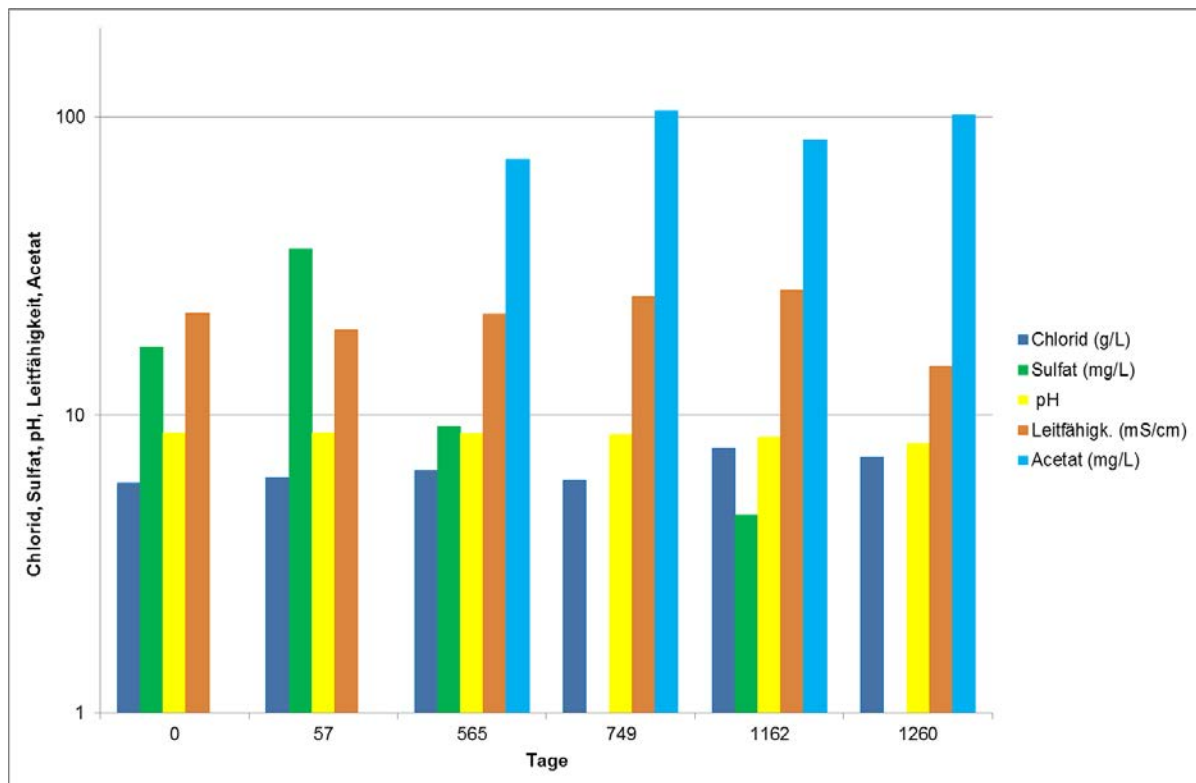


Figure 97: Course of pH value, chloride, sulphate and acetate in the formation water of the test field (Source: BOKU)

8.5.4 Modification of reservoir parameters

During the entire experiment, no decrease in the permeability of the reservoir could be observed, which suggests, that no microbial mass increase and the associated growth in the pore space has happened. On the contrary, the increase in permeability, which is typical for a new storage was measured. The increase is related to drying effects in the area close to the wellbore as the dry gas that is injected removes water from the pores of the reservoir rock. The composition of the reservoir water and the pH value in the water were also slightly changed during the field test. However, these changes could be observed to the same extent during the laboratory tests of the IFA Tulln. Thus, they are only another indicator for the project that microbiological activity takes place in the reservoir.

8.6 Material tests

In order to be able to test the various materials used in the facilities in reality, a material test track was installed in the test facility of the Underground Sun Storage project, which allowed the materials to be exposed to the gas flow during the test.

8.6.1 Cement

No hydrogen-induced damage was found either in the laboratory or on the cement samples exposed to the storage gas. The comparison of the measurement results shows that the behavior observed in the laboratory also occurs in the field test (see also 6.7).

8.6.2 Steels

As measured in the laboratory, no significant changes in material properties or even material damage were found in the steels used for the field test. It has thus been proven that a hydrogen content of 10% which does not exceed a partial pressure of 10 bar does not pose any problems for the steel materials used in RAG storage facilities (see also 6.4).

8.6.3 Elastomers

During the test, elastomer seals were installed in the completion as well as in the above-ground test facility of the field test. After completion of the test, these were removed again and subjected to an optical examination, in which no changes were detected. In addition, various common elastomers were also installed in the material test track during the field test. The materials used here showed minor changes in the mass and volumes of the material. However, since there are no references in the literature, the results from the field test are difficult to interpret and it is not possible to say clearly which of the changes can be attributed to hydrogen. However, the elastomers used as standard sealing elements at RAG showed the smallest changes in the investigations.

8.6.4 Well Integrity

As was already the case before the test was carried out, evidence was subsequently secured on the wells casing by means of ultrasonic measurement (USIT) and on the cementation by means of log measurement (CBL). Both measurements show that there were no changes during the test. It could thus be confirmed that the hydrogen does not endanger the integrity of the well or the cement sealing.

8.7 Modeling

The field test was also accompanied by a dynamic simulation of the reservoir. The aim was to find out to what extent the storage of hydrogen can be modeled and mapped with common software. A history match (HM) for the field Lehen based on a geological (static) model in PETREL was to be created. The software package ECLIPSE 300 compositional (E300) simulation was used to represent changes due to the addition of hydrogen to natural gas during storage in the Lehen HP3A reservoir (Well Lehen 2 (LEH-002); start 15 March 2016).

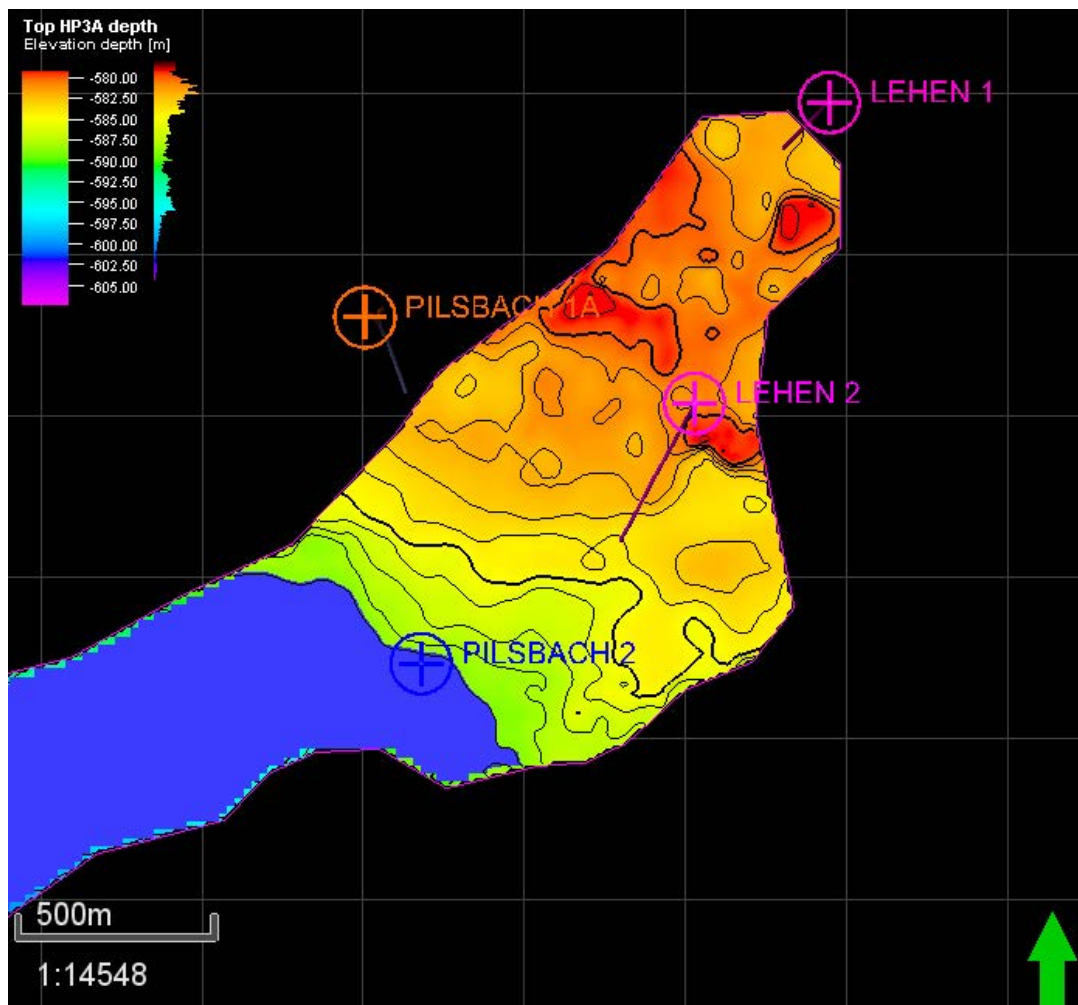


Figure 98: Structural map of the HP3 1A in the geological model

Summary

According to the geological (static) model of the HP3A deposit in Lehen, a history match was achieved with E300. The E300 was chosen because a gas mixture of natural gas and hydrogen was stored in the Lehen field. Good agreement (± 2 bar pressure difference) was achieved with the measured pressure values from the reservoir until the start of injection of the natural gas-hydrogen mixture in mid-March 2016. Thereafter, the match gradually deteriorated (pressure difference between ± 2 and 4 bar) between simulation and measured values, probably due to the cell size of 20mx20mx0.3m (LxWxH). This cell size is much smaller than is commonly used in modelling, but still too coarse for such a small reservoir as Poro-Perm changes occur at even smaller intervals.

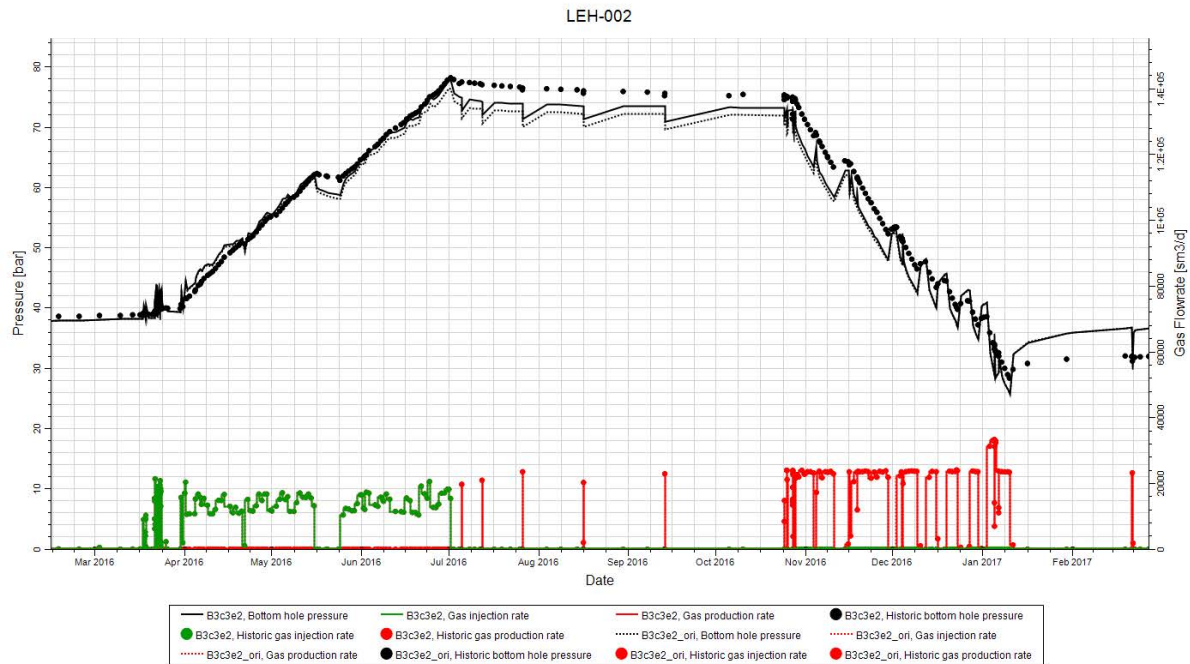


Figure 99: Updated history match for the 10 vol.% H₂ gas mixture case and the pure natural gas case until 27 February 2017

In addition to these model related problems, the software used was also classified as insufficient. Thus, it was not possible to correctly map the changes in the hydrogen concentration during the production phase. Also, the equation of state used by the software was not able to map the behavior of hydrogen (Figure 99) and had to be adapted with an empirical approximation. Last but not least, the diffusion and dissolution behavior of hydrogen is not represented with sufficient accuracy. In summary, it can be said that an extension of the commonly used software packages is necessary to optimally simulate the problem.

8.8 Summary of the results

No integrity problems induced by hydrogen could be detected during the entire operation of the field test. A continuous pressure monitoring of the possible gas flow paths in the well (tubing, annulus, annular space) could prove that the completion chosen for the field test is gas-tight.

An additional confirmation is provided by the observation of the hydrogen content in the well during the inclusion phase. During this phase gas samples were taken at regular intervals in order to observe the development of the gas mixture in the reservoir. The percentage of hydrogen gas measured at the end of each extraction was always almost equal to the value measured at the beginning of the next extraction (Figure 100). Thus a possible accumulation in the probe can be assumed, but not a diffusion out of the probe. It should also be noted here that at least 1000 Nm³ of gas were extracted with each sampling in order to actually measure gas from the reservoir and not gas that was only in the tubing.

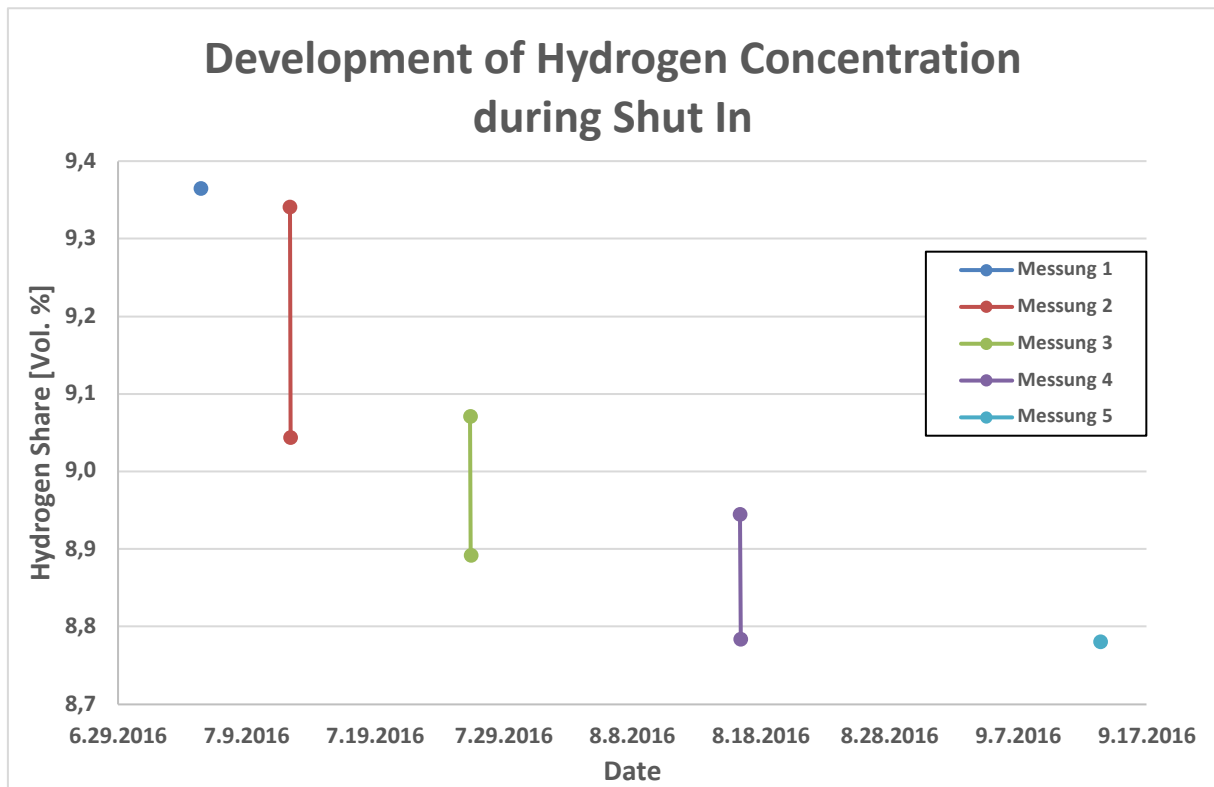


Figure 100: Development of the hydrogen concentration in the tubing with comparison of the respective final and initial concentrations

As a further measure to determine the well integrity, both the quality of the cementation and the wall thickness of the casing were determined before and after the field test. No changes were detected. Any deviations in the cement would have indicated that hydrogen migrates through the cement. In the case of casing, a change in the wall thickness would have indicated corrosion.

8.9 Reference to publications and other documents

Nr.	Studie/ Bericht/ Präsentation	Jahr	Autor
1	Interner Workshop Hychico	2016	RAG
2	Abschlussbericht zum Speicherbetriebsplan „Lehen 2 – Speicherstation (Untertage Sonnenspeicher)“ Auswertung der Ergebnisse	2017	Pichler; Bauer
3	ÖVGW Jahrestagung USS- Erneuerbare Energien Untertage Speichern	2017	Bauer
4	Präsentation Ergebnisse DVGW Clustersitzung	2017	Bauer

8.10 List of references

- [1] HUBER H., STETTER K.O. (2006): *Thermoplasmatales*, Prokaryotes (2006) 3:101-112 DOI: 10.1007/0-387-30743-5_7
- [2] WOLICKA, D., BORKOWSKI, A., (2012): *Microorganisms and Crude Oil*, University of Warsaw Poland, (2012)
- [3] CARR S.A., ORCUTT B.N., MANDERMACK K.W., SPEAR J.R. (2015): *Abundant Atribacteria in deep marine sediment from the Adélie Basin, Antarctica*, *Frontiers Microbiology* 2015 Aug 26;6:872. doi: 10.3389/fmicb.2015.00872. eCollection 2015
- [4] Lucia, „Measurements of H₂ solubility in saline solutions under reservoir conditions: preliminary results from project H₂STORE,“ European Geosciences Union General Assembly, Potsdam, 2015.
- [5] Lassin und e. al, Hydrogen solubility in pore water of partially saturated argillites: Application to Callovo-Oxfordian clayrock in the context of a nuclear waste geological disposal, Fontenay-aux-Roses, France: *Physics and Chemistry of the Earth* 36 (2011) 1721–1728, 2011.
- [6] Gesetz von Boyle Mariotte, „Wikipedia,“ [Online]. Available: https://de.wikipedia.org/wiki/Thermische_Zustandsgleichung_idealer_Gase. [Zugriff am 28 September 2017].

8.11 Contact details

RAG Austria AG
UGS Subsurface Management
Markus Pichler
Markus.pichler@rag-austria.at
Tel: 0043507245346
Schwarzenbergplatz 16
1015 Wien

UNIVERSITÄT FÜR BODENKULTUR WIEN
Department IFA-Tulln
Institut für Umweltbiotechnologie
a.o.Prof.DI Dr. Andreas P. Loibner
Konrad Lorenz Str. 20, A-3430 Tulln
Tel.: +43-1-47654-97470
Fax: +43-1-47654-97409
E-Mail: andreas.loibner@boku.ac.at
www.boku.ac.at

Autoren: A. Andiappan, M. Pichler, S. Bauer, J. Schritter, A.P. Loibner

9 Risk analysis and life cycle assessment

9.1 Task definition

In connection with the investigation of the hydrogen compatibility of underground gas storages, a risk assessment of possible dangers of underground hydrogen storage was carried out, as well as a life cycle analysis of the environmental impacts of feasible hydrogen storage scenarios.

The task of the risk assessment was to identify risks and safety aspects of underground hydrogen storage in a pore storage facility by means of a literature study with regard to future undertakings of this kind and to supplement these by means of expert interviews. The result will be presented in a list of the identified risks and safety aspects of the technology used in this project. Based on these results, a qualitative and quantitative risk assessment will be carried out, whereby the findings will be incorporated into an improved model for risk evaluation of underground hydrogen storage. This model will also be supported by a Monte Carlo simulation to contribute to a better understanding of the effects of critical risks. The methodology developed will allow the verification of the data obtained from the field test and contribute to a generic methodology for the evaluation of similar projects.

In addition to risk analysis, this section includes the implementation of an ecological assessment based on a Life Cycle Assessment (LCA) for potentially feasible - i.e. economically meaningful - scenarios of hydrogen storage, which were elaborated from the economic analyses (see Chapter 10). These scenarios were defined as fields of application and contain different aspects regarding value generation and potential customers. A special LCA software was used for the implementation of the ecological assessment and visualization. The results of the Life Cycle Assessment are included in the risk analysis.

9.2 Content presentation

This section is subdivided into the part of Risk Assessments and the part of Life-Cycle Assessments.

9.2.1 Risk analysis

The risk assessments were divided into a detailed survey of all system elements of underground storage and a comprehensive literature search to identify, record and present risks in a hazard matrix. The collected data were checked for parallelism between the system elements in order to be able to represent or exclude further hazards.

The created representation of these risks and dangers was subsequently used as the basis for a survey of experts to consider further risks and to complete this list.

Subsequently, the risks were analyzed qualitatively and quantitatively using a "bow-tie" analysis, which combines a fault tree analysis (FTA), a method for detailed fault analysis with a top-down approach, and an event tree analysis (ETA). Model uncertainties, which insist on

the assumption of independence between the different events, were taken into account by using fuzzy logic.

On the basis of these initial data and findings, the risks were again examined and evaluated according to the procedure model and methodology of the ISO 31000 Risk Management Process and processed using a specially developed methodological framework or procedure model (Figure 101).

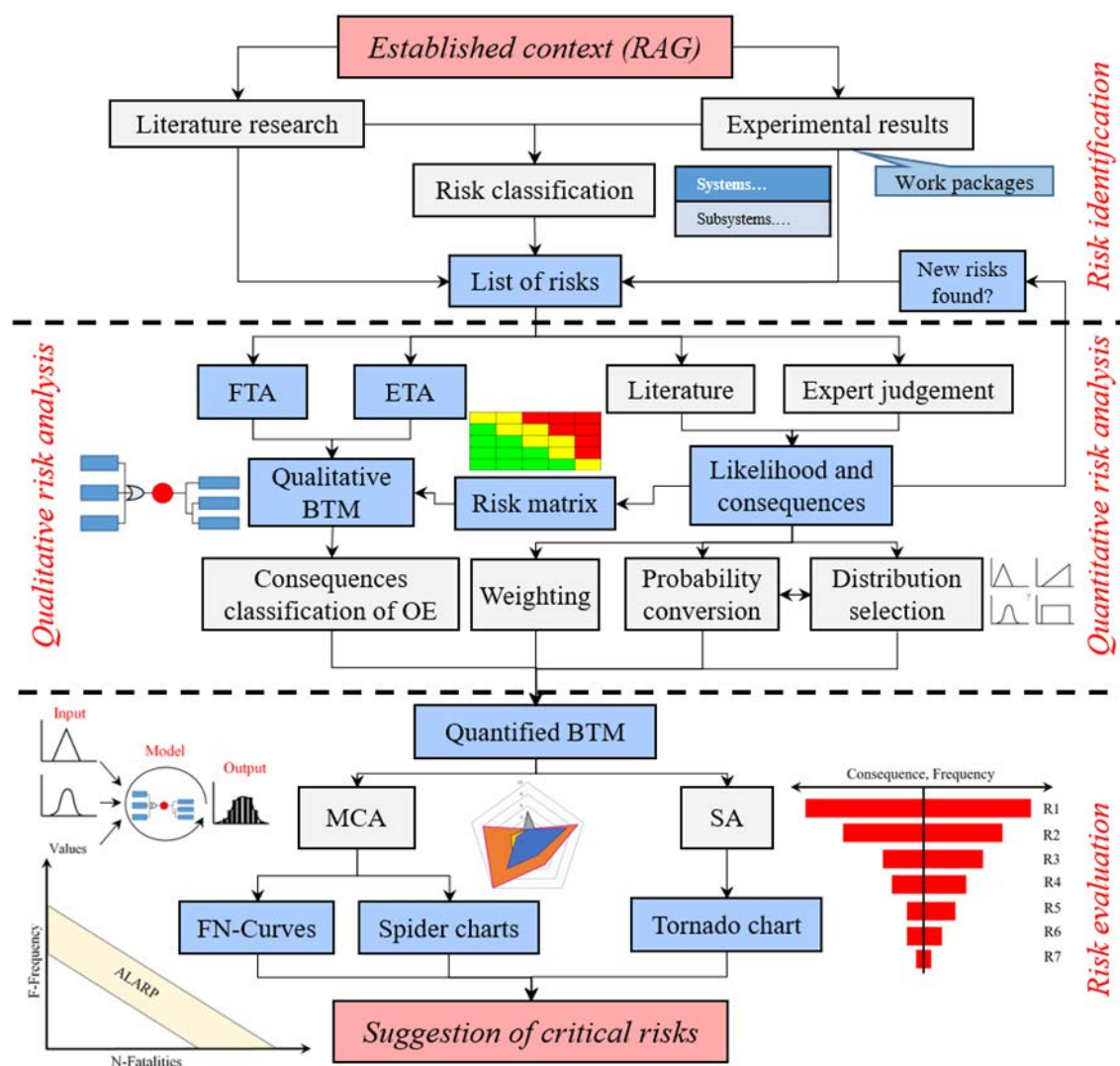


Figure 101: Procedure of the PtG RA (Tucovic, N. 2017).

This procedure model took into account the information gained up to that point and also made it possible to take into account newly gained findings from the other relevant work packages. Subsequently, a qualitative as well as a quantitative risk analysis takes place in this model, which is expressed as a result in a quantified Bow-Tie model.

This quantified Bow-Tie model is in turn subjected to a Monte Carlo analysis as well as a sensitivity analysis for further risk evaluation in order to identify critical risks and visualize them using a spider diagram, tornado representation and an FN curve. This visualization also supports the final results.

9.2.2 Life cycle assessment

The ecological assessment is based on the standards ISO 14040:2006 "Environmental management - Life cycle assessment - Principles and framework" and ISO 14044:2006 "Environmental management - Life cycle assessment - Requirements and guidance". Accordingly, the implementation of an LCA includes the following 4 phases:

- (1) Definition of objective and scope of investigation, to define width, depth and detail
- (2) Preparation of the Life Cycle Inventory (LCI)
- (3) Life cycle impact assessment
- (4) Phase of evaluation.

The LCA carried out is built around the "pilot plant" system, whereby the data and information required for the analysis were partly taken from upstream work packages. The following flow chart provides an overview of the system under consideration:

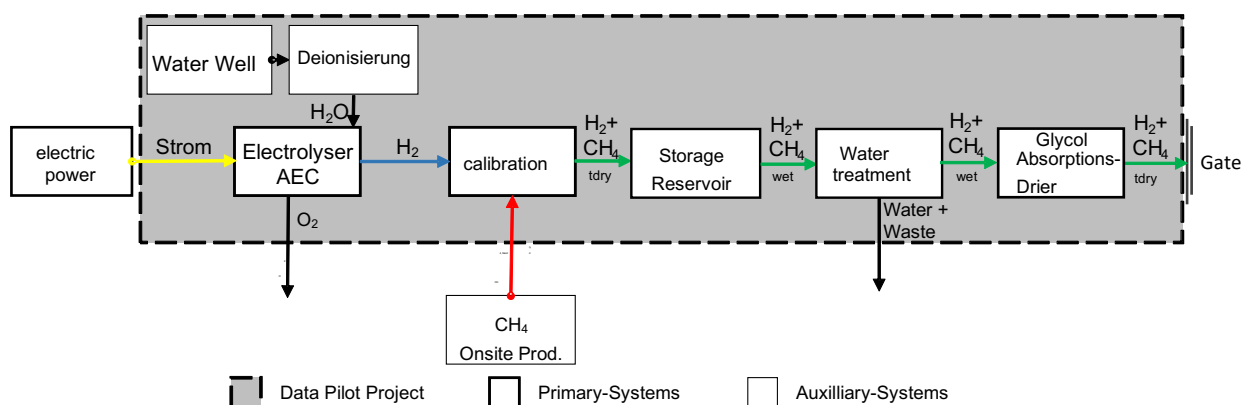


Figure 102: Flow diagram of the system boundary of the USS project (cf. Sledz, 2017 and Tschiggerl et al. 2017)

In coordination with the project consortium, two fields of application (AF 1 and 7 from the economic analysis) with economic implementation potential were selected for evaluation by means of a life cycle assessment:

- 1) Storage of renewable energy in a porous gas storage facilities (new product/new market)
 - a. Service - Provision of a storage facility for hydrogen in the porous storage facility
 - b. Renewable storage product from the porous storage facility
- 2) Production of a new renewable product
 - a. Mixture of hydrogen and methane for the fuel market
 - b. Pure hydrogen as a raw material for the chemical industry

9.3 Results and conclusions

9.3.1 Risk Analysis

The results of the risk assessment according to the above methodology are structured as follows:

a) Results of risk identification

The identified risks, which take into account both surface and underground risks, are shown in Figure 103 and listed in the following Table 27 to 30 (Tucovic, N 2017). They also take into account the results of the other work packages.

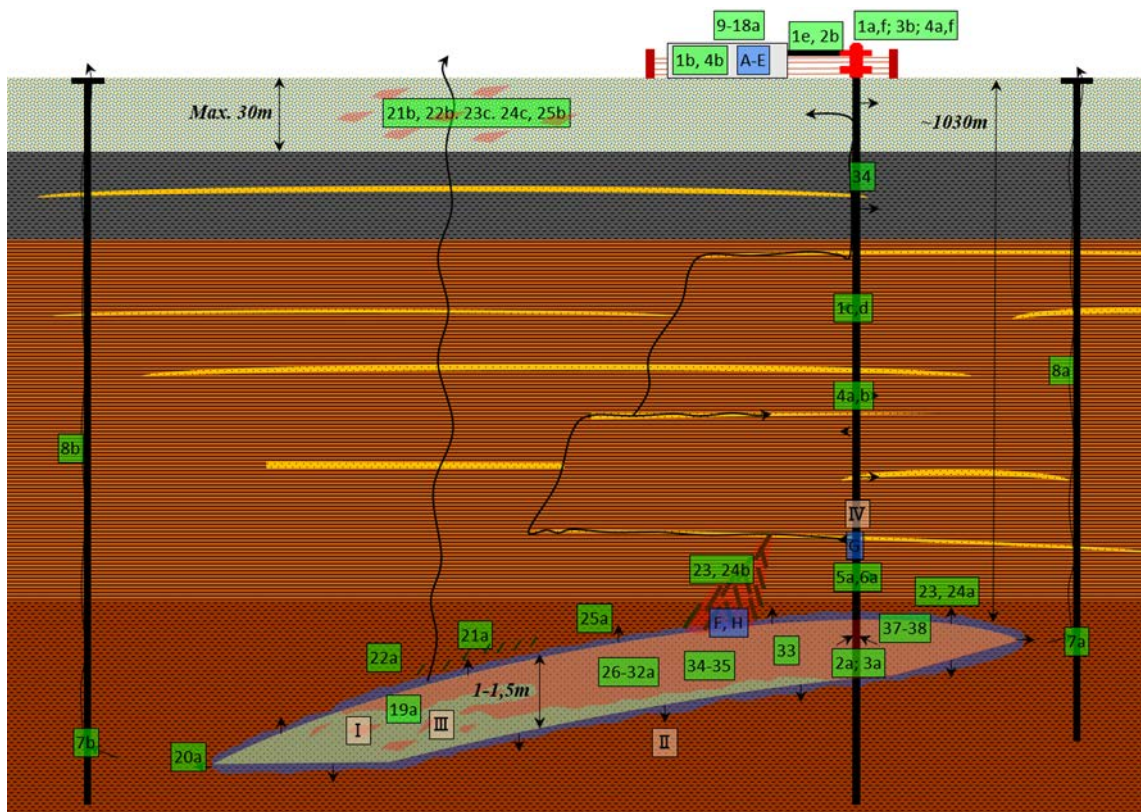


Figure 103: Simplified representation of the testbed with the respective labels of the identified risks (Tucovic, N. 2017)

Table 27: Identification of risks related to the components of the storage facility

FACILITY COMPONENTS RELATED RISKS – ETA			
<u>NO.</u>	<u>THREATS/HAZARDS</u>	<u>NO.</u>	<u>POTENTIAL OUTCOMES</u>
1	H ₂ embrittlement (steel)	1a	Leak valves
		1b	Leak compressor
		1c	Leak casing
		1d	Leak tubing
		1e	Leak pipes
		1f	Leak wellhead
2	Diffusion facility components	2a	Diffusion packers
		2b	Diffusion pipes
3	Blistering (elastomers)	3a	Leak packers
		3b	Leak sealing rings
4	Corrosion (steel)	4a	Leak valves
		4b	Leak compressor
		4c	Leak casing
		4d	Leak tubing
		4e	Leak pipes
		4f	Leak wellhead
5	Viscous flow cement	5a	Leak cement
6	Diffusion cement	6a	Leak cement
7	Nearby wells connected to reservoir	7a	Leak into PILS-001A
		7b	Leak into PILS-002
		7c	Leak into LEH-001
8	Poor abandoned nearby wells	8a	Leak through PILS-001A
		8b	Leak through PILS-002
		8c	Leak through LEH-001

Table 28: Identified risks related to human behavior

HUMAN RELATED RISKS – ETA			
<u>NO.</u>	<u>THREATS/HAZARDS</u>	<u>NO.</u>	<u>POTENTIAL OUTCOMES</u>
9	Poor SCADA	9a	Overfilling reservoir
		9b	No det. of reservoir irregularities
10	Poor equipment maintenance	10a	Leak due to maintenance
11	Unsuitable material from supplier	11a	Leak due to supplier

12	No quality checking of material	12a	Leak due to supplier
13	3rd party interference, sabotage	13a	Leak due to sabotage
14	Misbehavior from contractors	14a	Leak due to contractor
15	Bad signage	15a	Leak due to misconception

Table 29: Identified risks related to the environment

ENVIRONMENT RELATED RISKS – FTA			
NO.	<u>THREATS/HAZARDS</u>	NO.	<u>POTENTIAL OUTCOMES</u>
16	Flood	16a	Leak due to flood
17	Subsidence	17a	Leak due to subsidence
18	Earthquake	18a	Leak due to earthquake

Table 30: Risks not related to the equipment

NON-EQUIPMENT RELATED RISKS – FTA			
NO.	<u>THREATS/HAZARDS</u>	NO.	<u>POTENTIAL OUTCOMES</u>
19	Viscous fingering/lateral spreading	19a	Escape from trap
20	Reservoir not isolated	20a	Escape from trap
21	Existing fractures	21a	Leak to surrounding rocks
		21b	Leak up to groundwater and surface
22	Existing faults	22a	Leak to surrounding rocks
		22b	Leak up to groundwater and surface
23	Induced shear fractures	23a	Leak to surrounding rocks
		23b	Destruction of geological system
		23c	Leak up to groundwater and surface
24	Induced hydraulic fractures	24a	Leak to surrounding rocks
		24b	Destruction of geological system
		24c	Leak up to groundwater and surface
25	Induced capillary pressure	25a	Leak to surrounding rocks
		25b	Leak up to groundwater and surface
26	Methanogenesis	26a	Loss of gas mixture
27	Homoacetogenesis	27a	Loss of gas mixture
28	Sulphate reduction	28a	Loss of gas mixture

Table 31: Identified risks related with the destruction of the porous storage reservoir

DESTRUCTION OF THE RESERVOIR – FTA			
<u>NO.</u>	<u>THREATS/HAZARDS</u>	<u>NO.</u>	<u>POTENTIAL OUTCOMES</u>
29	Change of mineral abundance	29a	Destruction of pore space
30	Biomass accumulation	30a	Destruction of pore space
31	Change of aqueous species	31a	Destruction of pore space
32	pH-level change	32a	Destruction of pore space

Table 32: Identified hazards the increase the overall risk

REMAINING THREATS AND HAZARDS INCREASING OVERALL RISK – FTA			
<u>NO.</u>	<u>THREAT/HAZARD</u>	<u>NO.</u>	<u>INFLUENCING</u>
33	Generation of H ₂ S	33a	Corrosion risk increasing
		33b	Embrittlement risk increasing
		33c	Blistering risk increasing
		33d	Cement leak risk increasing
		33e	Fatality risk increasing
34	Static demixing	34a	Blistering risk increasing
		34b	Embrittlement risk increasing
		34c	Diffusion rate increasing
		34d	Cement leak risk increasing
		34e	Caprock leak risk increasing
		34f	Viscous fingering increasing
35	Dynamic demixing (pipes)	35a	Embrittlement risk increasing
		35b	Diffusion rate increasing
36	Dynamic demixing (reservoir)	36a	Diffusion rate increasing
		36b	Blistering risk increasing
		36c	Cement leak risk increasing
		36d	Caprock leak risk increasing
		36e	Viscous fingering increasing
37	Overfilling	37a	Caprock leak increasing
38	Too high injection rate	38a	Viscous fingering increasing

b) Summary of the results

When carrying out the risk assessment, the risk of an above-ground gas leak, i.e. an undefined mixing ratio of methane and hydrogen, was used as the most important criterion

(main event), since it can have a direct influence on the safety of the personnel at the facility.

Above-ground consideration

With regard to the case of an aboveground gas leak, the risks of human interference and corrosion were identified as the most likely causes.

In the case of human interference, sabotage was identified as the highest hazard, along with the misconduct of contractors. With regard to the risk factor corrosion, the compressor, wellhead and the piping of the plant were identified as risk elements or hazard elements to be considered.

The risk of material embrittlement due to hydrogen, on the other hand, was assessed as low, as the low hydrogen content in the gas mixture and the temperature and pressure in the plant are too low to cause material embrittlement.

It is therefore concluded that, whether with or without hydrogen in the gas mixture, the hazards to the surface equipment of the plant are corrosion and the human factor.

The result of the Monte Carlo analysis, related to the main event, gives a mean value for a significant surface leak of the gas mixture of "once in 7580 years", and corresponds predominantly to the results obtained from the literature study.

Subsequently, the further events after the occurrence of the main event were also considered according to frequency and presented in an FN curve (Figure 104).

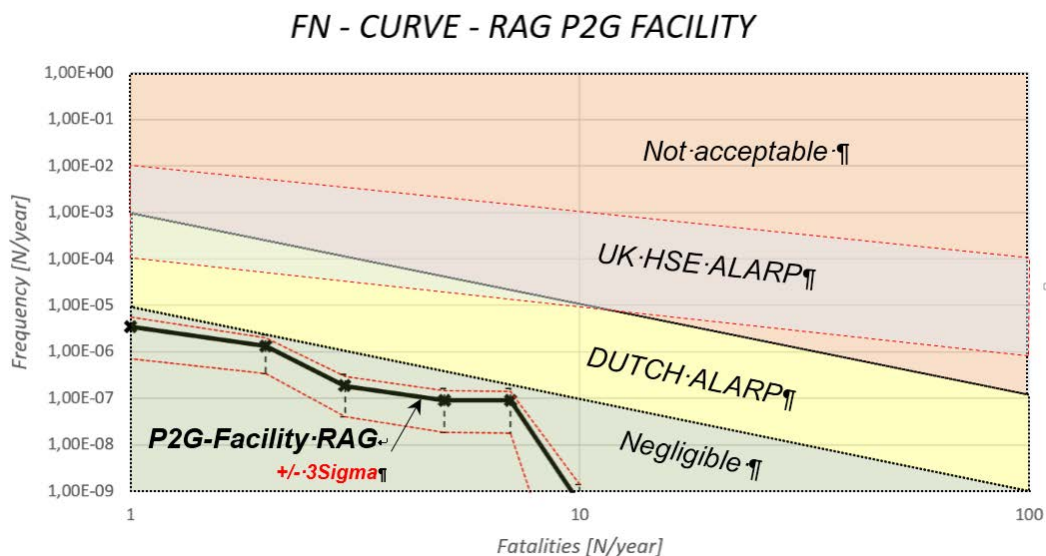


Figure 104: FN curve (black=average; dashed red = 3Sigma) of the RAG PtG plant (Tucovic, N. 2017)

The result clearly shows that the power-to-gas system falls below the current limit values and that there are no significant risks for people or the environment. It should be noted, however, that there are some discrepancies with regard to the literature comparison, which in turn leads to the conclusion that the definition is uncertain solely on the basis of expert opinions.

In the following, the main problems resulting from surface gas leakage were also presented in a spider diagram (Figure 105). In this graph, it is obvious that individuals and the public were identified as the most prominent characteristics. The environment has the lowest ranking in this graph, as the influence of an above-ground gas leak does not cause direct damage to the environment.

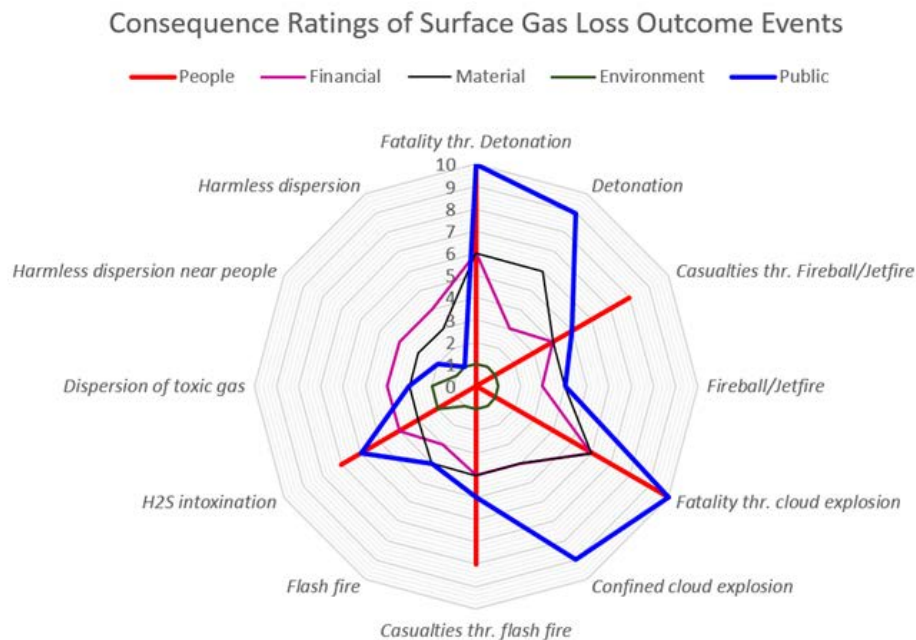


Figure 105: Spider diagram of the surface OE, evaluated by consequences (Tucovic, N. 2017)

Underground viewing

For the underground analysis of the risk assessment, it is pointed out that a possible hydrogen loss or damage to the geological system has no direct influence on the safety of the power-to-gas plant. The risks in this respect are therefore predominantly of a financial nature.

When considering the hazards of the underground equipment and the geological system, corrosion again stands out as the greatest threat, followed by methanogenesis and the viscous flow through the cementation of the borehole, for the main event considered.

The consideration of the results from the Monte Carlo analysis for the two Bow-Tie model observations carried out, indicate a probability of $5.98\text{E-}03$ for significant destruction of the geological system and $6.07\text{E-}03$ for significant loss of calorific value. However, it should be noted that there is a very high discrepancy in the probability of frequency per year in all studies considered and monitored. This uncertainty is due on the one hand to the different methodologies used to derive the frequency distributions and on the other hand to the different scenarios considered. Therefore, the applied frequency distribution is also subject to a high degree of uncertainty and should therefore be treated with caution.

The assessment of possible events in the underground risk assessment is summarized in the following diagram (Figure 106). The event with the highest ranking is the complete

destruction of the storage capacity. The associated financial aspect, followed by the effects on reputation, is identified by public perception as the greatest danger.

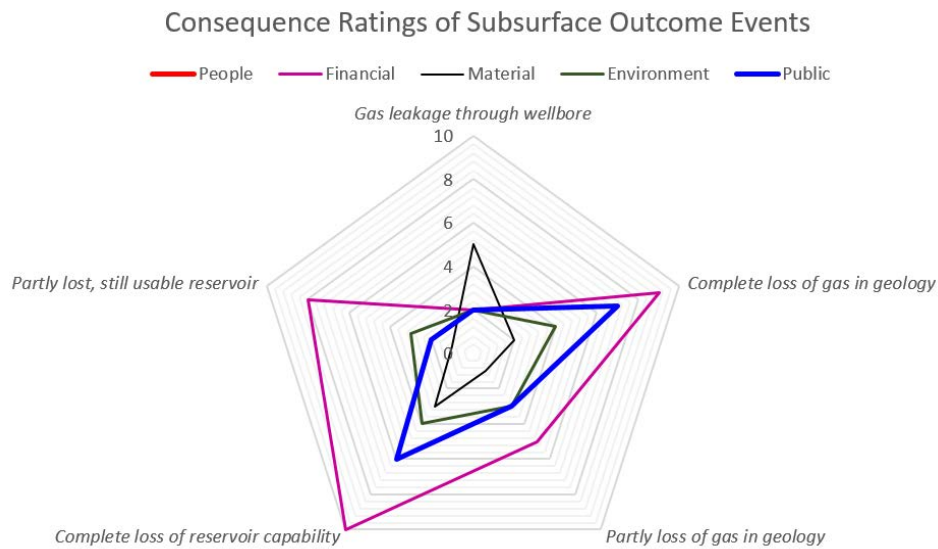


Figure 106: Spider diagram of underground OUs evaluated by consequences (Tucovic, N. 2017)

Finally, it can be stated that a gas mixture with a proportion of up to 10% hydrogen does not increase the risk of the considered power-to-gas plant including the geological reservoir compared to conventional natural gas reservoirs. All risks associated with an underground gas reservoir, including hydrogen, such as material embrittlement, diffusion, viscous fingering, or segregation, were considered in detail and were not considered significant. The only remaining risk from the addition of hydrogen is the proven increase in microbiological activity in the geological system and represents a pure financial risk for the company. Any impairment of the safety of the plant or personnel can be ruled out. The only exception would be a sulfate reduction by special bacteria which could lead to hydrogen sulfide generation in the reservoir. This is to be excluded for the considered case with probability bordering on certainty, however, it must be examined for further use cases.

This means that there are no obvious limitations which argue against a storage of up to 10% hydrogen in the considered underground porous storage facility.

Life cycle assessment

Based on the requirements of the ISO standards, the following results, which build on one another, result in the individual phases:

Phase 1: The system boundaries are determined by the process units used in the respective specific field of application. This results in the definition of the analysis as a gate-to-gate assessment, i.e. the phases of production, maintenance and recycling or disposal of the pilot plant as well as for energy generation are not included. The investigation focuses on the value-adding process of the generated products or services. The functionalities refer to the process modules of the pilot plant (see Figure 1 flowchart). The functional unit refers to the outputs (depending on the business model, these are hydrogen, synthetic methane, natural gas or

mixtures) of the fields of application investigated, which is why the energy content per MJ was used to make comparisons.

Phase 2: The Life Cycle Inventory is based on the analysis of all inputs and outputs of the process modules (depending on the field of application). Data were generated from upstream work packages (data sheets, pre-defined or measured data), from LCA databases (GaBi and data converted from Ecoinvent), as well as by applying conceptual designs to insufficient data (assumptions and estimates based on physical and chemical principles).

Phase 3: The impact assessment was implemented using the CML method. The calculation was performed with the software Umberto NXT Universal using the GaBi database. In order to include future possibilities, the LCA considers a hydrogen concentration of 10 vol.% in the gas network (current values for Austria and Germany are 4-5 vol.%). The impact assessment contains results for the following impact categories:

- Global warming potential (GWP)
- Ozone depletion (stratosphere) (ozone depletion potential, ODP)
- Human toxicity (Human Toxicological Classification Factor, HC)
- Aquatic Ecotoxicity (Ecological Classification Factor for Aquatic Ecosystems, ECA)
- Ecological Classification Factor for Terrestrial Ecosystems (ECT)
- Formation of photooxidants (Photochemical Ozone Creation Potential, POCP)
- Acidification potential (AP)
- Eutrophication (Nutrification Potential, NP)
- Depletion of abiotic resources (Abiotic Depletion Factor, ADF)

Furthermore, primary energy consumption was included in the impact assessment.

The following Figure 107 and Figure 108 show the flow diagram and the corresponding material flows (inputs and outputs) as well as their modelling using LCA software and data for application field 1b:

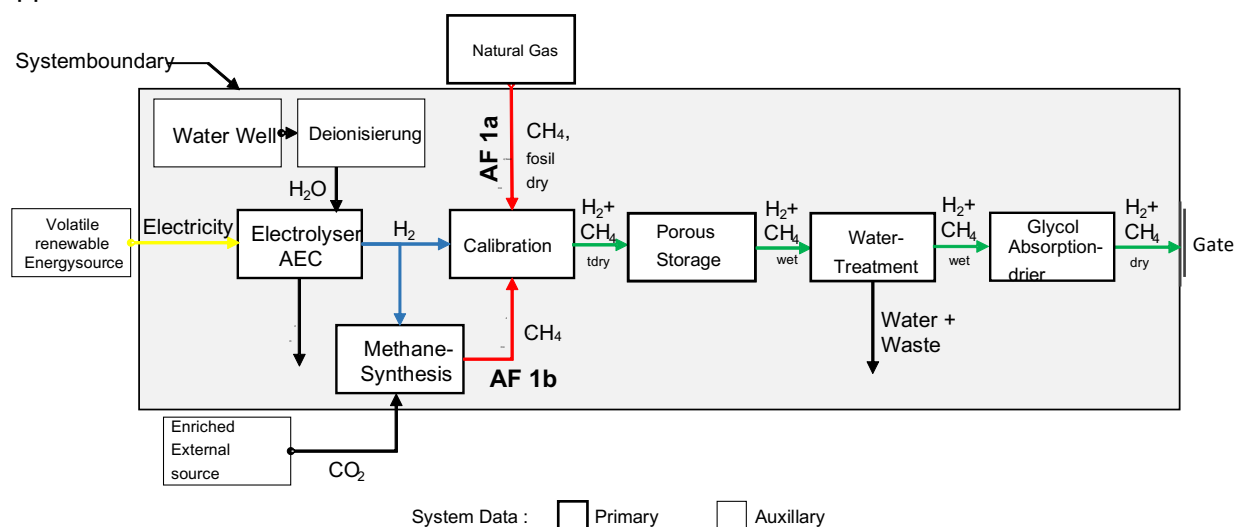


Figure 107: Flow diagram application field 1b (cf. Sledz, 2017 and Tschiggerl et al. 2017)

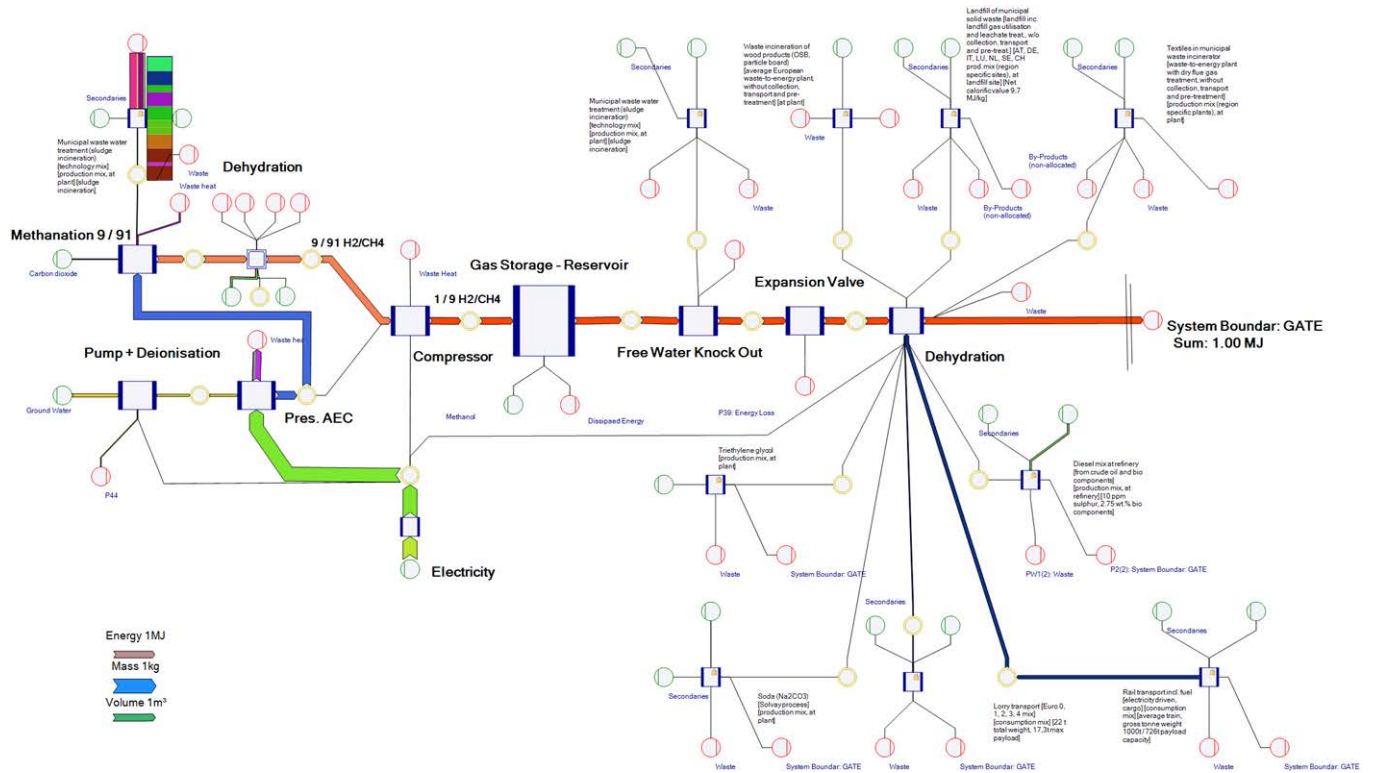


Figure 108: Modeling application field 1b (Sledz, 2017)

Phase 4: The impact assessment clearly showed that the energy source is decisive for the ecological impacts of the selected PtG application fields. The processes in the background dominate those in the foreground. Within the two fields of application, the electrolysis unit was identified as the most important energy consumer and its specific efficiency as a critical parameter. Figure 109 shows an extract from the environmental profile for application area 1b.

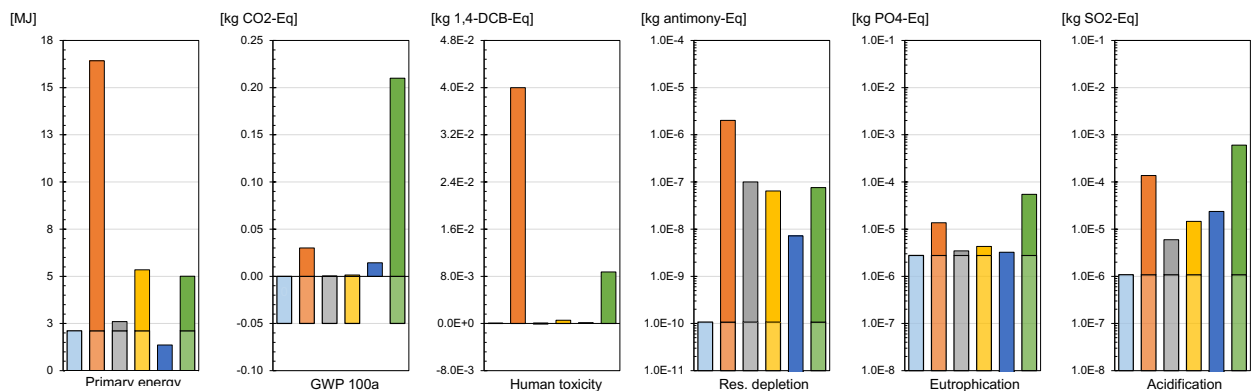


Figure 109: Extract from the environmental profile for field of application 1b (cf. Sledz, 2017 and Tschiggerl et al., 2017)

Risks that may be associated with hydrogen storage in porous geological formations are cement integrity, corrosion, hydrate development and microbiological growth that may cause hydrogen sulphide formation. According to Pichler (2013) and Schritter et al. (2016), and as a result of the microbiological investigations, underground storage would only be influenced by microbiological activities if electron acceptors such as CO₂ or sulphate were present. Since the results in the present field test and in comparable facilities were insignificant, they were not integrated into the LCA.

In general, it should be noted that the environmental indicators should not be compared as they concern different environmental impacts. As a consequence, no environmentally friendly product, field of application or energy source can be identified as the reasoning relates to the specific situation. Life cycle assessments are per se based on an iterative approach, in the present case data collection over a longer period would be useful, as well as the integration of the analysis in a broader context, e.g. with regard to synergies between PtG plants and plants requiring oxygen and waste heat. This should make it possible to make clearer statements regarding the ecological improvement potential and advantages of PtG technology.

9.4 Reference to publications and other documents

Two master theses were written in connection with the risk assessment. It is planned to publish an article focusing on the application of Monte Carlo analysis and sensitivity analysis and on the Bow-tie models.

In connection with the Life Cycle Assessment a master thesis was published and an article was presented at a conference lecture at the end of June 2017.

Below is a list of the publications that were produced within the scope of the work package:

- Sledz, Christian (2017): Life-Cycle Assessments of Power-to-Gas Business Models. Master Thesis, Montanuniversität Leoben.
- Tschiggerl, Karin; Sledz, Christian; Topic, Milan (2017): Evaluation of Environmental Impacts of Power-to-Gas Business Models. Vortrag 3rd International Conference on Energy and Environment, Porto 29. – 30. Juni.

9.5 List of references

Risiko Assessment (Literaturauszug)

Bücher

DGMK (Ed.) (2013): DGMK Research Report 756: Influence of Bio-methane and Hydrogen on the Microbiology of Underground Gas Storage. Hamburg: DGMK. ISBN 978-3-941-72136-4.

DGMK (Ed.) (2014): DGMK Research Report 752: Influence of Hydrogen on Underground Gas Storage. Hamburg: DGMK. ISBN 978-3-941-72148-7.

Papers und Artikel

Amid, A.; Mignard, D.; Wilkinson, M. (2016): Seasonal storage of hydrogen in a depleted natural gas reservoir. In: International Journal of Hydrogen Energy, Vol. 42, No. 12, pp. 5549-5558.

Carden, P. O.; Paterson, L. (1979): Physical, chemical and energy aspects of underground hydrogen storage. In: International Journal of Hydrogen Energy, Vol. 4, No. 6, pp. 559-569.

Ferdous, R.; Khan, F.; Sadiq, R.; Amyotte, P.; Veitch, B. (2012): Handling and updating uncertain information in bow-tie analysis. In: Journal of Loss Prevention in the Process Industries, Vol. 25, No. 1, pp. 8-19.

Hagemann, B.; Rasoulzadeh, M.; Panfilov, M.; Ganzer, L.; Reitenbach, V. (2016): Hydrogenization of underground storage of natural gas: Impact of hydrogen on the hydrodynamic and bio-chemical behavior. In: Computational Geoscience, Vol. 20, No. 3, pp. 595-606.

Panfilov, M. (2010): Underground Storage of Hydrogen: In Situ Self-Organisation and Methane Generation. In: Transport in Porous Media, Vol. 85, No. 3, pp. 841 – 865.

Paterson, L. (1983): The implications of fingering in underground hydrogen storage. In: International Journal of Hydrogen Energy, Vol. 8, No. 1, pp. 53-59.

Sercombe, J.; Vidal, R.; Galle, C.; Adenot, F. (2007): Experimental study of gas diffusion in cement paste. In: Cement and Concrete Research, Vol. 37, No. 4, pp. 579-588.

Sherif, S. A.; Barbir, F.; Veziroglu, T. N. (2003): Principles of Hydrogen Energy Production, Storage and Utilization. In: Journal of Scientific & Industrial Research, Vol. 62, No. 1, pp. 46-63.

Reporte, Publikationen, Diplomarbeiten und Dissertationen

Altfeld, K. (2013): H₂ Sensitivity of Seals, Valve and Compressors in High Pressure Natural Gas Systems. Final Report for the GERG Project, Brussels.

Altfeld, K.; Pinchbeck, D. (2013): Admissible Hydrogen Concentrations in Natural Gas Systems. Final Report for the GERG Project, Brussels.

Batisse, R. (2012): Existing Natural Gas Transmission Pipelines Tolerance to CH₄-H₂ Mixtures. Final Report for the GERG Project, Brussels.

DBI (Ed.) (2012): Abschlussbericht – Erarbeitung von Basisinformationen zur Positionierung des Energieträgers Erdgas im zukünftigen Energiemix in Österreich. AP 2: Evaluierung der existierenden Infrastrukturen auf Grundlage der ermittelten Potenziale, Leipzig.

DBI (Ed.) (2013): Admissible Hydrogen Concentrations Natural Gas Systems – Gas distribution. Final Report for the GERG Project, Brussels.

Deborah, K. (2008): Failure rates for underground gas storage: Significance for land use planning assessments. Research Report for HSE, HSE, Norwich.

Foh, S.; Novil, M.; Rockar, E.; Randolph, P. (1979): Underground Hydrogen Storage – Final Report. Technical Report for Department of Energy and Environment, Institute of Gas Technology, Chicago.

Lord, A. S. (2009): Overview of Geologic Storage of Natural Gas with Emphasis on Assessing the Feasibility of Storing Hydrogen. Research Report, Sandia National laboratories, Albuquerque.

Nadau, L. (2013): Underground Storage: literature survey of hydrogen and natural gas mixture behaviour. Final Report for the GERG Project, GERG, Brussels.

Life-Cycle Assessment (ausgewählte Literatur)

Europäische Kommission (Hrsg.). 2010. *EUROPE 2020 A strategy for smart, sustainable and inclusive growth*. Europäische Kommission, Brüssel (Mar).

Europäischer Rat (Hrsg.). 2011. *EUCO 2/1/11 REV 1*. Generalsekretariat des Rats. Brüssel (Feb.).

- Fthenakis, V.; Kim, H.C.; Alsema, E. 2008. "Emissions from Photovoltaic Life Cycle." *Environmental Science & Technology* 42, No. 6 (Mar), 2168-2174.
- Fthenakis, V.; Kim, H.C.; Frischknecht, R.; Rauegi, M.; Sinha, P.; Stucki, M. 2011. „Life Cycle Inventories and Life-Cycle Assessments of Photovoltaic Systems." Forschungsbericht, International Energy Agency PVPS Task 12, New York (Oct).
- Ganzer, L.; Reitenbach, V.; Pudlo, D.; Panfilov, M.; Albrecht, D.; Gaupp, R. 2013. „The H_2 STORE Project - Experimental and Numerical Simulation Approach to Investigate Processes in Underground Hydrogen Reservoir Storage". *Society of Petroleum Engineers*. doi:10.2118/164936-MS.
- Götz, M.; Lefebvre, J.; Mörs, F.; McDaniel Koch, A.; Graf, F.; Bajohr, S.; Reimert, R.; Kolb, T. 2016. „Renewable Power-to-Gas: A technological and economic review." *Renewable Energy* 8 (Jan), 1371-1390.
- Graf, F.; Götz, M.; Henel, M.; Schaaf, T.; Tichler, R. 2014. „Technoökonomische Studie von Power-to-Gas Konzepten." Forschungsbericht G3-01-12, DVGW, Bonn (Nov.).
- Hellweg, S.; Rubli, S.; Von Götz, N. 2016. „Ökologische Systemanalyse. Materialflussanalyse – Risikoanalyse – Ökobilanz." Vorlesungsskriptum, ETH Zürich, Zürich (Feb).
- International Energy Agency (Ed.). 2012. *World Energy Outlook 2012*. IEA. Paris.
- International Organization for Standardization (Ed.). 2006. *ISO 14044:2006 Environmental management—life-cycle assessment—requirements and guidelines*. ISO, Genf.
- Johnson M.W.; Suskewicz J. 2009. "How to jump-start the Clean Tech economy." *Harvard Business Review* 87, No.11 (Nov), 52-60.
- Klöppfer, W.; Grahl, B. 2012. *Ökobilanz (LCA): Ein Leitfaden für Ausbildung und Beruf*. Wiley, Weinheim.
- Lehner, M.; Tichler, R.; Steinmüller, H.; Koppe, M. 2014. *Power-to-Gas: Technology and Business Models*. Springer, Cham-Heidelberg et al.
- Makaruk, A.; Szivacz, J.; Bauer, S.; Schlegl, L. 2016. „Key role of membrane gas separations in the utilisation of an underground natural gas reservoir for the renewable energy storage." In Proceedings of the Spring Conference (Paris, France, Apr.21-22). Gas Processors Association Europe, Paris, n.p.
- Müller-Syring, G.; Henel, H.; Köppel, W.; Mlaker, H.; Sterner, M.; Höcher, T. 2013. „Entwicklung von modularen Konzepten zur Erzeugung, Speicherung und Einspeisung von Wasserstoff und Methan ins Erdgasnetz." Forschungsbericht G1-07-10, DVGW, Bonn (Feb).
- Pichler, M. 2013. "Assessment of hydrogen-rock interactions during geological storage of CH_4 - H_2 mixtures." Masterarbeit, Montanuniversität Leoben.
- Reiter, G.; Lindorfer, J. 2015. "Global warming potential of hydrogen and methane production from renewable electricity via power-to-gas technology." *The International Journal of Life-Cycle Assessment* 20, No.4 (Apr), 477-489.
- Reiter, G.; Lindorfer, J.; Tichler, R. (2015). „Projekt Underground.Sun.Storage: vertiefte Konzeption der Geschäftsmodelle für die ökonomische Bewertung." Forschungsbericht, Energie Institut JKU, Linz (Mar).
- Schaltegger, S.; Hansen, E.; Lüdeke-Freund, F. (2016). „Business Models for Sustainability: Origins, Present Research, and Future Avenues." *Organization & Environment* 29, No.1 (Mar), 3-10.
- Schritter, J.; Scherr, K.; Komm, R.; Backes, D.; Loibner, A.P. 2015. „Underground.Sun.Storage WP 3 – Microbial Processes in Hydrogen Exposed Reservoir: Hydrogen induced microbial processes as observed underground gas storage simulation experiments." Präsentation beim 3. Stakeholder Workshop Underground.Sun.Storage, Wien (Jun).
- Tichler, R.; Steinmüller, H.; Reiter, G. 2014. „Wirtschaftlichkeit und Systemanalyse von Power-to-Gas Konzepten." Forschungsbericht G3-01-12, DVGW, Bonn (Nov).
- United Nations (Ed.). 2015. *Transforming our world: the 2030 Agenda for Sustainable Development*. A/RES/70/1. UN, New York (Oct).
- United Nations Framework Convention on Climate Change (Ed.). 2015. *ADOPTION OF THE PARIS AGREEMENT – Proposal by the President –Draft decision –/CP.21. F FCCC/CP/2015/L.9/Rev.1*. UN FCCC, Paris (Dec).
- Valente, A.; Irabarren, D.; Dufour, D. 2017. "Life-cycle assessment of hydrogen energy systems: a review of methodological choices." *The International Journal of Life-Cycle Assessment* 22, No.3 (Mar), 346-363.

9.6 Contact details

Projektleiter

Hubert BIEDERMANN

o.Univ.-Prof. Dipl.-Ing. Dr. mont.

Vorstand Lehrstuhl und Department WBW

+43 (0) 3842 402 6000

hubert.biedermann@unileoben.ac.at

wbw.unileoben.ac.at

Weitere Ansprechpartner

Franz SIEGMETH

Dipl.-Ing. MBA, Senior Lecturer

+43 (0) 3842 402 6014

franz.siegmeth@unileoben.ac.at

Robin KÜHNAST

Dipl.-Ing., Wissenschaftlicher Mitarbeiter

+43 (0) 3842 402 6030

robin.kuehnast@unileoben.ac.at

Karin TSCHIGGERL

Mag., Wissenschaftliche Mitarbeiterin

+43 (0) 3842 402 6005

karin.tschiggerl@unileoben.ac.at

10 Economic and legal analyses

In this chapter, the different possible uses and fields of application of storage technology in the context of the entire power-to-gas system are examined in the context of economic and legal analyses. In addition, the potential of hydrogen injection into the Austrian natural gas grid is determined. In order to identify obstacles on the one hand and to propose possible future framework conditions on the other hand, an analysis of the existing legal system and an investigation of the social acceptance of power-to-gas is carried out.

10.1 Tasks

The tasks in the project part "Economic and legal analyses" include the following points:

1. Analysis of the current legal situation
2. Building on the basic technical results, draft legislative proposals to amend existing legislation with the aim of opening the system for the underground storage of hydrogen and helping to integrate it into the natural gas market.
3. Detailed analysis of the optimal system integration of hydrogen storage into the energy market
4. Detailed definition and analysis of the economic characteristics and impacts of hydrogen production and storage
5. Identification of potentials for cost reduction for the energy system
6. Quantifying the macroeconomic influences of the process

10.2 Content presentation

This chapter provides a detailed description of the content of the thematic blocks dealt with - legal analyses, potential of hydrogen injection into the Austrian natural gas grid, economic evaluation, social acceptance of power-to-gas.

10.2.1 Legal analyses

The legal analysis mainly deals with the (interim) storage of hydrogen and synthetic natural gas in the natural gas network. The first step explains how a power-to-gas plant can be integrated into an electricity and gas market model and who is allowed to construct and operate such a plant. Then the general professional and operational requirements will be shown. An important point in this context is also to examine the electricity and gas costs. Since the GWG 2011 is currently only applicable to natural gas and biogenic gases, the question arises as to whether and under what conditions power-to-gas products can also be included. Subsequently, the possibilities of re-electrification in an external plant as well as the participation of the power-to-gas plant in the control energy market in the form of negative secondary control will be investigated.

Another legal issue concerns the underground storage of power-to-gas products under the MinroG and natural gas storage under the GWG 2011.

Finally, an overview is given as to whether the power-to-gas plant can be subject to state access under the EnLG 2012 in the event of a crisis.

10.2.2 Potential of hydrogen injection into the Austrian natural gas grid

The aim of the present study is to estimate the potential of hydrogen injection in the Austrian natural gas grid in order to derive the potential for power-to-gas plants. The potential of hydrogen injection into the natural gas grid in Austria depends on numerous different factors. The most important factors are listed here:

- Permitted volume fraction of H₂ in natural gas (regulated in the directive ÖVGW-RL G31)
- Compliance with the combustion characteristics Wobbe index, calorific value and relative density (also regulated in the directive ÖVGW-RL G31)
- Compatibility of the various components and materials in the natural gas infrastructure (transport, storage and distribution of natural gas, measurement and control technology and end user applications)
- Natural gas flow with daily and seasonal fluctuations (maximum volume fraction H₂ as well as combustion characteristics must be observed at all times!)
- Generation structure of the power-to-gas plant or the renewable power generators (in particular wind turbines and photovoltaics)
- Removal of the power-to-gas plant or the renewable electricity producers from the feed-in point into the natural gas network.
- Location-specific parameters and load flows in the natural gas network (very large fluctuations, especially in small local networks)

The individual factors were taken into account in the estimates of the potential of H₂ injection into the natural gas network. The data were obtained from various literature sources, E-Control Austria and various gas network operators (example networks).

10.2.3 Economic valuation

The economic evaluation of power-to-gas is based on the calculation of specific production costs for hydrogen or methane in different fields of application. Due to the versatile application possibilities of Power-to-Gas in the energy system, numerous fields of application can be derived, whereby an economic evaluation was carried out for the following:

- 1) Storage of renewable energy in porous gas storages (new product/new market)
 - a. Service - Provision of a storage facility for hydrogen in the pore storage facility
 - b. Renewable storage product from the porous storage facility
- 2) Use of non-public gas pipelines (crude gas pipelines)
- 3) Substitution of replacement investments in electricity grid expansion
- 4) Optimization of load management (with a high proportion of volatile production)
- 5) Optimization of the operation of a wind power plant
 - a. Increasing the full load hours of a wind turbine as an alternative to shutdowns
 - b. Revenue optimization of a wind power plant - fulfillment of day-ahead forecasts with interim storage
- 6) Intermediate storage of electricity
 - a. Sale on the electricity market at optimal price times
 - b. Own use in the case of flexible tariffs - Optimization of procurement costs
- 7) Production of a new renewable product
 - a. for the fuel market
 - b. for the chemical industry
- 8) H₂ separation from natural gas - production of a renewable product (fuel/chemistry)
- 9) Supply of negative balancing energy

These fields of application are compared with the respective specific benchmarks in the energy system. In order to optimize the production costs and thus the economic efficiency of power-to-gas, various combinations of application fields are also investigated. The selection of suitable fields of application is based on the respective production costs.

The analysis of the economic effects of the power-to-gas technology for Austria was carried out for selected applications. Within the analysis on the one hand the comparative-static data of the use of the respective technology is given, on the other hand a macroeconomic simulation analysis is carried out based on these values, on the basis of which dynamic effects on the national economy can be quantified. These effects are determined with regard to their effect on the central macroeconomic variables of the gross domestic product, employment, current account, private consumption and investment.

A selection of scenarios was made for which the economic effects were analyzed. The selection was made with regard to their plausible implementation, the broadest possible differentiation between the scenarios and their data availability. The economic effects were simulated for the following fields of application:

- Field of application 5a (Optimization of the operation of a wind turbine)
- Field of application 7a (Production of a renewable product in the form of fuel (hydrogen or methane))
- Field of application 7b (production of a new product (hydrogen) for industrial use)

In addition, an analysis of the economic effects for the combination of the various fields of application was carried out.

10.2.4 Social Acceptance of Power-to-Gas

The aim is to develop the status quo with regard to the social acceptance of power-to-gas technology by researching existing studies, opinion polls and projects. Although the acceptance of power-to-gas plants and the feeding of hydrogen into the natural gas grid was not specifically investigated, there are already studies on the acceptance of hydrogen, especially in the mobility sector, the results of which can be at least partially applied to the power-to-gas process and discussed. The results will be presented in an Austrian context. At the same time, an overview of the secondary literature on the social acceptance of energy infrastructure projects, in particular of high-voltage lines and pumped storage power plants, will take place in order to discuss the experiences already gained with the problems and in dealing with acceptance problems and to transfer them to power-to-gas.

10.3 Results and conclusions

This chapter describes the results and conclusions of the thematic blocks dealt with - legal analyses, brand research, potential of hydrogen injection into the Austrian natural gas grid, economic evaluation, and social acceptance of power-to-gas.

10.3.1 Legal analyses

Due to the constantly increasing use of electrical energy from renewable sources, the question arises as to how surplus electricity can be used temporarily so that the corresponding generation plants do not have to be throttled or completely shut down or significant line capacities have to be built. The search for suitable storage technologies has led in particular to the idea of using electricity to produce hydrogen or, optionally, synthetic natural gas from it (power-to-gas). In particular, this means that the volatile share of electrical energy generated can be transferred to a storage medium and used for demand-oriented purposes. For example, it is possible to feed these energy sources into the natural gas grid first. If necessary, e.g. at times of low electricity generation, the power-to-gas products stored in the natural gas network can be taken out of the natural gas network for balance sheet purposes and returned to the grid in order to feed this electricity back into the electricity network. However, this approach is not the preferred option. The use in the transport sector, in the heat sector and in industry as process energy can also be presented.

The examination of the legal framework in Underground Sun Storage shows, however, that the current legal framework in Austria concerning storage and conversion facilities in general and power-to-gas facilities in particular is still very rudimentary, although initial steps have been taken in this direction to change this. Nevertheless, there are still numerous unresolved legal issues and associated uncertainties. For this reason, a first position paper was drawn up by several stakeholders in which selected legal problems and proposed changes were compiled. On the other hand, for this reason existing regulations concerning pumped storage power plants are often presented as a basis within the framework of the investigation. In addition, a brief digression into the German legal situation is undertaken again and again, as far as this appears sensible for the Austrian view. It becomes clear that in many segments power-to-gas plants in Germany are in a better legal position than equivalent plants in Austria.

The legal investigation in the context of power-to-gas technology in this project deals mainly with the possibility of (intermediate) storage of hydrogen and synthetic natural gas in the natural gas network. First of all, it is analyzed which market participants could be involved in the power-to-gas plant on both the electricity and gas side. At present, however, there is no defined integration into the Austrian energy market model. Therefore, the existing general energy law regulations must be used. Since the power-to-gas plant is likely to be the first step in obtaining electrical energy predominantly from the public grid, this technology - also in line with the highest court ruling on pumped storage power plants - is to be classified under electricity law as a purchaser, customer, grid user and end consumer. If at this point the applicability of the GWG 2011 is assumed, it must be noted in the case of pure hydrogen that, unlike synthetic natural gas, it may not be fed directly into the natural gas network in order to avoid damage to pipelines and customer plants. The hydrogen must therefore first be mixed with natural gas from the natural gas network to form a natural gas-hydrogen mixture. It is imperative that the gas to be fed into the grid meets the requirements of the relevant ÖVGW guidelines and is therefore compatible with the grid. On the gas side, the power-to-gas plant - insofar as it actually takes natural gas from the natural gas network for the purpose of adding it to pure hydrogen - functions as an extractor, network user and currently probably also as an end consumer and then as a natural gas company, producer, feeder, network user and, due to the wording of the law, also as a natural gas trader if the natural gas/hydrogen mixture or the synthetic natural gas is released into the natural gas network with the intention of making a profit.

It then examines who is allowed to build and operate such a plant at all. This will probably be anyone. From the point of view of unbundling law, however, this seems problematic for the grid operators. For example, a gas distribution network operator will probably not be allowed to operate such a technology at present. The same applies to both the electricity transmission network operator and the gas transport network operator. The situation could be different for the electricity distribution network operator, provided that the power-to-gas system itself does not generate electricity back into the grid.

In connection with the requirements of professional and plant law, it can be assumed that a free trade, but one subject to registration, as defined in the GewO 1994 is involved. Depending

on the minimum quantity available, it could also be a Seveso III plant due to the use of hazardous substances.

It was also important to shed light on the electricity costs for the power-to-gas plant. When electricity is purchased from the public grid, the system usage fees relevant for consumers are charged first. However, due to a temporary exemption pursuant to Section 111 (3) of the Electricity Industry and Organization Act (EIWOG), the grid usage charge and the grid loss charge are excluded from this in 2010. For this reason, the obligation to pay the green electricity flat rate and the green electricity subsidy contribution currently appears unclear. For example, the green electricity flat rate is levied "together with the respective grid utilization fee" and the green electricity subsidy contribution is to be paid "in proportion to the respective grid utilization and grid loss fees to be paid". The same applies to the CHP flat rate. In this context, it should be emphasized that pumped storage power plants do not have to pay either the green electricity levy or the CHP flat rate. With regard to the electricity levy, a taxable event is to be assumed for the time being. However, a tax exemption could possibly be considered. On the one hand, if the electrical energy is used to produce and transport natural gas; although the power-to-gas plant does not produce natural gas, it produces a natural gas substitute in the form of a natural gas-hydrogen mixture or synthetic natural gas for the purpose of feeding into the natural gas network. Therefore, a legal equalization with natural gas seems obvious. In the opinion of the Federal Ministry of Finance, the same also applies to biogas. On the other hand, if the electric energy is used for non-energy purposes. The problem is that the conversion of electricity into hydrogen or synthetic natural gas can also be seen as an energy consuming process. However, according to the Federal Ministry of Finance, there is also a non-energy purpose in the use of electric energy for the decomposition or conversion of substances such as electrolysis. The same generally applies to chemical or physical use. The first step in the power-to-gas process is electrolysis for the purpose of producing hydrogen. In addition, synthetic natural gas can optionally be produced from this hydrogen - and is thus based on electrolysis. Methanation can also be defined as a chemical use. The pure energy price, as well as the usage levy and the value added tax, however, are striking.

At present, the GWG 2011 does not explicitly regulate whether and under what conditions power-to-gas products may be fed into the natural gas grid, i.e. whether the GWG 2011 is applicable at all. This applies exclusively to (natural) gas and biogenic gases. However, it can certainly be argued that grid-compatible natural gas-hydrogen mixtures and synthetic natural gas should be subsumed under the scope of the GWG 2011, especially as biogas must first be upgraded to natural gas quality. This assumption is supported by the Natural Gas Directive 2009. Subject to the applicability of the GWG 2011 and compliance with the quality requirements, the following costs will be incurred on the gas side: When natural gas is procured from the natural gas grid for the purpose of mixing with hydrogen, the system usage fee for the user is currently the main charge, as are the natural gas supply and value-added tax. With regard to the natural gas levy, on the other hand, the possibility of a tax exemption could be obvious.

When (re-)feeding the natural gas/hydrogen mixture or the synthetic natural gas into the grid, the system usage fee for the feeder must be paid. Due to the systemic background, legal equivalence with biogenic gases should be sought with regard to the hydrogen content to be fed into the system or the synthetic natural gas.

In the case of re-electrification by an external power plant, the question arises as to the origin of the electric energy. It is therefore advisable to clarify that electricity, despite intermediate storage in the natural gas network, then consists of renewable energy sources, provided that the corresponding prerequisites (e.g. electricity extraction from a direct line) are fulfilled in the respective individual case. In addition, it must be determined to what extent the evidence must be deleted due to technical storage losses. A regulation regarding a possible feed-in tariff would also be informative.

Furthermore, the Underground Sun Storage project presented the possibility of a power-to-gas plant participating in the balancing energy market in the form of negative secondary regulation. In this context, the necessary prerequisites as well as any costs incurred were discussed.

Another legal issue is connected with the possibility of underground storage of Power-to-Gas products in accordance with the MinroG. The MinroG mainly regulates the storage of mineral raw materials, i.e. hydrocarbons of natural origin, which include crude oil and natural gas. However, the introduction of substances is also anchored. Thus, the individual storage projects are presented and an attempt is made to outline the scope of the terms hydrocarbons and substances. In this context, pure natural gas and synthetic natural gas fall under the term hydrocarbons. Pure hydrogen, on the other hand, is regarded as a substance.

Finally, an overview is given of whether power-to-gas products may be accessed in the event of a crisis. In this context, it seems conceivable that the power-to-gas plant could be temporarily affected on the electricity side by the control measure to secure electricity supply to purchase less electricity. On the gas side, on the other hand, instructions could be given to produce more natural gas-hydrogen mixtures or synthetic natural gas and feed it into the natural gas network in order to guarantee a secure supply. However, since the power-to-gas plant is also an end user in the case of the necessary enrichment of hydrogen with natural gas from the natural gas network, due to its necessary procurement, the steering measure of temporarily withdrawing less natural gas could also be relevant.

10.3.2 Potential of hydrogen injection into the Austrian natural gas grid

As the comprehensive investigation shows, the potential of hydrogen injection into the Austrian natural gas grid depends on several influencing factors. Standards and guidelines such as ÖVGW-RL 31, which regulate the maximum volume fraction of H₂ in natural gas as well as compliance with combustion parameters (Wobbe index, calorific value, relative density), are of major importance. Other limiting factors for H₂ injection are the compatibility of components and materials in the natural gas infrastructure and the daily and seasonal fluctuations in natural gas flow. In many cases, the physical properties of transport pipelines are less important than

gas supply contracts in determining whether natural gas flows through the pipeline, which can have a significant impact on the H₂ potential in the respective network section.

The injection of hydrogen must be considered separately depending on the network level, local conditions and customer structure. In the case of transit pipelines, it should be noted that the gas quality may vary depending on the origin of the natural gas and may already contain hydrogen. Here it must be clarified whether an additional H₂ feed-in and forwarding to the respective neighboring country is possible. Due to contracts and frequently changing injection and withdrawal processes, it is difficult to predict the flows and their direction in the transport pipeline. In the distribution network, on the other hand, the flow and direction of the natural gas follows physical conditions, with sales being subject to strong fluctuations in some cases, depending on the respective consumer structure.

According to ÖVGW-RL 31, the maximum H₂ content in Austria is currently 4 % by volume (and 2 % by volume at natural gas filling stations). The problem here, however, is that the gas quality in the existing natural gas network is mainly measured at transfer points to other network areas, countries and natural gas storage facilities. Combustion parameters essentially depend on the origin of the natural gas (Russia, North Sea). Unlike relative density, the Wobbe index causes the least difficulty. Thus, the limit value for the relative density for natural gas from Russia is already undercut at a volume share of 4-5 vol.% H₂. The Wobbe index can still be maintained even with a volume fraction of 15 vol.%, but compliance with the limit values for the calorific value from 10 vol.% H₂ is to be regarded as critical.

As far as the H₂ compatibility of individual components is concerned, there is a particular need for adjustment in the case of gas turbines as well as transport and storage compressors. Further adaptation is also required for CNG vehicles (currently max. 2 vol.% H₂) and process gas chromatographs (currently no H₂ measurable). With regard to the compatibility of H₂ in pore storages, however, a considerable need for research can be assumed.

The estimation of the potential of hydrogen in the Austrian natural gas network is based on a theoretical potential (annual gas consumption), taking into account the different annual gas consumption of industry and households, and on the calculation of the gas absorption capacity in the summer load case by Hofmann et al. (2005). The results for current and possible future framework conditions and limits are summarized in Figure 110. In addition, the figure lists those components of the natural gas network for which there is still a need for research or at least adaptation. The size of the rectangles provides information on the level of potential in relation to the other calculation methods.

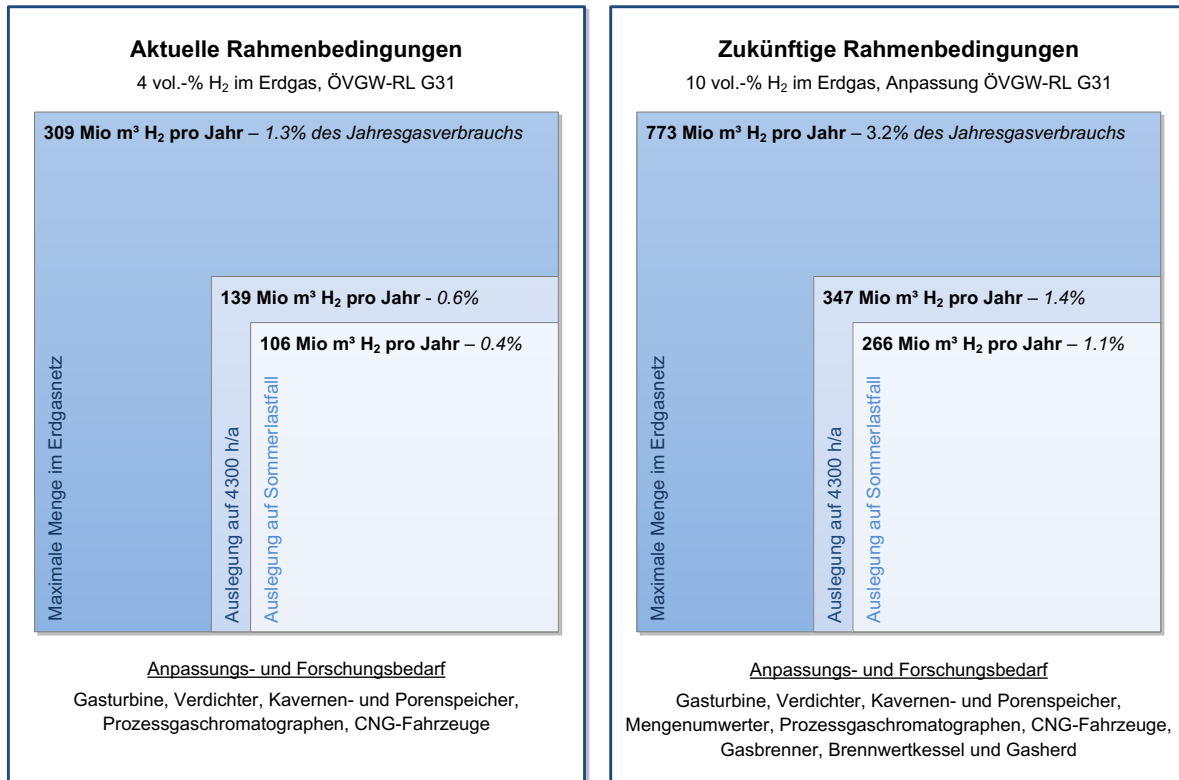


Figure 110: Potential of the annual H₂ injection into the Austrian natural gas grid Source: Energy Institute at the JKU Linz

Figure 110 shows the potential of H₂ injection into the Austrian natural gas grid for various calculation methods. The calculation of the maximum amount of H₂ in the natural gas network does not take into account the large differences in the natural gas flow during the year and represents the theoretical potential. If it is assumed that hydrogen is not produced continuously throughout the whole year (4300 full load hours per year), the potential is significantly reduced. A design of the feed-in for the summer load case (8h mean value) reduces the total potential again, but in this case it can be fed in all year round independent of the actual gas flow. Over an entire year, the potential is thus only slightly below that of 4300 full load hours per year when designed for the summer load case. Figure 110 also shows the amount that can be fed into the grid as a percentage of annual gas consumption. It should be noted here that the volumetric energy density of hydrogen is lower than that of methane (approx. 1/3 of the calorific value of methane). With a volume share of 4% by volume of hydrogen, only 1.3% of annual gas consumption is replaced in terms of energy content.

The analysis of different example networks showed that there are no typical consumption profiles, especially in network sections with predominantly industrial customers. Also the progressions of the regions and urban areas show differences and thus a range between 0 and 56% of the average flow rate was determined for the throughput in the summer load case (8h mean value). A detailed potential for hydrogen injection can only be determined separately for each grid area due to the different characteristics. However, the results scaled up to Austria can serve as guide values.

On the basis of the possible H₂ absorption capacity of the Austrian natural gas network (see Figure 110), the possible total installed capacity of power-to-gas plants and the storable electricity is estimated in the form of H₂ (see Figure 111).

If the power-to-gas plant is designed on the basis of the average absorption capacity of the natural gas network, a total capacity of 176 MW_{el} is possible under current conditions. When designed for the summer load case, the possible total output is already significantly reduced. Nevertheless, under current conditions (4 vol.% H₂ in natural gas) at least 1% of the electricity generated from wind and PV can still be stored in the form of H₂. The criteria according to which the power-to-gas plant is actually designed depend above all strongly on the respective field of application and the grid area under consideration. If the plant is designed for 4300 full load hours per year, there will be large differences in the total potential in terms of capacity and storable electricity quantity, as the plant only produces H₂ in 4300 h/a. Depending on the application, however, in addition to the total amount of storable electricity, the possible total output can be significant. This applies above all to the use of surpluses from wind and PV, where peak loads tend to occur at short notice and not throughout the year.

When storing surpluses from volatile electricity generation by wind turbines or photovoltaics, the characteristics of electricity generation and gas consumption in the different regions must also be taken into account. While in Burgenland and Lower Austria, for example, a high amount of electricity can be generated from wind power but only a low feed-in capacity into the natural gas grid, other provinces have high feed-in capacities (e.g. Upper Austria and Vienna) but only low electricity production from wind and photovoltaics.

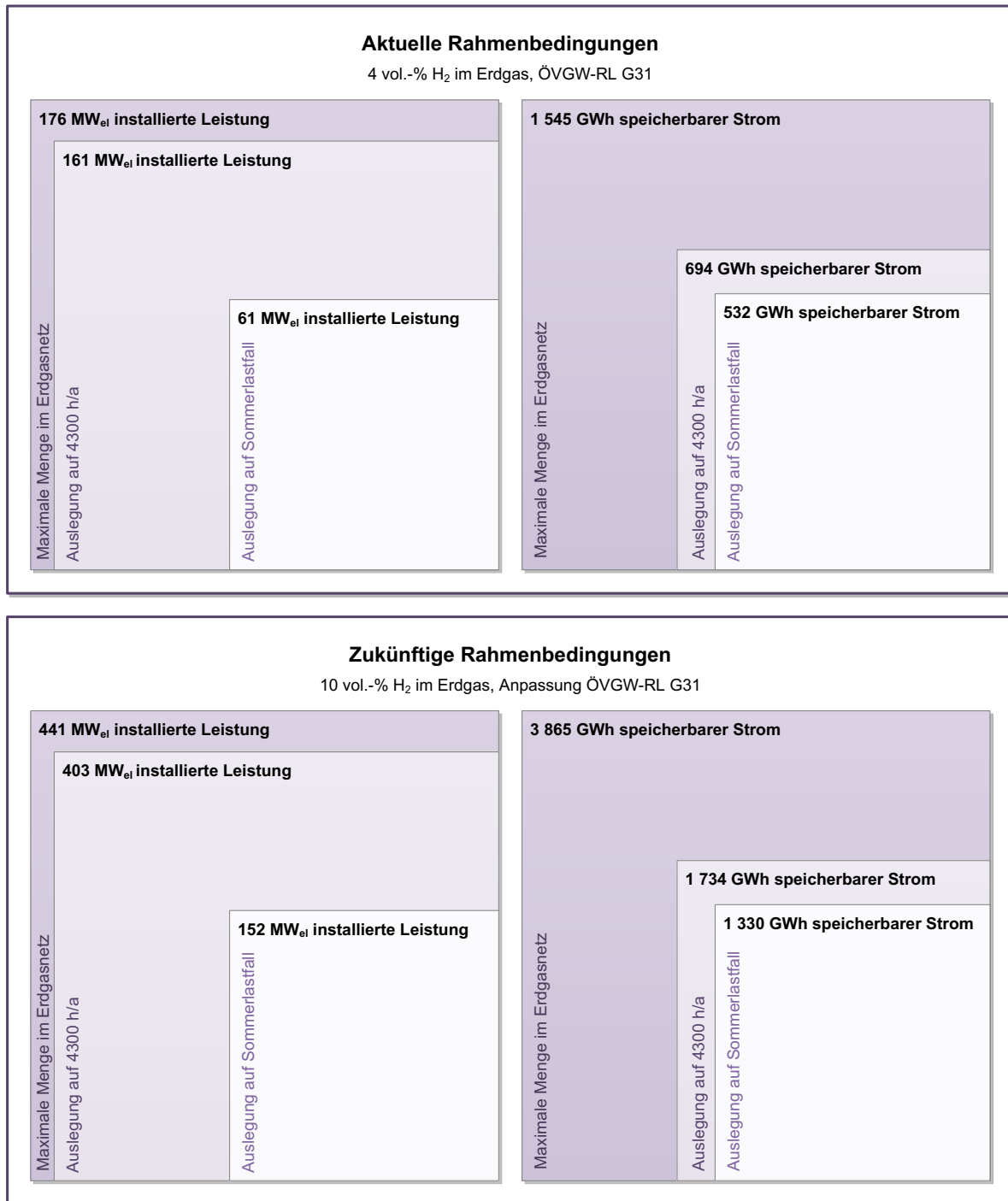


Figure 111: Possible total installed capacity of power-to-gas plants and storable electricity for the various H₂ feed-in capacities into the Austrian natural gas grid for current and future framework conditions. Source: Energy Institute at the JKU Linz

10.3.3 Economic valuation

For the economic evaluation of Power-to-Gas within the Underground Sun Storage project, the project consortium selected nine fields of application and evaluated eight of them quantitatively. The application fields differ in size, system benefit, product (hydrogen, methane or electricity) and the respective benchmark in the energy system.

The results for the individual fields of application are compared in Figure 112. In addition to the specific production costs for the respective product (hydrogen, methane or electricity), the full load hours achieved for the power-to-gas system are also shown, as these have a significant influence on the costs.

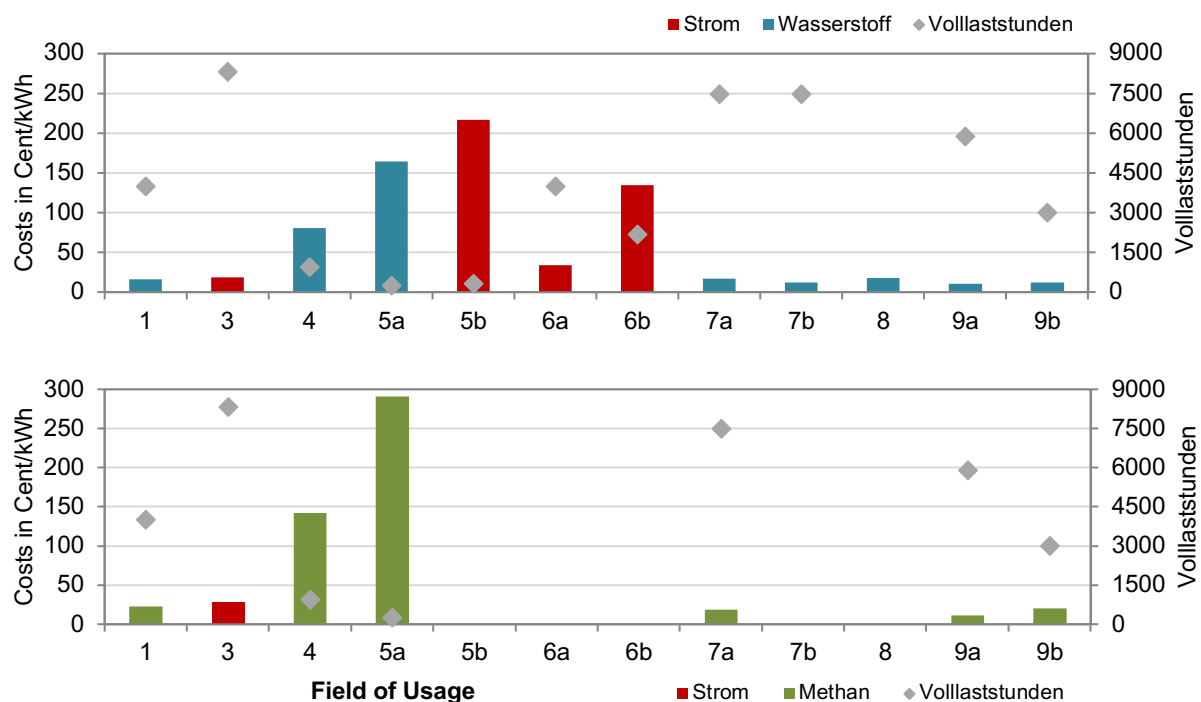


Figure 112: Overview of the production costs of the individual fields of application Source: *Energy Institute at JKU Linz*

Note: all values without VAT. In all fields of application, the values refer to the calorific value (LHV) of hydrogen and methane with the exception of the red columns, which refer to the electric current from hydrogen or methane.

- 1a) Storage of renewable energy in gas porous storage facilities - provision of storage facility as a service
- 1b) Storage of Renewable Energy in Gas Porous Storage - Renewable Storage Product from the Porous Storage
- 2) Utilization and use of non-public gas pipelines - qualitative assessment
- 3) Substitution of replacement investments in electricity grid expansion
- 4) Optimization of load management with high proportion of volatile production
- 5a) Optimizing the operation of a wind turbine by increasing full load hours as an alternative to shutdowns
- 5b) Optimization of the operation of a wind turbine by fulfilling the day-ahead forecast with intermediate storage
- 6a) Intermediate storage of electrical energy - sale on the electricity market at optimal price times
- 6b) Intermediate storage of electrical energy - own use in case of flexible tariffs
- 7a) Production of a new renewable product - Fuel market (hydrogen and methane)
- 7b) Production of a new renewable product - chemical product (hydrogen)
- 8) H2 separation from the natural gas
- 9a) Provision of negative control energy - cost-optimized full load hours
- 9b) Provision of negative balancing energy - 3000 h/a

The economic evaluation shows that individual fields of application, considered on their own, are usually associated with high production costs and that these depend strongly on the annual full load hours achieved by the power-to-gas system. Due to the additional components and the lower overall efficiency, the specific production costs of synthetic methane are higher than those of hydrogen. The use of re-electrification significantly reduces efficiency along the entire production chain and increases specific costs. At lower full load hours, the investment costs have a large influence on the electricity procurement costs. A significant reduction in investment costs can be expected in the future.

Compared with the benchmarks in the energy system, the production of a renewable product (field of application 7) and the provision of negative control energy (field of application 9) are of particular interest. This is mainly due to the high full load hours of these two fields of application. In other application fields, on the other hand, only very few full load hours are achieved and despite very low electricity procurement costs, as in the case of the use of surpluses from wind turbines (application field 5), the specific production costs are very high. In combination with other fields of application, these could be very interesting due to the low power procurement costs.

In order to optimize the economic efficiency by increasing the full load hours, a combination of several application fields was calculated in addition to the individual application fields. The combination includes the use of surplus electricity from wind turbines (250 h/a), the provision of negative control energy (3300 h/a) and an additional electricity purchase from the public grid at spot market prices (including proof of origin for renewable electricity). The hydrogen produced or, optionally, the synthetic methane are used as fuel or fed into the natural gas grid. The full load hours were set at 6000 h/a. The calculations were made for future (2025) costs and framework conditions and are shown in Figure 112.

The combination of the fields of application contributes to the increase in full load hours and thus brings considerable advantages in terms of economic efficiency. In future, specific production costs of around 13 cents per kWh of hydrogen or 18 cents per kWh of synthetic methane can be achieved.

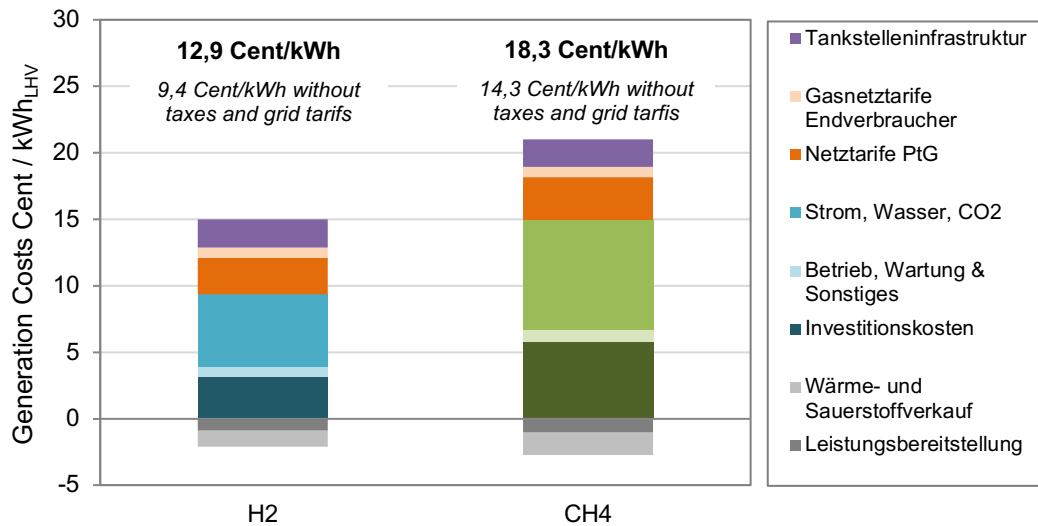


Figure 113: Composition of the specific production costs of hydrogen and methane from a power-to-gas plant with a rated output of 5 MWel at 6000 h/a. Source: Energy Institute at the JKU Linz

Note: all values without VAT. The values refer to the calorific value (LHV) of hydrogen and methane. Also included are the costs for the necessary filling station infrastructure and the final consumer levies.

In a sensitivity analysis, the influence of full load hours was also investigated for the combination. In the combination studied, an increase in full-load hours between 3500 and 8000 h/a has hardly any influence on the production costs, since the reduction in specific investment costs is offset by rising average electricity costs. From full load hours of approx. 3500 h/a, these are no longer decisive for the specific production costs. Higher full-load hours have the advantage of an overall increased production of H₂ or CH₄ and thus an increased substitution of fossil energy sources, but this also increases the overall electricity demand in the energy system.

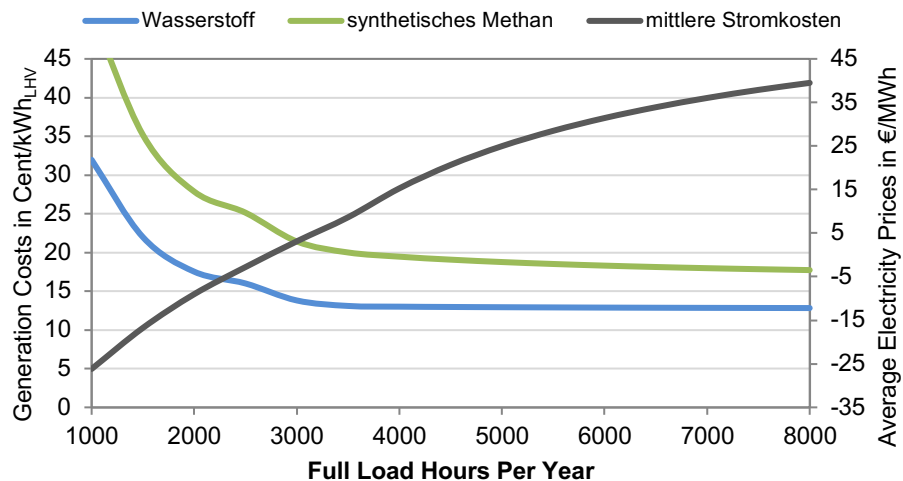


Figure 114: Sensitivity of production costs of H2 and CH4 from power-to-gas. Source: Energy Institute at JKU Linz

Note: all values without VAT. The values refer to the calorific value (LHV) of hydrogen and methane. Also included are the costs for the necessary filling station infrastructure and the final consumer levies.

Following the economic evaluation of all application fields and the combination of several application fields, the economic effects of individual application fields (5a, 7a, 7b) and those of the combination were simulated using the simulation model MOVE2 developed at the Energy Institute at the Johannes Kepler University Linz.

Since the fields of application and thus also the size of the systems and their capital expenditure are very different, comparability between the fields of application is only possible to a limited extent. What all plants have in common is that they lead to an increase in Austria's gross domestic product. This is fundamentally based on all applications:

- additional investment impulses through the construction of power-to-gas plants,
- a reduction in fossil energy imports,
- the increase in wages induced by economic growth and thus in disposable income,
- the resulting employment effects, and
- secondary effects resulting from the listed impacts.

In application case 7a and the combination there is an additional increase in private consumption due to the purchase of gas-powered vehicles.

The differences in the number of plants erected and the construction period are mainly due to the different time horizons for a possible application. An implementation of the application cases 7a to 7b would already be possible while there is currently no demand for application field 5a (no surplus hours from wind turbines). For this reason, for application field 5a, the construction of the turbines is simulated from 2020 onwards. The combination of the application fields represents a possible plant configuration as well as a potential future use under changed framework conditions and is quantified for the year 2025. Since it is still difficult to estimate the further development of this development, an installation of ten systems in one year was simulated. Table 33 provides an overview of the key results of the economic analysis.

Table 33: Summary of the central results of the economic analysis of application fields 5a, 7a, 7b and the combination of several application fields

	fields of application						
	5a		7a		7b	Combination	
	H ₂	CH ₄	H ₂	CH ₄	H ₂	H ₂	CH ₄
Installations constructed (total)	6	6	10	10	10	10	10
Construction period	6 years	6 years	10 years	10 years	10 years	1 year	1 year
Study period	2020-2030	2020-2030	2015-2030	2015-2030	2015-2030	15 years	15 years
Gross domestic product (in Mio. € p.a.)	0,58	3,47	26,91	30,95	19,35	54,94	60,20
Private consumption (in Mio. € p.a.)	0,65	1,05	5,84	6,92	2,18	29,32	27,85
Investments (in Mio. € p.a.)	1,48	2,53	4,37	9,91	4,62	6,03	12,63
Net exports (in Mio. € p.a.)	- 1,55	-0,15	16,71	14,12	12,55	19,59	19,72
Employees (Persons p.a.)	30	60	100	230	80	210	370

In general, it can be stated that in all cases the use of the methanation plant (CH₄) leads to more pronounced results. This is basically due to the higher investment costs of these plants, which trigger higher economic effects. With regard to the employment effects, a higher level is also achieved in the installation of methanation plants (CH₄) in all application cases.

10.3.4 Social acceptance of power-to-gas

In principle, the use of hydrogen as an energy carrier offers new opportunities for storing energy on the one hand and for use as an alternative fuel in the mobility sector on the other, in order to reduce dependence on fossil fuels. A key factor for the successful implementation of projects in the field of hydrogen mobility and the establishment of hydrogen filling stations is named as the "*social acceptance*" of the population. In order to promote the development of a so-called "*hydrogen economy*" in the future, not only technical, technological and economic aspects have to be taken into account in the implementation of power-to-gas plants, but also the social dimension, which is manifested by a wide variety of reactions from different actors in the fields of economy, politics and the public. The acceptance of the technology and the processes and outputs used with it is therefore important for a wide variety of stakeholders.

On the basis of studies already carried out in acceptance research, especially with regard to the expansion of renewable energy plants (e.g. wind power plants, hydropower plants) and energy infrastructures (e.g. expansion and conversion of the power grid infrastructure) as well

as hydrogen as fuel or as technology, the findings can also be discussed for the power-to-gas concept, which can be decisive for the acceptance of corresponding plants in planning and implementation (cf. e.g. [5], p.71). Power-to-Gas technology as well as the use of hydrogen as an energy carrier is a relatively new topic in Austria, which is why it is important to also address the perceptions and concerns when introducing these innovations into society (cf. [6], pp. 11 and [7]). This is important for those hydrogen applications in daily use, as experience from the mobility sector shows. In order to achieve a positive effect on "social acceptance" for hydrogen applications, it is essential to identify and address the most important target groups in order to analyse their fears and plan appropriate participation measures (cf. [6], p. 11f). At present, however, it is difficult to assess the extent to which the knowledge of the public (and here in particular the population) about the power-to-gas process, with its advantages and disadvantages, is pronounced, as corresponding empirical studies (e.g. in the form of surveys) are currently still lacking.

In this context, it is essential to identify those factors that influence the acceptance of the most diverse social groups. This includes not only the population and those directly affected, but also the economy (companies from industry, energy supply companies, trade associations), social groups (consumer associations, environmental associations) and opinion-forming institutions from the media and politics that deal with this topic (cf. [8], p. 68). Understanding the reasons for resistance and/or support of the new hydrogen technologies or the associated facilities (e.g. hydrogen filling stations, power-to-gas facilities) can help decision-makers or project managers to develop measures to obtain broader public support and also to improve communication to the public in this respect.

In order to gain further public attention for the topic of hydrogen technologies, a broad social debate is needed as well as images and contexts that connect to the everyday world of future users (cf. [9]). In the context of the acceptance issue, the creation of a positive image for hydrogen and the power-to-gas technology in the respective municipality and in the local population is important. It is also essential to address any fears raised about the respective project in order, for example, to exclude or minimize health effects (electromagnetic fields, electro smog) or nature conservation concerns. Also arguments for the necessity of the realization of the plant and their positive effect can influence the acceptance of the public accordingly. One argument could be that the negative effects associated with the expansion of the electricity grid can be reduced by power-to-gas plants in the sense that the existing electricity and gas infrastructure is used. In addition, a positive and communicated image of power-to-gas can contribute to the fact that the hydrogen required in the electrolysis process is generated entirely from renewable energies (wind power and solar energy) right from the start (cf. [10], p.20). However, commercialization does not take place until it has been shown to the wider public that the safety risks associated with hydrogen can be adequately dealt with. By introducing policy measures for technologies that are beneficial for society and the environment (safety standards, specific energy resources for the production of hydrogen for subsidy, influence on the design of the technological system, etc.), various concerns can be reduced among a wide range of actors. These in turn influence the choice of site for the power-to-gas installations, e.g. granting of permits for construction only for those sites where there are no safety concerns. Experience from the planning and implementation of other energy infrastructure projects, such as wind power plants or high-voltage lines/pylons, shows that the

plant should not interfere too much with the landscape (e.g. in the form of small container plants). The fact that power-to-gas plants use existing infrastructures such as the gas grid/power grid and existing wind turbines to transport methane can also be seen as a further advantage over other infrastructure measures.

In general, all those factors that influence the acceptance of a project must be addressed in the planning and implementation of future power-to-gas projects. As already mentioned, the dissemination of information about the general approval of the technology to the general public is conducive to positively influencing attitudes towards it. With regard to participation, on the one hand, different information possibilities can be used, as some good practice examples from the fields of hydrogen mobility, wind power and high-voltage power lines show. Here it is also important to involve those affected in the planning process and to strengthen the flow of information and transparency with regard to the advantages and disadvantages of the technology.

In order to achieve knowledge and awareness among different target groups for a hydrogen-based energy supply system and thus the path to a "hydrogen economy & society", the development and implementation of policies and strategies in the areas of awareness raising (reduction of prejudices and risk concerns) is recommended (cf. [11]). Demonstration projects in particular can raise awareness throughout society - not only among the broader civil society but also among stakeholders from industry, the public sector and other decision-makers. This will also create confidence (e.g. among potential users of hydrogen-powered vehicles) in the technology through demonstration in the form of infrastructure as well as through application (e.g. through the visibility of vehicles in public spaces). Targeted, honest and enlightening communication can promote the willingness to use and buy hydrogen technologies. Particularly in the case of hydrogen mobility, there is currently still some uncertainty regarding the acquisition costs of vehicles, the ecological sustainability of hydrogen and the classification of hydrogen in the context of electro mobility (cf. [8], p.70).

This shows that on the basis of existing secondary literature on "social acceptance" of various energy infrastructure measures not only technological and technical obstacles, but also the non-technical barriers along the development and dissemination of hydrogen-based technologies should be addressed (cf. [6], p. 34). A general need for action in the introduction of hydrogen technologies, in particular in the context of market preparation, can be identified, so that in impulse and flagship projects questions relating to acceptance in society can also be considered through objective information transfer and thus the need for information on hydrogen as an energy carrier in the population is covered (cf. [12]). An in-depth qualitative as well as quantitative analysis could provide a better understanding of the motives and arguments for/against a power-to-gas project in case of given acceptance problems on site.

The necessity and importance of social acceptance is generally emphasized in numerous studies carried out for large-scale projects of all kinds (e.g. also energy infrastructure measures) and it was also shown in which type and dimension acceptance problems arise in the respective project phases. It was shown that delays in the implementation of projects, e.g. in wind power plant construction or in the construction of new power grid infrastructures, are not exclusively due to resistance from local actors (e.g. local population and/or local politicians, associations and interest groups, initiatives), but that legal and institutional framework

conditions (e.g. duration of approval procedures, quality of expert opinions) often also play an important role in the implementation of corresponding projects. It remains to be seen to what extent the implementation of a power-to-gas plant will directly affect, for example, local residents or the population (provided that the plant is also built near residential areas). At present, the level of acceptance cannot be directly estimated by political decision-makers at various levels; they are currently not directly integrated into the approval of power-to-gas plants, for example. In this context, it is also important to clarify the future role of regional and local authorities in the approval process for power-to-gas plants.

In summary, it can be stated that the social consequences and the different levels of acceptance of different actors cannot yet be assessed due to the current research and development stage of power-to-gas, so that this paper also draws on the experience gained in the field of energy infrastructures and hydrogen technologies. The Hytrust project showed that *the present scenarios and roadmaps for the introduction of hydrogen technology do not take current and future social developments, perceptions and attributions of meaning into account*. Further social research on the acceptance of new technologies is therefore seen in this context as another important field of research (cf. [13]).

10.3.5 Summary of the report

The **legal analyses** deal with the current legal situation of underground storage of various energy sources, with a focus on hydrogen injection into existing gas storage facilities. Open points and problems were pointed out and the current legal situation of power-to-gas plants was analyzed in detail. From this, recommendations for the adaptation of the legal framework were formulated.

For the **economic evaluation** of Power-to-Gas within the project Underground Sun Storage, nine fields of application were selected and quantitatively evaluated in the project consortium. The application fields differ in size, system benefit, product (hydrogen, methane or electricity) and the respective benchmark in the energy system. Individual fields of application, considered on their own, are usually associated with high production costs and depend heavily on the annual full load hours achieved by the power-to-gas system. Due to the additional components and the lower overall efficiency, the specific production costs of synthetic methane are generally higher than those of hydrogen. The use of re-electrification significantly reduces efficiency along the entire production chain and increases specific costs. Particularly at lower full load hours, the investment costs have a major influence on the production costs, whereby a significant reduction in investment costs can be expected in the future.

In comparison with the benchmarks in the energy system, the production of a renewable product and the provision of negative control energy are of particular interest. This is mainly due to the high full load hours of these two fields of application. In other fields of application, however, only a few full load hours are achieved and despite very low electricity procurement costs, as in the case of the use of surpluses from wind turbines, the specific production costs are very high. In combination with other fields of application, however, these could be very interesting due to the low power procurement costs.

In order to optimize economic efficiency by increasing the full load hours, a combination of several application fields was considered in addition to the individual application fields. The combination includes the use of surplus electricity from wind power plants (250 h/a), the provision of negative control energy (3300 h/a) and an additional electricity purchase from the public grid at spot market prices (incl. proof of origin for renewable electricity). The hydrogen produced or, optionally, the synthetic methane are used as fuel or fed into the natural gas grid. The full load hours of the power-to-gas plant were set at 6000 h/a. This means that specific production costs of around 13 cents per kWh of hydrogen or 18 cents per kWh of synthetic methane can be achieved in future. A sensitivity analysis shows that an increase in the full load hours between 3500 and 8000 h/a in the investigated combination has hardly any influence on the production costs, since the reduction of the specific investment costs is compensated by the rising average electricity costs. Although higher full load hours have the advantage of an overall increased production of H_2 or CH_4 and thus an increased substitution of fossil fuels, this also increases the overall electricity demand in the energy system.

The **economic effects** of selected fields of application and those of the combination were simulated using the MOVE2 simulation model developed at the Energy Institute at JKU Linz. The size of the plants and their investments are very different and thus a comparison of the fields of application is only possible to a limited extent. What all systems have in common is that they lead to an increase in Austria's gross domestic product. This is fundamentally based on all applications:

- additional investment impulses through the construction of power-to-gas plants,
- a reduction in fossil energy imports,
- the increase in wages induced by economic growth and thus in disposable income,
- the resulting employment effects, and
- Secondary effects resulting from the listed impacts.

The production of a renewable product for the mobility sector and the combined field of application also leads to an increase in private consumption through the purchase of gas-powered vehicles. In general, it can be stated that in all cases the use of the methanation plant (CH_4) leads to more pronounced results. This is basically due to the higher investment costs of these plants, which trigger higher economic effects. With regard to the employment effects, a higher level is also achieved in the installation of methanation plants (CH_4) in all application cases.

The **potential of hydrogen injection** into the Austrian natural gas grid depends on several influencing factors, such as applicable standards and guidelines, H_2 -compatibility of the components, gas grid structure and natural gas flow rate. When feeding into transit pipelines, it should be noted that the gas quality varies depending on the origin of the natural gas and may already contain hydrogen. Here it must be clarified whether an additional H_2 feed-in and a transmission to the respective neighboring country is possible. In the case of transport pipelines, in many cases it is less the physical properties than the gas supply contracts that determine whether and how much natural gas flows through the pipeline. In the distribution network, on the other hand, the flow and direction of the natural gas follows physical conditions,

with sales being subject to strong fluctuations in some cases, depending on the respective consumer structure.

Standards and guidelines such as ÖVGW-RL 31, which regulate the maximum volume fraction of currently 4 vol.% H₂ in natural gas as well as compliance with combustion parameters (Wobbe index, calorific value, relative density), are of major importance. Combustion parameters essentially depend on the origin of the natural gas (Russia, North Sea). While the limit value for the relative density for natural gas from Russia is already undershot at a volume share of 4-5 vol. % H₂, the Wobbe index can still be maintained at a volume share of 15 vol.%. Compliance with the limit values for the calorific value from 10 vol. % H₂ is to be regarded as critical. As far as the H₂ compatibility of individual components is concerned, there is a particular need for adjustment in the case of gas turbines as well as transport and storage compressors. Further adaptation is also required for CNG vehicles (currently max. 2 vol. % H₂) and process gas chromatographs (currently no H₂ measurable). With regard to the compatibility of H₂ in pore storages, however, a considerable need for research can be assumed.

An analysis of various sample networks showed that the natural gas flows differed greatly and that there are no typical consumption profiles, especially in network sections with predominantly industrial customers. The potentials for hydrogen feed indicated in the analyses can therefore only serve as guide values; a detailed potential survey must be carried out separately for each network area due to the different nature of the gas. On the basis of the possible hydrogen absorption capacity of the Austrian natural gas grid, an estimate was made of the possible total installed capacity of power-to-gas plants and the electricity that can be stored in the form of H₂. While power-to-gas plants with a total capacity of 60 MWe_{el} can be integrated when designed for the lowest natural gas flow rate in the summer load case, the potential increases to a total of 176 MWe_{el} when designed for the average flow rate. Which criteria are used to design the power-to-gas plant depends strongly on the respective field of application, the network section under consideration and the alternative possible uses for the hydrogen produced. When storing surpluses from volatile power generation, the characteristics of power generation and gas consumption in the various regions must be taken into account above all. While in Burgenland and Lower Austria, for example, a high amount of electricity can be generated from wind power, but only a small feed-in capacity into the natural gas grid, other provinces have high feed-in capacities (e.g. Upper Austria and Vienna), but only low electricity production from wind and PV.

For the development of a so-called "Hydrogen Economy" (hydrogen economy), the **acceptance of the population** as an essential factor must be considered in addition to technological and economic aspects. However, the social consequences and different levels of acceptance of the various actors cannot yet be assessed due to the current research and development stage of power-to-gas, so that experience and studies from the fields of energy infrastructures and hydrogen technologies must be drawn upon. In the future, social accompanying research on the acceptance of power-to-gas will be seen as an important field of research.

In order to achieve a positive effect on the social acceptance of hydrogen applications, the respective target groups must be identified and the relevant influencing factors addressed. It is essential to involve those affected in the planning process and to address any fears raised about the respective project. Arguments for the necessity of the realization of the plant, the use of existing infrastructures and the resulting possible reduction of the negative effects of the expansion of the electricity grid as well as the complete production of hydrogen from renewable energy can have a positive influence on public acceptance. In addition, it must be shown that the safety risks associated with hydrogen can be adequately dealt with and that there is no excessive interference with the landscape. Especially in the case of hydrogen mobility, there is currently still some uncertainty regarding the acquisition costs of vehicles, the ecological sustainability of hydrogen and the classification of hydrogen in the context of electro mobility. In order to increase knowledge and awareness of a hydrogen-based energy system among the various target groups, the development of strategies in the area of awareness raising is recommended. Demonstration projects of all kinds play an important role and can strengthen confidence in the technology.

However, delays in the implementation of projects are not exclusively due to resistance from local actors, but are often also caused by legal and institutional framework conditions (e.g. duration of approval procedures). In this context, it is therefore important to clarify the future role of regional and local authorities in the approval process for power-to-gas plants.

On the basis of the legal and economic analyses in the Underground Sun Storage project, it can be stated that the development of the power-to-gas system needs to be accelerated from a technological and regulatory point of view, as well as from the perspective of intelligent business models, in order to be able to realize the positive economic and systemic contributions.

10.4 Reference to publications and other documents

The following table lists all documents and publications that have been generated during the Underground Sun Storage Project.

Nr.	Studie/Bericht/Präsentation	Jahr	Autoren
1	Bericht: Underground Sun Storage – Gesellschaftliche Akzeptanz von Power-to-Gas	2015	Ch. Friedl et al.
2	Bericht: Underground Sun Storage – Ökonomische Bewertung der Anwendungsfelder	2015	G. Reiter et al.
3	Bericht: Underground Sun Storage – Potential der Wasserstoff-Einspeisung in das österreichische Erdgasnetz	2015	G. Reiter et al.
4	Bericht: Underground Sun Storage – Rechtliche Analysen	2016	K. De Bruyn
5	Präsentation:	2015	R. Tichler

	EPCON 2015 - Neue Geschäftsmodelle – 29.04.2015 – Liegt die Zukunft in der Umwandlung von „überschüssiger“ Energie?		
6	Präsentation: IIR Fachkonferenz Hybride Netze 3.- 4. Dezember 2014, Mauerbach– Power-to-Gas als Schlüsseltechnologie für die Speicherung und Verwertung erneuerbarer Energien	2014	R. Tichler
7	Präsentation: 12. Österreichische Photovoltaik-Tagung – 5. November 2014 - Power-to-Gas - eine flexibel einsetzbare Technologie zur verbesserten Integration erneuerbarer Energieträger	2014	R. Tichler
8	Präsentation: 14th IAEE European Conference - Rome 2014 – Macroeconomic effects of the energy storage system power-to-gas	2014	R. Tichler
9	Präsentation: 11. Österreichisches Windenergie-Symposium – 4.12.2014 – Power-to-Gas - ein flexibles System zur optimierten Integration von Windenergie in das Energiesystem	2014	R. Tichler
10	Präsentation: Workshop APG – Energieinstitut an der JKU Linz / 26.11.2014 – Power-to-Gas - Auswirkungen auf Netze	2014	R. Tichler
11	Präsentation: 14. Symposium Energieinnovation Graz – Wirtschaftlichkeit von Power-to-Gas durch Kombination verschiedener Anwendungsfelder	2016	A. Zauner
12	Buchbeitrag: STORING ENERGY: with Special Reference to Renewable Energy Sources - Trevor M. Letcher - Elsevier Science & Tech, 2016 Chapter 19: Power-to-gas	2016	R. Tichler, S. Bauer
13	Buch: Power-to-Gas: Technology and Business Models, Springer 2014	2014	M. Lehner et al.

10.5 List of references

- [1] Reiter G, Lindorfer J. Möglichkeiten der Integration von Power-to-Gas in das bestehende Energiesystem. In: Steinmüller H., Schneider F., Hauer A. Jahrbuch Energiewirtschaft 2013, NWV-Verlag.
- [2] Steinmüller H, Tichler R et al. (2014) Power-to-Gas – Eine Systemanalyse. Markt- und Technologiescouting und -analyse. Im Auftrag des BMWFJ.
- [3] Tichler R, Lindorfer J, Friedl C, Reiter G, Steinmüller H (2014) FTI-Roadmap Power-to-Gas für Österreich. Berichte aus Energie- und Umweltforschung 50/2014, Bundesministerium für Verkehr, Innovation und Technologie.
http://www.energiesystemederzukunft.at/nw_pdf/1450_fti_roadmap_power_to_gas.pdf, Zugriff am 03.08.2015
- [4] M. Lehner, R. Tichler, H. Steinmüller, M. Koppe, Power-to-Gas: Technology and Business Models Springer Briefs in Energy, 2014.
- [5] Huijts, N.M.A., De Groot, J.I.M., Molin, E.J.E., van Wee, B. (2013) Intention to act towards a local hydrogen refuelling facility: Moral considerations versus self-interest. Transportation Research Part A: Policy and Practice 48, S.63-74

- [6] European Commission (2006) Introducing Hydrogen as an energy carrier. Safety, regulatory and public acceptance issues. European Commission. Luxembourg. Download unter: ftp://ftp.cordis.europa.eu/pub/fp7/energy/docs/hydrogen_22002_en.pdf (letzter Abruf: 19.2.2015)
- [7] Projekt Hytrust unter: <http://www.hytrust.de/de/aktuelles.html> (letzter Abruf am 27. Februar 2014).
- [8] Canzler, W., Deibel, I. (2011) Wasserstoffbasierte Technologien im Verkehr – auch eine Frage von Vertrauen und Vertrautsein. Artikel aus: Technikfolgenabschätzung, Theorie und Praxis, ISSN 1619-7523, Jg.20, Nr.1, 2011, S.68-70
- [9] Kaiser, M., Zimmer, R. (2013) Diskursanalyse von Positionen zur Wasserstoffmobilität. Arbeitsbericht Nr. 01 im Rahmen des Projektes „HyTrust Auf dem Weg in die Wasserstoffgesellschaft“. Unabhängiges Institut für Umweltfragen, Berlin. Download unter: http://www.hytrust.de/fileadmin/download/HT-AB-01_Diskursanalyse.pdf (letzter Abruf: 20. Februar 2015).
- [10] Krstacic-Galic, A., Marz, L. (2011) Konsenschancen des energietechnologischen Paradigmenwechsels: Das Beispiel der Wasserstoff- und Brennstoffzellentechnologie, WZB Discussion Paper, No. SP III 2011-402
- [11] Project Hysociety unter: http://ec.europa.eu/research/energy/pdf/6_hysociety_en.pdf und http://www.vgb.org/fue_projekt239.html (letzter Abruf: 27. Februar 2015).
- [12] Bundesministerium für Wirtschaft und Arbeit (2005) Strategiepapier zum Forschungsbedarf in der Wasserstoff-Energietechnologie; Strategiekreis Wasserstoff des Bundesministeriums für Wirtschaft und Arbeit, Forschungsbericht Nr. 546. München. Download unter: http://www.iphe.net/docs/Meetings/France_1-05/German_Strategy_Report.pdf (letzter Abruf: 27. Februar 2015)
- [13] http://www.fvee.de/fileadmin/politik/10.06.vision_fuer_nachhaltiges_energiekonzept.pdf (letzter Abruf: 27. Februar 2015).

10.6 Contact details

Energieinstitut an der Johannes Kepler Universität Linz

Dr. Robert Tichler

Altenberger Straße 69, 4040 Linz

Tel.: +43-732-2468-5656

Fax: +43-732-2468-5651

E-Mail: office@energieinstitut-linz.at

www.energieinstitut-linz.at

Autoren: R. Tichler, A. Zauner, M. Baresch, K. De Bruyn, C. Friedl, M. Furtlehner, S. Goers, J. Lindorfer, J. Mayerhofer, G. Reiter, M. Schwarz

11 Outlook and recommendations

The provision of large-volume and seasonal storage facilities is a key challenge in the conversion of our energy production to renewable fluctuating sources. Underground gas storage facilities are already fulfilling this storage task, but it remains to be seen how these facilities can be made accessible for renewable energy through a power-to-gas process. For the first time, therefore, the questions arising from hydrogen storage/mixing were investigated within the framework of an interdisciplinary project and including a field trial at a real gas reservoir. It could be determined:

For the geochemical, geophysical and material conditions investigated, no impairment of the storage integrity can be expected with hydrogen admixtures of 10 vol.% or 10 bar hydrogen partial pressure. Initial effects will occur when the reservoir is first exposed to hydrogen. There is still a need for research in the field of geochemistry and in particular on the solubility of hydrogen in reservoir water.

Within the framework of the Underground Sun Storage project, it was possible to demonstrate, in addition to the purely scientific findings, that the conversion of renewable energy into gas as a storable energy carrier is the solution for seasonal large-volume energy storage. The kind of energy storage is of decisive importance with an increasing of renewable energy in the energy mix. Especially in regard to the balance of seasonal fluctuations in the energy demand and the energy generation and thus ultimately to ensure security of supply at any time in the year.

The comprehensive, positive results were generated from a sandstone reservoir in the Austrian Molasse Basin, which is comparable to RAG's conventional natural gas storages. Due to the different situation in many other natural gas storage facilities (different type, different geological situation, etc...) the results cannot be easily transferred. The experience with the different investigation methods and interdisciplinary approaches with their results, however, provide a good guideline for the investigation of further storage formations and storage facilities. The essential parameters have been defined.

Open questions still concern possible operational effects in commercial operation caused by changes in the composition of the storage gas and thus also in the calorific value of the storage medium. The actual admission of hydrogen to the cross-border natural gas infrastructure can only take place in a pan-European perspective. It is therefore recommended that the next steps be taken at European level.

In summary, both the integrity of the storage facilities and the field test with the associated facilities were sufficiently confirmed over a period of four years. Thus it was possible not only to achieve valuable scientific results, but also to demonstrate the efficiency of the gas storage facilities in a renewable energy system.

In addition, potential was identified to use natural gas deposits as natural reactors for the microbiological methanation of hydrogen and carbon dioxide. This was the deciding factor for the follow-up project Underground Sun Conversion. In addition to the development of a seasonal storage solution for renewable energy, it could be possible to produce renewable natural gas and at the same time use the existing infrastructure without restrictions and thus develop a sustainable carbon cycle.

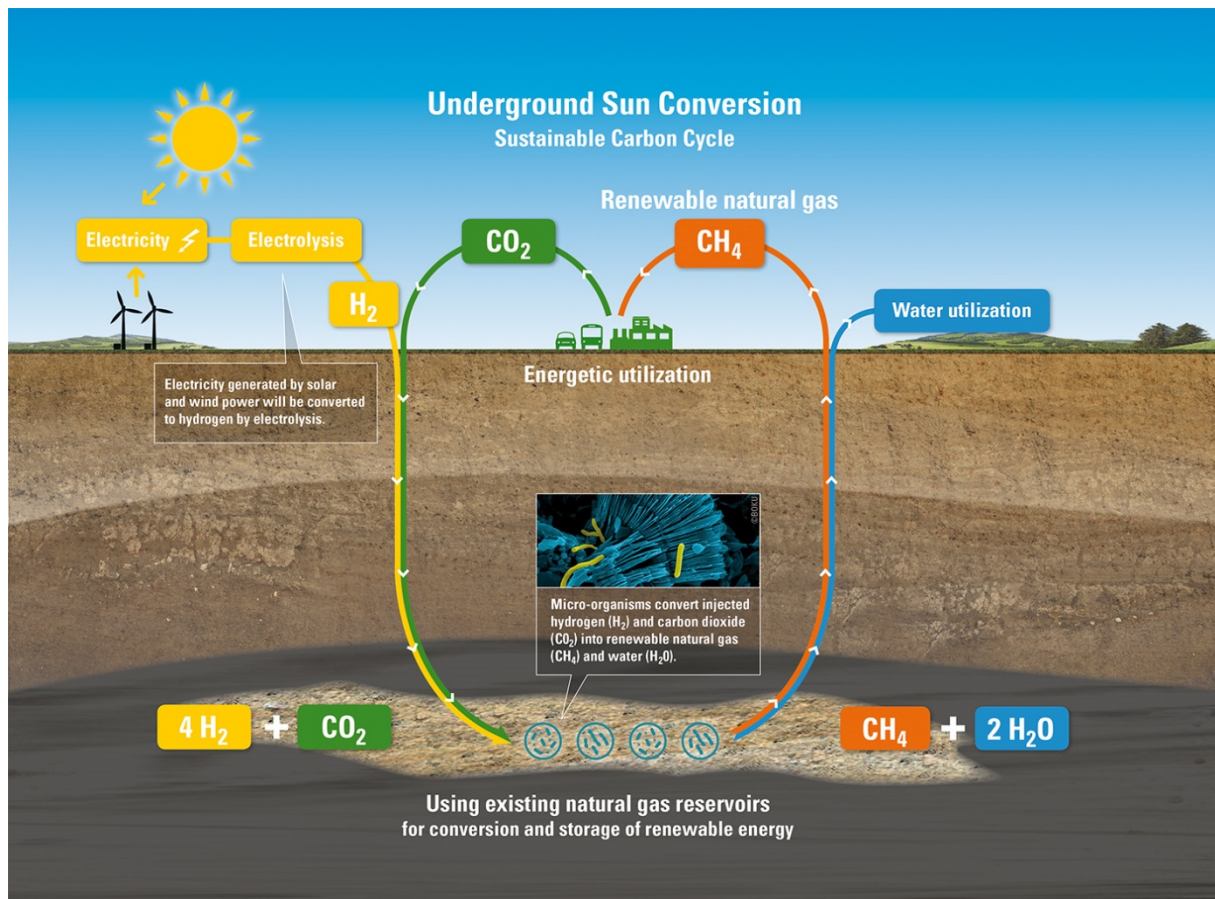


Figure 115: Underground Sun Conversion - A sustainable carbon cycle (Source: RAG)

Further information can be found at: www.underground-sun-conversion.at.

12 Appendix

Figure 1: System Image of energy storage via power to gas	14
Figure 2: Overview matrix H ₂ tolerance of selected elements in the natural gas network	15
Figure 3: Core of the cap rock from the well NU C2	19
Figure 4: Measuring site for determining gas permeability	21
Figure 5: Determined breakthrough curves at dry cores BA C1 and NU W8 at flow velocities of 3.5 cm/min.....	22
Figure 6: Comparison of the displacement function at the wet cores NU W8 /8.9 cm/min) and BA C1 (4.3 cm/min)	23
Figure 7: Comparison of the displacement curves measured on the water-saturated core BA C1 26 at flow velocities of 4.3 and 6.5 cm/min.	24
Figure 8: Pressure transmitter: a) Mounting position with safety valve; b) Lower reactor section; c) Upper reactor section.....	25
Figure 9: Data Acquisition Visualization.....	26
Figure 10: Process - Gas - Chromatograph with display of capillary tubes	26
Figure 11: Drying of the sand in the rotating tube (a), perforated plate with filter paper (b), reactor empty (c), reactor filled (d-e)	27
Figure 12: Pressure curve of reactor with 10 bar over the test period.....	29
Figure 13: Temperature curves of reactor 10 bar over the test period	29
Figure 14: Pressure curve reactor 10 bar and ambient temperature.....	30
Figure 15: CH ₄ /H ₂ ratio for reactor 10 bar.....	31
Figure 16: CH ₄ /H ₂ ratio for reactor 25 bar	31
Figure 17: CH ₄ /H ₂ ratio for reactor 40 bar	32
Figure 18: Breakthrough curves with 1st derivation at 10 bar reactor pressure	33
Figure 19: Breakthrough curves with 1st derivation at 20 bar reactor pressure	34
Figure 20: Breakthrough curves with 1st derivation at 10 bar reactor pressure	35
Figure 21: Breakthrough curves with 1st derivation at 20 bar reactor pressure	35
Figure 22: Breakthrough curves with 1st derivation at 10 bar reactor pressure and increased flow rate.....	36
Figure 23: Breakthrough curves with 1st derivation with methane as background gas, pressure 10 bar and test gas 8% H ₂ and 92% CH ₄	37
Figure 24: Breakthrough curves with 1st derivation with methane as background gas, pressure 10 bar and test gas 20% H ₂ and 80% CH ₄	37
Figure 25: Displacement of nitrogen at 10 bar and 8% H ₂ or at 20 bar and 20% H ₂	38
Figure 26: Displacement of the gas mixture at 10 bar and 8% or at 20 bar and 20% H ₂	39
Figure 27: Breakthrough curves with 1st derivation in wet conditions, pressure 10 bar.	40
Figure 28: Breakthrough curves wet conditions, pressure 20 bar.	40
Figure 29: Displacement of the mixture at 10 bar and 8% H ₂ at the wet core	41
Figure 30: Sections of geological modelling: digitization of structural maps, extraction of drilling markers from drilling protocols, seismic cube interpretation and flow simulation grid construction.....	42
Figure 31: Distribution of hydrogen concentration in the deposit over time.....	43
Figure 32: Comparison of the spatial distributions of CH ₄ and H ₂ in the reservoir.	43
Figure 33: H ₂ concentration vs. penetration depth of H ₂ into the surface layers.....	45
Figure 34: Core of hole BA C1 original sample (left) and after storage (right).....	46
Figure 35: Photos of the cores from the NU original sample (left) and after storage (right) ..	47

Figure 36: Core BA C1, (left) and core NU W8, (right); brightfield transmitted light, detail: 3.6 mm x 2.4 mm.....	48
Figure 37: Core BA C1, depth: 1319.14 m, (left: before storage, right: after storage), crossed polarizers, image section: 3.6 mm x 2.4 mm.....	48
Figure 38: Core NU W8, (left: before storage, right: after storage), crossed polarizers, image section: 3.6 mm x 2.4 mm	48
Figure 39: Flow apparatus	50
Figure 40: Core BA C1, depth: 1312.97 m, (left: before storage, right: after storage for 12 months)	51
Figure 41: Core NU W8 (left: before storage, right: after storage for 12 months).....	51
Figure 42: Moderately sorted, fine-grained, calcitically cemented litharenite	53
Figure 43: Overview of a porous, well sorted, fine-grained litharenite. The free pore space is blue.	53
Figure 44: Core BA C1, depth: 1310.94 m, (left: before storage, right: after storage for 12 months), crossed polarizers; detail: 900 μm x 600 μm	54
Figure 45: Core NU W8, (left: before storage, right: after storage for 12 months), crossed polarizers; image detail: 900 μm x 600 μm	54
Figure 46: H ₂ Sensitivity.....	57
Figure 47: Numerical errors	57
Figure 48: Pyrite Sensitivity	58
Figure 49: Pyrite sensitivity II	58
Figure 50: Limit value H ₂ (g)	59
Figure 51: Limit value H ₂ (g) without calcite and dolomite	59
Figure 52: pH value as a function of the added amount of substance H ₂ (g), without calcite/dolomite in the rock.....	60
Figure 53: Proposed geochemical modelling workflow as described in the text.....	61
Figure 54: Development of the pH static equilibrium model as a function of injected hydrogen fugacity.	62
Figure 55: Change in mineral composition during an injection year with an H ₂ partial pressure of 7.5 bar (Basic kinetic model based on the initial system of case study 3 and assuming the reactions of pyrite and pyrrhotite are in equilibrium). 63	63
Figure 56: pH change (Basic kinetic model based on the initial system of case study 3 and assuming the reactions of pyrite and pyrrhotite are in equilibrium).	63
Figure 57: Diagram Source: BOKU Wien.....	69
Figure 58: Reactor head with fittings	69
Figure 59: Isolated high-pressure bioreactors	69
Figure 60: Reservoir water Source: BOKU Wien (RAG)	70
Figure 61: Drill core.....	70
Figure 62: Primer pair V4.....	71
Figure 63: Filling of high-pressure bioreactors Source: BOKU Wien.....	72
Figure 64: Gas sampling Source: BOKU Wien.....	73
Figure 65: Opening of a reactor Source: BOKU Wien	74
Figure 66: Concentration curve of the gas components in reactors 1 and 4: 4 % H ₂ , 0,3 % CO ₂ in methane Source: BOKU	79
Figure 67: Concentration curve of the gas components in reactors 1 and 4: 10 % H ₂ , 0,3 % CO ₂ in methane, refilling on day 109 Source: BOKU.....	80
Figure 68: Discoloration of the outer edge of a drill core when the reactors are opened Source: BOKU.....	81

Figure 69: Concentration curve of the gas components in reactors 2 and 5: 10 % H ₂ , 0,3 % CO ₂ in methane Source: BOKU.....	82
Figure 70: Concentration curve of gas components in abiotic reactors 7 and 8: 10 % H ₂ , 2,5 % CO ₂ in methane Source: BOKU.....	83
Figure 71: Microbial consortia in reactors (start vs. end of hydrogen exposure) and formation water (test field). Representation on phylum level. Source: BOKU.....	84
Figure 72: Test setup for SSRTs, a) Tensile testing device with glass cell for the SSRTs at 1 bar,	88
Figure 73: Test setup for CLTs at 1 bar.....	89
Figure 74: Test setup for ageing tests at 1 bar.....	89
Figure 75: Arithmetic mean values of the elongations at fracture of the material L80.....	92
Figure 76: Arithmetic mean values of the elongations at break of the material P110.....	93
Figure 77: Elongations at break of materials 42CrMo4 QT, 42CrMo4 QTT, L360 and P235.....	94
Figure 78: Exemplary cement core.....	97
Figure 79: Comparison of X-ray diffractograms of the cement sample before and after storage.	98
Figure 80: Cement stone before storage at 200x magnification.	98
Figure 81: Cement paste after H ₂ storage at 200-fold magnification	99
Figure 82: Fragmented core after autoclave opening	100
Figure 83: Integration and function of a hydrogen separation plant on a pore storage tank	101
Figure 84: Relative permeances for hydrogen and hydrocarbons of a glassy polymer (polyimides).....	103
Figure 85: Concentration processes in the retentate-flow and in the permeate flow of the hydrogen separation plant during a storage-out process.....	104
Figure 86: Experimental membrane plant for the separation of hydrogen/natural gas mixtures in the research project Underground Sun Storage	104
Figure 87: Separation parameters of the plant in a hydrogen balancing mode	105
Figure 88: Separation parameters of the plant in a hydrogen separation plant.....	105
Figure 89: Schematic plant overview - main plants (Source: RAG).....	108
Figure 90: Course of the hydrogen concentration over the storage level	110
Figure 91: Course of the carbon dioxide concentration over the storage level.....	111
Figure 92: Comparative course of temperature development during the field test and the preparation phase	112
Figure 93: Filling of the reservoir water (Source: BOKU Vienna (RAG)).....	113
Figure 94: Sampler before entering the pneumatic gas lock (Source: BOKU Vienna (RAG))	114
Figure 95: Shifts of the microbial consortium in the formation water of the test field. Representation on phylum level (Source: BOKU).....	115
Figure 96: Comparison of the proportion of existing (DNA) and active (RNA) methanogens in the microbial consortium in the formation water of the test field (Source: BOKU).....	116
Figure 97: Course of pH value, chloride, sulphate and acetate in the formation water of the test field (Source: BOKU).....	118
Figure 98: Structural map of the HP3 1A in the geological model	120
Figure 99: Updated history match for the 10 vol.% H ₂ gas mixture case and the pure natural gas case until 27 February 2017	121

Figure 100: Development of the hydrogen concentration in the tubing with comparison of the respective final and initial concentrations	122
Figure 101: Procedure of the PtG RA (Tucovic, N. 2017).....	126
Figure 102: Flow diagram of the system boundary of the USS project (cf. Sledz, 2017 and Tschiggerl et al. 2017).....	127
Figure 103: Simplified representation of the testbed with the respective labels of the identified risks (Tucovic, N. 2017)	128
Figure 104: FN curve (black=average; dashed red = 3Sigma) of the RAG PtG plant (Tucovic, N. 2017).....	132
Figure 105: Spider diagram of the surface OE, evaluated by consequences (Tucovic, N. 2017)	133
Figure 106: Spider diagram of underground OUs evaluated by consequences (Tucovic, N. 2017)	134
Figure 107: Flow diagram application field 1b (cf. Sledz, 2017 and Tschiggerl et al. 2017)	135
Figure 108: Modeling application field 1b (Sledz, 2017).....	136
Figure 109: Extract from the environmental profile for field of application 1b (cf. Sledz, 2017 and Tschiggerl et al., 2017).....	136
Figure 110: Potential of the annual H ₂ injection into the Austrian natural gas grid <i>Source: Energy Institute at the JKU Linz</i>	149
Figure 111: Possible total installed capacity of power-to-gas plants and storable electricity for the various H ₂ feed-in capacities into the Austrian natural gas grid for current and future framework conditions. <i>Source: Energy Institute at the JKU Linz</i>	151
Figure 112: Overview of the production costs of the individual fields of application <i>Source: Energy Institute at JKU Linz</i>	152
Figure 113: Composition of the specific production costs of hydrogen and methane from a power-to-gas plant with a rated output of 5 MW _{el} at 6000 h/a. <i>Source: Energy Institute at the JKU Linz</i>	154
Figure 114: Sensitivity of production costs of H ₂ and CH ₄ from power-to-gas. <i>Source: Energy Institute at JKU Linz</i>	154
Figure 115: Underground Sun Conversion - A sustainable carbon cycle (Source: RAG) ...	167

Projektleitung und Gesamtkoordination:

DI Stephan Bauer

RAG Austria AG

Schwarzenbergplatz 16, 1015 Wien

www.rag-austria.at; www.underground-sun-storage.at

Projektpartner:

Axiom angewandte Prozeßtechnik Ges.m.b.H.

Wienerstraße 114, 2483 Ebreichsdorf

www.axiom.at

Verbund AG

Am Hof 6a, 1010 Wien

www.verbund.com

Montanuniversität Leoben

Lehrstuhl für Verfahrenstechnik des industriellen Umweltschutzes

Franz-Josef Straße 18, 8700 Leoben

www.unileoben.ac.at

Universität für Bodenkultur Wien

Department für Agrarbiotechnologie Tulln

Konrad Lorenz Straße 20, 3430 Tulln

Gregor Mendel Straße 33, 1180 Wien

www.boku.ac.at

Energieinstitut an der Johannes Kepler Universität Linz

Altenberger Straße 69, 4040 Linz

www.energieinstitut-linz.at